A NEW SPACE-TIME FINITE ELEMENT METHOD FOR THE DYNAMIC ANALYSIS OF TRUSS-TYPE STRUCTURES

JIE MA

BEng., MSc.

A thesis submitted in partial fulfilment of the requirements of Edinburgh Napier University, for the award of Doctor of Philosophy

School of Engineering and the Built Environment

Edinburgh Napier University

Edinburgh, U.K.

May 2015

Abstract

Truss-type structures are widely used in contemporary constructions. The dynamic analysis is very important to ensure the safety and the functionalities of these structures. The aim of this research was to propose a new method tailored for the dynamic analysis of linear truss-type structures. The proposed method is a single-step method underpinned by Unconventional Hamilton-type Variational Principles, and employing the finite element discretisation in both spatial and temporal domains.

To develop the proposed method, five Unconventional Hamilton-type Variational Principles tailor-made for truss-type structures were derived, preserving naturally all necessary conditions for the dynamic analysis without the introduction of any artificial factors. The resultant one-field and the two-filed formulations were used to build algorithms for the proposed method. The semi-discretisation treatment of the spatial and temporal domains was applied to these formulations. While the spatial discretisation was undertaken in the standard fashion, temporal discretisation was attempted with four different types of time finite elements. The convergence of the algorithms was examined in terms of the stability and the consistency properties. Numerical examples with different types of truss-type structures were given to verify the proposed method, and also to compare the performance of these algorithms against the existing analysis methods.

The proposed algorithms were shown to be second- or higher-order accurate when various time finite elements were employed. Compared to the widely used Average Acceleration Method (AAM), the proposed method produces highly accurate results. Larger time steps can be used without compromising the accuracy hence the computational costs may be reduced. Therefore, the proposed method can provide a fast and high-precision analysis solution for applications where these attributes are desired.

Declaration

I hereby declare that the contents of this thesis are of original and have been submitted solely to Edinburgh Napier University in partial fulfilment of the requirement for the degree of Doctor of Philosophy (PhD).

Jie Ma

Signed:

Dated: May/2015

Acknowledgement

I would like to express my appreciation and thanks to Dr Johnson Hexin Zhang and Dr Daniel Ridley-Ellis for their supervision and encouragement throughout the course of this research. Their advice and support have enriched me deeply in many aspects during this research.

I would also like to thank the Centre for Timber Engineering, Edinburgh Napier University for kindly providing the stipend during 2009 -2012. This research cannot be done without their financial support.

My special thank is reserved for my wife for her understanding and patience of my study, especially for she taking all responsibilities to look after the whole family, while coping with her work as well, when I was separated from them conducting my research. My thanks also extend to my parents and my daughter, for their support and encourage throughout the course of my research.

CONTENTS

List of Figures

CHAPTER 1

CHAPTER 3

CHAPTER 4

CHAPTER 5

CHAPTER 6

CHAPTER 7

CHAPTER 9

List of Tables

CHAPTER 5

CHAPTER 9

Notation

Unless otherwise stated in the text, the symbols used in this thesis are listed below in the order: Roman characters, Greek characters, miscellaneous character and acronyms. The units used in this thesis are System International (SI), or derived, units where possible.

Roman characters

c	viscous damping coefficient of the rod, per unit length
$\mathrm{f}(x)$	body force in the local system, per unit length
$\mathbf{f}$	body force vector
$\bar{f}$	body force field in local system
m	total number of truss rods
$\mathrm{m}(x)$	mass density of the truss rod, per unit length
n	total number of degree of freedoms

nd	total number of truss nodes
nr	total number of truss rods
$\mathrm{p}(x,t)$	momentum field
$\overline{\mathrm{p}}(x,0)$	initial momentum
$\mathbf{s}$	shape function for spatial discretisation
t	time coordinate
$u_{(\ )}$	displacement field
$\mathrm{u}(x,t)$	displacement field
$\tilde{\mathrm{u}}(x,t)$	prescribed displacement
$\overline{\mathrm{u}}(x,0)$	initial displacement
$\mathbf{u}(t)$	nodal displacement vector
$\mathbf{u_{ab}}$	nodal displacement vector of rod $\overline{ab}$ in the local coordinate system
$\mathrm{v}(x,t)$	velocity field
x	spatial coordinate
x_u	displacement boundary of the rod
x_N	traction boundary of the rod
$\mathrm{A}(x)$	cross-sectional area of the rod
$\mathbf{A}, \mathbf{A}_r$	amplification matrix
$\mathbf{C}_{(e)}$	elementary damping matrix
$\mathbf{C}$	global damping matrix
$D_{(\ )i}$	displacement components in the global system $(i = X, Y, Z)$
$\mathbf{D}(t)$	global nodal displacement vector
$\mathbf{D_{ab}}$	nodal displacement vector of rod $\overline{ab}$ in the global system
$\mathbf{D}^{(i)}(t)$	nodal displacement vector of the ith node
$\tilde{\mathbf{D}}(\tau)$	approximated displacement within time element
E	elastic modulus

$\mathbf{F}_{(e)}$	elementary body force vector
$\mathbf{F}(t)$	global body force vector
$\widehat{\mathbf{F}}(\tau)$	piecewise global body force vector within time element
$\mathbf{F}_n$	load operator
H	Hamiltonian of the system
$\mathbf{I}$	identity matrix
$\mathbf{K}_{(e)}$	elementary stiffness matrix
$\mathbf{K}$	global stiffness matrix
L, l	length of a truss rod
$\mathbf{L}(t)$	global nodal force vector
$\mathbf{L}(\tau)$	piecewise global nodal force vector within time element
$\mathbf{M}_{(e)}, \hat{\mathbf{M}}_e^{(i)}$	elementary mass matrix
$\mathbf{M}, \hat{\mathbf{M}}$	global mass matrix
$\mathrm{N}(x,t)$	axial force field
$\tilde{\mathrm{N}}(x,t)$	prescribed axial force
$\{N(x)\}$	linear interpolation operator
$\mathbf{P}(t)$	global nodal momentum vector
$\mathbf{P}^{(i)}(t)$	nodal momentum vector of the *ith* rod
$\mathbf{S}_e^{(i)}$	elementary shape function matrix
$\mathbf{S}$	global shape function matrix
T	kinetic energy
$\mathbf{T}$	transformation matrix
$\mathbf{T1}$	transformation vector
$\mathbf{U}, \mathbf{V}, \mathbf{W}$	state vector
W	work of conservative and non-conservative forces

Greek characters

$\delta(\ )$	variation operator
$\varepsilon(x,t)$	strain field
$\phi(\ ),\varphi(\ )$	time element shape function
ℓ	Laplace transform operator
$\lambda^{(\ )}$	eigenvalue of the amplification matrix
$\rho(\ )$	spectral radius
τ	dimensionless time
$\boldsymbol{\Psi},\boldsymbol{\Phi}$	time finite element approximation operator
Π,Γ	energy functionals

Miscellaneous character

$\mathcal{L}$	Lagrange density

Acronyms

DOF	Degree of Freedom
FDM	Finite Difference Method
FEM	Finite Element Method
GN*pj*	Generalised Newmark method with approximation of degree *p* for equations of order *j*
HLVA	Hamilton's Law of Varying Action
HWP	Hamilton's Weak Principle
MDOF	Multi-Degree-of-Freedom
PTI	Precise Time Integration
SDOF	Single-degree-f-Freedom
SS*pj*	Single Step with approximation of degree *p* for equations of order *j*
STFEM	Space-Time Finite Element Method
UHVP	Unconventional Hamilton-type variational principle

1. INTRODUCTION

1.1 Background

Truss-type structures are widely used in contemporary constructions. This type of structure is typically made of rod members connected by rigid joints, and the load is applied to the joint only. There is no bending moment within each rod member or at the interface between the rod and the joint. A truss-type structure may be in the form of a simple planar truss in a two-dimensional plane, or a space truss in the three-dimensional space. Figure 1.1.1 gives two typical examples of truss-type structures.

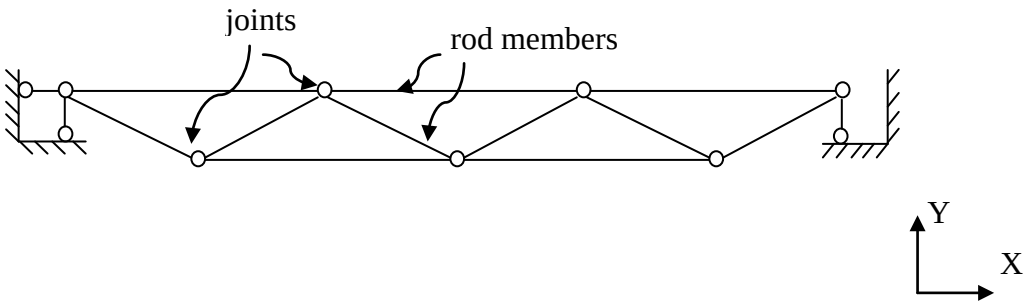

Figure 1.1.1a – A planar truss

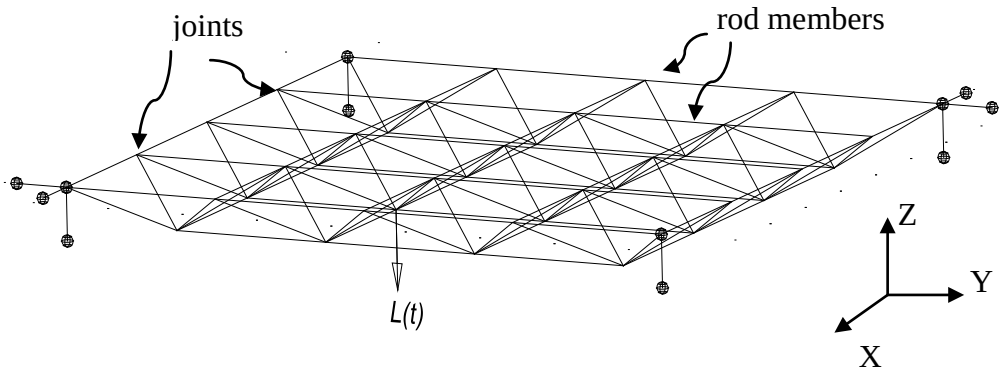

Figure 1.1.1b – A space truss

Truss-type structures have a long history in the civilisation development and can be traced back to medieval times when high pitched church roofs were built (Schueller, 1983). With the advance in the material production and construction techniques, truss-type structures have been increasingly adopted in modern applications for a large varieties of projects, such as but not limited to, bridges, open-space column-free buildings, industrial equipments and space structures, etc.. The Forth Railway Bridge is such a typical example.

Figure 1.1.2 – Forth Railway Bridge (Roelandts, n.d.)

Figure 1.1.3 – A typical truss roof of a modern facility (Anon., n.d.)

Figure 1.1.4 – A telescope disc (Anon., n.d.)

Figure 1.1.5 – A space station (Anon., n.d.)

During the service period, these structures are frequently subject to dynamic loads /effects, such as

- Wind excitation.
- Seismic load.
- Machinery/ occupants induced excitations.
- Stress wave propagation.
- etc.

As a result of these dynamic loads /effects, these structures can exhibit various dynamic characteristics, which need to be addressed in line with the particular requirements of the applications. In infrastructures and buildings, vibrations induced by the earthquake, wind or moving loads /parts /occupants can cause adverse effects, such as the resonance or excessive displacements of the structure. These results can lead to the over-stressing of structural members and even the failure of the entire structure. Typical examples included the collapse of the Tacoma Narrows Bridge in 1940 and the San Francisco–Oakland Bay Bridge failure in 1989. Therefore, the dynamic effects are critical to the structural safety.

Meanwhile, for certain types of applications, the vibration control is vital to ensure the functionality. For example, astronomy telescopes searching signals from the distant spaces are commonly required to be isolated from all sorts of vibrations, in order to satisfy the stringent signal processing criterion (e.g. displacement needs to be controlled in the ranges of a few nanometres) (Preumont, 2011). Vibration control systems are installed to minimise oscillations to acceptable level. The minimisation relies on the predication made by a dynamic analysis package, and this predication has to be computed to a high order of accuracy for its purpose, where fast and higher-order accurate algorithms would be desirable for the analysis. It can be seen that the dynamic analysis is paramount in many aspects.

When a truss-type structure is subject to a dynamic load, the structural members may have to sustain cyclic tension and compression forces. If the axial force exceeds a certain threshold, either the failure of brittle components or the buckling/yielding of the elastic members will occur. In the case of component failure, the stiffness of the system will change suddenly, and the force will be redistributed in the remaining members, and the whole system needs to be re-evaluated. In the case of buckling/yielding, the post-buckling behaviour of the structural members can be very complex, involving lateral deflections and inelastic cyclic of truss members as shown in Figure 1.1.6. This inelastic post-buckling cyclic behaviour of the truss member was discussed by Malla et al. (2011) and some valuable insights have been obtained. However, the linearity is not the issue that this research is aiming to address, because this study is focused on a new fundamental dynamic analysis method for truss-type structures. A tailored made variational theory and the resultant analysis method are developed for this purpose. Although it is presented for the linear cases only in this thesis, the theory and the method could be expanded to non-linear cases, using a similar developing procedure demonstrated in this research.

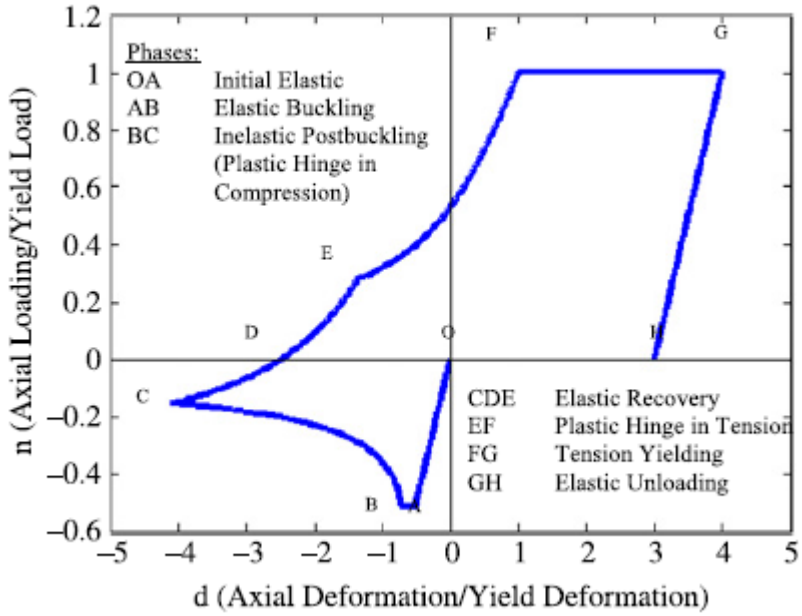

Figure 1.1.6 – Post-buckling inelastic cyclic behaviour of truss member (Malla et al., 2011)

A survey of the literature found that current studies regarding the dynamic analysis of truss structures are based on either the direct integration methods or the modal decomposition method. The central difference scheme was used by Yu, Li and Luo (2011); the popular average acceleration method of the Newmark's family was used by various authors (Thai and Kim, 2011; Malla et al., 2011). Gao (2007) used modal decomposition method for his random seismic response analysis. The paper of Koohestani and Kaveh (2010) discussed special treatment to system matrices to break down a large eigenproblem into a smaller one and thus facilitate the modal decomposition method.

However, these methods are known to have various drawbacks. For the modal decomposition method, first of all, it is limited to linear systems only. Secondly, as modern truss-type structures tend to contain many structural elements hence the number of degree-of-freedoms can get very large. It is known that the eigenproblem associated with the modal decomposition method is very difficult to solve for large systems. In practice, lower frequency modes are often considered and other modes are omitted in the analysis; however the result without the

contributions of intermediate and high frequencies will not be able to meet the requirement in high precision applications such as vibration control problems and shock wave problems. Thirdly, Duhamel time integration may have to be used if there is no analytical solution corresponding to particular excitation forces, however, this exercise is very expensive computationally.

Direct integration methods do not have the issues associated with the modal decomposition method. However, there are a few issues for this type of methods, namely, the numerical stability, numerical dissipation and the order of accuracy. For the stability issue, this type of methods can be grouped into conditionally stable schemes and unconditionally stable ones. The central difference method found in the literature is a conditionally stable method hence the time step has to be very small to satisfy the stability requirement. It is desirable to use unconditionally stable methods, so that the results obtained can be assured not to "blow up" due to inappropriate time steps. The average acceleration method of the Newmark's family is a popular method belongs to the group of methods possessing the unconditional stability. However, it does not have the desired property of numerical dissipation (Hilber and Hughes, 1978). The spurious higher mode responses may not be damp out without the numerical dissipation, and hence the solution may be contaminated. Various improvements have been made to introduce numerical dissipation (Wilson, 1968; Hilber, Hughes and Taylor, 1977; Chung and Hulbert, 1993). However these methods introduce algorithmic damping not only in the desired high frequency range, but more or less in the low frequency range as well, therefore these methods all produce bigger period and amplitude errors than the original average acceleration method (Hilber and Hughes, 1978; Chung and Hulbert, 1993). The direct integration methods use certain assumed variation pattern for the acceleration, velocity and displacement. Because these assumptions are not flexible, it is often found the accuracy of direct integration method is not high. The average acceleration method and those improved methods are only second-order accurate, and the central difference method is even first-order accurate. To improve the accuracy of the results, the time step has to be reduced from a relatively large value to much smaller values,

and the reduction depends on what level of accuracy is required. The use of smaller time step inevitably means more calculations need to be done for the same problem, and hence the computational cost will increase, sometimes, dramatically. From the numerical examples presented in Chapter 9, it can be seen that this increased computational cost will make the direct integration method less favourable for high-precision applications.

In light of these drawbacks, the search for higher-order accurate methods with improved algorithmic attributes has always been a major interest of the research community. Several alternative linear analysis methods have been proposed recently for the structural dynamics in general. It is suggested that higher-order algorithms can offer benefits such as suitable for long-term evaluation and preserving system invariants (Fung, 1999a). Larger time step can also be used without compromising the accuracy. These alternatives include higher-order methods based on the Newmark scheme (Kim et al, 1997; Fung, 1998b), the precise time integration methods (Zhong and William, 1994; Fung, 2006; Wang and Au, 2009), collocation methods (Golley, 1996; Wang and Au, 2004; Rostami, 2012), differential quadrature method (Fung 2001a), various new weighted residual methods (Golley, 1999; Fung, 2003b; Idesman, 2007) and the variational methods (Luo, Huang and Zhang, 2003; Luo, Liang and Li, 2007; Grossi and Albaracin, 2007).

In this research the so-called Unconventional Hamilton-type Variational Principle (UHVP) (Luo et al., 2003) is used to underpin the development of a new linear analysis method for truss-type structures, which utilises finite element discretisation in both spatial and temporal domains to derive higher-order algorithms. The UHVP based method offers a series of advantages for the dynamic analysis, such as:

- No knowledge is required for solving the partial differential equation.
- No need for separate treatments of solution and altering the forcing function as used in some recent methods.

- Straightforward and intuitive.
- Possesses solid mathematical ground.
- A wide range of governing relations is included.
- Several existing variational laws / principles are embraced.

Several higher-order algorithms are obtained with this method, and the numerical characteristics of these algorithms are discussed in this thesis. The developed algorithms are compared with the popular average acceleration method in terms of the accuracy and efficiency.

1.2 Objectives

The objective of this research is to construct a new, tailor-made system of variational theory for the dynamic analysis of truss-type structures, and to develop a new space-time finite element method accordingly. To achieve this objective, it is necessary to accomplish the following sub-objectives:

(1) To develop a system of Unconventional Hamilton-type Variational Principles tailored for truss-type structures.

(2) To lay a solid theoretical foundation for the development of a space-time finite element method for truss-type structures, which can be extended to other applications (such as non-linear and multi-physics problems).

(3) To propose a new approach to develop the space-time finite element for truss-type structures based on the proposed UHVP.

(4) To develop a tailor-made procedure for construction of the space-time finite element method for truss-type structures based on the proposed UHVP.

(5) To test the stability, consistency, accuracy, and the efficiency of the proposed finite element method with different temporal interpolation schemes.

(6) To verify the proposed variational principles and the space-time finite element method with numerical examples.

1.3 Methodology

To develop a new analysis method, various approaches emerged recently have been reviewed and evaluated, and Unconventional Hamilton-type Variational Principle is chosen to underpin the proposed method after the review. However, in order to develop the proposed method, tailored principles preserving and utilising the characteristics of truss-type structures are required. To this end, five bespoke principles suitable for this type of structures are proposed. The one-field (displacement) and two-field (displacement and momentum) formulations are used for the subsequent development of the new analysis method since these two principles contain enough and necessary field variables for the problem and lead to the most economic equation sets.

Having derived the UHVP integration formulations, the space-time finite element method is utilised to take the advantages offered by these formulations in the aim to construct higher-order algorithms. The semi-discretisation treatment of the space-time domain is selected. While the spatial discretisation is rather standard, four time finite elements are considered in the temporal domain to obtain the different numerical properties. These time finite elements are based on the Hermite cubic polynomials and the Lagrange polynomials of various orders.

It is important to evaluate the numerical characteristics of the resultant algorithms. The convergence is a key issue in this regard. Since the convergence can be verified by judging the stability and consistency (Hughes, 1987), the algorithms derived are investigated in these two respects.

Numerical examples are also required to verify the performance of the proposed algorithms. This is done by comparing the solutions obtained from the algorithms with the results from the analytical method (modal decomposition method) and

the average acceleration method. The absolute and relative errors are used to compare these schemes.

1.4 Organisation of the thesis

The structure of the thesis is as follows:

In Chapter 1, the background of dynamic analysis of truss-type structures, research objectives and the adopted methodology have been presented.

Chapter 2 reviews the current research on linear dynamic analysis of truss-type structures, and the weakness of these methods is highlighted. In order to find suitable alternative methods, various established linear analysis methods and emerging methods proposed recently for structures in general are reviewed and discussed in detail. Unconventional Hamilton-type variational principle is chosen to underpin the proposed method for the dynamic analysis of truss-type structures.

The development of variational methods for dynamic problems is presented in Chapter 3. Firstly Hamilton's Principle is examined and its unfitness for dynamic analysis is clarified. The first suitable variational principle - Gurtin's principle and its variants are presented next. Another important branch, Hamilton's Law of Varying Action (HLVA) is reviewed subsequently and some further developments related to HLVA are also presented. Finally, the recently proposed unconventional Hamilton-type variational principle (UVHP) in the general form is introduced. The relationship between UVHP and other variation law / principles is discussed.

Chapter 4 derives five tailored UVHPs for truss-type structures. In each of the principles a pair of functionals is found. It is proved that the governing equations and the initial / boundary conditions will be recovered naturally when the variation of either functional is made to vanish. The principles employ up to five independent fields, and these fields can be reduced by admitting various control

equations as prerequisites, so that a series of simplified principles are derived systematically.

Time finite elements are reviewed in Chapter 5. Two fundamental aspects of implementing the finite element in the temporal domain are presented first, and the choice of this research is explained. Various time finite elements suitable for initial-value problems are reviewed. Four time finite elements for the proposed method are presented in detail.

In Chapter 6, two classes of space-time finite element algorithms based on the unconventional Hamilton-type variational principle are developed. Firstly, the one-field and two-field variational formulations are presented. The finite element discretisation of the spatial domain is then applied to each variational formulation, resulting in a set of integro-differential equations. Subsequently these equations are transformed into a set of algebraic equations with the finite element discretisation in time, from which the space-time finite element algorithms specific for truss-type structures are found.

The stability of the proposed algorithms is investigated in Chapter 7 by examining the spectral radius of the amplification matrix of each algorithm. It is found that these algorithms possess different stability properties; three out of four algorithms are conditionally stable, and one algorithm is unconditionally stable.

In Chapter 8 the consistency of the proposed algorithms is investigated by the comparison of the numerical amplification matrix with the exact one, and finding the leading truncation error term. It is found these algorithms are consistent. While the one-field algorithm is second-order accurate with the cubic Hermite time element, the order of accuracy of the two-field algorithms seems to be proportional to the order of the time approximation. Second- and higher- order results can be generated.

The performance of the proposed algorithms is evaluated in four numerical examples in Chapter 9, and the results are compared with reference schemes. It is found that the UVHP algorithms produce much improved results compared to the Average Acceleration Method (AAM) using the same time step, at the same time, the computational cost for UVHP algorithms can be lower. To improve the accuracy of the AAM results, much increased computational cost is demanded. In contrast, these additional costs can be lower for UVHP algorithms as well.

The final Chapter summarises the thesis and presents the conclusions of the research, areas for further studies are also recommended.

Chapter 2 Overview of Linear Dynamic Analysis Methods

2.1 Introduction

This chapter reviews the current dynamic analysis methods for truss-type structures and newly emerged methods for structural dynamics in general. First, current methods for truss-type structures are reviewed in Section 2.2. It is found the current research in this area is still restricted to modal decomposition method and a couple of direct integration methods; however, there are several drawbacks with these classical methods, which are discussed in Section 2.3. Section 2.3 also examines other established main-stream linear analysis methods and various dynamic analysis methods proposed recently for structural dynamics in general, in order to identify suitable alternatives to the current methods. These methods include different types of direct integration methods, higher-order methods based on Newmark scheme, precise time integration method, weighted residual methods, collocation methods, differential quadrature method and variational methods.

2.2 Current research on dynamic analysis of truss-type structures

There are relatively few studies on dynamic analysis of truss-type structures in the literature. The review conducted by this author found that the existing methods used for either linear or non-linear truss-type structures can be classified into two categories

- Modal decomposition method
- Direct integration method

Modal decomposition method

Koohestani and Kaveh (2010) proposed a special technique to deal with the eigenproblem associated with free vibration and buckling of cyclically repeated space truss structures. Advantage is taken of the cylindrical coordinate system to obtain system matrices in a special pattern, which decomposes the eigenproblem into smaller sub-problems easy to solve. In this fashion decomposition method for the dynamic analysis can be facilitated. However, this treatment can only be applied the particular type of truss. In addition, the forced vibration of trusses is not considered. There are other research apply the modal decomposition method directly, see Gao (2007) for example, without addressing the associated eigenproblems.

Direct integration method

Two direct integration methods are found in the literature. In one paper by Yu, Li and Luo (2011), the discretised motion equations are solved with the central difference method. However this method is conditionally stable only and this method is only first-order accurate. In one paper discussing nonlinear time-history analysis of truss structures (Thai and Kim, 2011), the response of each time step is solved initially with the average acceleration method (AAM) of the Newmark family, which is then inputted into the iteration process for the nonlinearity consideration. In the paper of Malla et al. (2011) the AAM is also used to solve the dynamic equations considering post-buckling behaviours of the structure. The Newmark family method will be reviewed in detail in the next subsection.

2.3 Linear analysis methods for structural dynamic problems

In this section the classical methods and newly emerged methods for linear dynamic analysis are reviewed, including modal decomposition method, various direct integration methods, higher-order methods based on Newmark scheme, precise time integration methods, weighted residual methods, collocation method, differential quadrature method and variational methods.

2.3.1 Equation of motion

The structural dynamic problem can be expressed conveniently with the equation of motion. For a Single-Degree-of-Freedom (SDOF) system this equation is in the following form

$$m\ddot{u}(t)+c\dot{u}(t)+ku(t)=f(t) \tag{2.3.1a}$$

where m,c,k,f are the mass, damping coefficient, stiffness coefficient and excitation force respectively. $u(t)$ is the displacement field to be determined and the superimposed dot represents the time differentiation operation of the field. $f(t)$ is the time-varying force. The initial condition can be expressed as

$$\begin{aligned} u(0)&=u_0 \\ \dot{u}(0)&=\dot{u}_0 \end{aligned} \tag{2.3.1b}$$

The analytical solutions are available if Eq. (2.3.1a) is homogenous, i.e. $f(t)=0$. This corresponding solution is called the homogenous solution. Analytical solutions are also known for a few types of non-homogenous equations. However, if the excitation force is of an arbitrary type, then the Duhamel integral may have to be used to find the so-called “particular solution” related to the force. So the solution of the problem in Eq. (2.3.1) is given by the summation of the homogenous solution $u_h(t)$ and the particular solution $u_p(t)$.

$$u(t)=u_h(t)+u_p(t) \tag{2.3.2}$$

The homogenous solution $u_h(t)$ can be found in many textbooks such as (Tedesco et al., 1999) and the particular solution can be found by using the Duhamel integral as

$$u_p(t) = \int_0^t f(\tau) h(t-\tau)\, d\tau \tag{2.3.3}$$

where $h(\ )$ is the impulsive response function of the system.

For a Multi-Degree-of-Freedom (MDOF) system, the equation of motion can be put into a matrix format as below in which the boldface characters represent corresponding vectors/ matrices of the system

$$\mathbf{M}\ddot{\mathbf{U}}(t) + \mathbf{C}\dot{\mathbf{U}}(t) + \mathbf{K}\mathbf{U}(t) = \mathbf{F}(t) \tag{2.3.4a}$$

With the initial condition

$$\begin{aligned} \mathbf{U}(0) &= \mathbf{U}_0 \\ \dot{\mathbf{U}}(0) &= \dot{\mathbf{U}}_0 \end{aligned} \tag{2.3.4b}$$

The solution of an MDOF system can be obtained using many methods, which are to be reviewed in the following sub-section.

2.3.2 Classical methods of dynamic analysis

Modal decomposition method and Duhamel integration

This method was developed for solving dynamic problems for linear MDOF systems. It has been well established that the response of a linear MDOF system can be obtained from its modal response components (Hughes, 1987; Zienkiewicz, 1977), as long as the physical damping of the system is of orthogonal type and satisfies the Caughey condition $\mathbf{C}\mathbf{M}^{-1}\mathbf{K} = \mathbf{K}\mathbf{M}^{-1}\mathbf{C}$. The modal decomposition method transforms the original coupled MDOF equations (in the form of Eq. (2.3.4)) into a set of uncoupled SDOF differential equations (in the form of Eq. (2.3.1)), which can be solved individually by using analytical solutions or the Duhamel integration. The solutions of these uncoupled equations are then

combined to obtain the response of the original system.

High precision result at any desired time instance can be obtained with the modal decomposition method. However, in order to obtain the uncoupled equations, it is required to solve the eigenproblem associated with the dynamic system first, and that would be a difficult, even impossible, task for a system with large number of degree-of-freedoms. In addition, the Duhamel integration per se is rather computationally expensive to find the response history, especially for systems with large numbers of DOFs. Therefore, improvements have been proposed to tackle these difficulties. Successful efforts have been made by Liu to replace the Duhamel integration by the piecewise Lagrange polynomial approximation (Liu, 2001) and the Birkhoff polynomial approximation (Liu, 2002) of the load functions. However, the overall accuracy is compromised as the particular solution thus obtained is inherently less accurate than the homogeneous solution.

Direct integration methods

This family of methods use various finite difference discretisation techniques in the time domain to transform the original differential equations into a set of algebraic equations, which can be solved much easier. Many widely used methods belong to this category. The early direct integration methods include the central difference method, the Newmark's family of methods (Newmark, 1959) , Wilson-θ method (Wilson, 1968), HHT-α method (Hilber et al., 1977), Houbolt method (Houbolt, 2012), Park method (Park, 1975), Bossak method and Bazzi-Anderheggen method (Bazzi and Anderheggen, 1982). Recently some more methods have been added into this big family, including an explicit and unconditionally stable method proposed by Itzkowitz and Levit (1987), the improved Houbolt's family of methods (Chung and Hulbert, 1994), the generalised-α method (Chung and Hulbert, 1993), the generalised average acceleration method promoted by Kim et al (1997), the sub-time step method by Fung (1997b, 2001b).

It is impossible to review all direct integration methods in this chapter; therefore a few typical ones are selected and presented in what follows. For a more comprehensive review of these various schemes, the reader is referred to the work of Dokainish and Subbaraj (1989) and Subbaraj and Dokainish (1989).

One of the most influential methods for structural dynamics is the Newmark method. In this method, the approximated displacement $\mathbf{u}_{n+1}$ and velocity $\mathbf{v}_{n+1}$ at the end of the time step $t = t_{n+1}$ are solved from the following equations

$$\begin{aligned}
&\mathbf{u}_{n+1} = \mathbf{u}_n + \Delta t \mathbf{v}_n + \Delta t^2 \frac{(1-2\beta)}{2} \ddot{\mathbf{u}}_n + \Delta t^2 \beta \ddot{\mathbf{u}}_{n+1} \\
&\dot{\mathbf{u}}_{n+1} = \dot{\mathbf{u}}_n + \Delta t (1-\gamma) \ddot{\mathbf{u}}_n + \Delta t \gamma \ddot{\mathbf{u}}_{n+1} \\
&\mathbf{M}\ddot{\mathbf{u}}_n + \mathbf{C}\dot{\mathbf{u}}_n + \mathbf{K}\mathbf{u}_n = \mathbf{F}_n \\
&\mathbf{M}\ddot{\mathbf{u}}_{n+1} + \mathbf{C}\dot{\mathbf{u}}_{n+1} + \mathbf{K}\mathbf{u}_{n+1} = \mathbf{F}_{n+1}
\end{aligned} \tag{2.3.5}$$

where Δt is the time step and $\Delta t = t_{n+1} - t_n$. Two parameters β and γ are in place to control the algorithmic properties. It is required that $2\beta \geq \gamma \geq 1/2$ to ensure an unconditionally stable numerical scheme. When $\gamma = 1/2$ the resulting schemes are second-order accurate but non-dissipative; while $\gamma > 1/2$ the algorithm becomes dissipative, but the accuracy decreases to first-order. Other existing methods can be derived with different β, γ values. If $\gamma = 1/2$ and $\beta = 1/12$ the implicit method of Fox and Goodwin (Fox and Goodwin, 1949) arises; when $\gamma = 1/2$ and $\beta = 1/6$ the linear acceleration method is obtained and if $\gamma = 1/2$ and $\beta = 1/4$ the average acceleration method is derived.

Since the original Newmark method can only generate either dissipative first-order accurate algorithms or non-dissipative second-order algorithms, various proposals have been put forward to alter this type of method to have the desired

numerical stability and dissipation properties. Among the second-order accurate algorithms are Wilson-θ method, HHT-α method, collocation method (Hilber and Hughes, 1978), WBZ-α method (Wood et al., 1980), generalised-α method (Chung and Hulbert, 1993).

2.3.3 Newly developed methods

Higher-order methods based on the Newmark scheme

A fourth-order algorithm was obtained by Tarnow and Simo (1994) using a sub-marching procedure applied to the Newmark method. The resulting algorithm is non-dissipative, and the accuracy is not as good as other fourth-order methods. The concept of average acceleration used in the original Newmark method was generalised by Kim et al. (1997), a higher-order and unconditionally stable algorithm was achieved. However, this algorithm is also non-dissipative. Dissipative, unconditionally stable and higher-order accurate schemes were derived by Fung with the sub-stepping procedure (Fung, 1997b,c, 2001b; Fung and Chow, 1999, 2002). The essence of sub-stepping procedure is to evaluate the responses at the sub-time step locations with Newmark method individually, and then combine these responses with the corresponding weighting factors to obtain the solution at the end of the time step. The algorithm is unconditionally stable and the dissipation is controllable with an ultimate spectral radius parameter. The accuracy is related to the number of sub-time steps and can be adjusted to the desired order. These sub-time step locations can be determined by the roots of a polynomial, which in turn can be given explicitly in terms of the ultimate spectral radius parameter and the number of the sub-time steps. The weighting factors can be solved from a set of algebraic equations once the sub-time step locations are determined. However, there are several drawbacks with this method:

- Complex time step has to be used if the desired order of accuracy exceeds three; computational cost is hence higher due to the high cost of computation of complex numbers.

- Excitation force needs to be modified to maintain the same accuracy of the particular solution as the homogeneous solution.
- Excitation force needs to be extrapolated in case of sub-step positions are outside of the current time step.

Precise Time Integration (PTI) Methods

Zhong and William(1994) proposed a time integration method, called the precise time step integration method, for a high precision analysis of structural dynamics. In their method, with the assistance of a new variable $\mathbf{Y}$,

$$\mathbf{Y} = \mathbf{M}\dot{\mathbf{U}} + \frac{\mathbf{C}\mathbf{U}}{2} \tag{2.3.6}$$

the second-order differential equation Eq. (2.3.4) was transformed into a first-order equation

$$\dot{\mathbf{Y}} = \left(\frac{\mathbf{C}\mathbf{M}^{-1}\mathbf{C}}{4} - \mathbf{K} \right)\mathbf{U} - \frac{\mathbf{C}\mathbf{M}^{-1}}{2}\mathbf{Y} + \mathbf{F} \tag{2.3.7}$$

Combined with the velocity expression derived from Eq. (2.3.6)

$$\dot{\mathbf{U}} = -\frac{\mathbf{M}^{-1}\mathbf{C}}{2}\mathbf{U} + \mathbf{M}^{-1}\mathbf{Y} \tag{2.3.8}$$

A matrix equation was derived as

$$\dot{\mathbf{V}} = \mathbf{H}\mathbf{V} + \mathbf{F}' \tag{2.3.9}$$

in which

$$\mathbf{V}=\begin{Bmatrix}\mathbf{U}\\ \mathbf{Y}\end{Bmatrix};\quad \mathbf{H}=\begin{bmatrix}-\dfrac{\mathbf{M}^{-1}\mathbf{C}}{2} & \mathbf{M}^{-1}\\ \dfrac{\mathbf{C}\mathbf{M}^{-1}\mathbf{C}}{4}-\mathbf{K} & -\dfrac{\mathbf{C}\mathbf{M}^{-1}}{2}\end{bmatrix};\quad \mathbf{F}'=\begin{Bmatrix}\mathbf{0}\\ \mathbf{F}\end{Bmatrix} \tag{2.3.10}$$

The load term $\mathbf{F}$ was assumed to vary linearly within the time step (t_k, t_{k+1}). The general solution was obtained as the following

$$\mathbf{V}_{k+1}=\mathbf{T}(\Delta t)\times\left\{\mathbf{V}_k+\mathbf{H}^{-1}\left(\mathbf{F}_k'+\mathbf{H}^{-1}\mathbf{F}_{k+1}'\right)\right\}-\mathbf{H}^{-1}\left(\mathbf{F}_k'+\mathbf{H}^{-1}\mathbf{F}_{k+1}'+\mathbf{F}_{k+1}'\times\Delta t\right) \tag{2.3.11}$$

in which $\Delta t=t_{k+1}-t_k$ and the amplification matrix was

$$\mathbf{T}(\Delta t)=\exp(\mathbf{H}\times\Delta t) \tag{2.3.12}$$

The high precision of Zhong's algorithm lies in the accurate calculation of the exponential matrix $\mathbf{T}$. The key to this is dividing the time step into a large number of segments with the length being $\tau=\Delta t/2^N$ $(\text{integer } N\geq 20)$ and using the following 2^N property

$$\mathbf{T}(\Delta t)=\exp(\mathbf{H}\times\Delta t)=\left\{\exp\left(\mathbf{H}\times\frac{\Delta t}{2^N}\right)\right\}^{2^N}=\left\{\exp(\mathbf{H}\times\tau)\right\}^{2^N} \tag{2.3.13}$$

When $N=20$, $2^N=1048576$, therefore τ is such a small figure that a truncated Taylor expansion can be used to approximate $\exp(\mathbf{H}\times\tau)$ very accurately.

$$\exp(\mathbf{H}\times\tau)\cong\mathbf{I}+\left(\mathbf{H}\times\tau+\frac{(\mathbf{H}\times\tau)^2}{2!}+\frac{(\mathbf{H}\times\tau)^3}{3!}+\frac{(\mathbf{H}\times\tau)^4}{4!}\right)=\mathbf{I}+\mathbf{T}_a \tag{2.3.14}$$

It is then followed by

$$\mathbf{T}(\Delta t) = \{\mathbf{I} + \mathbf{T}_a\}^{2^N} \tag{2.3.15}$$

A scaling and squaring technique was used for the calculation of Eq. (2.3.15) to obtain $\mathbf{T}$. The accuracy of Zhong's method was only affected by the accuracy of the matrix inversion of $\mathbf{H}$ and the load approximation. The selection of the time step Δt can be made considerably large (as long as the load approximation is acceptable for such a time step) and independent to the modal frequencies of the structural system. However, as shown in Eqs. (2.3.14) and (2.3.15), the computation of $\mathbf{T}(\Delta t)$ involved multiple matrix operations, which made the computation not so efficient for large systems.

To reduce the computational effort, Fung (1997a) proposed a similar precise time step integration method. The second-order equation of motion was tackled directly, and the solution was expressed using the initial conditions, the steady-state response in addition to the step-response and impulsive-response matrices. With the steady-state response studied by others (Leung, 1986), Fung's work focused on the derivation of the step-response and impulsive-response matrices, in which the scaling and squaring technique was employed as well to make the time segment small enough for the precise calculation of the matrices using the truncated Taylor series. In contrast to Zhong's original method, the symmetry of matrices was introduced, and the relations between the response matrices and their time derivatives were investigated in order to improve the computational efficiency. As demonstrated in his paper, the accuracy was high, but the stability of the method was unconditionally unstable or conditionally stable at the most, depending on the order of the Taylor expansion.

Efforts have been made to improve the PTI method through many other ways, interested reader is referred to the works of (Lin et al., 1995; Shen et al., 1995; Gu et al., 2001) for more details. In particular, the truncated Taylor expansion of the

exponential function was replaced by the Padé approximation (Wang and Au, 2009) and the generalised Padé approximation (Fung, 2005; Wang and Au, 2009) in the evaluation of the matrix exponential function to attain unconditional stability and controllable numerical dissipation. Wang and Au (2009) further replaced the linear approximation of the excitation forces by three different types of quadrature formulations to eliminate the errors associated with the matrix inversion, thus the accuracy was further improved. The order of accuracy can be set as desired by adjusting the algorithmic parameters.

In these works mentioned above the matrix multiplications are still required; consequently the computational cost is still high for large systems. Fung (2006) proposed an improved version of PTI method to tackle this problem, in which the computational efficiency was firstly improved by reducing the dimension of the exponential matrix $\exp\left(\mathbf{H}\times\Delta t\right)$ through the Krylov subspace method. The efficiency was further improved by using the Padé approximation instead of the truncated Taylor series in the evaluation of the exponential matrix, along with transforming the inhomogeneous governing equation into an equivalent homogeneous one, by the dimensional expanding method (Wang et al., 2002), to avoid seeking the particular solution.

However there are several drawbacks with the precise time step integration method:

- Computational cost is high due to the multiplication of the system matrix.
- Accuracy will be compromised if the inversion of the amplification matrix is still used.
- Particular solution is less accurate compared to the homogenous solution. Dimension expansion method can be used to avoid seeking the particular solution, however, at a price of increased computational cost.

Weighted residual methods

The weighted residual method is widely used for various problems. As popular for solving the static problems, it is not surprising that this method is also widely-used for various initial-value problems, including structural dynamics. Zienkiewicz and co-authors (1984) re-derived many direct integration methods under the unified SSpj framework using weighted residual method. However, other found the straightforward application of the weighted residual method in the time domain did not offer advantages over existing finite difference methods (Segerlind, 1989). In the 1990's, time-discontinuous Galerkin method was introduced by Hughes and Hulbert for dynamic analysis (Hughes and Hulbert, 1988; Hulbert and Hughes, 1990; Hulbert, 1992; Hughes and Stewart, 1996). In their approach, the temporal and spatial domains are discretised simultaneously forming unstructured meshes to capture discontinuities or sharp changes in the solution. The trial functions for the displacement and velocity, as well as the test function, are allowed to be discontinuous between the "space-time slabs" generated from the simultaneous discretisation. These quantities are then substituted in the Galerkin formulation for finding the solution; additional least-squares term may be incorporated to enhance the stability. The algorithm thus obtained is unconditionally stable and third-order accurate for linear elastodynamics problems. However, the scheme is asymptotic annihilating thus too dissipative in the high-frequency range.

It is desired that the numerical schemes to be unconditionally stable, high order of accuracy and with adjustable numerical dissipation. Many weighted residual based methods can only have up to second-order accuracy if unconditional stability is guaranteed, and they are either non-dissipative at all or over-dissipative at the high-frequency end. This issue was successfully solved by Fung in a series of works. In the work of Fan and Fung (1997a,b), a general framework was proposed to offer algorithms with those desired properties. The equation of motion was transformed into first-order form, and the Lagrange finite elements were used for the trial and test functions. The trial functions were interpolated

through one more node than that of the test functions in order to keep the number of the unknowns equal to the number of equations after the incorporation of the initial conditions. This algorithm is unconditionally stable and up to fourth-order accurate. In addition, the dissipation is fully controllable with an algorithmic parameter. The time-continuous Galerkin methods (such as SS*pj* algorithms) and the time-discontinuous Galerkin method can be unified into this framework.

Another weighted residual based method called the weighting parameter method was proposed by Fung later on for the same purpose. The cubic Hermite time element was employed for the time approximation of the displacement (Fung, 1996). The residual of the governing equation was then weighted by two weighting functions. However these weighting functions were not specified in the first place, rather, four weighting parameters were introduced to solve the weighted equation. The weighting parameters used were the time integration of the inner product of the weighting functions with the trial functions, which also controlled the algorithmic characteristics, such as accuracy and dissipation. The weighted parameters were obtained by comparing the numerical solution with the analytical solution and eliminating the leading term of the truncated error. Two families of algorithms were derived. One posses the third-order accuracy and is asymptotically annihilating; the other posses the fourth-order accuracy and has no numerical dissipation at all. Unconditional stability is achievable for both families. A similar treatment was used by Golley (1999) where eight undetermined parameters were used in his scheme. These parameters were selected subsequently with the aim to minimise errors, guarantee unconditional stability and improve numerical efficiency. The numerical dissipation is fully controllable in this treatment.

The weighting parameter method was further developed recently. Fung (1999a,b) used weighting parameters instead of weighting functions in the recurrence formulation, the undetermined values at the end of time step were related to the initial values through the weighting parameter matrix. The weighting parameters

were so selected that the Padé approximation (or the generalized Padé approximation) of the exponential function in the analytical solution of the original equation was re-produced. Once the weighting parameters were determined the end value could then be worked out. It leads to an unconditionally stable algorithm of at least *n*th-order accurate with controllable dissipation (n is the number of the undetermined coefficients in the displacement approximation). However, additional weighting parameters might be required to maintain the accuracy of the algorithm under certain circumstances. The displacement approximation can also be related to the Taylor expansion of the exact solution to predetermine some of the coefficients (Fung, 2000a, 2003c). The order of accuracy of the unconditionally stable method was increased to $2n$. In another two papers by Fung (2003a,b), the initial and final displacement and velocity were weakly enforced at the beginning and the end of the time step, the accuracy was further improved to $2n+3$. This treatment also provided a unified framework for various continuous, time-discontinuous and bi-discontinuous Galerkin schemes.

A new time-continuous Galerkin method was proposed recently by Idesman (2007). This method offers the improved accuracy and reduction in computation time compared to the standard time-continuous Galerkin methods. The trial functions and test functions were in the form of power series for the displacement and velocity fields. Additional weighting scalar functions were utilised to provide additional numerical dissipation. The unknown quantities at the end of the time step can be attained by a direct solver or a predictor/ multi-corrector procedure. The method is unconditionally stable and the numerical dissipation is controllable. Idesman also presented a strategy to combine small/null and large numerical dissipation methods for the treatment of the spurious oscillations encountered in problems such as wave propagations.

In general this category of method produces highly accurate results, although there might be additional costs, such as additional weighting parameters or stabilizing functions are required to solve the solution accurately.

Collocation methods

The concept of the collocation method is very easy to understand - it requires the governing equation to be satisfied at the specified time nodes thus the unknown coefficients in the field approximation can be determined, and consequently the displacement/ velocity at the end of the time step can be worked out subsequently. The Wilson-θ method is a typical example of the collocation method. Simple it may seem, yet this method is capable of producing high precision results if suitable collocation points are used, thus the choice of the collocation points is crucial.

Golley (1996) presented a fourth-order accurate algorithm in which a cubic approximation of the displacement was used and two Gauss points were chosen as the collocation points, however the algorithm is only conditionally stable. Fung (2000b) proposed an unconditionally stable high-order collocation method whose order of accuracy is controllable. The concept of weighted parameter is used again there and the collocation points are given by the roots of a polynomial in terms of the ultimate amplification factor, which in turn is adjustable.

The combination of weighted residual and point collocation method was utilised by Wang and Au (2004), leading to an unconditionally stable high-order algorithm. A fifth-order time finite element was employed to approximate the displacement field with the displacements, velocities and accelerations at both ends of the time step, one of the two collocation points was chosen with a θ parameter as used in the Wilson-θ method while the other at the end of the time step. In addition, the weighted residual was required to vanish within the time step where another parameter was introduced. These parameters influence the algorithmic accuracy, stability and dissipation. The dissipation can be adjusted with several parameters. The procedure is less straightforward than other weighted residual methods.

Rostami et al. (2012) chose the equally-spaced points within the time step as the collocation points, in combination with the quartic B-spline approximation of the displacement field, to construct a conditionally stable scheme.

Differential quadrature method

The differential quadrature method was initially proposed by Bellman and Casti (1971), and introduced by Fang et al. (1999) for structural dynamic problems. Later, a more general application of this technique was utilised in combination with the point collocation method by Fung for initial value problems of various orders (Fung, 2001a, 2001c). The key tool used in this method is to approximate the time derivatives of a target function with the weighted function values at distinct sampling points within the time interval. Initial values can be incorporated explicitly during the process. The approximated quantities are then substituted into the governing equation directly, leading to a set of algebraic equations in terms of the function values at all sampling points. Once these values are solved for, the end value is then obtained by the Lagrange interpolation. The accuracy and the stability of the scheme depend on the selection of the n sampling points. In general, the scheme is at least nth-order accurate, and the order of accuracy can be further improved to $2n-1$ or $2n$ for the end values of the time step if the sampling points are chosen as the roots of a polynomial in terms of a dissipation parameter. The given scheme is unconditionally stable with controllable dissipation. This method was also shown to be equivalent to the implicit Runge-Kutta collocation method (Fung, 2002b). The method is shown to be applicable to nonlinear problems as well (Liu and Wang, 2008).

Variational methods

In additional to the methods reviewed as above, variational methods have also been applied to dynamic problems. In fact, this type of method is also the earliest method applied to the dynamic problems. Typical examples can be found in (Courant, 1943; Gurtin, 1963; Argyris and Scharpf, 1969; Levinson, 1976). Informations such as the governing equation and the initial conditions can be

derived by finding the stationarity of a variational statement. In fact, the governing equation even needs not to be used to solve the problem. It is often found that variational methods offer several significant advantages, such as the expediency of manipulation; ease of incorporation of constraints and boundary conditions; free choice of reference system (Courant, 1943; Lanczos, 1970). Particularly, for time-dependent problems, variational methods may offer solutions directly without any knowledge of solving the partial differential equation involved (Bailey, 1976), thus this type of method is also very appealing. There are several variational principles/ laws for dynamic problems, including Hamilton's Law of Varying Action, Hamilton's Weak Principle, Gurtin's Principle and its simplified variants.

Recently a novel type of variational principle, so-called Unconventional Hamilton-type Variational Principle (Luo et al., 2003), has been proposed and applied to various initial-value problems. Satisfactory results are obtained (Huang et al., 2006; Jiang and Luo, 2008; Li and Luo, 2007; Luo et al., 2006). This type of principle has a solid mathematical foundation and takes full account of the characteristics of dynamic systems, which is not fully satisfied by other variational principles/ laws. In addition, it embraces several existing variational principles and laws. Therefore it is of interest to explore this principle to construct a new method for the dynamic analysis of truss-type structures.

2.4 Summary

In this chapter, existing analysis methods for truss-type structures and various recently developed methods for linear structural dynamics in general are reviewed. Modal decomposition method can be used to find analytical homogeneous solutions. However, it is generally difficult to solve the associated eigenproblem for large systems in the first place. Meanwhile, the forced vibration has to be calculated with either the expensive Duhamel integration method or various force approximation techniques at a price of compromised accuracy. Various direct

integration methods are among those popular methods in use. However, the accuracy for many well-known schemes is limited to second-order if unconditionally stable solutions are desired. In addition, the numerical damping is normally not adjustable. The family of precise time integration methods can achieve high precision numerical results by calculating the amplification matrix with nominal errors. Several variants of this method and the associated advantages and drawbacks are reviewed. Weighted residual method is another popular type of method. Several higher-order and unconditionally stable algorithms with controllable dissipation were proposed recently, although additional computational cost might be incurred. Collocation method can produce highly accurate results however the choice of the collocation points is crucial.

Various variational principles and laws have also been used and offer several advantages for the dynamic problem. The recently proposed Unconventional Hamilton-type Variational Principles (UHVP) has a solid mathematical foundation and takes full account of the characteristics of dynamic systems. This variational principle is used to underpin the proposed analysis method in this research.

Chapter 3 Variational Methods for Initial-value Problems

3.1 Introduction

Problems of structural dynamics belong to the category of initial-value problem, therefore, the existing variational methods for this category in general are reviewed in this chapter to provide a general introduction on available approaches. Variational principles and statements for elastodynamic problems are of primary interest. Firstly, the unfitness of the well-known Hamilton's Principle for initial-value problems is examined, followed by the review of Gurtin type principles and some simplified variants. However, the derivation of Gurtin type principles is quite cumbersome, and the resultant algorithms are computationally expensive due to the convolution operation employed. Variational approaches without the convolution operator are examined next with particular emphasis on Hamilton's Law of Varying Action and its variations. In the final part of this chapter, a novel type of variational principle called Unconventional Hamilton-type Variational Principles is reviewed. This type of principle not only contains all necessary relations and conditions for initial-value problems, but also embraces some established variational laws and principles, such as Hamilton's Law of Varying Action and others.

3.2 Preliminary

Let an arbitrary volume V be enclosed by its boundary S, which in turn can be divided into two complementary disjoint subsets S_σ and S_u. A traction is prescribed on S_σ, denoted as $\overline{T}$. The displacement is prescribed on S_u, denoted as $\overline{u}$. S_σ and S_u satisfy

$$S = S_\sigma \bigcup S_u \text{ and } S_\sigma \bigcap S_u = 0 \tag{3.2.1}$$

$\boldsymbol{n} = (n_1, n_2, n_3)$ is the outward pointing normal to the boundary.

3.3 Variational methods for initial-value problems

Analytical mechanics, or the variational approach of mechanics, examines two scalar quantities, the "kinetic energy" and the "potential energy" of the studied system, and seeks the solution from the point of view of energy. Originated by Leibniz, and further developed by Euler, Lagrange and Hamilton, as well as many modern scholars, this subject becomes an indispensable foundation for mechanics.

Hamilton's principle is one of the best-known variational principles, and indeed this principle was adopted in the early years for structural dynamics (Argyris & Scharpf, 1969). It is not difficult to find that this principle is still referred to in current textbooks (for example the classical one by Tedesco (1999)) and papers (Heppler et al., 2003, Grossi and Albaracin, 2007). However, Hamilton's principle does not satisfy the pre-conditions for initial-value problems and is hence not really suitable for this type of problem, including structural dynamics. The reason is discussed as below.

3.3.1 The unfitness of Hamilton's principle for initial-value problems

Hamilton (1834, 1835) presented a variational approach for the determination of the motion of objects. However, his philosophy was somehow mis-interpreted in the historical development of the analytical mechanics, and what is now called "Hamilton's Principle" is actually not what Hamilton promoted in his original work (Bailey, 1975a).

Being a "constrained variational principle" (Chen, 1990), Hamilton's principle is suitable for boundary-value problems, where the unknown field attains pre-determined values at the lower and upper temporal boundaries thus the variation of the functional vanishes at both boundaries. It is easy to see that this is not the case for initial-value problems since the value at the upper boundary is not known at all. Many researchers have pointed out the flaws using this principle for initial-value problems (Gurtin, 1964a; Tiersten, 1968; Tonti, 1973; Reddy, 1976; Simkins, 1981):

1) The first order derivative operator ($\partial/\partial t$) used in the initial-value problems are not self-adjoint with respect to the following operator used in Hamilton's principle.

$$\langle u_1, u_2 \rangle = \int_V \int_{t_0}^{t_1} \left\{ u_1(x,t)\, u_2(x,t) \right\} dt dV \tag{3.3.1}$$

2) Incorrect zero velocity / momentum condition would arise at the upper temporal boundary.

3) Initial conditions of the problems are not included in Hamilton's principles

4) Spatial boundary conditions need to be imposed as constraints.

The first and the fourth points are quite straightforward, and the second and third points may be illustrated as follows.

Let $T = \frac{1}{2} m\dot{u}\dot{u}$ and $V = \frac{1}{2} kuu$ denote the kinetic energy and the potential energy of a single mass-spring system, respectively. f is a conservative force. With Hamilton's principle one has

$$\delta\int_{t_0}^{t_1}(\mathrm{T}-\mathrm{V})dt+\delta\int_{t_0}^{t_1}(f\,\mathrm{u})dt=0 \tag{3.3.2a}$$

or

$$\delta\int_{t_0}^{t_1}\left(\frac{1}{2}m\dot{u}\dot{u}-\frac{1}{2}kuu\right)dt+\delta\int_{t_0}^{t_1}(f\,\mathrm{u})dt=0 \tag{3.3.2b}$$

Performing the variation operation and integrating the kinetic energy term by part gives

$$\int_{t_0}^{t_1}(-m\ddot{u}-ku+f)\delta\,\mathrm{u}\,dt+m\dot{u}\delta\,\mathrm{u}\Big|_{t=t_0}^{t=t_1}=0 \tag{3.3.3}$$

Satisfaction of Eq. (3.3.3) hints that in addition to the control equation

$$-m\ddot{u}-ku+f=0 \tag{3.3.4}$$

another condition arises, viz.

$$m\dot{u}\delta\,\mathrm{u}\Big|_{t=t_0}^{t=t_1}=0 \tag{3.3.5}$$

It should be noted that one of the trailing terms $m\dot{u}\delta\,\mathrm{u}\Big|_{t=t_0}$ vanishes due to $\delta\,\mathrm{u}\Big|_{t=t_0}=0$ for the given initial displacement in the variational context, therefore Eq. (3.3.5) becomes

$$m\dot{u}\delta\,\mathrm{u}\Big|^{t=t_1}=0 \tag{3.3.6}$$

Eq. (3.3.6) implies the velocity $\dot{u}$ (or the momentum $m\dot{u}$) at the instant t_1 has to equal to zero since the variation of the displacement $\delta \mathrm{u}$ does not necessarily vanish at the upper temporal boundary. This postulation, however, is obviously at fault. It is also clear that the initial conditions, i.e., the initial displacement and initial velocity, are not included in either Eqs. (3.3.2) or (3.3.3).

As pointed out by Tonti (1973), methods based on Hamilton's principle ignore the initial conditions for the first time derivatives of the unknown variables at the lower temporal boundary; and insert various artificial conditions at the upper temporal boundary, transforming the initial-value problem into a boundary-value problem. However, this boundary-value problem is not equivalent to the original initial-value problem and does not in general give the same solution. The only benefit of this transformation is that the control equation found with the transformed boundary-value problem is the differential equations of the original initial-value problem.

3.3.2 Gurtin's variational principles

The breakthrough came when Gurtin (1963, 1964a, 1964b) introduced a novel type of variational principles for linear initial-value problems. Gurtin transformed the original problem to an equivalent boundary-value problem containing the governing equations and the initial conditions implicitly, by using a convolution operator in the following bilinear form.

$$u_1 * u_2(x,t) = \int_0^t \{u_1(x,t-\tau)u_2(x,\tau)\}d\tau \tag{3.3.7}$$

Gurtin gave a general variational principle with the displacement u, the strain tensor e and the stress tensor τ as the independent variables. In the principle, a functional, which can be regarded as "a function of functions" was used to

incorporate the relationships of these variable fields for the dynamic problem. The functional given by Gurtin was $\Lambda(\mathbf{u},\mathbf{e},\boldsymbol{\tau})$ as the following

$$\begin{aligned}\Lambda(\mathbf{u},\mathbf{e},\boldsymbol{\tau}) = &\frac{1}{2}\int_V c_{ijkl}(x)\left[t * e_{ij} * e_{kl}\right](x,t)\,dx + \frac{1}{2}\int_V \rho(x)\left[u_i * u_i\right](x,t)\,dx \\ &- \int_V \left[t * \tau_{ij} * e_{ij}\right](x,t)\,dx - \int_V \left[\left(t * \tau_{ij,j} + f_i\right) * u_i\right](x,t)\,dx \\ &+ \int_{S_u}\left[t * T_i * \overline{u}_i\right](x,t)\,dx + \int_{S_\sigma}\left[t * \left(T_i - \overline{T}_i\right) * u_i\right](x,t)\,dx\end{aligned} \tag{3.3.8}$$

Taking variation of $\Lambda(\mathbf{u},\mathbf{e},\boldsymbol{\tau})$ and making it to vanish will lead to a set of admissible fields satisfying the governing equation, strain-displacement relation, the stress-strain relation as well as the initial conditions and boundary conditions simultaneously. Several more principles were also given by Gurtin, in which different relations and boundary conditions were met in the selection of the variable set. When the variations of the functionals are made to vanish, the governing equation, the initial condition and the rest of boundary conditions will be obtained.

Gurtin's method uses Laplace transform and inverse Laplace transform. Reddy(1976) argued additional errors would be introduced in these transforms. However Gurtin's method is a great achievement in developing variational principles for initial-value problems, and many have been inspired to find more variational principles in this approach (Wilson and Nickell, 1966, Nickell and Sackman, 1968, Sandhu and Pister, 1970, Tonti, 1973, Herrera and Bielak, 1974, Reddy, 1976, Gellert, 1978, Bhutani and Gupta, 1982, Luo and Cheung, 1988, Peng et al., 1996). Indeed, the convolution technique is still applied in recent dynamic algorithms (Soares Jr, 2011, Panagiotopoulos and Manolis, 2011).

Tonti (1973) pointed out the Laplace transform and the inverse-Laplace transform were not actually necessary for finding the equivalent control equations. He demonstrated a method to obtain directly the integro-differential equations given

by Gurtin. Further, Tonti highlighted that initial-value problem in the original differential equation form could be deduced directly from the stationarity of suitable functionals.

Reddy (1976) presented a modified Gurtin-type variational principle for viscoelasticity problems, also using the convolution bilinear operator. The resulting control equations are in the original differential equation form, not as the one in Gurtin's integro-differential form. The underpinning theory for Reddy's procedure is a theorem proven by Vainberg et. al.(1964). This theorem states that, if an operator $N(\ )$ is of potential, then a functional $J(u)$ can be found as

$$J(u) = J(u_0) + \int_{u_0}^{u} \langle N(u), du \rangle \tag{3.3.9a}$$

Where

$$\langle u_1, u_2 \rangle = \int_V \int_0^{t_0} \left[u_1(x,t) u_2(x,t) \right] dt dx \tag{3.3.9b}$$

Reddy casted the control equations for linear viscoelastic problems into an operator form, including:

- Strain-displacement relation
- Equation of motion
- Stress-strain relations
- Displacement and traction boundary conditions
- Displacement and velocity initial conditions

By utilising Vainberg's theorem, a functional can be found whose stationarity leads to the solution of the linear viscoelastic problem. The functional given is

$$
\begin{aligned}
J = {} & \frac{1}{2}\left[\rho\dot{u}_m, \dot{u}_m\right] + \left[\sigma^{ij}, \frac{1}{2}\left(u_{i,j} + u_{j,i}\right) - \gamma_{ij}\right] - \left[\rho f_m, u_m\right] \\
& + \frac{1}{2}\left[\dot{G}^{ijkl} * \gamma_{kl} + E^{ijkl}\gamma_{kl}, \gamma_{ij}\right] - \left[T^m, u_m - \bar{u}_m\right]_{S_u} \\
& - \left[\bar{T}^m, u_m\right]_{S_\sigma} + \left[\rho\left(\dot{u}_m - v_m\right), u_m\right]_0 - \frac{1}{2}\left[\rho\left(u_m - 2d_m\right), \dot{u}_m\right]_0
\end{aligned}
\tag{3.3.10}
$$

in which

$$a * b = \int_0^t a(x,\tau)\, b(x, t-\tau)\, d\tau$$

$$\left[a, b\right] = \int_V \int_0^t a(x,\tau)\, b(x, t-\tau)\, dx\, d\tau$$

$$\left[a, b\right]_S = \int_S \int_0^t a(x,\tau)\, b(x, t-\tau)\, dS\, d\tau$$

$$\left[a, b\right]_0 = \int_V \left\{a(x,\tau)\, b(x, t-\tau)\right\}\Big|_{\tau=0}^{t} dx$$

It is noticeable that various authors, Gurtin (1964a), Sandhu and Pister (1970) and Reddy (1976) all demonstrated the feasibility of generating particular variational functionals from a general one, by allowing certain boundary conditions to be met at the outset. In Gurtin's work (1964a), for example, the functional given in Eq. (3.3.8) can be reduced to

$$
\begin{aligned}
\Phi(\mathbf{u}, \mathbf{e}, \boldsymbol{\tau}) = {} & \frac{1}{2}\int_V \rho(x)\left[u_i * u_i\right](x,t)\, dx + \frac{1}{2}\int_V \left[t * \tau_{ij} * e_{ij}\right](x,t)\, dx \\
& - \int_V \left[f_i * u_i\right](x,t)\, dx - \int_{S_\sigma} \left[t * \bar{T}_i * u_i\right](x,t)\, dx
\end{aligned}
\tag{3.3.11}
$$

when the strain-displacement relations $e_{ij} = \frac{1}{2}\left(u_{i,j} + u_{j,i}\right)$, the stress-strain relations $\tau_{ij} = c_{ijkl} e_{kl}$ and the boundary conditions $u_i = \hat{u}_i$ are admitted in the selection of the set of variables $\mathbf{u}$, $\mathbf{e}$ and $\boldsymbol{\tau}$.

However the drawback with these functionals given by Gurtin, Sandhu and Pister, Reddy as well as Herrera and Bielak (1974) is that they all contain double convolution operations in the form $u_1 * u_2 * u_3$, which makes the computations rather cumbersome and expensive.

3.3.3 Variational formulations without convolution operator

To avoid the convolution computation and construct more straightforward variational formulations, other treatments have been explored by many researchers. One effort was made by Tiersten (1968) to introduce the boundary and initial conditions into the variational statements with the aid of Lagrange multipliers. However, while boundary conditions were built into the variational statement via Lagrange multipliers, the initial conditions were introduced with the weighting terms, not Lagrange multipliers, thus his method is a mixed method. Inspired by Tiersten's work, Simkins (1978) used purely Lagrange multipliers and constructed variational statements containing the governing equation, boundary conditions, as well as the initial conditions naturally. The trial solution hence can be chosen freely.

From the equation of motion,

$$\frac{\partial U}{\partial u_k} + \rho \ddot{u}_k - \sigma_{lk,l} = 0 \tag{3.3.12}$$

where U is the potential energy of the system, σ_{lk} the stress tensor.

Along with the boundary conditions

$$u_k - \overline{u}_k = 0 \qquad \text{on } S_u \tag{3.3.13a}$$

$$\overline{F}_k - n_l \sigma_{lk} = 0 \quad \text{on } S_\sigma \tag{3.3.13b}$$

and the initial conditions (the barred quantities are the given initial values)

$$u_k(t_0)-\bar{u}_k(t_0)=0, \qquad \dot{u}_k(t_0)-\bar{v}_k(t_0)=0 \tag{3.3.14}$$

A variational formulation can be constructed

$$\begin{aligned}&\int_{t_0}^{t_1}\int_V\left(\frac{\partial U}{\partial u_k}+\rho\ddot{u}_k-\sigma_{lk,l}\right)\delta u_k dVdt+\int_{t_0}^{t_1}\int_{S_\sigma}\left(\bar{F}_k-n_l\sigma_{lk}\right)\delta\lambda_k^{(1)}dVdt\\&+\int_{t_0}^{t_1}\int_{S_u}\left(u_k-\bar{u}_k\right)\delta\lambda_k^{(2)}dVdt+\int_V\left[u_k(t_0)-\bar{u}_k(t_0)\right]\delta\lambda_k^{(3)}dV\\&+\int_V\left[\dot{u}_k(t_0)-\bar{v}_k(t_0)\right]\delta\lambda_k^{(4)}dV=0\end{aligned} \tag{3.3.15}$$

The Lagrange multipliers, $\delta\lambda_k^{(i)}$ $(i=1,2,3,4)$, can be determined by the elimination of redundant boundary conditions, after applying the divergence theorem and integration by parts to Eq. (3.3.15) for several times. However, as Simkins admitted, “the identification of which boundary terms are to be eliminated does not always proceed from obvious physical consideration”. Smith (1979) questions Simkins’ method is not a variational method but a weighted residual method in nature, because there is no functional and “therefore nothing to vary”. In his response, Simkins (1979) highlights the distinct difference between a weighted residual method and a variational method – while the analyst makes the choice of weighting functions and determines how the residual is weighted in the former method, “the physical law or balance make the choices automatically” in the latter.

Chen (1990) presented a procedure to obtain an unconstrained variational statement for dynamic problems, by virtue of the so-called Principle of Total Virtual Action. According to Chen, the total virtual action of a system consists five individual parts.

The first part is the basic virtual action of system integrated over the space –time domain $V\times[t_0,t_1]$.

$$\delta A_H=\delta\int_{t_0}^{t_1}\int_V L\,dV\,dt \tag{3.3.16}$$

where $L=\frac{1}{2}\rho\dot{u}_i\dot{u}_i-\frac{1}{2}C_{ijkl}u_{i,j}u_{k,l}$ is the Lagrange density of the system.

The second part is the virtual action contributed by the prescribed body force f_i,

$$\delta A_b=\delta\int_{t_0}^{t_1}\int_V f_i u_i\,dV\,dt \tag{3.3.17}$$

The third part is due to the surface force T_i over the boundary, $S\times[t_0,t_1]$

$$\delta A_S=\delta\int_{t_0}^{t_1}\int_{S_\sigma}\overline{T}_i u_i\,ds\,dt+\delta\int_{t_0}^{t_1}\int_{S_u}T_i\left(u_i-\overline{u}_i\right)ds\,dt \tag{3.3.18}$$

The fourth part is the change of the action at the temporal boundaries t_0 and t_1

$$\begin{aligned}\delta A_t=&\left\{\delta\int_V\left\{P_i-\rho\left[\dot{u}_i\left(t_0\right)-\overline{v}_i^{(0)}\right]\right\}\left[u_i-\overline{u}_i^{(0)}\right]d\Omega\right\}_{t=t_0}\\&-\left\{\delta\int_V\left\{P_i-\rho\left[\dot{u}_i\left(t_1\right)-\overline{v}_i^{(1)}\right]\right\}\left[u_i-\overline{u}_i^{(1)}\right]d\Omega\right\}_{t=t_1}\end{aligned} \tag{3.3.19}$$

in which P_i is the "density of generalised momentum over V"; $\overline{u}_i^{(0)}$ and $\overline{v}_i^{(0)}$ are the given initial displacement and velocity. $\overline{u}_i^{(1)}$ and $\overline{v}_i^{(1)}$ are the counterparts at the upper time boundary. The quantity $\rho\left[\dot{u}_i\left(t_0\right)-\overline{v}_i^{(0)}\right]$ is an impulse required for the jump of velocity at t_j in case $\dot{u}_i\left(t_j\right)\neq\overline{v}_i^{(j)}$.

The fifth part is needed for cases where discontinuity in time occurs, the contribution of the impulse $\overline{P}_i$ at the instance t^* ($t_0 < t^* < t_1$) is

$$\delta A_P = \int_V \overline{P}_i \delta u_i \left(t^*\right) dV \tag{3.3.20}$$

Adding up all five parts one has

$$\delta A_T = \delta A_H + \delta A_b + \delta A_S + \delta A_t + \delta A_P \tag{3.3.21}$$

Vanishing of the total virtual action δA_T will give the satisfaction of the motion equation and boundary conditions as well as the initial conditions, as expressed in Eqs. (3.3.13) to (3.3.14). In addition, the relation between the momentum and the velocity are also satisfied at both temporal termini.

3.3.4 Hamilton's Law of Varying Action

Parallel to various approaches to construct aforementioned variational formulations, different treatments to the boundary variations have also been explored. In a paper published by Pian and O'Brien (Geradin 1974) an "extended form" of Hamilton's principle was used.

$$\int_{t_0}^{t_1} \left(\delta T - \delta U + \delta Q\right) dt = \int_V \left(m\dot{u}\delta u\right) dV \Big|_{t_0}^{t_1} \tag{3.3.22}$$

It is found that the theory underpinning this equation was later on named as "Hamilton's Law of Varying Action".

Classical form of Hamilton's Law of Varying Action

Bailey reviewed the original work of Hamilton (1834, 1835) and examined the philosophy and concepts regarding Hamilton's Principle in the literature. He highlighted that the theory presented in Hamilton's work was actually not what has been known as Hamilton's Principle (1975a, 1975b, 1976), and the significance of the original work was far beyond Hamilton's Principle. Bailey referred Hamilton's theory as Hamilton's Law of Varying Action (HLVA), – taken from Hamilton's own words, "*Law of Varying Action*" (Hamilton, 1834). For stationary systems, Hamilton's Principle can be derived from this law and has been successfully applied to boundary-value problems. Nevertheless, as Bailey pointed out, Hamilton's Principle has also long been mis-applied to non-stationary systems but failed to produce direct solutions.

By "stationary", the system is supposed to satisfy the following condition:

$$\left[\frac{\partial \mathrm{T}}{\partial \dot{\mathrm{u}}_i}\delta \mathrm{u}_i\right]\Big|_{t=t_0}^{t=t_1} = 0 \tag{3.3.23}$$

Hamilton's Law of Varying Action states (Bailey, 1975a)

$$\delta\int_{t_0}^{t_1}\left(\mathrm{T}+\mathrm{W}\right)dt - \left[\frac{\partial \mathrm{T}}{\partial \dot{\mathrm{u}}_i}\delta \mathrm{u}_i\right]\Big|_{t=t_0}^{t=t_1} = 0 \tag{3.3.24}$$

T is the kinetic energy of the system; W is the work done by the conservative and non-conservative forces, although some argues that there is no such functional for non-conservative forces since their work are "path dependent" (Smith and Smith, 1977, Smith, 1977).

Obviously, when the system is stationary, HLVA is reduced to Hamilton's Principle as

$$\delta\int_{t_0}^{t_1}\left(\mathrm{T}+\mathrm{W}\right)dt=0 \tag{3.3.25}$$

However, in contrast to the requirements of vanishing of variations at time extremities imposed on Hamilton's Principle, $\delta \mathrm{u}_i\big|_{t=t_0}=\delta \mathrm{u}_i\big|^{t=t_1}=0$, HLVA places no such restrictions by introducing the negative of these trailing terms in the equation, thus more general approximating functions are allowed in HLVA. The historical development of HLVA and Hamilton's Principle was reviewed in the paper named "A New Look at Hamilton's Principle" (Bailey, 1975a) . There had been a debate on variations of the trailing terms, with Smith and Smith on one side while Bailey on the other. Bailey (1975a) suggests, while $\delta \mathrm{u}_i$ and $\delta \dot{\mathrm{u}}_i$ vanish at the instant $t=0$ due to the fact u_i and $\dot{\mathrm{u}}_i$ are the known initial conditions, *"it is impossible, unless the answer is known in advance, to choose* t_1 *to be that instant in time at which* $\left(\partial T\big/\partial \dot{q}_i\right)\delta q_i=0$*"*. This point of view was presented in a series of his work published in the 1970's and stressed again in his later work within the context of calculus of variations (Bailey, 1987). There is no need for any artificial postulations for the variations of boundary terms, simply because they are cancelled off when the variation of the kinetic energy is taken by part, with only the motion equation remaining.

$$\begin{aligned}&\left[\frac{\partial \mathrm{T}}{\partial \dot{\mathrm{u}}_i}\delta \mathrm{u}_i\right]\Big|_{t=t_0}^{t=t_1}+\int_{t_0}^{t_1}\left(-\frac{d}{dt}\frac{\partial \mathrm{T}}{\partial \dot{\mathrm{u}}_i}+\frac{\partial \mathrm{T}}{\partial \mathrm{u}_i}+\mathrm{Q}_i\right)\delta \mathrm{u}_i\,dt-\left[\frac{\partial \mathrm{T}}{\partial \dot{\mathrm{u}}_i}\delta \mathrm{u}_i\right]\Big|_{t=t_0}^{t=t_1}\\&=\int_{t_0}^{t_1}\left(-\frac{d}{dt}\frac{\partial \mathrm{T}}{\partial \dot{\mathrm{u}}_i}+\frac{\partial \mathrm{T}}{\partial \mathrm{u}_i}+\mathrm{Q}_i\right)\delta \mathrm{u}_i\,dt=0\end{aligned} \tag{3.3.26}$$

In Bailey's work, the direct solution is obtained when the displacement field approximated with a power series and the initial conditions, is substituted into Eq. (3.3.24). The trial function is in the form

$$\mathrm{u}_i = \mathrm{u}_{i0} + \dot{\mathrm{u}}_{i0}\, t_1 \tau + \sum_{j=2}^{N} A_{ij} \tau^j \qquad \left(\tau = t \big/ t_1 \right) \tag{3.3.27}$$

where u_{i0} and $\dot{\mathrm{u}}_{i0}$ are the initial displacement and velocity, respectively. A_{ij} are the coefficients to be solved for by the satisfaction of Eq. (3.3.24). $\tau \in [0,1]$ is a dimensionless time. The approximated solution converges to the exact one when the number of terms N is increased. When the problem at hand is simple enough, and N is big enough, the solution obtained is the analytical one. However, as some recent research has pointed out that Bailey's approach may result in ill-conditioned equations when N is increased (Sheng, 1998a). In addition, Bailey's algorithm is only conditionally stable (Fung, 2003d).

Other forms of Hamilton's Law of Varying Action

Baruch and Riff (1982) argue that in addition to the two treatments of temporal boundary variations presented in the work of Bailey and Smith and Smith, there are another four possible combinations of boundary variations, resulting six "correct formulations" for initial-value problems. They suggest that any combination of the displacement and velocity at any arbitrary instant may be used as "initial values" for the problem at hand, because "the physical solution of a given dynamic problem exists and it is unique". The displacement trial functions, and consequently the velocity trial function, are different for each formulation, in order to allow for different vanishing boundary variations. The variations were constructed from the same set used for the trial functions, in the classical variational manner. Each of these six formulations was deemed "correct". These six formulations can be summarised briefly as the following.

Formulation 1

$$\begin{aligned} &\delta \int_{t_0}^{t_1} (T - V)\, dt + \int_{t_0}^{t_1} f\, \delta u dt - \frac{\partial T}{\partial \dot{u}(t_1)} \delta u(t_1) = 0 \\ &\delta u(t_0) = 0; \delta \dot{u}(t_0) = 0 \end{aligned} \tag{3.3.28a}$$

This formulation is of HLVA form used by Bailey, the variations of initial displacement and velocity vanish.

Formulation 2

$$\begin{aligned}&\delta\int_{t_0}^{t_1}(T-V)\,dt+\int_{t_0}^{t_1} f\,\delta u dt=0\\&\delta u(t_0)=0;\delta u(t_1)=0\end{aligned}\tag{3.3.28b}$$

This formulation is the classical form of Hamilton's Principle, when the force f is conservative.

Formulation 3

$$\delta\int_{t_0}^{t_1}(T-V)\,dt+\int_{t_0}^{t_1} f\,\delta u dt-\left[\frac{\partial \mathrm{T}}{\partial \dot{\mathrm{u}}}\delta \mathrm{u}\right]\Big|_{\substack{t=t_1\\t=t_0}}=0\tag{3.3.28c}$$

This formulation is of the classical form of HLVA, combined with the vanishing boundary variations

$$\delta\dot{u}(t_0)=0;\delta\dot{u}(t_1)=0$$

Formulation 4

$$\begin{aligned}&\delta\int_{t_0}^{t_1}(T-V)\,dt+\int_{t_0}^{t_1} f\,\delta u dt+\frac{\partial T}{\partial\dot{u}(t_0)}\delta u(t_0)=0\\&\delta u(t_1)=0;\delta\dot{u}(t_1)=0\end{aligned}\tag{3.3.28d}$$

Formulation 5

$$\begin{aligned}&\delta\int_{t_0}^{t_1}(T-V)\,dt+\int_{t_0}^{t_1} f\,\delta u dt-\frac{\partial T}{\partial\dot{u}(t_1)}\delta u(t_1)=0\\&\delta u(t_0)=0;\delta\dot{u}(t_1)=0\end{aligned}\tag{3.3.28e}$$

Formulation 6

$$\delta\int_{t_0}^{t_1}(T-V)\,dt+\int_{t_0}^{t_1} f\,\delta u dt+\frac{\partial T}{\partial \dot{u}(t_0)}\delta u(t_0)=0 \qquad \delta\dot{u}(t_0)=0;\delta u(t_1)=0 \tag{3.3.28f}$$

The vanishing temporal boundary variations can be presented in pairs in the following figure.

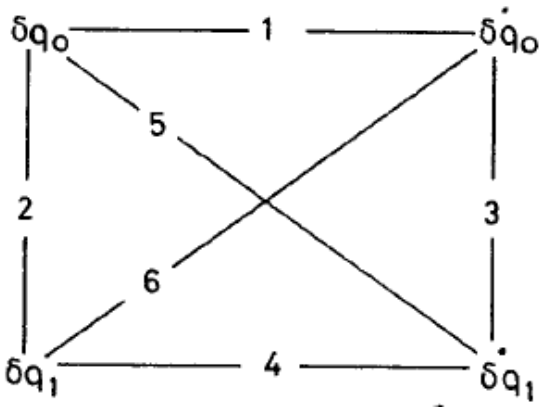

Figure 3.3.1 – Combinations of vanishing variations (Baruch and Riff, 1982)

The drawbacks with Baruch and Riff's argument are two-fold. Firstly, it is difficult to justify the assumptions made for some of the formulations from the point of view of physics; Secondly, given $6n$ "correct formulations" for a system with n numbers of DOFs, there would exist 6^n sets of simultaneous equations for the problem. Which set(s) of formulations are capable of producing the desired accuracy and how to choose the "right" set are unexplained. Furthermore, as pointed out in the reply of Simkins (1983), there would be more than 6 formulations for a SDOF system with Baruch and Riff's concept, if one treats the variations of any arbitrary instant within the time domain as the initial conditions.

Borri et al. (1985) adopted a two-field formulation of HLVA with the generalised momentum replacing the velocities in the trailing terms. He referred to the principle as "Hamilton's Weak Principle" (HWP),

$$\int_{t_0}^{t_1}\left(\delta L+\delta\bar{L}\right)dt = p\delta \mathrm{u}\Big|_{t=t_0}^{t=t_1} \tag{3.3.29}$$

in which $\delta\bar{L}=\mathrm{f}\,\delta\mathrm{u}$ is the virtual work of the generalised conservative and non-conservative forces. $p=\partial L/\partial\dot{u}$ the generalised momentum. The advantages of adopting the momentum field p rather than the velocity field $\dot{u}$ are two-fold.

Firstly, the velocity-momentum conditions are incorporated in the variational statement as demonstrated in a later paper (Peters and Izadpanah, 1988). If one takes $L=\frac{1}{2}m\dot{u}^2-\frac{1}{2}ku^2$ for an SDOF system, the expansion of Eq. (3.3.29) is

$$\int_{t_0}^{t_1}\left(ku+m\ddot{u}-f\right)\delta u dt+\left[p\left(t_1\right)-m\dot{u}\left(t_1\right)\right]\delta u\left(t_1\right)-\left[p\left(t_0\right)-m\dot{u}\left(t_0\right)\right]\delta u\left(t_0\right) = 0 \tag{3.3.30}$$

Without any constraints on the boundary variations, the satisfaction of Eq. (3.3.30) demands that the control equation in the integrand along with the momentum conditions on the temporal extremities to be met for any possible variations. In the classical form of HLVA, however, these momentum conditions are cancelled off, only the control equation is obtained.

Secondly, it is argued that the quantity $p(t)/m$ should converge more rapidly to the velocity field than the first time derivative of $u(t)$ does, due of the sensitivity of the first time derivative used in the approximation of $\dot{u}(t)$ (Peters and Izadpanah, 1988).

A direct solution is obtained through the HWP combined with a simple assumption on the displacement field (linear interpolation) and velocity field (average value) over the time interval $[t_0,t_1]$ $(\Delta t = t_1 - t_0)$. The corresponding variations are in the context of the classical calculus of variation.

$$u(t) = \left(1 - \frac{t-t_0}{\Delta t}\right) u(t_0) + \frac{t-t_0}{\Delta t} u(t_1) \tag{3.3.31a}$$

$$\dot{u}(t) = \left[u(t_1) - u(t_0)\right] \Big/ \Delta t \tag{3.3.31b}$$

$$\delta u(t) = \left(1 - \frac{t-t_0}{\Delta t}\right) \delta u(t_0) + \frac{t-t_0}{\Delta t} \delta u(t_1) \tag{3.3.31c}$$

$$\delta \dot{u}(t) = \left[\delta u(t_1) - \delta u(t_0)\right] \Big/ \Delta t \tag{3.3.31d}$$

Substitution of Eqs. (3.3.31) into Eq. (3.3.30) yields

$$\frac{m}{\Delta t} u(t_0) - \frac{m}{\Delta t} u(t_1) + \int_{t_0}^{t_1} \left(1 - \frac{t-t_0}{\Delta t}\right) \mathrm{f}(t) dt + p(t_0) = 0 \tag{3.3.32a}$$

$$-\frac{m}{\Delta t} u(t_0) + \frac{m}{\Delta t} u(t_1) + \int_{t_0}^{t_1} \left(\frac{t-t_0}{\Delta t}\right) \mathrm{f}(t) dt - p(t_1) = 0 \tag{3.3.32b}$$

with the aid of $p(t_i) = m\dot{u}(t_i)\,(i = 0,1)$ an explicit recurrence scheme arises immediately

$$u(t_1) = u(t_0) + \dot{u}(t_0)\Delta t + \frac{\Delta t}{m} \int_{t_0}^{t_1} \left(1 - \frac{t-t_0}{\Delta t}\right) \mathrm{f}(t) dt \tag{3.3.33a}$$

$$\dot{u}(t_1) = \dot{u}(t_0) + \frac{1}{m} \int_{t_0}^{t_1} \mathrm{f}(t)\, dt \tag{3.3.33b}$$

Borri et al. (1985) further argued that, while the structure of the scheme being maintained, other interpolation functions could be used for the solution.

A similar variational statement given by Peters and Izadpanah (1988), as a special case of their bilinear formulation for elastodynamics can be given as

$$\delta\int_{t_0}^{t_1}\left(\tfrac{1}{2}Ku^2-\tfrac{1}{2}M\dot{u}^2\right)dt=\int_{t_0}^{t_1}F\delta u dt-P(t_1)\delta u(t_1)+P(t_0)\delta u(t_0) \tag{3.3.34}$$

in which u is the unknown displacement, and K, M, F and P are the stiffness, mass , force and momentum, respectively.

The left-hand side of Eq. (3.3.34) is the negative variation of action, and because

$$\int_{t_0}^{t_1}\left(F\delta u\right)dt=\int_{t_0}^{t_1}\left(\frac{dP}{dt}\delta u\right)dt=\int_{P(t_0)}^{P(t_1)}\left(\delta u\right)dP \tag{3.3.35}$$

it is then not difficult to see the right-hand side of Eq. (3.3.34) can be regarded as the "virtual action" during the time interval and cross the temporal boundaries, with the term of "virtual action" defined as the time integral of the virtual work. Thus, Peters and Izadpah made the observation that the sum of the variation of action and the virtual action must vanish for the time interval $[t_0,t_1]$.

The two authors further point out that, in either HLVA or Hamilton's Principle based formulations, the velocity natural conditions are absent, therefore velocity constraints are required for the approximating solution u, implying the displacement field has to be C^1 class functions rather than more general C^0 class ones.

Sheng et al. (1998a, 1998b) summarised the work of Bailey, Baruch and Riff, Simkins as well as Wu (1977). The various HLVA based formulations of these authors are unified and presented in a framework with the assistance of free

variables. Both the one-field and mixed field formulations are given. Two different treatments of initial conditions were presented therein.

The first treatment enforces the initial conditions directly by linking the variations at two temporal end-points with a user-specified parameter matrix $\boldsymbol{\alpha}$. This treatment reduces the number of equations to match the number of the unknowns. It generates constrained parameterised formulations in the primal form similar to the one-field formulation given by the classical HLVA, or in a mixed form similar to the two-field one as proposed by Borri et al. (1985).

Primal form

Using HLVA as the starting point and assuming that the temporal boundary variations are interrelated with a linear function, Sheng obtains

$$\begin{aligned} &\delta\int_{t_0}^{t_1} L dt + \int_{t_0}^{t_1} \delta \mathrm{W}\, dt - \left[\frac{\partial L}{\partial \dot{\mathbf{u}}}\delta\mathbf{u}\right]\Big|_{t=t_0}^{t=t_1} = 0 \\ &\text{with } \delta\mathbf{Q}\big|_{t=t_0} = \boldsymbol{\alpha}\delta\mathbf{Q}\big|_{t=t_1} \end{aligned} \tag{3.3.36}$$

where $\mathbf{Q} = \left[\mathbf{u}, \dot{\mathbf{u}}\right]^T$ presenting the initial conditions.

Mixed form

In the mixed form, the Hamiltonian $H = \dot{\mathbf{u}}^T\mathbf{p} - L$ is used, the equivalent to Eq. (3.3.36) is

$$\begin{aligned} &\int_{t_0}^{t_1}\left(\dot{\mathbf{u}}^T\delta\mathbf{p} + \mathbf{p}^T\delta\dot{\mathbf{u}} - \delta H + \delta \mathrm{W}\right)dt = \mathbf{p}^T\delta\mathbf{u}\Big|_{t=t_0}^{t=t_1} \\ &\text{with } \delta\mathbf{Q}\big|_{t=t_0} = \boldsymbol{\alpha}\,\delta\mathbf{Q}\big|_{t=t_1} \end{aligned} \tag{3.3.37}$$

where $\mathbf{Q} = \left[\mathbf{u}, \mathbf{p}\right]^T$ gives the initial displacement and momentum. $\boldsymbol{\alpha}$ is the parameter matrix. For an SDOF system, $\boldsymbol{\alpha}$ is a two by two matrix

$$\boldsymbol{\alpha} = \begin{bmatrix} a_1 & b_1 \\ a_2 & b_2 \end{bmatrix} \tag{3.3.38}$$

In the second treatment, initial conditions are not directly imposed, yet they are incorporated with the aid of a penalty matrix $\boldsymbol{\alpha}$. This generates unconstrained parameterised formulations, and the number of the unknowns matches the number of equations by adding more unknowns stemmed from $\boldsymbol{\alpha}$. The primal form and the mixed form are available respectively.

Primal form

$$\delta\int_{t_0}^{t_1} L dt + \int_{t_0}^{t_1} \delta \mathrm{W}\, dt - \left[\frac{\partial \mathrm{L}}{\partial \dot{\mathbf{u}}}\delta\mathbf{u}\right]\Big|_{t=t_0}^{t=t_1} + \mathbf{Q}^T\boldsymbol{\alpha}\delta\mathbf{Q} = 0 \tag{3.3.39}$$

where $\mathbf{Q} = \left[\mathbf{u}(0) - \mathbf{u}_0, \dot{\mathbf{u}}(0) - \dot{\mathbf{u}}_0\right]^T$, in which $\mathbf{u}(0)$ and $\dot{\mathbf{u}}(0)$ are the vectors approximated at the initial time $t = t_0$ while $\mathbf{u}_0$ and $\dot{\mathbf{u}}_0$ are the given initial vectors. The dimension of the parameter matrix $\boldsymbol{\alpha}$ is the same as in the first approach.

Mixed form

$$\int_{t_0}^{t_1}\left(\dot{\mathbf{u}}^T\delta\mathbf{p} + \mathbf{p}^T\delta\dot{\mathbf{u}} - \delta\mathbf{H} + \mathbf{f}^T\delta\mathbf{u}\right)dt - \mathbf{p}^T\delta\mathbf{u}\Big|_{t=t_0}^{t=t_1} + \mathbf{Q}^T\boldsymbol{\alpha}\delta\mathbf{Q} = 0 \tag{3.3.40}$$

in this case, $\mathbf{Q} = \left[\mathbf{u}(0) - \mathbf{u}_0, \mathbf{p}(0) - \mathbf{p}_0\right]^T$. $\mathbf{u}(0)$ and $\mathbf{p}(0)$ are the approximated values while $\mathbf{u}_0$ and $\mathbf{p}_0$ are the prescribed initial values.

Sheng et al. argue three advantages of this parameterised approach:

- The optimal approximation may be derived when the parameter matrix $\boldsymbol{\alpha}$ is properly selected, which is normally determined by a prior/ posterior analysis. Although, as the authors admit, the exact solutions for most practical problems are difficult to obtain.

- The resulting algorithms have controllable dissipation properties, which cover the spectrum from non-dissipative to asymptotic annihilating.

- High order accurate algorithms can be obtained.

However, there are some issues with Sheng's formulations:

- The calculated initial values $\mathbf{u}(0), \dot{\mathbf{u}}(0)$ or $\mathbf{u}(0), \mathbf{p}(0)$ by the unconstrained parameterised formulation may not equal to the given initial conditions values $\mathbf{u}_0, \dot{\mathbf{u}}_0$ or $\mathbf{u}_0, \mathbf{p}_0$.

- There will be more unknowns to solve ($a_1, a_2, \cdots, a_n, b_1, b_2, \cdots, b_n$), hence the computational cost are higher.

3.4 Unconventional Hamilton-type Variational Principles

The search for new variational methods has not stopped. Having applied successfully a novel approach for the derivation of variational principles in Gurtin's convolution form (Luo and Cheung, 1988), Luo extended this approach into constructing the so-called Unconventional Hamilton-type Variational Principle for various linear and non-linear problems (Luo et al., 2002; Luo et al., 2003; Huang et al., 2006; Luo et al., 2006; Li and Luo, 2007; Li et al., 2007; Luo et al., 2007; Jiang and Luo, 2008). In this type of variational principles, boundary conditions and initial conditions are not required to be met a priori, and the

stationarity of the first variation of the functional will recover all information needed for solving the time-varying problem, including control equations, boundary conditions and initial conditions.

Unconventional Hamilton-type Variational Principle employs up to five independent field variables to take full account of the time-varying characteristics, more general than any other known variational principles or variational statements for the same problem.

In the case of linear elastodynamics, Unconventional Hamilton-type Variational Principle in the fundamental form, starts from a basic relation.

$$\begin{aligned}&\int_{t_0}^{t_1}\int_V \left\{ p_i\dot{u}_i + \dot{p}_i u_i \right\} dVdt - \int_{t_0}^{t_1}\int_V \left\{ \sigma_{ij}u_{i,j} + \sigma_{ij,j}u_i \right\} dVdt + \int_{t_0}^{t_1}\oint_S \left\{ \left(\sigma_{ij}u_i \right) n_j \right\} dSdt \\ &-\int_V \left\{ p_i(t_1)u_i(t_1) - p_i(t_0)u_i(t_0) \right\} dV = 0\end{aligned} \tag{3.4.1}$$

This relation is the product of the following two equations.

The first one is based on the integration by parts.

$$\int_{t_0}^{t_1}\int_V \left\{ p_i\dot{u}_i + \dot{p}_i u_i \right\} dVdt - \int_V \left\{ p_i(t_1)u_i(t_1) - p_i(t_0)u_i(t_0) \right\} dV = 0 \tag{3.4.2}$$

The second is based on the divergence theorem.

$$\int_{t_0}^{t_1}\int_V \left\{ \sigma_{ij}u_{i,j} + \sigma_{ij,j}u_i \right\} dVdt - \int_{t_0}^{t_1}\oint_S \left\{ \left(\sigma_{ij}u_i \right) n_j \right\} dSdt = 0 \tag{3.4.3}$$

Eq. (3.4.1) is then simply obtained by subtracting Eq. (3.4.3) from Eq. (3.4.2).

In order to construct the desired principle, some manipulations are required. Firstly, advantage is taken from the following equation.

$$p_i v_i = \frac{1}{2}\rho v_i v_i + \frac{1}{2\rho} p_i p_i - \frac{1}{2\rho}\left(p_i - \rho v_i\right)\left(p_i - \rho v_i\right) \tag{3.4.4}$$

in which the two fields p_i and v_i are independent to each other and do not need to satisfy the momentum – velocity constraint $p_i = \rho v_i$.

Another equation will be utilised is

$$\sigma_{ij}\varepsilon_{ij} = \frac{1}{2}E_{ijkl}\varepsilon_{ij}\varepsilon_{kl} + \frac{1}{2}C_{ijkl}\sigma_{ij}\sigma_{kl} + \frac{1}{2}\left(\sigma_{ij} - E_{ijkl}\varepsilon_{kl}\right)\left(\varepsilon_{ij} - C_{ijkl}\sigma_{kl}\right) \tag{3.4.5}$$

Again, σ_{ij} and ε_{ij} are independent filed, and do not necessarily satisfy $\sigma_{ij} = E_{ijkl}\varepsilon_{kl}$ or $\varepsilon_{ij} = C_{ijkl}\sigma_{kl}$ a priori.

Rewrite terms $p_i\dot{u}_i$ and $\sigma_{ij}u_{i,j}$ in Eq. (3.4.1) as the following, by virtue of Eqs. (3.4.4) and (3.4.5)

$$p_i\dot{u}_i = \frac{1}{2}\rho v_i v_i + \frac{1}{2\rho} p_i p_i - \frac{1}{2\rho}\left(p_i - \rho v_i\right)\left(p_i - \rho v_i\right) - p_i\left(v_i - \dot{u}_i\right) \tag{3.4.6}$$

and

$$\begin{aligned}\sigma_{ij}u_{i,j} = {} & \frac{1}{2}E_{ijkl}\varepsilon_{ij}\varepsilon_{kl} + \frac{1}{2}C_{ijkl}\sigma_{ij}\sigma_{kl} + \frac{1}{2}\left(\sigma_{ij} - E_{ijkl}\varepsilon_{kl}\right)\left(\varepsilon_{ij} - C_{ijkl}\sigma_{kl}\right) \\ & - \sigma_{ij}\left[\varepsilon_{ij} - \frac{1}{2}\left(u_{i,j} + u_{j,i}\right)\right]\end{aligned} \tag{3.4.7}$$

After substituting Eqs. (3.4.6) and (3.4.7) into Eq. (3.4.1), the terms on the left-hand side of Eq. (3.4.1) can be grouped into two complementary parts, Π and Γ, each representing an energy/work functional. The work done by conservative and non-conservative forces are taken into account by the addition into one functional and the deduction from the other, thus the total action of these forces are balanced off. In this process, the restricted variation technique (Rosen, 1954) is applied to the work of non-conservative forces, dealing with the issue of "no work function exists for non-conservative forces" (Lanczos, 1970). Initial conditions are also manipulated in the same way.

The two complementary energy functionals are denoted as $\Pi_{(\ )}$ and $\Gamma_{(\ )}$, with the subscript indicating the number of independent fields used in the functionals. For each pair of $\Pi_{(\ )}$ and $\Gamma_{(\ )}$, there always exists

$$\Pi_{(\ )} + \Gamma_{(\ )} = 0 \tag{3.4.8}$$

stemmed from the original equation, Eq. (3.4.1). All additional terms introduced into this equation are complementary as well, i.e., some is added to one functional; but is subtracted from the other at the same time.

In the most general form considering all five independent fields for the linear elastodynamics, the functionals are

$$
\begin{aligned}
\Pi_5 = & \int_{t_0}^{t_1}\int_V \left\{\frac{1}{2}\rho v_i v_i - p_i\left(v_i - \dot{u}_i\right)\right\} dV dt \\
& + \int_{t_0}^{t_1}\int_V \left\{-\frac{1}{2}E_{ijkl}\varepsilon_{ij}\varepsilon_{kl} + \sigma_{ij}\left[\varepsilon_{ij} - \frac{1}{2}\left(u_{i,j} + u_{j,i}\right)\right] + f_i u_i - c\overset{\circ}{\dot{u}}_i u_i\right\} dV dt \\
& + \int_{t_0}^{t_1}\oint_{S_\sigma}\left\{\overline{T}_i u_i\right\} dS dt + \int_{t_0}^{t_1}\oint_{S_u}\left\{\sigma_{ij} n_j\left[u_i - \overline{u}_i\right]\right\} dS dt \\
& + \int_V \left\{\begin{array}{l} \alpha\, \overset{\circ}{p}_i(t_1)\overset{\circ}{u}_i(t_1) - \overset{\circ}{p}_i(t_1)u_i(t_1) + \overline{p}_i(t_0)u_i(t_0) \\ + p_i(t_0)\overset{\circ}{u}_i(t_0) - p_i(t_0)\overline{u}_i(t_0) - \beta\, \overset{\circ}{p}_i(t_0)\overset{\circ}{u}_i(t_0) \end{array}\right\} dV
\end{aligned}
\tag{3.4.9}
$$

and

$$
\begin{aligned}
\Gamma_5 = & \int_{t_0}^{t_1}\int_V \left\{\frac{1}{2\rho}p_i p_i - \frac{1}{2\rho}\left(p_i - \rho v_i\right)\left(p_i - \rho v_i\right) + \dot{p}_i u_i\right\} dV dt \\
& + \int_{t_0}^{t_1}\int_V \left\{-\frac{1}{2}C_{ijkl}\sigma_{ij}\sigma_{kl} - \frac{1}{2}\left(\sigma_{ij} - E_{ijkl}\varepsilon_{kl}\right)\left(\varepsilon_{ij} - C_{ijkl}\sigma_{kl}\right) - \sigma_{ij,j}u_i - f_i u_i + c\overset{\circ}{\dot{u}}_i u_i\right\} dV dt \\
& + \int_{t_0}^{t_1}\oint_{S_\sigma}\left\{\left[\sigma_{ij} n_j - \overline{T}_i\right]u_i\right\} dS dt + \int_{t_0}^{t_1}\oint_{S_u}\left\{\sigma_{ij} n_j \overline{u}_i\right\} dS dt \\
& + \int_V \left\{\begin{array}{l} \left(1-\alpha\right)\overset{\circ}{p}_i(t_1)\overset{\circ}{u}_i(t_1) - p_i(t_1)\overset{\circ}{u}_i(t_1) - \overline{p}_i(t_0)u_i(t_0) \\ + \overset{\circ}{p}_i(t_0)u_i(t_0) + p_i(t_0)\overline{u}_i(t_0) - \left(1-\beta\right)\overset{\circ}{p}_i(t_0)\overset{\circ}{u}_i(t_0) \end{array}\right\} dV
\end{aligned}
\tag{3.4.10}
$$

in which the barred quantities are the prescribed values at the spatial and temporal boundaries. The ones with the superscript ^{o} are the restricted quantities during the variation (Rosen, 1954). This technique gives a formal presentation of the same treatment to the "fixed" quantities in some early works (Argyris and Scharpf, 1969, Fried, 1969) and improves the clarity of the consequent formulation. α and β are the coefficients assisting the construction of the functionals, the value of which are not required to be determined.

The vanishing of the first variation of $\Pi_{(\,)}$ and $\Gamma_{(\,)}$, any one of these two, will naturally lead to the control equation, all boundary conditions and the initial

conditions. Functionals preserving all these information can only be found with Gurtin's convolution approach, Simkins' Lagrange multiplier approach and Chen's total virtual action approach, otherwise only partial boundary condition but no initial conditions can be derived. However, the computation required by Gurtin's approach is rather cumbersome and expensive in execution because of the convolution operation. Although the Lagrange multiplier approach does not require convolution computation, the determination of multiple multipliers is less straightforward. The total virtual action approach is an exception, which has the merit of both ease of computation and preservation, similar to Luo's approach.

There are two distinctive characters about Luo's approach. First, this type of principle offers a simple, straightforward and mathematically solid foundation to underpin the development of variational methods for various problems. Second, the functionals thus derived always come in pairs, meaning more functionals can be found to suit the particular problem at hand.

Furthermore, it can be proved that other variational principles, such as HLVA and Hamilton's Weak Principle can be re-produced from Unconventional Hamilton-type Variational Principle. For instance, when the displacement and traction boundary conditions, velocity – displacement relation, strain – displacement relation and stain – stress relation are satisfied at the outset, which have to be true for a valid solution, Eq. (3.4.9) becomes

$$\begin{aligned}\hat{\Pi}_5 = &\int_{t_0}^{t_1}\int_V \left\{\frac{1}{2}\rho v_i v_i - \frac{1}{2}E_{ijkl}\varepsilon_{ij}\varepsilon_{kl}\right\}dVdt + \int_{t_0}^{t_1}\int_V \left\{ f_i u_i - c\overset{o}{u}_i u_i\right\}dVdt \\ &+ \int_{t_0}^{t_1}\oint_{S_\sigma}\left\{\overline{T}_i u_i\right\}dSdt + \int_{t_0}^{t_1}\oint_{S_u}\left\{\sigma_{ij}n_j\left[u_i - \overline{u}_i\right]\right\}dSdt \\ &+ \int_V \begin{Bmatrix} \alpha\, \overset{o}{p}_i(t_1)\overset{o}{u}_i(t_1) - \overset{o}{p}_i(t_1)u_i(t_1) + \overline{p}_i(t_0)u_i(t_0) \\ + p_i(t_0)\overset{o}{u}_i(t_0) - p_i(t_0)\overline{u}_i(t_0) - \beta\, \overset{o}{p}_i(t_0)\overset{o}{u}_i(t_0)\end{Bmatrix} dV\end{aligned} \tag{3.4.11}$$

The first integrand is the Lagrangian density. The summation of the second, third and forth integrations is the action of the forces within the volume and at the boundaries. The variation of Eq. (3.4.11) can be put as

$$\begin{aligned}\delta\hat{\Pi}_5 = \delta\int_{t_0}^{t_1}\int_V L dV dt + \int_{t_0}^{t_1}\int_V \delta\bar{L} dV dt \\ + \int_V \left\{-p_i(t_1)\delta u_i(t_1) + \bar{p}_i(t_0)\delta u_i(t_0) + \left[u_i(t_0) - \bar{u}_i(t_0)\right]\delta p_i(t_0)\right\} dV\end{aligned} \tag{3.4.12}$$

The vanishing of Eq. (3.4.12), along with the admission of initial condition $u_i(t_0) = \bar{u}_i(t_0)$ and $p_i(t_0) = \bar{p}_i(t_0)$ give

$$\delta\hat{\Pi}_5 = \int_{t_0}^{t_1}\int_V \left(\delta L + \delta\bar{L}\right) dV dt + \int_V \left\{-p_i(t_1)\delta u_i(t_1) + p_i(t_0)\delta u_i(t_0)\right\} dV = 0 \tag{3.4.13}$$

This equation is identically the Eq. (3.3.29) given by Borri (1985), and is also equivalent to the HLVA equation Eq. (3.3.24).

3.5 Summary

In this chapter, various variational approaches for initial-value problems are reviewed. In general, these approaches can be grouped into two categories as shown in Figure 3.5.1.

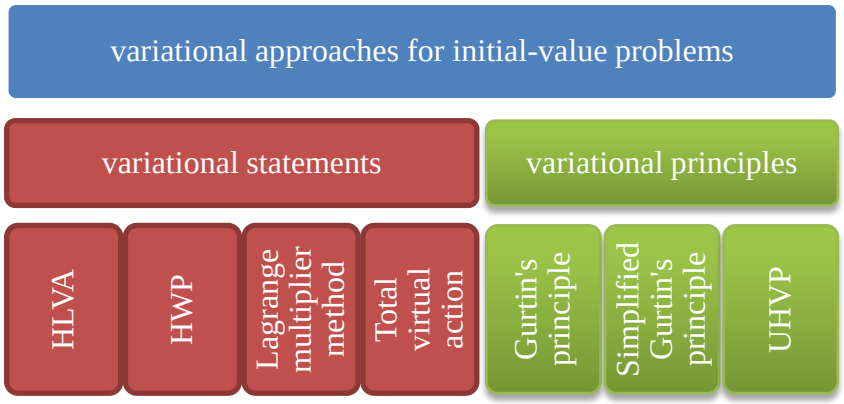

Figure 3.5.1 – Variational approaches for initial-value problem

The first category is the variational statement approach where no functional is available, including Lagrange multiplier method, Hamilton's Law of Varying Action (HLVA), Hamilton's Weak Principle (HWP), Total Virtual Action Principle. When these statements are made to vanish, the control equation for the problem will be obtained. Apart from the initial velocity/ momentum conditions is contained in HWP, the initial conditions are not satisfied automatically in these variational statements. Instead, initial conditions have to be incorporated into the approximating function or introduced with Lagrange multipliers. The second category is the variational principle approach, including Gurtin's variational principle and it simplified versions, as well as Unconventional Hamilton-type Variational Principle (UHVP). All boundary conditions and initial conditions are implied in the functional provided by each particular principle. When the functional is varied and made to vanish, those boundary/initial conditions will be recovered naturally.

The two approaches differ in the presence of a variational functional. A variational functional not only leads to a variational statement which can be used to find the solution, it also discloses the relationship between various quantities from an energy perspective, as demonstrated by the complimentary functionals given by UVHP.

In the UVHP framework, more variable fields are employed thus fully characterising the dynamic system. Moreover, it is found that UHVP embraces some existing of the variational laws/ principles such as HLVA, Hamilton's Principle and HWP.

Chapter 4 Unconventional Hamilton-type Variational Principles for Truss-type Structures

4.1 Introduction

Given the advantages discussed in Chapter 3, Luo's Unconventional Hamilton-type Variational Principle theory is adopted in this chapter to underpin the development of new algorithms for the dynamic analysis of truss-type structures. Several authors have successfully applied Luo's theory to various particular problems; different Unconventional Hamilton-type Variational Principles (UHVPs) were found for particular problems (Li, Luo and Huang 2007, Li and Luo 2007, Luo et al. 2002, Luo, Zhu and Yuan 2006). In this chapter, several UHVPs tailored for truss-type structures are established. Up to five independent variable fields, including the displacement, velocity, momentum, axial force and strain, are employed to derive these principles. These principles are inter-related in that simplified principles with fewer independent variable fields can be derived from a general one, when certain conditions are met at the outset, as demonstrated in previous works (Gurtin 1964; Sandhu and Pister 1971; Reddy 1976; Luo and Cheung 1988).

4.2 Assumptions

In the current discussion, the standard truss model is adopted, and the following assumptions are made within the scope of this research:

- The structural deformation due to the loadings is relatively small compared to the overall geometry of the structure, and thus can be treated as a linear deformation.

- The nodes of the structure are rigid. Therefore, there is no energy loss at these nodes throughout the course of the dynamic action.
- The kinetic energy associated with each node is negligible, due to the facts that the mass of a node is small compared to the mass of the rods connected.
- All material is homogenous and isotropic.
- The structural damping is of linear viscous type.

4.3 Governing equations and boundary/ initial conditions for the dynamics of truss-type structures

For a differential section of an arbitrary truss rod in the dynamic equilibrium shown in Figure 4.3.1, its dynamic characteristics can be represented by the following equations and conditions.

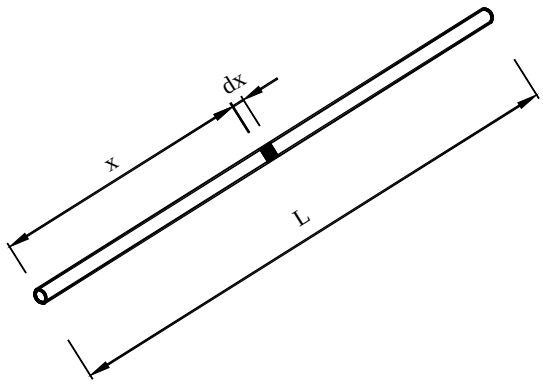

Figure 4.3.1 - A differential section in a typical truss rod

1) Velocity – displacement equation:

Two frequently encountered quantities in structural dynamics are the displacement $u(\ )$ and velocity $v(\ )$. By definition, the relation of the two is

$$\mathrm{v}(x,t)-\frac{\partial \mathrm{u}(x,t)}{\partial t}=0 \tag{4.3.1}$$

where $\frac{\partial}{\partial t}$ is the differentiation operator with respect to time *t*, and x is the spatial coordinate.

2) Momentum – velocity equation:

The velocity $\mathrm{v}(\ )$ is also related to the momentum $\mathrm{p}(\ )$. Follow the definition in classical mechanics, the relation of these two is

$$\mathrm{p}(x,t)-\mathrm{m}(x)\mathrm{v}(x,t)=0 \tag{4.3.2a}$$

or

$$\mathrm{v}(x,t)-\frac{1}{\mathrm{m}(x)}\mathrm{p}(x,t)=0 \tag{4.3.2b}$$

where $\mathrm{m}(x)$ is the mass density per unit length, measured along the longitudinal axis of the rod.

3) Equation of motion:

$$\frac{\partial \mathrm{N}(x,t)}{\partial x}+\mathrm{f}(x)-c\frac{\partial \mathrm{u}(x,t)}{\partial t}-\frac{\partial \mathrm{p}(x,t)}{\partial t}=0 \tag{4.3.3a}$$

or

$$\frac{\partial \mathrm{N}(x,t)}{\partial x}+\mathrm{f}(x)-c\frac{\partial \mathrm{u}(x,t)}{\partial t}-\mathrm{m}\frac{\partial^2 \mathrm{u}(x,t)}{\partial t^2}=0 \tag{4.3.3b}$$

where $\mathrm{N}(x,t)$ is the axial force field and $\frac{\partial \mathrm{N}(x,t)}{\partial x}$ is the infinitesimal increment along the longitudinal axis; $\mathrm{f}(x)$ is the projection of the body force on the

longitudinal axis, per unit length; c is the viscous damping coefficient per unit length of the rod and $c\dfrac{\partial \mathrm{u}(x,t)}{\partial t}$ is the viscous damping force; $\mathrm{m}\dfrac{\partial^2 \mathrm{u}(x,t)}{\partial t^2}$ is the inertia force. This equation represents the dynamic equilibrium of the studied section and can be illustrated in the following figure.

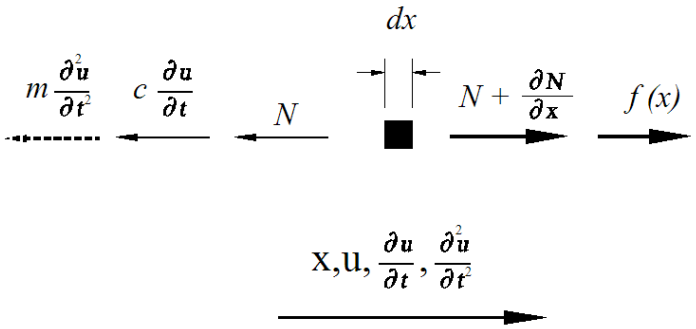

Figure 4.3.2 - Dynamic equilibrium of a differential section

4) Strain – displacement equation:

The stain $\varepsilon(\ )$ measures the deformation of the rod. It is known from the theory of elasticity that the strain field is related to the relative displacement of particles, and one has the following equation

$$\varepsilon(x,t)-\frac{\partial \mathrm{u}(x,t)}{\partial x}=0 \tag{4.3.4}$$

5) Axial force – strain equation:

Follow Hooke's Law, the relation between the axial force field and the strain field can be easily obtained by incorporating the stress – force relation $\mathrm{N}=\mathrm{A}\sigma$

$$\mathrm{N}(x,t)-E\,\mathrm{A}(x)\varepsilon(x,t)=0 \tag{4.3.5}$$

where E is the elastic modulus and $\mathrm{A}(x)$ is the cross-sectional area of the rod.

For an arbitrary section, there are two types of spatial boundary. The first type is the displacement boundary where the displacement can be prescribed for any point of time; the other one is the traction boundary where the external force at the boundary can be prescribed for any point of time. The next two conditions are related to these two types of boundary

6) Traction boundary condition:

$$\mathrm{N}(x,t)-\overline{\mathrm{N}}(x,t)=0 \text{ on } \chi_N \tag{4.3.6}$$

where $\overline{\mathrm{N}}(x,t)$ is the given axial force on the traction boundary, χ_N .

7) Displacement boundary condition:

$$\mathrm{u}(x,t)-\overline{\mathrm{u}}(x,t)=0 \text{ on } \chi_u \tag{4.3.7}$$

where $\overline{\mathrm{u}}(x,t)$ is the given displacement on the displacement boundary, χ_u

8) Initial conditions:

$$\mathrm{u}(x,0)-\overline{\mathrm{u}}(x,0)=0 \tag{4.3.8a}$$

$$\begin{aligned}&\mathrm{v}(x,0)-\overline{\mathrm{v}}(x,0)=0\\ &or\\ &\mathrm{p}(x,0)-\overline{\mathrm{p}}(x,0)=0\end{aligned} \tag{4.3.8b}$$

where $\overline{\mathrm{u}}(x,0)$, $\overline{\mathrm{v}}(x,0)$ and $\overline{\mathrm{p}}(x,0)$ are the given initial displacement field, initial velocity field and initial momentum field at the time $t=0$, respectively.

These equations incorporate the relations for a linear system to support the development of the proposed linear analysis method. However various other relations, such as non-linear relations and multi-physics relations, can be used as well in the similar fashion to consider different behaviours, and thus particular variational principles may be developed for those applications.

4.4 A fundamental integral relation

Let the length of a differential section be dx, the length of the rod be L, as shown in Figure 4.3.1. The time derivative of a quantity is denoted by a dot over the quantity, e.g. $\frac{\partial \mathrm{u}(x,t)}{\partial t} = \dot{\mathrm{u}}(x,t)$. $[0,t_1]$ is the time interval of interest.

For two arbitrary and independent continuous fields $\mathrm{p}(x,t)$ and $\mathrm{u}(x,t)$, it can be easily verified that the following equation always holds

$$\int_0^{t_1}\int_0^{L}\left\{\mathrm{p}(x,t)\dot{\mathrm{u}}(x,t)+\dot{\mathrm{p}}(x,t)\mathrm{u}(x,t)\right\}dxdt-\int_0^{L}\left\{\mathrm{p}(x,t)\mathrm{u}(x,t)\Big|_{t=0}^{t=t_1}\right\}dx=0 \qquad (4.4.1)$$

In the same fashion, one has the following equation for another two arbitrary and independent continuous fields $\mathrm{N}(x,t)$ and $\mathrm{u}(x,t)$:

$$\int_0^{t_1}\int_0^{L}\left\{\mathrm{N}(x,t)\frac{\partial \mathrm{u}(x,t)}{\partial x}+\frac{\partial \mathrm{N}(x,t)}{\partial x}\mathrm{u}(x,t)\right\}dxdt-\int_0^{t_1}\left\{\mathrm{N}(x,t)\mathrm{u}(x,t)\Big|_{x=0}^{x=L}\right\}dt=0 \qquad (4.4.2)$$

Subtracting Eq. (4.4.2) from Eq. (4.4.1) yields

$$\begin{aligned}&\int_0^{t_1}\int_0^{L}\left\{\mathrm{p}(x,t)\dot{\mathrm{u}}(x,t)+\dot{\mathrm{p}}(x,t)\mathrm{u}(x,t)\right\}dxdt\\&\quad-\int_0^{t_1}\int_0^{L}\left\{\mathrm{N}(x,t)\frac{\partial \mathrm{u}(x,t)}{\partial x}+\frac{\partial \mathrm{N}(x,t)}{\partial x}\mathrm{u}(x,t)\right\}dxdt\\&\qquad+\int_0^{t_1}\left\{\mathrm{N}(x,t)\mathrm{u}(x,t)\Big|_{x=0}^{x=L}\right\}dt-\int_0^{L}\left\{\mathrm{p}(x,t)\mathrm{u}(x,t)\Big|_{t=0}^{t=t_1}\right\}dx=0\end{aligned}\tag{4.4.3}$$

Eq. (4.4.3) is the underpinning equation for the Unconventional Hamilton-type Variational Principles tailored for truss-type structures. Two complementary functionals can be constructed out of this equation, and it will be proven later on that both of these two functionals, when varied and made to vanish, can lead to the governing equations and all boundary and initial conditions.

4.5 Unconventional Hamilton-type variational principles for truss-type structures

In this section, five variational principles are derived for the dynamic analysis of truss-type structures. In these principles, up to five physical fields, namely, the displacement field $\mathrm{u}(x,t)$, velocity field $\mathrm{v}(x,t)$, momentum field $\mathrm{p}(x,t)$, axial force field $\mathrm{N}(x,t)$ and strain field $\varepsilon(x,t)$, are treated initially as independent to each other. This independence allows finding the Euler equations associated with the functionals exactly as the governing equations and boundary / initial conditions given in Section 4.3. Therefore, it demonstrates the dynamic characteristics of truss-type structures are fully preserved in the presented variational principle. Another four variational principles with less independent fields are obtained subsequently once one or more governing equations is/are satisfied a priori at the outset. In this fashion, the relationships between these variational principles are also revealed.

4.5.1 Five-field unconventional Hamilton-type variational principle

Treat five variable fields as independent. The first term in the first integrand of Eq. (4.4.3) can be re-written as

$$\begin{aligned}&\mathrm{p}(x,t)\dot{\mathrm{u}}(x,t)\\&=\frac{1}{2}\mathrm{m}(x)\mathrm{v}^2(x,t)+\frac{1}{2\mathrm{m}(x)}\mathrm{p}^2(x,t)\\&-\frac{1}{2\mathrm{m}(x)}\left[\mathrm{p}(x,t)-\mathrm{m}(x)\mathrm{v}(x,t)\right]^2-\mathrm{p}(x,t)\left[\mathrm{v}(x,t)-\dot{\mathrm{u}}(x,t)\right]\end{aligned} \tag{4.5.1}$$

Moreover, the first term in the second integrand of Eq. (4.4.3) can be re-written as

$$\begin{aligned}&\mathrm{N}(x,t)\frac{\partial \mathrm{u}(x,t)}{\partial x}\\&=\frac{1}{2}E\,\mathrm{A}(x)\varepsilon^2(x,t)+\frac{1}{2E\,\mathrm{A}(x)}\mathrm{N}^2(x,t)\\&+\frac{1}{2}\left[\mathrm{N}(x,t)-E\,\mathrm{A}(x)\varepsilon(x,t)\right]\left[\varepsilon(x,t)-\frac{1}{E\,\mathrm{A}(x)}\mathrm{N}(x,t)\right]\\&-\mathrm{N}(x,t)\left[\varepsilon(x,t)-\frac{\partial \mathrm{u}(x,t)}{\partial x}\right]\end{aligned} \tag{4.5.2}$$

In the following discussion, (x) and (x,t) are omitted for brevity, unless they are required to be specified to clarify the boundary values. By virtue of Eqs. (4.5.1) and (4.5.2), Eq. (4.4.3) may be written in the form

$$\Pi_5(\mathrm{p},\mathrm{v},\mathrm{u},\mathrm{N},\varepsilon)+\Gamma_5(\mathrm{p},\mathrm{v},\mathrm{u},\mathrm{N},\varepsilon)=0 \tag{4.5.3}$$

with

$$\Pi_5(\mathrm{p},\mathrm{v},\mathrm{u},\mathrm{N},\varepsilon)=\int_0^{t_1}\int_0^{L}\left\{\frac{1}{2}\mathrm{m}\mathrm{v}^2-\mathrm{p}\left[\mathrm{v}-\dot{\mathrm{u}}\right]\right\}dxdt+\hat{\Pi}_3(\mathrm{u},\mathrm{N},\varepsilon)+\overset{o}{\Pi}(\mathrm{p},\mathrm{u}) \tag{4.5.4}$$

$$\Gamma_5(\mathrm{p},\mathrm{v},\mathrm{u},\mathrm{N},\varepsilon)=\int_0^{t_1}\int_0^L\left\{\frac{1}{2\mathrm{m}}\mathrm{p}^2-\frac{1}{2\mathrm{m}}[\mathrm{p}-\mathrm{mv}]^2+\dot{\mathrm{p}}\mathrm{u}\right\}dxdt+\hat{\Gamma}_3(\mathrm{u},\mathrm{N},\varepsilon)+\overset{o}{\Gamma}(\mathrm{p},\mathrm{u}) \tag{4.5.5}$$

and

$$\begin{aligned}&\hat{\Pi}_3(\mathrm{u},\mathrm{N},\varepsilon)\\&=\int_0^{t_1}\int_0^L\left\{-\frac{1}{2}EA\varepsilon^2+\mathrm{N}\left[\varepsilon-\frac{\partial\mathrm{u}}{\partial x}\right]+\left[\mathrm{f}-\mathrm{c}\overset{o}{\mathrm{u}}\right]\mathrm{u}\right\}dxdt\\&+\int_0^{t_1}\left\{\mathrm{N}(x,t)\left[\mathrm{u}(x,t)-\bar{\mathrm{u}}(x,t)\right]\Big|_{x_u=0}^{x_u=L}+\bar{\mathrm{N}}(x,t)\mathrm{u}(x,t)\Big|_{x_N=0}^{x_N=L}\right\}dt\end{aligned} \tag{4.5.6}$$

$$\begin{aligned}&\hat{\Gamma}_3(\mathrm{u},\mathrm{N},\varepsilon)\\&=\int_0^{t_1}\int_0^L\left\{-\frac{1}{2EA}\mathrm{N}^2-\frac{1}{2}[\mathrm{N}-EA\varepsilon]\left[\varepsilon-\frac{1}{EA}\mathrm{N}\right]-\frac{\partial\mathrm{N}}{\partial x}\mathrm{u}-\left[\mathrm{f}-c\overset{o}{\mathrm{u}}\right]\mathrm{u}\right\}dxdt\\&+\int_0^{t_1}\left\{\mathrm{N}(x,t)\bar{\mathrm{u}}(x,t)\Big|_{x_u=0}^{x_u=L}+\left[\mathrm{N}(x,t)-\bar{\mathrm{N}}(x,t)\right]\mathrm{u}(x,t)\Big|_{x_N=0}^{x_N=L}\right\}dt\end{aligned} \tag{4.5.7}$$

$$\begin{aligned}&\overset{o}{\Pi}(\mathrm{p},\mathrm{u})\\&=\int_0^L\left\{\begin{array}{l}\alpha\,\overset{o}{\mathrm{p}}(x,t_1)\overset{o}{\mathrm{u}}(x,t_1)-\overset{o}{\mathrm{p}}(x,t_1)\mathrm{u}(x,t_1)+\bar{\mathrm{p}}(x,0)\mathrm{u}(x,0)\\+\mathrm{p}(x,0)\overset{o}{\mathrm{u}}(x,0)-\mathrm{p}(x,0)\bar{\mathrm{u}}(x,0)-\beta\,\overset{o}{\mathrm{p}}(x,0)\overset{o}{\mathrm{u}}(x,0)\end{array}\right\}dx\end{aligned} \tag{4.5.8}$$

$$\begin{aligned}&\overset{o}{\Gamma}(\mathrm{p},\mathrm{u})\\&=\int_0^L\left\{\begin{array}{l}(1-\alpha)\overset{o}{\mathrm{p}}(x,t_1)\overset{o}{\mathrm{u}}(x,t_1)-\mathrm{p}(x,t_1)\overset{o}{\mathrm{u}}(x,t_1)-\bar{\mathrm{p}}(x,0)\mathrm{u}(x,0)\\+\overset{o}{\mathrm{p}}(x,0)\mathrm{u}(x,0)+\mathrm{p}(x,0)\bar{\mathrm{u}}(x,0)-(1-\beta)\overset{o}{\mathrm{p}}(x,0)\overset{o}{\mathrm{u}}(x,0)\end{array}\right\}dx\end{aligned} \tag{4.5.9}$$

$\Pi_5(\mathrm{p},\mathrm{v},\mathrm{u},\mathrm{N},\varepsilon)$ and $\Gamma_5(\mathrm{p},\mathrm{v},\mathrm{u},\mathrm{N},\varepsilon)$ are two complementary functionals in which the work done by external forces over the time interval $[0,t_1]$ may be introduced

as $\int_0^{t_1}\int_0^{L}\left[\mathrm{f}-\mathrm{c}\overset{\mathrm{o}}{\dot{\mathrm{u}}}\right]\mathrm{u}\,dxdt$. The fields with the superscript o are the restricted ones when variations are taken (Rosen 1954). These fields are to be held as invariable, e.g., $\delta\overset{o}{\mathrm{p}}(x,t_1)=0$; the superscript are to be removed once the variation is completed, e.g., $\delta\left(\overset{o}{\mathrm{p}}(x,t_1)\mathrm{u}(x,t_1)\right)=\mathrm{p}(x,t_1)\delta\mathrm{u}(x,t_1)$. α and β are the coefficients assisting the construction of the functionals, the value of which are not required for the forthcoming derivations.

Principle one

If and only if a set of fields, comprising $\mathrm{p},\mathrm{v},\mathrm{u},\mathrm{N},\varepsilon$, is the solution of a dynamic problem fulfilling Eqs. (4.3.1), (4.3.2), (4.3.3), (4.3.4), (4.3.5), (4.3.6), (4.3.7), (4.3.8a) and (4.3.8b), this set satisfies

$$\delta\Pi_5(\mathrm{p},\mathrm{v},\mathrm{u},\mathrm{N},\varepsilon)=0 \text{ and } \delta\Gamma_5(\mathrm{p},\mathrm{v},\mathrm{u},\mathrm{N},\varepsilon)=0$$

Proof

By taking variation of Π_5, one has

$$\begin{aligned}&\delta\Pi_5(\mathrm{p},\mathrm{v},\mathrm{u},\mathrm{N},\varepsilon)\\&=\int_0^{t_1}\int_0^{L}\left\{\mathrm{mv}\,\delta\mathrm{v}-\mathrm{p}\left[\delta\mathrm{v}-\delta\dot{\mathrm{u}}\right]-\left[\mathrm{v}-\dot{\mathrm{u}}\right]\delta\mathrm{p}\right\}dxdt+\delta\hat{\Pi}_3(\mathrm{u},\mathrm{N},\varepsilon)+\delta\overset{o}{\mathrm{I}}(\mathrm{p},\mathrm{u})\end{aligned}\qquad(4.5.10)$$

since

$$\begin{aligned}
&\int_0^{t_1}\int_0^{L}\{\mathrm{p}\,\delta\dot{\mathrm{u}}\}dxdt \\
&=\int_0^{L}\int_0^{t_1}\left\{\mathrm{p}\frac{\partial}{\partial t}\delta\mathrm{u}\right\}dtdx=\int_0^{L}\left\{\mathrm{p}\,\delta\mathrm{u}\Big|_{t=0}^{t=t_1}-\int_0^{t_1}\frac{\partial \mathrm{p}}{\partial t}\delta\mathrm{u}\,dt\right\}dx \\
&=\int_0^{L}\left\{\mathrm{p}\left(x,t_1\right)\delta\mathrm{u}\left(x,t_1\right)-\mathrm{p}\left(x,0\right)\delta\mathrm{u}\left(x,0\right)\right\}dx-\int_0^{t_1}\int_0^{L}\{\dot{\mathrm{p}}\,\delta\mathrm{u}\}dxdt
\end{aligned} \tag{4.5.11}$$

therefore Eq. (4.5.10) can be re-written as

$$\begin{aligned}
&\delta\Pi_5\left(\mathrm{p},\mathrm{v},\mathrm{u},\mathrm{N},\varepsilon\right) \\
&=\int_0^{t_1}\int_0^{L}\{[m\mathrm{v}-\mathrm{p}]\delta\mathrm{v}-\dot{\mathrm{p}}\,\delta\mathrm{u}-[\mathrm{v}-\dot{\mathrm{u}}]\delta\mathrm{p}\}dxdt+\delta\hat{\Pi}_3\left(\mathrm{u},\mathrm{N},\varepsilon\right)+\delta\overset{o}{\Pi}\left(\mathrm{p},\mathrm{u}\right) \\
&+\int_0^{L}\left\{\mathrm{p}\left(x,t_1\right)\delta\mathrm{u}\left(x,t_1\right)-\mathrm{p}\left(x,0\right)\delta\mathrm{u}\left(x,0\right)\right\}dx
\end{aligned} \tag{4.5.12}$$

where

$$\begin{aligned}
&\delta\hat{\Pi}_3\left(\mathrm{u},\mathrm{N},\varepsilon\right) \\
&=\int_0^{t_1}\int_0^{L}\left\{-EA\varepsilon\delta\varepsilon+\mathrm{N}\left[\delta\varepsilon-\frac{\partial\delta\mathrm{u}}{\partial x}\right]+\left[\varepsilon-\frac{\partial\mathrm{u}}{\partial x}\right]\delta\mathrm{N}+[\mathrm{f}-c\dot{\mathrm{u}}]\delta\mathrm{u}\right\}dxdt \\
&+\int_0^{t_1}\left\{\left[\mathrm{u}\left(x,t\right)-\bar{\mathrm{u}}\left(x,t\right)\right]\delta\mathrm{N}\left(x,t\right)\Big|_{x_u=0}^{x_u=L}+\mathrm{N}\left(x,t\right)\delta\mathrm{u}\left(x,t\right)\Big|_{x_u=0}^{x_u=L}+\bar{\mathrm{N}}\left(x,t\right)\delta\mathrm{u}\left(x,t\right)\Big|_{x_N=0}^{x_N=L}\right\}dt
\end{aligned} \tag{4.5.13}$$

since

$$\begin{aligned}
&\int_0^{t_1}\int_0^{L}\left\{\mathrm{N}\frac{\partial\delta\mathrm{u}}{\partial x}\right\}dxdt \\
&=\int_0^{t_1}\int_0^{L}\left\{\frac{\partial}{\partial x}\left(\mathrm{N}\,\delta\mathrm{u}\right)-\frac{\partial\mathrm{N}}{\partial x}\delta\mathrm{u}\right\}dxdt \\
&=\int_0^{t_1}\left\{\mathrm{N}\left(x,t\right)\delta\mathrm{u}\left(x,t\right)\Big|_{x_u=0}^{x_u=L}+\mathrm{N}\left(x,t\right)\delta\mathrm{u}\left(x,t\right)\Big|_{x_N=0}^{x_N=L}-\int_0^{L}\left[\frac{\partial\mathrm{N}}{\partial x}\delta\mathrm{u}\right]dx\right\}dt
\end{aligned} \tag{4.5.14}$$

consequently Eq. (4.5.13) can be expressed as

$$
\begin{aligned}
&\delta\hat{\Pi}_3\left(\mathrm{u},\mathrm{N},\varepsilon\right)\\
&=\int_0^{t_1}\int_0^{L}\left\{\left[\mathrm{N}-EA\varepsilon\right]\delta\varepsilon+\left[\varepsilon-\frac{\partial\,\mathrm{u}}{\partial x}\right]\delta\,\mathrm{N}+\left[\frac{\partial\,\mathrm{N}}{\partial x}+\mathrm{f}-\mathrm{c}\,\dot{\mathrm{u}}\right]\delta\,\mathrm{u}\right\}dxdt\\
&+\int_0^{t_1}\left\{\left[\mathrm{u}\left(x,t\right)-\bar{\mathrm{u}}\left(x,t\right)\right]\delta\,\mathrm{N}\left(x,t\right)\Big|_{x_u=0}^{x_u=L}+\left[\bar{\mathrm{N}}\left(x,t\right)-\mathrm{N}\left(x,t\right)\right]\delta\,\mathrm{u}\left(x,t\right)\Big|_{x_N=0}^{x_N=L}\right\}dt
\end{aligned}
\tag{4.5.15}
$$

The variation of $\overset{o}{\Pi}\left(\mathrm{p},\mathrm{u}\right)$ is

$$
\begin{aligned}
&\delta\overset{o}{\Pi}\left(\mathrm{p},\mathrm{u}\right)\\
&=\int_0^{L}\left\{-\mathrm{p}\left(x,t_1\right)\delta\,\mathrm{u}\left(x,t_1\right)+\bar{\mathrm{p}}\left(x,0\right)\delta\,\mathrm{u}\left(x,0\right)+\left[\mathrm{u}\left(x,0\right)-\bar{\mathrm{u}}\left(x,0\right)\right]\delta\,\mathrm{p}\left(x,0\right)\right\}dx
\end{aligned}
\tag{4.5.16}
$$

Substituting Eqs. (4.5.15) and (4.5.16) into Eq. (4.5.12) yields

$$
\begin{aligned}
&\delta\Pi_5\left(\mathrm{p},\mathrm{v},\mathrm{u},\mathrm{N},\varepsilon\right)\\
&=\int_0^{t_1}\int_0^{L}\left\{\begin{array}{l}\left[\mathrm{mv}-\mathrm{p}\right]\delta\,\mathrm{v}+\left[\dot{\mathrm{u}}-\mathrm{v}\right]\delta\,\mathrm{p}+\left[\mathrm{N}-EA\varepsilon\right]\delta\varepsilon\\+\left[\varepsilon-\dfrac{\partial\,\mathrm{u}}{\partial x}\right]\delta\,\mathrm{N}+\left[\dfrac{\partial\,\mathrm{N}}{\partial x}+\mathrm{f}-\mathrm{c}\,\dot{\mathrm{u}}-\dot{\mathrm{p}}\right]\delta\,\mathrm{u}\end{array}\right\}dxdt\\
&+\int_0^{t_1}\left\{\left[\mathrm{u}\left(x,t\right)-\bar{\mathrm{u}}\left(x,t\right)\right]\delta\,\mathrm{N}\left(x,t\right)\Big|_{x_u=0}^{x_u=L}+\left[\bar{\mathrm{N}}\left(x,t\right)-\mathrm{N}\left(x,t\right)\right]\delta\,\mathrm{u}\left(x,t\right)\Big|_{x_N=0}^{x_N=L}\right\}dt\\
&+\int_0^{L}\left\{\left[\bar{\mathrm{p}}\left(x,0\right)-\mathrm{p}\left(x,0\right)\right]\delta\,\mathrm{u}\left(x,0\right)+\left[\mathrm{u}\left(x,0\right)-\bar{\mathrm{u}}\left(x,0\right)\right]\delta\,\mathrm{p}\left(x,0\right)\right\}dx
\end{aligned}
\tag{4.5.17}
$$

Sufficiency proof:

Suppose the set $\mathrm{p},\mathrm{v},\mathrm{u},\mathrm{N},\varepsilon$ is the solution of the mixed problem including Eqs. (4.3.1), (4.3.2), (4.3.3), (4.3.4), (4.3.5), (4.3.6), (4.3.7), (4.3.8a) and (4.3.8b),

substituting these conditions into Eq. (4.5.17) yields $\delta\Pi_5\left(\mathrm{p},\mathrm{v},\mathrm{u},\mathrm{N},\varepsilon\right)=0$ naturally.

Necessity proof:

Assume Eq. (4.5.17) equals to zero for any variations of the five fields, then it arrives naturally that the products in square brackets have to vanish simultaneously, on the consideration that the variations $\delta\,\mathrm{v},\,\delta\,\mathrm{p},\,\delta\varepsilon,\,\delta\,\mathrm{N},\,\delta\,\mathrm{u}$ are arbitrary and independent to each other. This implies the simultaneous satisfaction of Eqs. (4.3.1), (4.3.2a), (4.3.3), (4.3.4), (4.3.5), (4.3.6), (4.3.7), (4.3.8a) and (4.3.8b), and proves that this set is the solution of the problem.

It can be seen from above that $\Pi_5\left(\mathrm{p},\mathrm{v},\mathrm{u},\mathrm{N},\varepsilon\right)$ is a functional whose Euler equations are exactly the governing equations and boundary / initial conditions for a truss-type structure. Compared with the other variational statements reviewed in Chapter 3, it can be seen that in addition to the advantage of the direct incorporation of all initial conditions in formulation, more conditions such as the constitutive one are also satisfied within the space – time volume and on the boundary. These conditions are contained naturally without using any artificial multipliers or convolution operators.

In a similar fashion, it is found

$$\begin{aligned}&\delta\Gamma_5\left(\mathrm{p},\mathrm{v},\mathrm{u},\mathrm{N},\varepsilon\right)\\&=\int_0^{t_1}\int_0^{L}\left\{\frac{1}{\mathrm{m}}\mathrm{p}\,\delta\,\mathrm{p}-\frac{1}{\mathrm{m}}\left[\mathrm{p}-\mathrm{mv}\right]\left[\delta\,\mathrm{p}-\mathrm{m}\,\delta\,\mathrm{v}\right]+\dot{\mathrm{p}}\,\delta\,\mathrm{u}+\mathrm{u}\,\delta\,\dot{\mathrm{p}}\right\}dxdt+\delta\hat{\Gamma}_3\left(\mathrm{u},\mathrm{N},\varepsilon\right)+\delta\overset{o}{\Gamma}\left(\mathrm{p},\mathrm{u}\right)\end{aligned}\tag{4.5.18}$$

in which

$$
\begin{aligned}
&\delta\hat{\Gamma}_3(\mathrm{u},\mathrm{N},\varepsilon)\\
&=\int_0^{t_1}\int_0^{L}\left\{\begin{array}{l}
-\dfrac{1}{EA}\mathrm{N}\,\delta\mathrm{N}-\dfrac{1}{2}\left[\mathrm{N}-EA\varepsilon\right]\left[\delta\varepsilon-\dfrac{1}{EA}\delta\mathrm{N}\right]\\
-\dfrac{1}{2}\left[\delta\mathrm{N}-EA\delta\varepsilon\right]\left[\varepsilon-\dfrac{1}{EA}\mathrm{N}\right]\\
-\dfrac{\partial\mathrm{N}}{\partial x}\delta\mathrm{u}-\dfrac{\partial\delta\mathrm{N}}{\partial x}\mathrm{u}-\left[\mathrm{f}-c\overset{\circ}{\mathrm{u}}\right]\delta\mathrm{u}
\end{array}\right\}dxdt\\
&+\int_0^{t_1}\left\{\begin{array}{l}
\overline{\mathrm{u}}(x,t)\,\delta\mathrm{N}(x,t)\Big|_{x_u=0}^{x_u=L}+\mathrm{u}(x,t)\,\delta\mathrm{N}(x,t)\Big|_{x_N=0}^{x_N=L}\\
+\left[\mathrm{N}(x,t)-\overline{\mathrm{N}}(x,t)\right]\delta\mathrm{u}(x,t)\Big|_{x_N=0}^{x_N=L}
\end{array}\right\}dt
\end{aligned}
\tag{4.5.19}
$$

and

$$
\begin{aligned}
&\delta\overset{o}{\Gamma}(\mathrm{p},\mathrm{u})\\
&=\int_0^{L}\left\{\left[\mathrm{p}(x,0)-\overline{\mathrm{p}}(x,0)\right]\delta\mathrm{u}(x,0)+\overline{\mathrm{u}}(x,0)\,\delta\mathrm{p}(x,0)-\mathrm{u}(x,t_1)\,\delta\mathrm{p}(x,t_1)\right\}dx
\end{aligned}
\tag{4.5.20}
$$

The integration $\int_0^{t_1}\int_0^{L}\{\mathrm{u}\,\delta\dot{\mathrm{p}}\}dxdt$ in Eq. (4.5.18) may be transformed by integration by parts as

$$
\begin{aligned}
&\int_0^{t_1}\int_0^{L}\{\mathrm{u}\,\delta\dot{\mathrm{p}}\}dxdt\\
&=\int_0^{L}\int_0^{t_1}\left\{\frac{\partial}{\partial t}(\mathrm{u}\,\delta\mathrm{p})-\dot{\mathrm{u}}\,\delta\mathrm{p}\right\}dtdx=\int_0^{L}\left\{\mathrm{u}\,\delta\mathrm{p}\Big|_{t=0}^{t=t_1}-\int_0^{t_1}\dot{\mathrm{u}}\,\delta\mathrm{p}\,dt\right\}dx
\end{aligned}
\tag{4.5.21}
$$

similarly the term $\int_0^{t_1}\int_0^{L}\left\{\dfrac{\partial\delta\mathrm{N}}{\partial x}\mathrm{u}\right\}dxdt$ in Eq. (4.5.19) may be transformed as

$$
\begin{aligned}
&\int_0^{t_1}\int_0^{L}\left\{\frac{\partial\delta \mathrm{N}}{\partial x}\mathrm{u}\right\}dxdt \\
&=\int_0^{t_1}\int_0^{L}\left\{\frac{\partial}{\partial x}\left(\mathrm{u}\,\delta \mathrm{N}\right)-\frac{\partial \mathrm{u}}{\partial x}\delta \mathrm{N}\right\}dxdt \\
&=\int_0^{t_1}\left\{\mathrm{u}\left(x,t\right)\delta \mathrm{N}\left(x,t\right)\Big|_{x_u=0}^{x_u=L}+\mathrm{u}\left(x,t\right)\delta \mathrm{N}\left(x,t\right)\Big|_{x_N=0}^{x_N=L}-\int_0^{L}\left[\frac{\partial \mathrm{u}}{\partial x}\delta \mathrm{N}\right]dx\right\}dt
\end{aligned}
\tag{4.5.22}
$$

By virtue of Eq. (4.5.22), Eq. (4.5.19) may be re-written as

$$
\begin{aligned}
&\delta\hat{\Gamma}_3\left(\mathrm{u},\mathrm{N},\varepsilon\right) \\
&=\int_0^{t_1}\int_0^{L}\left\{\left[\frac{\partial \mathrm{u}}{\partial x}-\varepsilon\right]\delta \mathrm{N}+\left[EA\varepsilon-\mathrm{N}\right]\delta\varepsilon-\left[\frac{\partial \mathrm{N}}{\partial x}+\mathrm{f}-c\overset{\mathrm{o}}{\mathrm{u}}\right]\delta \mathrm{u}\right\}dxdt \\
&+\int_0^{t_1}\left\{\left[\bar{\mathrm{u}}\left(x,t\right)-\mathrm{u}\left(x,t\right)\right]\delta \mathrm{N}\left(x,t\right)\Big|_{x_u=0}^{x_u=L}+\left[\mathrm{N}\left(x,t\right)-\bar{\mathrm{N}}\left(x,t\right)\right]\delta \mathrm{u}\left(x,t\right)\Big|_{x_N=0}^{x_N=L}\right\}dt
\end{aligned}
\tag{4.5.23}
$$

The substitution of Eqs. (4.5.20), (4.5.21) and (4.5.23) into Eq. (4.5.18) yields

$$
\begin{aligned}
&\delta\Gamma_5\left(\mathrm{p},\mathrm{v},\mathrm{u},\mathrm{N},\varepsilon\right) \\
&=\int_0^{t_1}\int_0^{L}\left\{\begin{array}{l}\left[\mathrm{p}-\mathrm{mv}\right]\delta \mathrm{v}+\left[\mathrm{v}-\dot{\mathrm{u}}\right]\delta \mathrm{p}+\left[EA\varepsilon-\mathrm{N}\right]\delta\varepsilon \\ +\left[\dfrac{\partial \mathrm{u}}{\partial x}-\varepsilon\right]\delta \mathrm{N}-\left[\dfrac{\partial \mathrm{N}}{\partial x}+\mathrm{f}-\mathrm{c}\dot{\mathrm{u}}-\dot{\mathrm{p}}\right]\delta \mathrm{u}\end{array}\right\}dxdt \\
&+\int_0^{t_1}\left\{\left[\bar{\mathrm{u}}\left(x,t\right)-\mathrm{u}\left(x,t\right)\right]\delta \mathrm{N}\left(x,t\right)\Big|_{x_u=0}^{x_u=L}+\left[\mathrm{N}\left(x,t\right)-\bar{\mathrm{N}}\left(x,t\right)\right]\delta \mathrm{u}\left(x,t\right)\Big|_{x_N=0}^{x_N=L}\right\}dt \\
&+\int_0^{L}\left\{\left[\mathrm{p}\left(x,0\right)-\bar{\mathrm{p}}\left(x,0\right)\right]\delta \mathrm{u}\left(x,0\right)+\left[\bar{\mathrm{u}}\left(x,0\right)-\mathrm{u}\left(x,0\right)\right]\delta \mathrm{p}\left(x,0\right)\right\}dx
\end{aligned}
\tag{4.5.24}
$$

It can be proved in a similar manner that, the sufficient and necessary condition of $\delta\Gamma_5\left(\mathrm{p},\mathrm{v},\mathrm{u},\mathrm{N},\varepsilon\right)=0$ is the simultaneous satisfaction of Eqs. (4.3.1) through to (4.3.8b), which means $\Gamma_5\left(\mathrm{p},\mathrm{v},\mathrm{u},\mathrm{N},\varepsilon\right)$ is another functional whose Euler equations are the governing equations and boundary / initial conditions.

This completes the proof of *Principle one*.

4.5.2 Four-field unconventional Hamilton-type variational principle

When the relation of p and v is admitted as a prerequisite as per Eq. (4.3.2), a variational principle with four independent fields $\mathrm{p},\mathrm{u},\mathrm{N},\varepsilon$ may be derived as follows.

The two complementary functionals can be found by substituting Eq. (4.3.2) into Eqs. (4.5.4) and (4.5.5), yielding

$$\Pi_4\left(\mathrm{p},\mathrm{u},\mathrm{N},\varepsilon\right)=\int_0^{t_1}\int_0^{L}\left\{\mathrm{p}\dot{\mathrm{u}}-\frac{1}{2\mathrm{m}}\mathrm{p}^2\right\}dxdt+\hat{\Pi}_3\left(\mathrm{u},\mathrm{N},\varepsilon\right)+\overset{o}{\Pi}\left(\mathrm{p},\mathrm{u}\right) \tag{4.5.25}$$

and

$$\Gamma_4\left(\mathrm{p},\mathrm{u},\mathrm{N},\varepsilon\right)=\int_0^{t_1}\int_0^{L}\left\{\frac{1}{2\mathrm{m}}\mathrm{p}^2+\dot{\mathrm{p}}\mathrm{u}\right\}dxdt+\hat{\Gamma}_3\left(\mathrm{u},\mathrm{N},\varepsilon\right)+\overset{o}{\Gamma}\left(\mathrm{p},\mathrm{u}\right) \tag{4.5.26}$$

$\Pi_4\left(\mathrm{p},\mathrm{u},\mathrm{N},\varepsilon\right)$ and $\Gamma_4\left(\mathrm{p},\mathrm{u},\mathrm{N},\varepsilon\right)$ are a pair of complementary functionals which satisfy

$$\Pi_4\left(\mathrm{p},\mathrm{u},\mathrm{N},\varepsilon\right)+\Gamma_4\left(\mathrm{p},\mathrm{u},\mathrm{N},\varepsilon\right)=0 \tag{4.5.27}$$

Principle two

If and only if a set of fields, comprising $\mathrm{p},\mathrm{u},\mathrm{N},\varepsilon$, is the solution of a dynamic problem fulfilling Eqs. (4.3.1), (4.3.3), (4.3.4), (4.3.5), (4.3.6), (4.3.7), (4.3.8a) and (4.3.8b), this set satisfies

$\delta\Pi_4\left(\mathrm{p},\mathrm{u},\mathrm{N},\varepsilon\right)=0$ and $\delta\Gamma_4\left(\mathrm{p},\mathrm{u},\mathrm{N},\varepsilon\right)=0$

Proof

By taking variation of Π_4, one has

$$\begin{aligned}&\delta\Pi_4\left(\mathrm{p},\mathrm{u},\mathrm{N},\varepsilon\right)\\&=\int_0^{t_1}\int_0^{L}\left\{\mathrm{p}\,\delta\dot{\mathrm{u}}+\dot{\mathrm{u}}\,\delta\mathrm{p}-\frac{1}{\mathrm{m}}\mathrm{p}\,\delta\mathrm{p}\right\}dxdt+\delta\hat{\Pi}_3\left(\mathrm{u},\mathrm{N},\varepsilon\right)+\delta\overset{o}{\Pi}\left(\mathrm{p},\mathrm{u}\right)\end{aligned}\tag{4.5.28}$$

Substituting Eqs. (4.5.11), (4.5.15) and (4.5.16) into Eq. (4.5.28) yields

$$\begin{aligned}&\delta\Pi_4\left(\mathrm{p},\mathrm{u},\mathrm{N},\varepsilon\right)\\&=\int_0^{L}\int_0^{t_1}\left\{\left[\dot{\mathrm{u}}-\frac{1}{\mathrm{m}}\mathrm{p}\right]\delta\mathrm{p}+\left[\frac{\partial\mathrm{N}}{\partial x}+\mathrm{f}-c\,\dot{\mathrm{u}}-\dot{\mathrm{p}}\right]\delta\mathrm{u}+\left[\mathrm{N}-EA\varepsilon\right]\delta\varepsilon+\left[\varepsilon-\frac{\partial\mathrm{u}}{\partial x}\right]\delta\mathrm{N}\right\}dtdx\\&+\int_0^{t_1}\left\{\left[\mathrm{u}\left(x,t\right)-\bar{\mathrm{u}}\left(x,t\right)\right]\delta\mathrm{N}\left(x,t\right)\Big|_{x_u=0}^{x_u=L}+\left[\bar{\mathrm{N}}\left(x,t\right)-\mathrm{N}\left(x,t\right)\right]\delta\mathrm{u}\left(x,t\right)\Big|_{x_N=0}^{x_N=L}\right\}dt\\&+\int_0^{L}\left\{\left[\bar{\mathrm{p}}\left(x,0\right)-\mathrm{p}\left(x,0\right)\right]\delta\mathrm{u}\left(x,0\right)+\left[\mathrm{u}\left(x,0\right)-\bar{\mathrm{u}}\left(x,0\right)\right]\delta\mathrm{p}\left(x,0\right)\right\}dx\end{aligned}\tag{4.5.29}$$

Bearing in mind the governing equations (4.3.2) are now the prerequisite of this principle, thus are satisfied in the outset. As proved in *Principle one*, all the square brackets have to vanish when the functional $\Pi_4\left(\mathrm{p},\mathrm{u},\mathrm{N},\varepsilon\right)$ finds its stationarity, meaning

$$\dot{\mathrm{u}}-\frac{1}{\mathrm{m}}\mathrm{p}=0\quad\text{i.e.,}\qquad\dot{\mathrm{u}}=\frac{1}{\mathrm{m}}\mathrm{p}\tag{4.5.30}$$

By using Eq. (4.3.2b), it is easy to find

$$\dot{\mathrm{u}} = \frac{1}{\mathrm{m}}\mathrm{p} = \mathrm{v} \tag{4.5.31}$$

It is clear that all governing equations are contained in $\delta\Pi_4(\mathrm{p},\mathrm{u},\mathrm{N},\varepsilon)=0$ implicitly or explicitly.

In a similar fashion, performing the variation on the functional $\Gamma_4(\mathrm{p},\mathrm{u},\mathrm{N},\varepsilon)$

$$\delta\Gamma_4(\mathrm{p},\mathrm{u},\mathrm{N},\varepsilon) = \int_0^{t_1}\int_0^{L}\left\{\frac{1}{\mathrm{m}}\mathrm{p}\,\delta\mathrm{p}+\dot{\mathrm{p}}\,\delta\mathrm{u}+\mathrm{u}\,\delta\dot{\mathrm{p}}\right\}dxdt + \delta\hat{\Gamma}_3(\mathrm{u},\mathrm{N},\varepsilon) + \delta\overset{o}{\Gamma}(\mathrm{p},\mathrm{u}) \tag{4.5.32}$$

Substituting Eqs. (4.5.21), (4.5.23) and (4.5.20) into Eq. (4.5.32) gives

$$\begin{aligned}
&\delta\Gamma_4(\mathrm{p},\mathrm{u},\mathrm{N},\varepsilon)\\
&=\int_0^{t_1}\int_0^{L}\left\{\left[\frac{1}{\mathrm{m}}\mathrm{p}-\dot{\mathrm{u}}\right]\delta\mathrm{p}-\left[\frac{\partial\mathrm{N}}{\partial x}+\mathrm{f}-\mathrm{c}\,\dot{\mathrm{u}}-\dot{\mathrm{p}}\right]\delta\mathrm{u}+\left[EA\varepsilon-\mathrm{N}\right]\delta\varepsilon+\left[\frac{\partial\mathrm{u}}{\partial x}-\varepsilon\right]\delta\mathrm{N}\right\}dxdt\\
&+\int_0^{t_1}\left\{\left[\bar{\mathrm{u}}(x,t)-\mathrm{u}(x,t)\right]\delta\mathrm{N}(x,t)\Big|_{x_u=0}^{x_u=L}+\left[\mathrm{N}(x,t)-\bar{\mathrm{N}}(x,t)\right]\delta\mathrm{u}(x,t)\Big|_{x_N=0}^{x_N=L}\right\}dt\\
&+\int_0^{L}\left\{\left[\mathrm{p}(x,0)-\bar{\mathrm{p}}(x,0)\right]\delta\mathrm{u}(x,0)+\left[\bar{\mathrm{u}}(x,0)-\mathrm{u}(x,0)\right]\delta\mathrm{p}(x,0)\right\}dx
\end{aligned} \tag{4.5.33}$$

Once again, all governing equations are presented implicitly and explicitly in the statement $\delta\Gamma_4(\mathrm{p},\mathrm{u},\mathrm{N},\varepsilon)=0$.

The sufficiency and necessity proofs are similar to the ones of *Principle one*. $\Pi_4(\mathrm{p},\mathrm{u},\mathrm{N},\varepsilon)$ and $\Gamma_4(\mathrm{p},\mathrm{u},\mathrm{N},\varepsilon)$ are, therefore, a pair of complementary functionals suitable for the dynamics of truss-type structures. This completes the proof of *Principle two*.

4.5.3 Three-field unconventional Hamilton-type variational principle

One may obtain one pair of complementary functionals when Eqs. (4.3.1) and (4.3.2) are admitted and hence the fields p and v are replaced with $\dot{\mathrm{u}}$ at the outset. $\mathrm{u}, \mathrm{N}, \varepsilon$ are the remaining independent fields.

By substituting Eqs. (4.3.1) and (4.3.2) into Eqs. (4.5.4) and (4.5.5), one has

$$\Pi_3(\mathrm{u},\mathrm{N},\varepsilon)=\int_0^{t_1}\int_0^L\left\{\frac{1}{2}\mathrm{m}\dot{\mathrm{u}}^2\right\}dxdt+\hat{\Pi}_3(\mathrm{u},\mathrm{N},\varepsilon)+\overset{o}{\hat{\Pi}}(\mathrm{u}) \tag{4.5.34}$$

and

$$\Gamma_3(\mathrm{u},\mathrm{N},\varepsilon)=\int_0^{t_1}\int_0^L\left\{\frac{1}{2\mathrm{m}}(\mathrm{m}\dot{\mathrm{u}})^2+\frac{\partial(\mathrm{m}\dot{\mathrm{u}})}{\partial t}\mathrm{u}\right\}dxdt+\hat{\Gamma}_3(\mathrm{u},\mathrm{N},\varepsilon)+\overset{o}{\hat{\Gamma}}(\mathrm{u}) \tag{4.5.35}$$

where

$$\begin{aligned}\overset{o}{\hat{\Pi}}(\mathrm{u})=\int_0^L\{&\alpha\,\mathrm{m}\overset{o}{\dot{\mathrm{u}}}(x,t_1)\overset{o}{\mathrm{u}}(x,t_1)-\mathrm{m}\overset{o}{\dot{\mathrm{u}}}(x,t_1)\mathrm{u}(x,t_1)+\mathrm{m}\overline{\dot{\mathrm{u}}}(x,0)\mathrm{u}(x,0)\\&+\mathrm{m}\dot{\mathrm{u}}(x,0)\overset{o}{\mathrm{u}}(x,0)-\mathrm{m}\dot{\mathrm{u}}(x,0)\overline{\mathrm{u}}(x,0)-\beta\,\mathrm{m}\overset{o}{\dot{\mathrm{u}}}(x,0)\overset{o}{\mathrm{u}}(x,0)\}dx\end{aligned} \tag{4.5.36}$$

and

$$\begin{aligned}\overset{o}{\hat{\Gamma}}(\mathrm{u})=\int_0^L\{&(1-\alpha)\,\mathrm{m}\overset{o}{\dot{\mathrm{u}}}(x,t_1)\overset{o}{\mathrm{u}}(x,t_1)-\mathrm{m}\dot{\mathrm{u}}(x,t_1)\overset{o}{\mathrm{u}}(x,t_1)-\mathrm{m}\overline{\dot{\mathrm{u}}}(x,0)\mathrm{u}(x,0)\\&+\mathrm{m}\overset{o}{\dot{\mathrm{u}}}(x,0)\mathrm{u}(x,0)+\mathrm{m}\dot{\mathrm{u}}(x,0)\overline{\mathrm{u}}(x,0)-(1-\beta)\,\mathrm{m}\overset{o}{\dot{\mathrm{u}}}(x,0)\overset{o}{\mathrm{u}}(x,0)\}dx\end{aligned} \tag{4.5.37}$$

Again, α and β are the coefficients assisting the construction of the functionals, the value of which are not required in the following discussion.

$\Pi_3\left(\mathrm{u},\mathrm{N},\varepsilon\right)$ and $\Gamma_3\left(\mathrm{u},\mathrm{N},\varepsilon\right)$ are a pair of complementary functionals such that

$$\Pi_3\left(\mathrm{u},\mathrm{N},\varepsilon\right)+\Gamma_3\left(\mathrm{u},\mathrm{N},\varepsilon\right)=0 \tag{4.5.38}$$

Principle three

If and only if a set of fields, comprising $\mathrm{u},\mathrm{N},\varepsilon$, is the solution of a dynamic problem fulfilling Eqs. (4.3.3), (4.3.4), (4.3.5), (4.3.6), (4.3.7), (4.3.8a) and (4.3.8b), this set satisfies

$$\delta\Pi_3\left(\mathrm{u},\mathrm{N},\varepsilon\right)=0 \text{ and } \delta\Gamma_3\left(\mathrm{u},\mathrm{N},\varepsilon\right)=0$$

Proof

Taking variation of $\Pi_3\left(\mathrm{u},\mathrm{N},\varepsilon\right)$, one has

$$\delta\Pi_3\left(\mathrm{u},\mathrm{N},\varepsilon\right)=\int_0^{t_1}\int_0^{L}\left\{\mathrm{m}\dot{\mathrm{u}}\,\delta\dot{\mathrm{u}}\right\}dxdt+\delta\hat{\Pi}_3\left(\mathrm{u},\mathrm{N},\varepsilon\right)+\delta\overset{o}{\hat{\Pi}}\left(\mathrm{u}\right) \tag{4.5.39}$$

Integrating the first integral by parts

$$\int_0^{t_1}\int_0^{L}\left\{\mathrm{m}\dot{\mathrm{u}}\,\delta\dot{\mathrm{u}}\right\}dxdt=\int_0^{L}\left\{\mathrm{m}\dot{\mathrm{u}}\,\delta\mathrm{u}\Big|_{t=0}^{t=t_1}-\int_0^{t_1}\left\{\mathrm{m}\frac{\partial^2\mathrm{u}}{\partial t^2}\delta\mathrm{u}\right\}dt\right\}dx \tag{4.5.40}$$

and expand the term $\delta\overset{o}{\hat{\Pi}}\left(\mathrm{u}\right)$ in Eq. (4.5.40) as

$$\begin{aligned}\delta \overset{o}{\hat{\Pi}}(\mathrm{u}) = \int_0^L \{ &- \mathrm{m}\dot{\mathrm{u}}(x,t_1)\delta \mathrm{u}(x,t_1) + \mathrm{m}\bar{\dot{\mathrm{u}}}(x,0)\delta \mathrm{u}(x,0) \\ &+ \left[\mathrm{u}(x,0) - \bar{\mathrm{u}}(x,0)\right]\delta\left(\mathrm{m}\dot{\mathrm{u}}(x,0)\right)\}dx\end{aligned} \tag{4.5.41}$$

Substituting Eqs. (4.5.15), (4.5.40) and (4.5.41) into Eq. (4.5.39), yields

$$\begin{aligned}&\delta \Pi_3(\mathrm{u},\mathrm{N},\varepsilon) \\ &= \int_0^L \int_0^{t_1} \left\{ \left[\frac{\partial \mathrm{N}}{\partial x} + \mathrm{f} - c\dot{\mathrm{u}} - \mathrm{m}\frac{\partial^2 \mathrm{u}}{\partial t^2} \right]\delta \mathrm{u} + \left[\mathrm{N} - EA\varepsilon\right]\delta\varepsilon + \left[\varepsilon - \frac{\partial \mathrm{u}}{\partial x} \right]\delta \mathrm{N} \right\} dtdx \\ &+ \int_0^{t_1} \left\{ \left[\mathrm{u}(x,t) - \bar{\mathrm{u}}(x,t)\right]\delta \mathrm{N}(x,t)\Big|_{x_u=0}^{x_u=L} + \left[\bar{\mathrm{N}}(x,t) - \mathrm{N}(x,t)\right]\delta \mathrm{u}(x,t)\Big|_{x_N=0}^{x_N=L} \right\} dt \\ &+ \int_0^L \left\{ \mathrm{m}\left[\bar{\dot{\mathrm{u}}}(x,0) - \dot{\mathrm{u}}(x,0)\right]\delta \mathrm{u}(x,0) + \left[\mathrm{u}(x,0) - \bar{\mathrm{u}}(x,0)\right]\delta\left(\mathrm{m}\dot{\mathrm{u}}(x,0)\right) \right\} dx\end{aligned} \tag{4.5.42}$$

Similarly, take variation of $\Gamma_3(\mathrm{u},\mathrm{N},\varepsilon)$

$$\delta \Gamma_3(\mathrm{u},\mathrm{N},\varepsilon) = \int_0^{t_1}\int_0^L \left\{ \mathrm{m}\dot{\mathrm{u}}\,\delta\dot{\mathrm{u}} + \mathrm{m}\frac{\partial^2 \mathrm{u}}{\partial t^2}\delta \mathrm{u} + \mathrm{u}\,\delta\frac{\mathrm{m}\partial^2 \mathrm{u}}{\partial t^2} \right\} dxdt + \delta \hat{\Gamma}_3(\mathrm{u},\mathrm{N},\varepsilon) + \delta \overset{o}{\hat{\Gamma}}(\mathrm{u}) \tag{4.5.43}$$

It can be seen that

$$\begin{aligned}&\int_0^{t_1}\int_0^L \left\{ \mathrm{mu}\,\delta\frac{\partial^2 \mathrm{u}}{\partial t^2} \right\} dxdt \\ &= \int_0^{t_1}\int_0^L \left\{ \mathrm{mu}\frac{\partial^2 \delta \mathrm{u}}{\partial t^2} \right\} dxdt = \int_0^L \left\{ \mathrm{u}\,\delta\left(\mathrm{m}\dot{\mathrm{u}}\right)\Big|_{t=0}^{t=t_1} \right\} dx - \int_0^{t_1}\int_0^L \left\{ \mathrm{m}\dot{\mathrm{u}}\,\delta\dot{\mathrm{u}} \right\} dxdt\end{aligned} \tag{4.5.44}$$

and

$$\delta \overset{o}{\hat{\Gamma}}(\mathrm{u}) = \int_0^L \{ \bar{\mathrm{u}}(x,0)\delta\left(\mathrm{m}\dot{\mathrm{u}}(x,0)\right) - \mathrm{u}(x,t_1)\delta\left(\mathrm{m}\dot{\mathrm{u}}(x,t_1)\right) + \mathrm{m}\left[\dot{\mathrm{u}}(x,0) - \dot{\bar{\mathrm{u}}}(x,0)\right]\delta\mathrm{u}(x,0)\} dx \tag{4.5.45}$$

By virtue of Eqs. (4.5.23), (4.5.44) and (4.5.45), it is found Eq. (4.5.43) may now be transformed as

$$\begin{aligned}
&\delta\Gamma_3(\mathrm{u},\mathrm{N},\varepsilon) \\
&= \int_0^{t_1}\int_0^L \left\{ \left[EA\varepsilon - \mathrm{N}\right]\delta\varepsilon + \left[\frac{\partial \mathrm{u}}{\partial x} - \varepsilon\right]\delta\mathrm{N} - \left[\frac{\partial \mathrm{N}}{\partial x} + \mathrm{f} - \mathrm{c}\dot{\mathrm{u}} - \mathrm{m}\frac{\partial^2 \mathrm{u}}{\partial t^2}\right]\delta\mathrm{u} \right\} dxdt \\
&+ \int_0^{t_1} \left\{ \left[\bar{\mathrm{u}}(x,t) - \mathrm{u}(x,t)\right]\delta\mathrm{N}(x,t)\Big|_{x_u=0}^{x_u=L} + \left[\mathrm{N}(x,t) - \bar{\mathrm{N}}(x,t)\right]\delta\mathrm{u}(x,t)\Big|_{x_N=0}^{x_N=L} \right\} dt \\
&+ \int_0^L \left\{ \mathrm{m}\left[\dot{\mathrm{u}}(x,0) - \dot{\bar{\mathrm{u}}}(x,0)\right]\delta\mathrm{u}(x,0) + \left[\bar{\mathrm{u}}(x,0) - \mathrm{u}(x,0)\right]\delta\left(\mathrm{m}\dot{\mathrm{u}}(x,0)\right) \right\} dx
\end{aligned} \tag{4.5.46}$$

In a similar fashion to the proof of Principle one, and bearing in mind that Eqs. (4.3.1) and (4.3.2) are the preconditions of this principle, it can be observed in the variational statements Eqs. (4.5.42) and Eq. (4.5.46) that all Governing equations have to be satisfied when the stationarity of $\Pi_3(\mathrm{u},\mathrm{N},\varepsilon)$ and $\Gamma_3(\mathrm{u},\mathrm{N},\varepsilon)$ are found, thus $\Pi_3(\mathrm{u},\mathrm{N},\varepsilon)$ and $\Gamma_3(\mathrm{u},\mathrm{N},\varepsilon)$ are a pair of complementary functionals for a dynamic problem. This completes the proof for *Principle three*.

4.5.4 Two-field unconventional Hamilton-type variational principle

When the relations Eqs. (4.3.2), (4.3.4) and (4.3.5) are admitted as prerequisites, a two-field variational principle with only p and u as the independent fields may be derived as follows.

Substituting Eqs. (4.3.2), (4.3.4) and (4.3.5) into Eqs. (4.5.4) and (4.5.5), one has

$$\Pi_2(\mathrm{p},\mathrm{u})=\int_0^{t_1}\int_0^{L}\left\{\mathrm{p}\dot{\mathrm{u}}-\frac{1}{2\mathrm{m}}\mathrm{p}^2\right\}dxdt+\hat{\Pi}_1(\mathrm{u})+\overset{o}{\Pi}(\mathrm{p},\mathrm{u}) \tag{4.5.47}$$

and

$$\Gamma_2(\mathrm{p},\mathrm{u})=\int_0^{t_1}\int_0^{L}\left\{\frac{1}{2\mathrm{m}}\mathrm{p}^2+\dot{\mathrm{p}}\mathrm{u}\right\}dxdt+\hat{\Gamma}_1(\mathrm{u})+\overset{o}{\Gamma}(\mathrm{p},\mathrm{u}) \tag{4.5.48}$$

whereas $\overset{o}{\Pi}(\mathrm{p},\mathrm{u})$ and $\overset{o}{\Gamma}(\mathrm{p},\mathrm{u})$ are given by Eqs. (4.5.8) and (4.5.9) respectively,

$$\begin{aligned}&\hat{\Pi}_1(\mathrm{u})\\&=\int_0^{t_1}\int_0^{L}\left\{-\frac{1}{2}EA\left(\frac{\partial\mathrm{u}}{\partial x}\right)^2+\left[\mathrm{f}-\mathrm{c}\overset{\mathrm{o}}{\dot{\mathrm{u}}}\right]\mathrm{u}\right\}dxdt\\&+\int_0^{t_1}\left\{EA\frac{\partial\mathrm{u}(x,t)}{\partial x}\left[\mathrm{u}(x,t)-\bar{\mathrm{u}}(x,t)\right]\Big|_{\substack{x_u=L\\x_u=0}}+\bar{\mathrm{N}}(x,t)\mathrm{u}(x,t)\Big|_{\substack{x_N=L\\x_N=0}}\right\}dt\end{aligned} \tag{4.5.49}$$

$$\begin{aligned}&\hat{\Gamma}_1(\mathrm{u})\\&=\int_0^{t_1}\int_0^{L}\left\{-\frac{1}{2}EA\left(\frac{\partial\mathrm{u}}{\partial x}\right)^2-EA\frac{\partial^2\mathrm{u}}{\partial x^2}\mathrm{u}-\left[\mathrm{f}-c\overset{\mathrm{o}}{\dot{\mathrm{u}}}\right]\mathrm{u}\right\}dxdt\\&+\int_0^{t_1}\left\{EA\frac{\partial\mathrm{u}(x,t)}{\partial x}\bar{\mathrm{u}}(x,t)\Big|_{\substack{x_u=L\\x_u=0}}+\left[EA\frac{\partial\mathrm{u}(x,t)}{\partial x}-\bar{\mathrm{N}}(x,t)\right]\mathrm{u}(x,t)\Big|_{\substack{x_N=L\\x_N=0}}\right\}dt\end{aligned} \tag{4.5.50}$$

It can be easily verified that

$$\Pi_2(\mathrm{p},\mathrm{u})+\Gamma_2(\mathrm{p},\mathrm{u})=0 \tag{4.5.51}$$

Therefore they are a pair of complementary functionals.

Principle four

If and only if a set of fields, comprising p,u, is the solution of a dynamic problem fulfilling Eqs. (4.3.1), (4.3.3), (4.3.6), (4.3.7), (4.3.8a) and (4.3.8b), this set satisfies

$$\delta\Pi_2\left(\mathrm{p},\mathrm{u}\right)=0 \text{ and } \delta\Gamma_2\left(\mathrm{p},\mathrm{u}\right)=0$$

Proof

Taking variation of $\Pi_2\left(\mathrm{p},\mathrm{u}\right)$, one has

$$\begin{aligned}&\delta\Pi_2\left(\mathrm{p},\mathrm{u}\right)\\&=\int_0^{t_1}\int_0^{L}\left\{\mathrm{p}\,\delta\dot{\mathrm{u}}+\left[\dot{\mathrm{u}}-\frac{1}{\mathrm{m}}\mathrm{p}\right]\delta\mathrm{p}\right\}dxdt+\delta\hat{\Pi}_1\left(\mathrm{u}\right)+\delta\overset{o}{\Pi}\left(\mathrm{p},\mathrm{u}\right)\end{aligned}\tag{4.5.52}$$

and the variation of $\hat{\Pi}_1\left(\mathrm{u}\right)$ is given by

$$\begin{aligned}&\delta\hat{\Pi}_1\left(\mathrm{u}\right)\\&=\int_0^{t_1}\int_0^{L}\left\{-EA\frac{\partial\mathrm{u}}{\partial x}\delta\frac{\partial\mathrm{u}}{\partial x}+\left[\mathrm{f}-\mathrm{c}\overset{\mathrm{o}}{\dot{\mathrm{u}}}\right]\delta\mathrm{u}\right\}dxdt\\&+\int_0^{t_1}\left\{\begin{array}{l}\delta\left(EA\dfrac{\partial\mathrm{u}\left(x,t\right)}{\partial x}\right)\left[\mathrm{u}\left(x,t\right)-\bar{\mathrm{u}}\left(x,t\right)\right]\Big|_{x_u=0}^{x_u=L}\\+EA\dfrac{\partial\mathrm{u}\left(x,t\right)}{\partial x}\delta\mathrm{u}\left(x,t\right)\Big|_{x_u=0}^{x_u=L}+\bar{\mathrm{N}}\left(x,t\right)\delta\mathrm{u}\left(x,t\right)\Big|_{x_N=0}^{x_N=L}\end{array}\right\}dt\end{aligned}\tag{4.5.53}$$

Using integration by parts, the first term in the first integrand may be expressed as

$$\begin{aligned}
&\int_0^{t_1}\int_0^{L}\left\{-EA\frac{\partial \mathrm{u}}{\partial x}\delta\frac{\partial \mathrm{u}}{\partial x}\right\}dxdt \\
&=\int_0^{t_1}\int_0^{L}\left\{EA\frac{\partial^2 \mathrm{u}}{\partial x^2}\delta \mathrm{u}\right\}dxdt-\int_0^{t_1}\left\{EA\frac{\partial \mathrm{u}(x,t)}{\partial x}\delta \mathrm{u}(x,t)\Big|_{x_u=0}^{x_u=L}\right\}dt \\
&-\int_0^{t_1}\left\{EA\frac{\partial \mathrm{u}(x,t)}{\partial x}\delta \mathrm{u}(x,t)\Big|_{N_u=0}^{N_u=L}\right\}dt
\end{aligned} \tag{4.5.54}$$

Therefore $\delta\hat{\Pi}_1(\mathrm{u})$ is transformed as

$$\begin{aligned}
&\delta\hat{\Pi}_1(\mathrm{u}) \\
&=\int_0^{t_1}\int_0^{L}\left\{\left[EA\frac{\partial^2 \mathrm{u}}{\partial x^2}+\mathrm{f}-\mathrm{c}\dot{\mathrm{u}}\right]\delta \mathrm{u}\right\}dxdt \\
&+\int_0^{t_1}\left\{\begin{array}{l}\delta\left(EA\dfrac{\partial \mathrm{u}(x,t)}{\partial x}\right)\left[\mathrm{u}(x,t)-\bar{\mathrm{u}}(x,t)\right]\Big|_{x_u=0}^{x_u=L} \\ +\left[\bar{\mathrm{N}}(x,t)-EA\dfrac{\partial \mathrm{u}(x,t)}{\partial x}\right]\delta \mathrm{u}(x,t)\Big|_{x_N=0}^{x_N=L}\end{array}\right\}dt
\end{aligned} \tag{4.5.55}$$

Substituting Eqs. (4.5.11), (4.5.16) and (4.5.55) into Eq. (4.5.52), one has

$$\begin{aligned}
&\delta\Pi_2(\mathrm{p},\mathrm{u}) \\
&=\int_0^{t_1}\int_0^{L}\left\{\left[\dot{\mathrm{u}}-\frac{1}{\mathrm{m}}\mathrm{p}\right]\delta \mathrm{p}+\left[EA\frac{\partial^2 \mathrm{u}}{\partial x^2}+\mathrm{f}-\mathrm{c}\dot{\mathrm{u}}-\dot{\mathrm{p}}\right]\delta \mathrm{u}\right\}dxdt \\
&+\int_0^{t_1}\left\{\left[\mathrm{u}(x,t)-\bar{\mathrm{u}}(x,t)\right]\delta\left(EA\frac{\partial \mathrm{u}(x,t)}{\partial x}\right)\Big|_{x_u=0}^{x_u=L}\right\}dt \\
&+\int_0^{t_1}\left\{\left[\bar{\mathrm{N}}(x,t)-EA\frac{\partial \mathrm{u}(x,t)}{\partial x}\right]\delta \mathrm{u}(x,t)\Big|_{x_N=0}^{x_N=L}\right\}dt \\
&+\int_0^{L}\left\{\left[\bar{\mathrm{p}}(x,0)-\mathrm{p}(x,0)\right]\delta \mathrm{u}(x,0)+\left[\mathrm{u}(x,0)-\bar{\mathrm{u}}(x,0)\right]\delta \mathrm{p}(x,0)\right\}dx
\end{aligned} \tag{4.5.56}$$

Taking variation of $\Gamma_2(\mathrm{p},\mathrm{u})$, one has

$$\delta\Gamma_2(\mathrm{p},\mathrm{u})=\int_0^{t_1}\int_0^{L}\left\{\frac{1}{\mathrm{m}}\mathrm{p}\,\delta\mathrm{p}+\dot{\mathrm{p}}\,\delta\mathrm{u}+\mathrm{u}\,\delta\dot{\mathrm{p}}\right\}dxdt+\delta\hat{\Gamma}_1(\mathrm{u})+\delta\overset{o}{\Gamma}(\mathrm{p},\mathrm{u}) \tag{4.5.57}$$

The variation of $\hat{\Gamma}_1(\mathrm{u})$ is given by

$$\begin{aligned}
&\delta\hat{\Gamma}_1(\mathrm{u})\\
&=\int_0^{t_1}\int_0^{L}\left\{-EA\frac{\partial\mathrm{u}}{\partial x}\delta\frac{\partial\mathrm{u}}{\partial x}-EA\frac{\partial^2\mathrm{u}}{\partial x^2}\delta\mathrm{u}-EA\mathrm{u}\,\delta\left(\frac{\partial^2\mathrm{u}}{\partial x^2}\right)-\left[\mathrm{f}-c\dot{\mathrm{u}}\right]\delta\mathrm{u}\right\}dxdt\\
&+\int_0^{t_1}\left\{\delta\left(EA\frac{\partial\mathrm{u}(x,t)}{\partial x}\right)\overline{\mathrm{u}}(x,t)\Big|_{x_u=0}^{x_u=L}+\left[EA\frac{\partial\mathrm{u}(x,t)}{\partial x}-\overline{\mathrm{N}}(x,t)\right]\delta\mathrm{u}(x,t)\Big|_{x_N=0}^{x_N=L}\right\}dt\\
&+\int_0^{t_1}\left\{\delta\left[EA\frac{\partial\mathrm{u}(x,t)}{\partial x}\right]\mathrm{u}(x,t)\Big|_{x_N=0}^{x_N=L}\right\}dt
\end{aligned} \tag{4.5.58}$$

Therefore $\delta\Gamma_2(\mathrm{p},\mathrm{u})$ is obtained by substituting Eqs. (4.5.20), (4.5.21) and (4.5.58) into Eq. (4.5.57),

$$\begin{aligned}
&\delta\Gamma_2(\mathrm{p},\mathrm{u})\\
&=\int_0^{t_1}\int_0^{L}\left\{\left[\frac{1}{\mathrm{m}}\mathrm{p}-\dot{\mathrm{u}}\right]\delta\mathrm{p}+\left[EA\frac{\partial^2\mathrm{u}}{\partial x^2}+\mathrm{f}-c\dot{\mathrm{u}}-\dot{\mathrm{p}}\right]\delta\mathrm{u}\right\}dxdt\\
&+\int_0^{t_1}\left\{\left[\overline{\mathrm{u}}(x,t)-\mathrm{u}(x,t)\right]\delta\left(EA\frac{\partial\mathrm{u}(x,t)}{\partial x}\right)\Big|_{x_u=0}^{x_u=L}\right\}dt\\
&+\int_0^{t_1}\left\{\left[EA\frac{\partial\mathrm{u}(x,t)}{\partial x}-\overline{\mathrm{N}}(x,t)\right]\delta\mathrm{u}(x,t)\Big|_{x_N=0}^{x_N=L}\right\}dt\\
&+\int_0^{L}\left\{\left[\mathrm{p}(x,0)-\overline{\mathrm{p}}(x,0)\right]\delta\mathrm{u}(x,0)+\left[\overline{\mathrm{u}}(x,0)-\mathrm{u}(x,0)\right]\delta\mathrm{p}(x,0)\right\}dx
\end{aligned} \tag{4.5.59}$$

It is clear from Eqs. (4.5.56) and (4.5.59) that the Euler equations given by both $\Pi_2(\mathrm{p},\mathrm{u})$ and $\Gamma_2(\mathrm{p},\mathrm{u})$ are the boundary condition $\overline{\mathrm{u}}(x,t)-\mathrm{u}(x,t)=0$ on the

displacement boundary x_u (Eq. 4.3.7); as well as the initial conditions Eqs. (4.3.8a) and (4.3.8b), plus the following two equations

$$\frac{1}{\mathrm{m}}\mathrm{p}-\dot{\mathrm{u}}=0 \tag{4.5.60}$$

and

$$EA\frac{\partial^2 \mathrm{u}}{\partial x^2}+\mathrm{f}-\mathrm{c}\dot{\mathrm{u}}-\dot{\mathrm{p}}=0 \tag{4.5.61}$$

With the precondition Eq. (4.3.2b), Eq. (4.5.60) is essentially the governing equation (4.3.1), i.e.

$$\frac{1}{\mathrm{m}}\mathrm{p}-\dot{\mathrm{u}}=\mathrm{v}-\dot{\mathrm{u}}=0 \tag{4.5.62}$$

With the prerequisites Eqs. (4.3.4) and (4.3.5), the Euler equation (4.5.61) is in fact the governing equation (4.3.3)

$$EA\frac{\partial^2 \mathrm{u}}{\partial x^2}+\mathrm{f}-\mathrm{c}\dot{\mathrm{u}}-\dot{\mathrm{p}}=\frac{\partial}{\partial x}\left(EA\varepsilon\right)+\mathrm{f}-\mathrm{c}\dot{\mathrm{u}}-\dot{\mathrm{p}}=\frac{\partial \mathrm{N}}{\partial x}+\mathrm{f}-\mathrm{c}\dot{\mathrm{u}}-\dot{\mathrm{p}}=0 \tag{4.5.63}$$

Therefore all governing equations are obtained in the variations of $\Pi_2\left(\mathrm{p},\mathrm{u}\right)$ and $\Gamma_2\left(\mathrm{p},\mathrm{u}\right)$, and this two functionals are consequently a set of complementary functionals for the dynamic problems of truss-type structures. This completes the proof of *Principle four*.

4.5.5 One-field unconventional Hamilton-type variational principle

When the governing equations (4.3.1), (4.3.2), (4.3.4) and (4.3.5) are admitted in $\Pi_5(\mathrm{p},\mathrm{v},\mathrm{u},\mathrm{N},\varepsilon)$ and $\Gamma_5(\mathrm{p},\mathrm{v},\mathrm{u},\mathrm{N},\varepsilon)$ one more pair of functionals are found with u is the only remaining field.

The two functionals $\Pi_1(\mathrm{u})$ and $\Gamma_1(\mathrm{u})$ are as follows

$$\Pi_1(\mathrm{u})=\int_0^{t_1}\int_0^{L}\left\{\frac{1}{2}\mathrm{m}\,\dot{\mathrm{u}}^2\right\}dxdt+\hat{\Pi}_1(\mathrm{u})+\overset{o}{\hat{\Pi}}(\mathrm{u}) \tag{4.5.64}$$

and

$$\Gamma_1(\mathrm{u})=\int_0^{t_1}\int_0^{L}\left\{\frac{1}{2}\mathrm{m}\dot{\mathrm{u}}^2+\frac{\partial(\mathrm{m}\dot{\mathrm{u}})}{\partial t}\mathrm{u}\right\}dxdt+\hat{\Gamma}_1(\mathrm{u})+\overset{o}{\hat{\Gamma}}(\mathrm{u}) \tag{4.5.65}$$

Where $\hat{\Pi}_1(\mathrm{u})$ and $\hat{\Gamma}_1(\mathrm{u})$ are given by Eqs. (4.5.49) and (4.5.50) respectively, and $\overset{o}{\hat{\Pi}}(\mathrm{u})$ and $\overset{o}{\hat{\Gamma}}(\mathrm{u})$ are given by Eqs. (4.5.36) and (4.5.37).

$\Pi_1(\mathrm{u})$ and $\Gamma_1(\mathrm{u})$ are a pair of complementary functionals such that

$$\Pi_1(\mathrm{u})+\Gamma_1(\mathrm{u})=0 \tag{4.5.66}$$

Principle five

If and only if u is the solution of a dynamic problem fulfilling Eqs. (4.3.3), (4.3.6), (4.3.7), (4.3.8a) and (4.3.8b), this field satisfies

$$\delta\Pi_1(\mathrm{u})=0 \text{ and } \delta\Gamma_1(\mathrm{u})=0$$

Proof

By taking variation of $\Pi_1(\mathrm{u})$, one has

$$\delta\Pi_1(\mathrm{u}) = \int_0^{t_1}\int_0^{L}\{\mathrm{m}\,\dot{\mathrm{u}}\,\delta\,\dot{\mathrm{u}}\}dxdt + \delta\hat{\Pi}_1(\mathrm{u}) + \delta\overset{o}{\hat{\Pi}}(\mathrm{u}) \tag{4.5.67}$$

By virtue of Eqs. (4.5.40), (4.5.41) and (4.5.55), one has

$$\begin{aligned}
&\delta\Pi_1(\mathrm{u}) \\
&= \int_0^{t_1}\int_0^{L}\left\{\left[EA\frac{\partial^2\mathrm{u}}{\partial x^2} + \mathrm{f} - \mathrm{c}\dot{\mathrm{u}} - \mathrm{m}\frac{\partial^2\mathrm{u}}{\partial t^2}\right]\delta\,\mathrm{u}\right\}dxdt \\
&+\int_0^{t_1}\left\{\left[\mathrm{u}(x,t) - \bar{\mathrm{u}}(x,t)\right]\delta\left(EA\frac{\partial\,\mathrm{u}(x,t)}{\partial x}\right)\Big|_{\substack{x_u=L\\x_u=0}}\right\}dt \\
&+\int_0^{t_1}\left\{\left[\bar{\mathrm{N}}(x,t) - EA\frac{\partial\,\mathrm{u}(x,t)}{\partial x}\right]\delta\,\mathrm{u}(x,t)\Big|_{\substack{x_N=L\\x_N=0}}\right\}dt \\
&+\int_0^{L}\left\{\mathrm{m}\left[\dot{\bar{\mathrm{u}}}(x,0) - \dot{\mathrm{u}}(x,0)\right]\delta\,\mathrm{u}(x,0) + \left[\mathrm{u}(x,0) - \bar{\mathrm{u}}(x,0)\right]\delta\left(\mathrm{m}\dot{\mathrm{u}}(x,0)\right)\right\}dx
\end{aligned} \tag{4.5.68}$$

Similarly, taking variation of $\Gamma_1(\mathrm{u})$, one has

$$\delta\Gamma_1(\mathrm{u}) = \int_0^{t_1}\int_0^{L}\left\{\mathrm{m}\dot{\mathrm{u}}\,\delta\,\dot{\mathrm{u}} + \mathrm{m}\frac{\partial^2\mathrm{u}}{\partial t^2}\delta\,\mathrm{u} + \mathrm{m}\mathrm{u}\,\delta\frac{\partial^2\mathrm{u}}{\partial t^2}\right\}dxdt + \delta\hat{\Gamma}_1(\mathrm{u}) + \delta\overset{o}{\hat{\Gamma}}(\mathrm{u}) \tag{4.5.69}$$

Substitution of Eqs. (4.5.23), (4.5.44) and (4.5.45) into Eq. (4.5.69) gives

$$
\begin{aligned}
&\delta\Gamma_1(\mathrm{u}) \\
&= \int_0^{t_1}\int_0^{L}\left\{-\left[EA\frac{\partial^2 \mathrm{u}}{\partial x^2}+\mathrm{f}-\mathrm{c}\dot{\mathrm{u}}-\mathrm{m}\frac{\partial^2 \mathrm{u}}{\partial t^2}\right]\delta \mathrm{u}\right\}dxdt \\
&+\int_0^{t_1}\left\{\left[\bar{\mathrm{u}}(x,t)-\mathrm{u}(x,t)\right]\delta\left(EA\frac{\partial \mathrm{u}(x,t)}{\partial x}\right)\Big|_{\substack{x_u=L\\ x_u=0}}\right\}dt \\
&+\int_0^{t_1}\left\{\left[EA\frac{\partial \mathrm{u}(x,t)}{\partial x}-\bar{\mathrm{N}}(x,t)\right]\delta \mathrm{u}(x,t)\Big|_{\substack{x_N=L\\ x_N=0}}\right\}dt \\
&+\int_0^{L}\left\{\left[\mathrm{m}\dot{\mathrm{u}}(x,0)-\mathrm{m}\dot{\bar{\mathrm{u}}}(x,0)\right]\delta \mathrm{u}(x,0)+\left[\bar{\mathrm{u}}(x,0)-\mathrm{u}(x,0)\right]\delta\left(\mathrm{m}\dot{\mathrm{u}}(x,0)\right)\right\}dx
\end{aligned}
\tag{4.5.70}
$$

By making use of Eqs. (4.3.4) and (4.3.5), one of the Euler equations obtained in Eqs. (4.5.68) and (4.5.70), $EA\frac{\partial \mathrm{u}(x,t)}{\partial x}-\tilde{\mathrm{N}}(x,t)=0$, is equal to the traction boundary condition Eq. (4.3.6). Another one, $\mathrm{m}\dot{\mathrm{u}}(x,0)-\mathrm{m}\dot{\bar{\mathrm{u}}}(x,0)=0$, is in fact one of the initial conditions Eq. (4.3.8b) with the assistance of Eqs. (4.3.1) and (4.3.2a). Thus all governing equations have to be satisfied when the two functionals find their stationarity. The sufficiency and necessity proofs are similar to that in the proof of Principle one, consequently it is clear that $\Pi_1(\mathrm{u})$ and $\Gamma_1(\mathrm{u})$ are a pair of complementary variational principles for the dynamics of truss-type structures. This completes the proof of *Principle five*.

4.6 Summary

Five Unconventional Hamilton-type Variational Principles are presented for truss-type structures in this chapter. *Principle one* is the most general one with five independent variable fields. It takes full account of the dynamic characteristics of a truss-type system. Furthermore, it also incorporates boundary conditions and initial conditions without using Lagrange multipliers or any artificial coefficients. The derivation of the principle is straightforward and has a solid mathematic foundation. In addition, each principle yields a pairs of functionals; either one can

be selected to construct numerical algorithms for dynamic solutions. This feature makes this principle distinctive to other variational principles and laws. Unlike Gurtin's principle, the presented variational formulation involves no convolution operators hence the computation cost is reduced. The other four UHVPs are the simplified version of *Principle one* with less variable fields when certain control equations are set as a priori. Simplified versions offer computational advantage due to fewer unknowns to solve. This feature is explored in the remaining chapters to construct a space-time finite element method for the dynamic analysis of truss-type structures.

Chapter 5 Finite Elements in the Temporal Domain

5.1 Introduction

Traditionally dynamic problems were solved with various finite difference methods in the temporal domain (Richymyer and Morton, 1967; Newmark, 1962). Following the fruitful applications of the finite element method (FEM) in the spatial domain, it becomes promising and natural to extend the FEM into the temporal domain as well for time-varying problems. Finite element in time offers "a unified solution strategy for the space-time domain which could give synergistic improvements in computational efficiency"; "finite element in time could be tuned to give minimum error at points for which the greatest accuracy is desired" (Peters and Izadpanah, 1988). The variational principles presented in the last chapter lead to several corresponding weak formulations for truss-type structures and facilitate a unified solution procedure as suggested by Peters and Izadpanah.

In this chapter, two fundamental aspects of implementing time finite element are discussed briefly, i.e., the global approximation and piecewise approximation; the simultaneous discretisation and semi-discretisation and the associated advantage and disadvantage are presented. Various time finite elements used in the literatures are reviewed next, followed by the introduction of the time finite elements adopted in the present study.

5.2 Global approximation or piecewise approximation

Finite element in time can be implemented in two ways. The first one is the global approximation, where time finite elements are applied to the entire time domain and the unknown values for all time nodes are coupled together and solved simultaneously; the second is to divide the time domain into successive time intervals and seeking solutions in a stepwise fashion, i.e., using the known values

(either the initial conditions or the results of the previous time step) as the input to advance the results at the end of the current time step. This procedure is repeated until the end of the time domain is reached. There are pros and cons associated with each method, which are summarised in the following table.

	pros	cons
Global approximation	● Presenting time finite element and spatial finite element in an uniform framework. ● Results of higher accuracy may be obtained. [1,2]	● More unknowns to be solved thus leading to significant bigger equation set to be solved. ● Less satisfaction in the algorithmic stability compared to piecewise approximation. [1]
Piecewise approximation	● Smaller equation system which can be solved more economically. ● Improved algorithmic stability.	● Accuracy may be compromised[1], due to error accumulation in each step, but it can be improved if smaller time steps are used.

1. (Baruch and Riff, 1984)
2. (Howard and Penny, 1978)

Table 5.2.1 – Comparison of global and piecewise approximations

In the presented research, the piecewise approximation, which is of the single-step type, is adopted for the proposed numerical scheme, on the consideration of low computational cost and the stability reasons. Meanwhile, as highlighted by Howard and Penny (1978), the accuracy can be maintained by the suitable choice of time step length.

5.3 Simultaneous discretisation or semi-discretisation

There are two approaches to apply the finite element method in the temporal domain. The first approach is found in the early publications of the time finite element study, where time was treated as an additional dimension along with the spatial dimensions (Oden, 1969); the resulting space-time domain was discretised

with shape functions based on both the spatial and the temporal coordinates, therefore some refers this treatment as Space-Time Finite Element Method (STFEM) (Bajer, 1986). Mathematically, this discretisation procedure may be expressed as

$$\xi(x,t) = \sum_i N_i(x,t)\hat{\xi}_i(x,t) \tag{5.3.1}$$

in which $N_i(x,t)$ is the shape function, $\hat{\xi}_i(x,t)$ are the general coordinates of the pivot points. The STFEM approach has been successfully applied to a one-dimensional problem (Yu and Hsu, 1985), as well as to multi-dimensional problems (Kim, 2001; Bajer, 1986; Hughes and Hulbert; 1988). It is found particularly useful for problems with sharp changes in solutions, such as wave propagation problems (Hulbert and Hughes, 1990). However, the disadvantages of this approach are two-fold. The first one is that the resultant equation sets are bigger in size thus would require more computational resource to handle (Kim, 2003); the other is that the algorithmic stability issue becomes more sensitive, especially for non-rectangular space-time elements (Bajer, 1986).

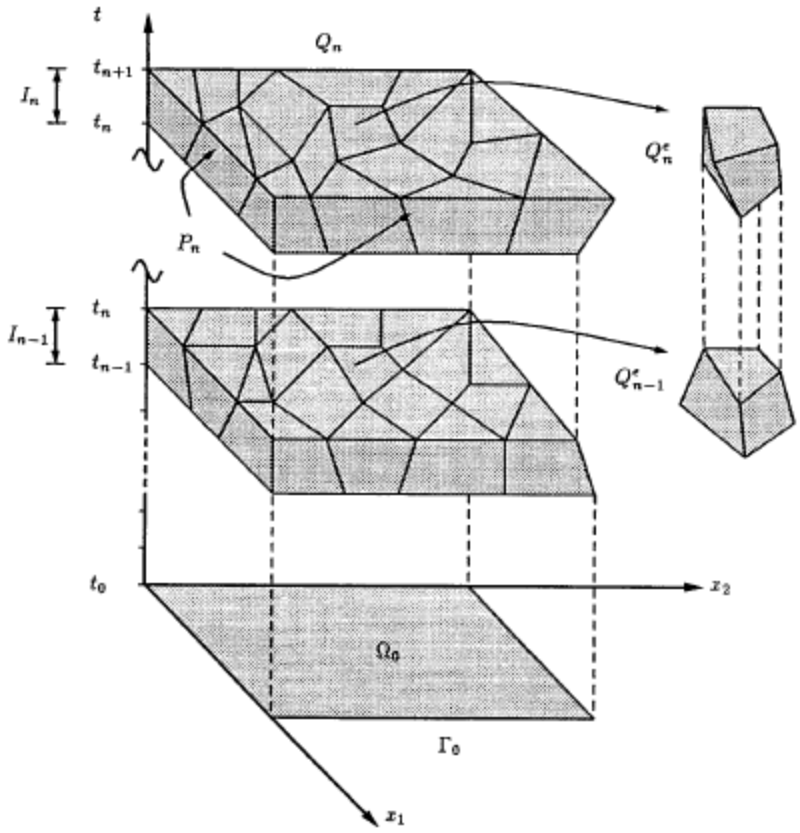

Figure 5.3.1- A simultaneous space-time finite element discretisation (Hughes and Stewart, 1996)

The second approach is the so-called “semi-discretisation” approach, i.e., the dynamic system is firstly discretised in the spatial domain, leading to either the equations of motion in the form of a set of ordinary differential equations, or an energy functional containing these equations implicitly. Finite element treatment in time is then applied to approximate the time-dependent variable field(s) thus a set of algebraic equations are obtained, which can be solved with various schemes. This discretisation procedure may be expressed as

$$\xi(x,t) = \sum_i N_i(t)\hat{\xi}_i(x,t) \tag{5.3.2}$$

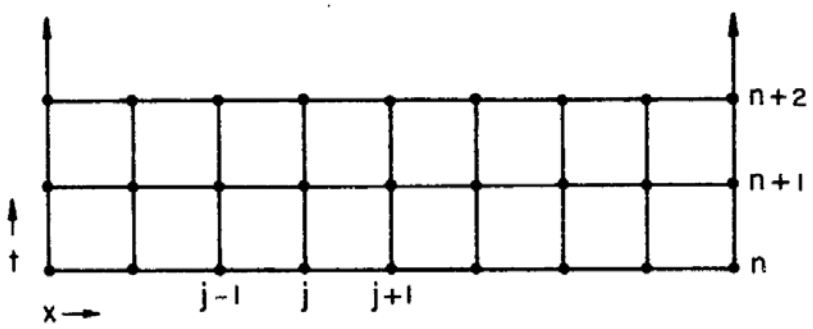

Figure 5.3.2 – A semi-discretisation of the space-time domain (Cushman, 1979)

There are abundant research works adopting this approach for various problems (Gellert, 1978; Golley, 1996; Lee and Kwak, 1993; Golley and Amer, 1999) because of the ease of implementation in the algorithm and less demanding for the computational resources.

Although these two approaches deal with the same task with different tactics, it has been shown that the STFEM approach is equivalent to the semi-discretisation one, if rectangular space-time elements are used (Sanz-Serna, 1983). In addition, given the drawbacks of STFEM, Zienkiewicz stated that the benefit of the STFEM approach for structural dynamics was limited (1977). For problems involving high frequency elements, however, the merits of STFEM are evident, such as capable of capturing accurately discontinuities in the solution and ease of adopting unstructured mesh in the space-time domain (Hughes and Hulbert, 1988; Hulbert and Hughes, 1990; Hulbert, 1992; Cella et al., 1980) .

In the present research, the semi-discretisation approach is adopted due to its convenience.

5.4 A review of time finite elements in the semi-discretisation application

The pioneers of the finite element in time were Argyris and Scharpf (1969) and Fried (1969). Since the publication of their research, the application of time finite

elements have been further explored by Zienkiewicz (1977) and many others (Riff and Baruch, 1984; Hulbert and Hughes, 1990; Bailey, 1975; Cushman, 1979).

Various approximation functions have been used for the approximation in the temporal domain, including cubic Hermite polynomials, Lagrange polynomials and B-splines, as well as power series and Taylor series.

Cubic Hermite time element

One of the most popular interpolation functions is the cubic Hermite polynomials. Starting from Hamilton's Principle, Argyris and Scharpf (1969) used these functions for the displacement approximation and the first derivates for the velocity approximation in their formulation. The algorithm was second-order accurate. They demonstrated their procedure could be extended further for the adaptation of shape functions of arbitrary orders.

The same approximation was used by Fried (1969) and Geradin (1974) in their stepwise algorithms. Geradin found that, when the cubic Hermite approximation was directly applied, the resultant algorithm was only conditionally stable. To overcome this problem, the same treatment used by Bathe and Wilson (1972) was employed to derive an unconditionally stable algorithm while the accuracy was affected only slightly. The response at the end of the time step was obtained in a two – step procedure: 1) the response at the end of a slightly larger time step is evaluated first; 2) the desired response is to be interpolated from that response and the initial values. It may be illustrated in the following figure.

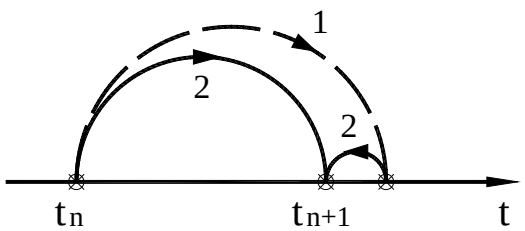

Figure 5.4.1- Geradin's unconditionally stable procedure (Geradin, 1974)

In a variational formulation proposed by Riff and Baruch (1984), the displacement and the velocity were identically approximated with the cubic Hermite functions and the first derivatives of these functions. However, in contrast to the calculus of variations, the variation of the approximated field was based on the second derivatives of the cubic Hermite polynomials. A conditionally stable algorithm was attained.

A similar approach was proposed by Golley and Amer (1999). In their procedure, the cubic Hermite polynomials and their first and second derivatives were used for the approximation of the displacement, velocity and acceleration respectively. These approximated quantities were then substituted into the governing equation and the residual was found. The weighted residuals, expressed as the functions of eight weighted integrals, were made to vanish to give rise to a recurrence formulation for the evaluation of the end values. These weighted integrals were determined on the consideration of algorithmic accuracy, stability, desired dissipation and numerical characteristics.

Lagrange time element

In addition to the Hermite polynomials, another popular choice for the time approximation is the Lagrange polynomials. A typical application was given by Fung (1998), in which the displacement and the momentum were treated as independent variables in a variational formulation. While these quantities were approximated with Lagrange polynomials of a given order, their variations were approximated with a different polynomial of one order lower. The resultant algorithms were found to be unconditionally stable with controllable numerical dissipation.

The performance of three types of Lagrange time finite elements was investigated in terms of accuracy, stability and numerical dissipation (Fan et al., 1997). The three types of Lagrange polynomials used for the approximation were:

- Lagrange polynomial
- Piecewise discontinuous Lagrange polynomial
- Piecewise continuous Lagrange polynomial

The equation of motion was expressed in the first order form and solved by the generalised Galerkin method. The test functions were taken as polynomials of one order less than that of the trial functions. It was found that

- With various combinations of trial functions and test functions, accuracy of different orders can be achieved, ranging from second-order to sixth-order.

- Various numerical dissipation was obtained. While unconditionally stable, non-dissipative algorithms can be obtained with the Lagrange polynomials, unconditionally stable and asymptotic annihilating algorithms can be derived with the piecewise discontinuous Lagrange polynomials. A third case exist when the piecewise continuous Lagrange polynomials were adopted; the result can have desired dissipation between the first two cases.

The effect of using lower order test functions were verified by Sheng et al. (1998) in their Hamilton's law based formulation.

The application of Lagrange approximation to arbitrary load functions was successfully used to avoid the expensive Duhamel integration for the particular solutions (Liu, 2001), and a semi-analytical algorithm of structural analysis based on the modal decomposition method was thus obtained.

Different types of approximating functions can be used in conjunction. In a paper by Gellert (1978), both the cubic Hermite polynomials and the second-order Lagrange polynomials were used, while the former was employed to approximate

the displacement, and latter is used for the load interpolation. A similar treatment was given by Golley and Amer (1999) with more combinations.

B-spline and power series

Recently, B-spline functions have been utilised for the time finite element approximation (Rostami et al., 2012). The velocity and the acceleration were derived from the time derivatives of the displacement approximation. These quantities were substituted into the control equation at the collocation points. High accuracy can be achieved. This algorithm is an explicit one, therefore, it has the advantage of high computational efficiency, but it also shares the drawback of conditional stability as other explicit algorithms.

Another type of time approximation function is the power series, which can be regarded as the general form of the Hermite and the Lagrange polynomials. A power series is normally in the following form,

$$x(t) = \sum^{n} \alpha_n t^n \quad n = 0,1,2,\cdots \tag{5.4.1}$$

The initial values (displacement and velocity) can be enforced strongly in the displacement approximation as demonstrated in a series of works by Bailey. Alternatively, these initial values can be enforced only weakly as shown in (Fung, 2003a, 2003b). Many established algorithms use power series approximation, including the Houbolt algorithm, the Wilson-Farhoomand procedures, the HHT method, and so on, Zienkiewicz et al. (1984) put forward a general framework unifying these algorithms and classified them under the category of the *SSpj* algorithms (Single Step with approximation of degree *p* for equations of order *j*). In many applications, the power approximation is only up to third-order.

Higher-order power series was attempted in later researches. Howard and Penny (1978) proposed a power series of the fifth-order (quintic element) for the

displacement approximation in order to account for the continuity of accelerations at the time element boundaries. The authors found with this approximation the errors were reduced significantly compared with the popular cubic Hermite approximation. However, this scheme was a conditionally stable one. An unconditionally stable algorithm based on the same fifth-order approximation was presented by Wang and Au (2004), in their approach the weighted residual method and the collocation method were combined and two parameters were put in place to control the stability and the accuracy. The solution was found to be fifth-order accurate.

High order accurate algorithm based on a power series of the order n with undetermined coefficients was proposed by Fung (2000). The power series was utilised to approximate the displacement field while the velocity and acceleration were subsequently derived from the time derivatives of the displacement field. The second-order differential governing equations were then transformed into a set of algebraic equations in terms of the coefficients. Once these coefficients were solved, the end value sought for was then obtained by back substitution. The accuracy and the stability of this scheme depend on the selection of n collocation parameters. In general, the scheme is at least nth-order accurate, and the order of accuracy can be further improved to $2n-1$or $2n$ if the collocation parameters are chosen as the roots of a polynomial in terms of the ultimate amplification factor. The given scheme is unconditionally stable one with controllable dissipation.

Although it is found many unconditionally stable algorithm were constructed with trial functions and test functions of different orders, as reviewed in the subsections of the Hermite and the Lagrange time elements. Idesman (2007, 2011) present an unconditionally stable time-continuous Galerkin method with trial functions and test functions of the same order, which also has controllable numerical dissipation.

In this research, several suitable time finite elements are identified for the proposed UHVP algorithms, including the cubic Hermite element, Lagrange elements of various orders. These time finite elements are reviewed next.

5.5 Time finite element employed in the study

5.5.1 Cubic Hermite time element

The cubic Hermite time finite element offers a straightforward way to incorporate the initial displacement and velocity into the unknown displacement field approximation, which is very convenient for structural dynamic problems.

Typical, the cubic Hermite polynomials may be expressed as Eq. (5.5.1), where $\tau = t/\Delta t$ is the local dimensionless time within the time step Δt.

$$\begin{aligned} &\phi_0 = 1 - 3\tau^2 + 2\tau^3; \qquad \phi_1 = 3\tau^2 - 2\tau^3; \\ &\varphi_0 = \tau - 2\tau^2 + \tau^3; \qquad \varphi_1 = \tau^3 - \tau^2 \qquad \tau \in [0,1] \end{aligned} \tag{5.5.1}$$

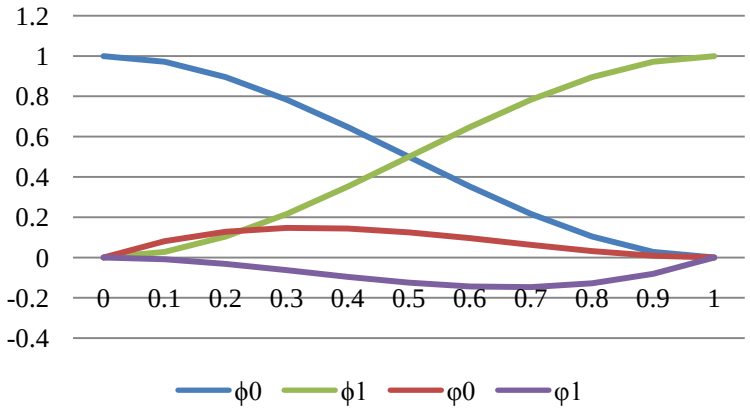

Figure 5.5.1 – Plot of the cubic Hermite polynomials

Accordingly the first derivatives with respect to τ are

$$\frac{d}{d\tau}\phi_0 = -6\tau + 6\tau^2; \qquad \frac{d}{d\tau}\phi_1 = 6\tau - 6\tau^2;$$
$$\frac{d}{d\tau}\varphi_0 = 1 - 4\tau + 3\tau^2; \qquad \frac{d}{d\tau}\varphi_1 = 3\tau^2 - 2\tau \qquad \tau \in [0,1] \tag{5.5.2}$$

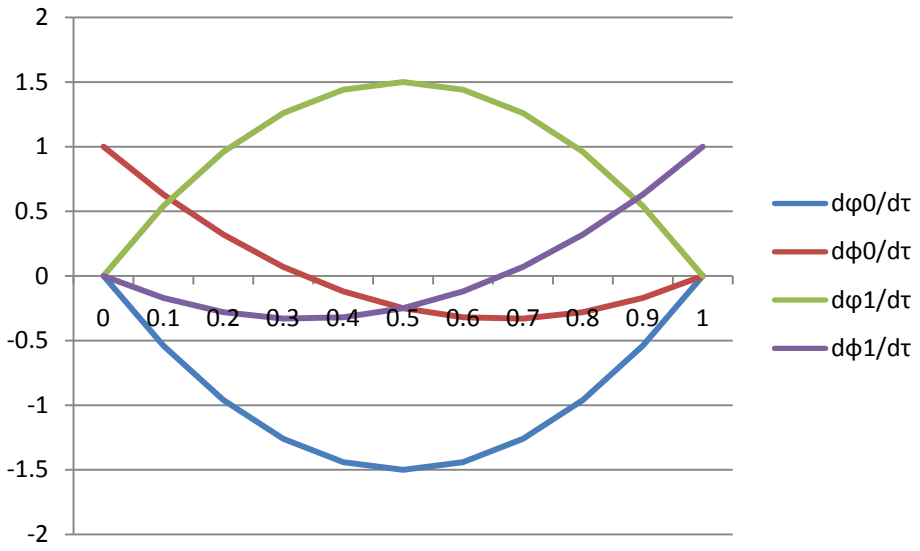

Figure 5.5.2 – Plot of first derivatives of the cubic Hermite polynomials

Using the cubic Hermite polynomials, the piecewise displacement field within a time interval [0,1] as shown in Figure 5.5.3 is approximated with the time nodal values of the displacement and velocity at the two time boundaries, $\hat{u}_0, \hat{u}_1, \hat{v}_0, \hat{v}_1$.

$$u(\tau) = \hat{u}_0\phi_0 + \hat{u}_1\phi_1 + (\hat{v}_0\Delta\tau)\varphi_0 + (\hat{v}_1\Delta\tau)\varphi_1 \qquad (\Delta\tau = 1) \tag{5.5.3}$$

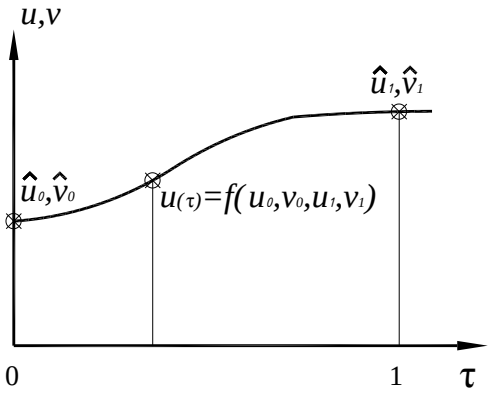

Figure 5.5.3 – The cubic Hermite approximation

The velocity field is derived accordingly as

$$v(\tau)=\frac{d\tau}{dt}\frac{du(\tau)}{d\tau}=\frac{1}{\Delta t}\left(\hat{u}_0\frac{d\phi_0}{d\tau}+\hat{u}_1\frac{d\phi_1}{d\tau}+(\hat{v}_0\Delta\tau)\frac{d\varphi_0}{d\tau}+(\hat{v}_1\Delta\tau)\frac{d\varphi_1}{d\tau}\right) \quad (5.5.4)$$
$$(\Delta\tau=1)$$

It can be easily verified that the approximated displacement and velocity will give the initial values at $\tau=0$ and the end values at $\tau=1$.

5.5.2 Lagrange time elements

Various Lagrange time elements may be constructed with the corresponding Lagrange polynomials. A standard Lagrange polynomial can be expressed with several pivot points $(\hat{x}_i,\hat{y}_i),(i=0,1,2,...,n)$ in the following form (Gerald and Wheatley, 1994)

$$\phi_i=\prod_{j=0,\,j\neq i}^{n}\frac{(x-\hat{x}_j)}{(\hat{x}_i-\hat{x}_j)} \quad (5.5.5)$$

Consequently the unknown field, for example the displacement field can be approximated with the values $\hat{u}_i$ at n pivot points

$$u(t) = \sum_{i=0}^{n} \phi_i \hat{u}_i \tag{5.5.6}$$

The order of the approximation is determined by the parameter n. When $n=1$, the approximation becomes a linear one. The linear approximation has been used in many early earlier publications. When $n=2$ the approximation is also referred as "quadratic interpolation" (Lee and Kwak, 1993).

In this research, Lagrange elements of various orders are used, including the second-, third- and fifth- order elements, respectively. These time finite elements are shown to give different characteristics to the resultant algorithms, and these characteristics are to be discussed in Chapters 7 & 8.

Second order interpolation

In the second order interpolation, the shape functions ϕ_i are

$$\begin{aligned} \phi_0 &= \frac{1}{2}(\tau-1)(\tau-2); \\ \phi_1 &= \tau(2-\tau); \\ \phi_2 &= \frac{1}{2}\tau(\tau-1) \qquad (\tau \in [0,2]) \end{aligned} \tag{5.5.7}$$

in which τ is again the dimensionless time. The three functions are plotted as below.

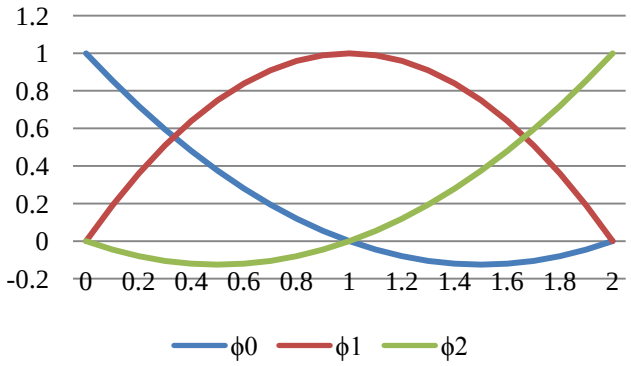

Figure 5.5.4 – Second order Lagrange polynomials

Third order interpolation

In the third order interpolation, the four shape functions ϕ_i are

$$\begin{aligned}
\phi_0 &= \frac{-1}{6}(\tau-1)(\tau-2)(\tau-3);\\
\phi_1 &= \frac{1}{2}\tau(\tau-2)(\tau-3);\\
\phi_2 &= \frac{-1}{2}\tau(\tau-1)(\tau-3);\\
\phi_3 &= \frac{1}{6}\tau(\tau-1)(\tau-2) \qquad (\tau\in[0,3])
\end{aligned} \tag{5.5.8}$$

They can be shown graphically as below

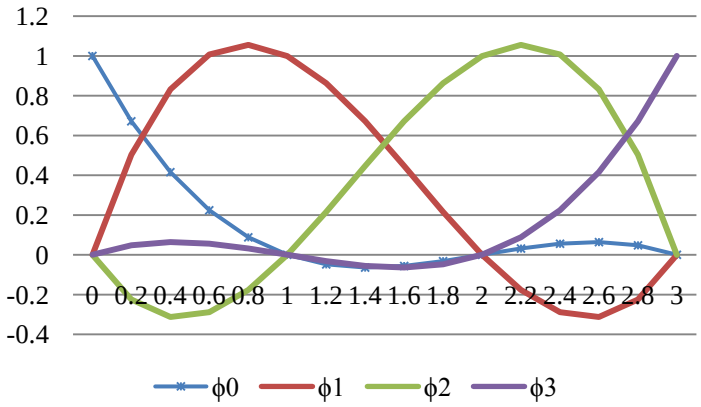

Figure 5.5.5 – Third order Lagrange polynomials

Fifth order interpolation

The fifth order interpolation is also used in the present study, for which the shape functions ϕ_i are

$$\begin{aligned}
\phi_0 &= \frac{-1}{120}(\tau-1)(\tau-2)(\tau-3)(\tau-4)(\tau-5);\\
\phi_1 &= \frac{1}{24}\tau(\tau-2)(\tau-3)(\tau-4)(\tau-5);\\
\phi_2 &= \frac{-1}{12}\tau(\tau-1)(\tau-3)(\tau-4)(\tau-5);\\
\phi_3 &= \frac{1}{12}\tau(\tau-1)(\tau-2)(\tau-4)(\tau-5);\\
\phi_4 &= \frac{-1}{24}\tau(\tau-1)(\tau-2)(\tau-3)(\tau-5);\\
\phi_5 &= \frac{1}{120}\tau(\tau-1)(\tau-2)(\tau-3)(\tau-4) \qquad \tau\in[0,5]
\end{aligned} \tag{5.5.9}$$

These shape functions are plotted as below

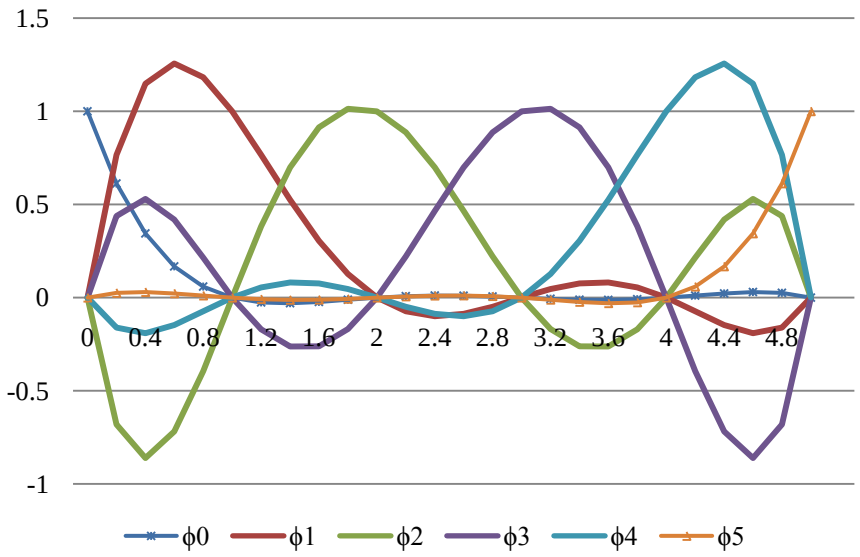

Figure 5.5.6 – Fifth order Lagrange polynomials

As shown in the plots, the *ith* shape function ϕ_i attains unity and the other ϕ_j $(j \neq i)$ all diminish at the *ith* pivot point; therefore the approximated field will

obtain the prescribed values at these pivot points. Obviously, the more pivot points, the more accurate the approximation within the time interval.

5.6 Summary

In this chapter, different ways of applying finite element discretisation in the temporal domain for dynamic problems is briefly reviewed. The piecewise approximation and semi-discretisation approach of applying time finite element are chosen for the present research. Time finite elements in existing literatures are reviewed, and particular ones suitable for the proposed space-time finite element algorithms are presented.

Chapter 6 One-field and Two-field UHVP Algorithms

6.1 Introduction

Based on the Unconventional Hamilton-type variational principles presented in Chapter 4, two algorithms are developed here to offer direct solutions for the dynamics of truss-type structures. These two algorithms are based on the one-field principle (*Principle five*) and the two-field principle *(Principle four*) respectively. The reasons for the adoption of these two particular principles lie in two aspects:

- It is well-understood that the status of a dynamic system can only be determined by describing its displacement and the momentum /velocity. The two-field principle yields the formulation employing nothing but exactly these two variable fields, therefore, the two-field principle is the most suitable choice. The mixed formulation thus generated may also offer certain algorithmic advantages, such as unconditional stability. (Fung et al., 1998). On the other hand, the status of a system can also be described if the velocity and displacement fields are linked together by differentiation operation, therefore the one-field principle can also be adopted.

- These two principles are also economic choices since there are fewer unknowns to be solved. For an *n*-DOFs system, these two principles both render *2n* numbers of unknowns, while other UHVPs would result in *3n*, *4n* and *5n* unknowns respectively.

In section 6.2, two variational formulations are given for the one-field and two-field UHVP algorithms. The derivation of these two types of space-time finite element algorithms is then presented in section 6.3. For each algorithm, the semi-

discretisation approach is adopted, where the spatial discretisation is performed first in a standard finite element procedure. The time discretisation using different time finite elements is presented next. The whole time domain is divided into successive sub-intervals, and the formulations for the end values within the time sub-interval are given. The solution from the current sub-interval is used as the initial values for the next sub-interval, and hence forms a single step time marching scheme. Summary are given in section 6.3.

6.2 Variational formulations for one-field and two-field algorithms

The variational expressions presented in the Chapter 4 are established on the basis of an individual rod member. To analyse the response of the entire structure, the contributions from all rod members need to be taken into account. To this end, variational formulations for individual rods are summed up to reflect the dynamic equilibrium of the whole structure. Consequently, for a structure with nr numbers of rods this summation is in the form of

$$\begin{aligned}&\delta\sum_{i=1}^{nr}\ \Pi_2^{(i)}\left(\mathrm{p},\mathrm{u}\right)\\&=\delta\sum_{i=1}^{nr}\ \int_0^{t_f}\int_0^{l^{(i)}}\left\{\mathrm{p}\dot{\mathrm{u}}-\frac{1}{2\mathrm{m}}\mathrm{p}^2\right\}dxdt+\delta\sum_{i=1}^{nr}\ \hat{\Pi}_1^{(i)}\left(\mathrm{u}\right)+\delta\sum_{i=1}^{nr}\ \overset{o}{\Pi}{}^{(i)}\left(\mathrm{p},\mathrm{u}\right)=0\end{aligned}\tag{6.2.1}$$

based on *Principle four*, and

$$\begin{aligned}&\delta\sum_{i=1}^{nr}\ \Pi_1^{(i)}\left(\mathrm{u}\right)\\&=\delta\sum_{i=1}^{nr}\ \int_0^{t_f}\int_0^{l^{(i)}}\left\{\frac{1}{2}\mathrm{m}\dot{\mathrm{u}}^2\right\}dxdt+\delta\sum_{i=1}^{nr}\ \hat{\Pi}_1^{(i)}\left(\mathrm{u}\right)+\delta\sum_{i=1}^{nr}\ \overset{o}{\hat{\Pi}}{}^{(i)}\left(\mathrm{u}\right)=0\end{aligned}\tag{6.2.2}$$

based on *Principle five*.

Here the functional Π is used for finding the solution. However, it should be noted that the other functional Γ is equivalent for this purpose, as proved in chapter 4.

For a solution of the problem, the boundary and initial conditions Eqs. (4.3.7) and (4.3.8a, b) have to be satisfied, in addition, by choosing carefully the trial functions $\mathrm{p}(x,t)$, $\mathrm{u}(x,t)$ to ensure these conditions are indeed fulfilled in the forthcoming derivation, the last two equations may be reduced as

$$\begin{aligned}
&\delta\sum_{i=1}^{nr}\ \Pi_2{}^{(i)}\left(\mathrm{p},\mathrm{u}\right)=\\
&\delta\sum_{i=1}^{nr}\ \int_0^{t_f}\int_0^{l^{(i)}}\left\{\mathrm{p}\dot{\mathrm{u}}-\frac{1}{2\,\mathrm{m}}\mathrm{p}^2-\frac{EA}{2}\left(\frac{\partial\,\mathrm{u}}{\partial x}\right)^2\right\}dxdt\ +\sum_{i=1}^{nr}\ \int_0^{t_f}\int_0^{l^{(i)}}\left\{\left[f-c\,\dot{\mathrm{u}}\right]\delta\,\mathrm{u}\right\}dxdt\\
&+\sum_{i=1}^{nr}\ \int_0^{t_f}\left\{\overline{\mathrm{N}}\,\delta\,\mathrm{u}\Big|_{x=0}^{x=l^{(i)}}\right\}dt+\sum_{i=1}^{nr}\ \int_0^{l^{(i)}}\left\{-\mathrm{p}\left(x,t_f\right)\delta\,\mathrm{u}\left(x,t_f\right)\right\}dx=0
\end{aligned}\tag{6.2.3}$$

and

$$\begin{aligned}
&\delta\sum_{i=1}^{nr}\ \Pi_1{}^{(i)}\left(\mathrm{u}\right)\\
&=\delta\sum_{i=1}^{nr}\ \int_0^{t_f}\int_0^{l^{(i)}}\left\{\frac{1}{2}\mathrm{m}\,\dot{\mathrm{u}}^2-\frac{EA}{2}\left(\frac{\partial\,\mathrm{u}}{\partial x}\right)^2\right\}dxdt+\sum_{i=1}^{nr}\ \int_0^{t_f}\int_0^{l^{(i)}}\left\{\left[f-c\,\dot{\mathrm{u}}\right]\delta\,\mathrm{u}\right\}dxdt\\
&+\sum_{i=1}^{nr}\ \int_0^{t_f}\left\{\overline{\mathrm{N}}\,\delta\,\mathrm{u}\Big|_{x=0}^{x=l^{(i)}}\right\}dt+\sum_{i=1}^{nr}\ \int_0^{l^{(i)}}\left\{-\mathrm{m}\,\dot{\mathrm{u}}\left(x,t_f\right)\delta\,\mathrm{u}\left(x,t_f\right)\right\}dx=0
\end{aligned}\tag{6.2.4}$$

Eqs. (6.2.3) and (6.2.4) are the underpinning formulations for the development of the one-field and the two-field UHVP algorithms in the following derivation.

6.3 UHVP based space-time finite element algorithms

In this section, two classes of space-time finite element algorithms are adopted to obtain direct solutions of the dynamics of truss-type structures.

The space-time finite element schemes have demonstrated its advantages in many publications for cases where higher accuracy is desired. In the construction of the presented algorithms, the structural system is firstly discretised in the spatial domain, followed by a separate discretisation in the temporal domain. This discretisation procedure belongs to the category of so-called “semi-discretisation”.

In the following subsections, the one-field algorithm and the two-field algorithm are presented respectively.

6.3.1 One-field variable algorithm

6.3.1.1 Discretisation in the spatial domain

The standard finite element discretisation procedure is adopted here. The displacement field of a rod is approximated with its nodal displacement values. To that end, a global coordinate system for the entire structure and a separate local coordinate systems for each rod are set up. In a truss-type structure, all external loadings are applied to the node(s) only, and each truss rod bears only tension/compression forces and undergoes deformations along the axial direction. Thus, for an arbitrary rod, on the assumption of small structural deformation, its displacement field can be simplified as a one-dimensional one along the axial direction. Therefore the local coordinate system is set conveniently along this axial direction as well.

For a typical truss rod $\overline{ab}$ in the Euclidian global system *OXYZ*, six displacement components are required to describe the deformation of $\overline{ab}$. Let D_{aX}, D_{aY}, D_{aZ} be the components for the node a; whereas D_{bX}, D_{bY}, D_{bZ} for the node b, as shown in Figure. 6.3.1a. In Figure 6.3.1b, the resultant nodal displacements of each node are denoted as u_a and u_b in the local coordinate system. By comparison of Figure 6.3.1a and Figure6.3.1b, it is easy to see that the following relations

$$u_a = D_{aX}\cos\alpha + D_{aY}\cos\beta + D_{aZ}\cos\gamma \tag{6.3.1a}$$

$$u_b = D_{bX}\cos\alpha + D_{bY}\cos\beta + D_{bZ}\cos\gamma \tag{6.3.1b}$$

in which $\cos\alpha$, $\cos\beta$ and $\cos\gamma$ are the directional cosines with respect to the global axes OX, OY and OZ, respectively.

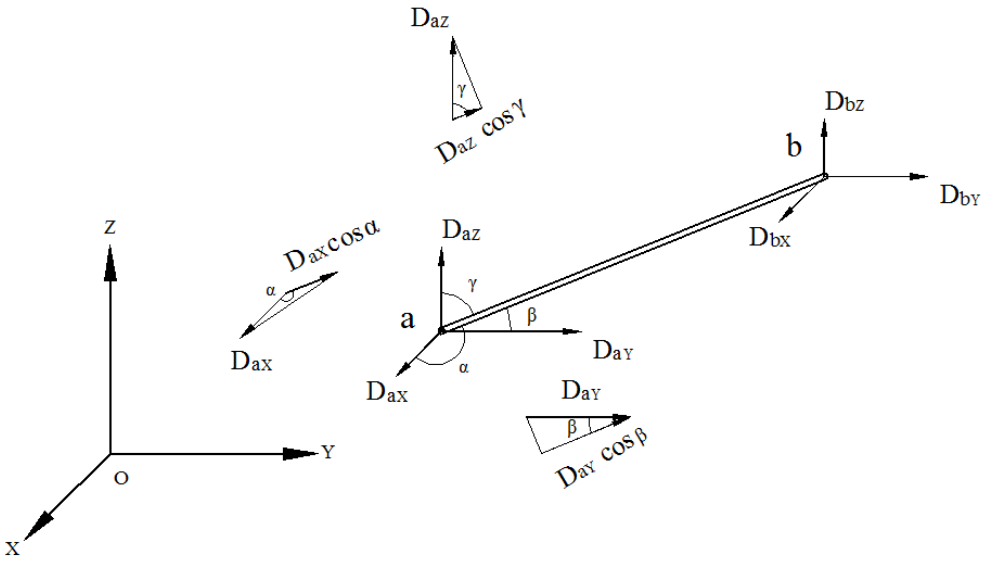

Figure 6.3.1a – Nodal displacements in the global coordinate system

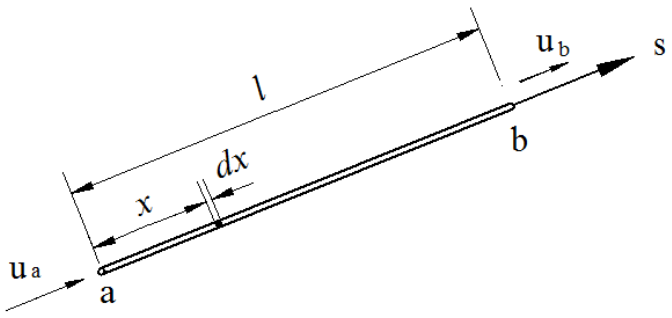

Figure 6.3.1b – Nodal displacements in the local coordinate system

Eqs. (6.3.1a) and (6.3.1b) can be couched in the matrix format as follows

$$\mathbf{u_{ab}} = \mathbf{T} \times \mathbf{D_{ab}} \tag{6.3.2}$$

in which

$$\mathbf{u_{ab}} = \begin{Bmatrix} u_a \\ u_b \end{Bmatrix} \tag{6.3.3}$$

$$\mathbf{D_{ab}} = \{ D_{aX}, D_{aY}, D_{aZ}, D_{bX}, D_{bY}, D_{bZ} \}^T \tag{6.3.4}$$

$\mathbf{T}$ is the transformation matrix

$$\mathbf{T} = \begin{bmatrix} \mathbf{T1}_{1\times 3} & \{0\}_{1\times 3} \\ \{0\}_{1\times 3} & \mathbf{T1}_{1\times 3} \end{bmatrix} \tag{6.3.5}$$

in which

$$\mathbf{T1} = \{ \cos\alpha \quad \cos\beta \quad \cos\gamma \} \tag{6.3.6}$$

Once $\mathbf{u}_{ab}$ is obtained, the displacement field measured in the local coordinate system can be interpolated from this vector. A linear interpolation operator $\mathbf{s}(x)$ is employed for this purpose, which is

$$\mathbf{s}(x) = \left\{ \frac{l-x}{l} \quad \frac{x}{l} \right\} \tag{6.3.7}$$

where l is the length of the rod, therefore,

$$u(x,t) = \mathbf{s}(x) \times \mathbf{u}_{ab} = \mathbf{s}(x) \times \mathbf{T} \times \mathbf{D}_{ab}(t) \tag{6.3.8}$$

The term $\frac{\partial \mathrm{u}}{\partial x}$ in Eq. (6.2.4) can thus be transformed as

$$\frac{\partial \mathrm{u}(x,t)}{\partial x} = \frac{\partial \mathbf{s}(x)}{\partial x} \times \mathbf{T} \times \mathbf{D}_{ab}(t) \tag{6.3.9}$$

where

$$\frac{\partial \mathbf{s}(x)}{\partial x} = \frac{1}{l}\{-1 \quad 1\} \tag{6.3.10}$$

Meanwhile, the first order time derivative of the displacement field may be written as

$$\dot{u}(x,t) = \mathbf{s}(x) \times \mathbf{T} \times \dot{\mathbf{D}}_{ab}(t) \tag{6.3.11}$$

The body force $\mathbf{f} = \{ f_X, f_Y, f_Z \}^T$ described in the global system can be translated into the local coordinate system for each rod as f

$$f = f_X \cos\alpha + f_Y \cos\beta + f_Z \cos\gamma \tag{6.3.12a}$$

i.e.

$$f = \mathbf{T1} \times \mathbf{f} \tag{6.3.12b}$$

The term $\int_0^{t_f} \left\{ \bar{\mathrm{N}}\, \delta \mathrm{u} \Big|_{x=0}^{x=l^{(i)}} \right\} dt$ in Eq. (6.2.4) represents the virtual actions of the axial forces at the nodal positions. Under the assumptions made in Chapter 4, the sum of these virtual actions $\sum_{i=1}^{nr} \int_0^{t_f} \left\{ \bar{\mathrm{N}}\, \delta \mathrm{u} \Big|_{x=0}^{x=l^{(i)}} \right\} dt$ is equal to the sum of the virtual actions of the exciting forces applied to all nodes because there is no energy loss at these nodes.

For instance, in the case of Figure 6.3.2, this relation is

$$\sum_{i=1}^{4} \int_0^{t_f} \left\{ \bar{\mathrm{N}}\, \delta \mathrm{u} \Big|_{x=0}^{x=l^{(i)}} \right\} dt = \int_0^{t_f} \left\{ \mathbf{L}(t)^T \times \delta \mathbf{D} \right\} dt \tag{6.3.13}$$

where $\mathbf{L}(t)$ is the nodal force vector; $\mathbf{D}$ is the nodal displacement vector.

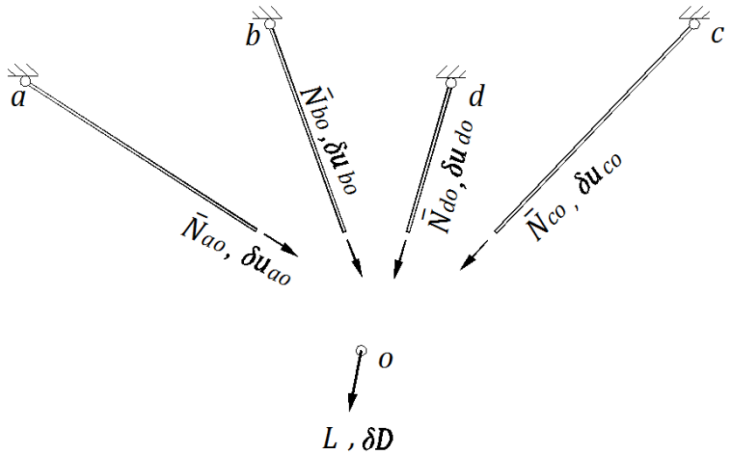

Figure 6.3.2 - Virtual actions of nodal force and axial forces

Thus Eq. (6.2.4) can be re-written as

$$\begin{aligned}
&\delta\sum_{i=1}^{nr}\ \Pi_1^{(i)}\left(\mathrm{u}\right)\\
&=\delta\sum_{i=1}^{nr}\ \int_0^{t_f}\int_0^{l^{(i)}}\left\{\frac{1}{2}\mathrm{m}\,\dot{\mathrm{u}}^2-\frac{EA}{2}\left(\frac{\partial\,\mathrm{u}}{\partial x}\right)^2\right\}dxdt+\sum_{i=1}^{nr}\ \int_0^{t_f}\int_0^{l^{(i)}}\left\{\left[\,f-c\,\dot{\mathrm{u}}\right]\delta\,\mathrm{u}\right\}dxdt\\
&+\sum_{j=1}^{nd}\ \int_0^{t_f}\left\{\mathbf{L}^{(j)T}\times\delta\mathbf{D}^{(j)}\right\}dt+\sum_{i=1}^{nr}\ \int_0^{l^{(i)}}\left\{-\mathrm{m}\,\dot{\mathrm{u}}\left(x,t_f\right)\delta\,\mathrm{u}\left(x,t_f\right)\right\}dx=0
\end{aligned}\tag{6.3.14}$$

here *nd* is the total number of the nodes of the truss-structure.

By virtue of Eqs. (6.3.8), (6.3.9), (6.3.11) and (6.3.12b), Eq. (6.3.14) is now

$$\begin{aligned}
&\delta\sum_{i=1}^{nr}\ \Pi_1^{(i)}\left(\mathrm{u}\right)\\
&=\sum_{i=1}^{nr}\int_0^{t_f}\int_0^{l^{(i)}}\left\{\begin{array}{l}\dot{\mathbf{D}}^{(i)}\left(t\right)^T\times\left(\mathbf{T}^T\times\mathbf{s}^T\times\mathrm{m}\times\mathbf{s}\times\mathbf{T}\right)^{(i)}\times\delta\dot{\mathbf{D}}^{(i)}\left(t\right)\\ -\mathbf{D}^{(i)}\left(t\right)^T\times\left(\mathbf{T}^T\times\dfrac{\partial\mathbf{s}^T}{\partial x}\times EA\times\dfrac{\partial\mathbf{s}}{\partial x}\times\mathbf{T}\right)^{(i)}\times\delta\mathbf{D}^{(i)}\left(t\right)\end{array}\right\}dxdt\\
&+\sum_{i=1}^{nr}\int_0^{t_f}\int_0^{l^{(i)}}\left\{\begin{array}{l}\left(\mathbf{T1}\times\mathbf{f}\times\mathbf{s}\times\mathbf{T}\right)^{(i)}\times\delta\mathbf{D}^{(i)}\left(t\right)\\ -\dot{\mathbf{D}}^{(i)}\left(t\right)^T\times\left(\mathbf{T}^T\times\mathbf{s}^T\times c\times\mathbf{s}\times\mathbf{T}\right)^{(i)}\times\delta\mathbf{D}^{(i)}\left(t\right)\end{array}\right\}dxdt\\
&+\sum_{j=1}^{nd}\int_0^{t_f}\left\{\mathbf{L}^{(j)}\left(t\right)^T\times\delta\mathbf{D}^{(j)}\left(t\right)\right\}dt-\sum_{i=1}^{nr}\int_0^{l^{(i)}}\left\{\dot{\mathbf{D}}^{(i)}\left(t_f\right)^T\times\left(\mathbf{T}^T\times\mathbf{s}^T\times\mathrm{m}\times\mathbf{s}\times\mathbf{T}\right)^{(i)}\times\delta\mathbf{D}^{(i)}\left(t_f\right)\right\}dx\\
&=0
\end{aligned}\tag{6.3.15}$$

It is noted that the terms $\left(\mathbf{T}^T\times\mathbf{s}^T\times\mathrm{m}\times\mathbf{s}\times\mathbf{T}\right)^{(i)}$, $\left(\mathbf{T}^T\times\dfrac{\partial\mathbf{s}^T}{\partial x}\times EA\times\dfrac{\partial\mathbf{s}}{\partial x}\times\mathbf{T}\right)^{(i)}$ and $\left(\mathbf{T}^T\times\mathbf{s}^T\times c\times\mathbf{s}\times\mathbf{T}\right)^{(i)}$ are all related to the properties of each rod element,

including material properties and geometrical properties, Eq. (6.3.15) can be put in the following form

$$\begin{aligned}
&\delta\sum_{i=1}^{nr}\Pi_1^{(i)}(\mathrm{u})\\
&=\sum_{i=1}^{nr}\int_0^{t_1}\left\{\dot{\mathbf{D}}^{(i)}(t)^T\times\mathbf{M}_{(e)}^{(i)}\times\delta\dot{\mathbf{D}}^{(i)}(t)-\mathbf{D}^{(i)}(t)^T\times\mathbf{K}_{(e)}^{(i)}\times\delta\mathbf{D}^{(i)}(t)\right\}dt\\
&+\sum_{i=1}^{nr}\int_0^{t_1}\left\{\mathbf{F}_{(e)}^{(i)}\times\delta\mathbf{D}^{(i)}(t)-\dot{\mathbf{D}}^{(i)}(t)^T\times\mathbf{C}_{(e)}^{(i)}\times\delta\mathbf{D}^{(i)}(t)\right\}dt\\
&+\sum_{j=1}^{nd}\int_0^{t_f}\left\{\mathbf{L}^{(j)}(t)^T\times\delta\mathbf{D}^{(j)}(t)\right\}dt-\sum_{i=1}^{nr}\left\{\dot{\mathbf{D}}^{(i)}(t_f)^T\times\mathbf{M}_{(e)}^{(i)}\times\delta\mathbf{D}^{(i)}(t_f)\right\}\\
&=0
\end{aligned}\tag{6.3.16}$$

in which

$$\mathbf{M}_{(e)}^{(i)}=\int_0^{l^{(i)}}\left\{\mathbf{T}^T\times\mathbf{s}^T\times\mathrm{m}\times\mathbf{s}\times\mathbf{T}\right\}^{(i)}dx \tag{6.3.17a}$$

$$\mathbf{K}_{(e)}^{(i)}=\int_0^{l^{(i)}}\left\{\mathbf{T}^T\times\frac{\partial\mathbf{s}^T}{\partial x}\times EA\times\frac{\partial\mathbf{s}}{\partial x}\times\mathbf{T}\right\}^{(i)}dx \tag{6.3.17b}$$

$$\mathbf{F}_{(e)}^{(i)}=\int_0^{l^{(i)}}\left\{\mathbf{T}\mathbf{1}\times\mathbf{f}\times\mathbf{s}\times\mathbf{T}\right\}^{(i)}dx \tag{6.3.17c}$$

$$\mathbf{C}_{(e)}^{(i)}=\int_0^{l^{(i)}}\left\{\mathbf{T}^T\times\mathbf{s}^T\times c\times\mathbf{s}\times\mathbf{T}\right\}^{(i)}dx \tag{6.3.17d}$$

are the elementary matrices/ vector for the *ith* rod.

For the spatial discretisation of the entire structure, let $\mathbf{D}(t)$ contain the nodal displacement components for all nodes.

$$\mathbf{D}(t)=\left\{D_{1X},D_{1Y},D_{1Z},D_{2X},\ldots,D_{ndX},D_{ndY},D_{ndZ}\right\}^T=\left\{D_1,D_2,\ldots,D_n\right\}^T \tag{6.3.18}$$

and n is the number of degree of freedom of the structure. Let $\mathbf{L}(t)$ be the global nodal force vector,

$$\mathbf{L}(t)=\left\{L_{1X},L_{1Y},L_{1Z},L_{2X},\ldots,L_{ndX},L_{ndY},L_{ndZ}\right\}^T=\left\{L_1,L_2,\ldots,L_n\right\}^T \tag{6.3.19}$$

Following the standard discretisation procedure, the variational expression for a truss-type system is in the following form

$$\int_0^{t_f}\left\{\dot{\mathbf{D}}(t)^T\times\mathbf{M}\times\delta\dot{\mathbf{D}}(t)+\left[\mathbf{F}(t)^T+\mathbf{L}(t)^T-\mathbf{D}(t)^T\times\mathbf{K}-\dot{\mathbf{D}}(t)^T\times\mathbf{C}\right]\times\delta\mathbf{D}(t)\right\}dt$$
$$-\dot{\mathbf{D}}(t_f)^T\times\mathbf{M}\times\delta\mathbf{D}(t_f)=0 \tag{6.3.20}$$

wherein the time-invariant $\mathbf{M}$, $\mathbf{K}$ and $\mathbf{C}$ are the assembled global matrices related to the mass, stiffness and damping properties, and $\mathbf{F}(t)$ is the discretised body force vector. Upon this equation, time finite element can be introduced for deriving a direct solution of the dynamic problem.

6.3.1.2 Discretisation in the temporal domain

To find out the solution for the desired time interval, the entire time domain $[0,t_f]$ is divided into successive sub-intervals of equal-length as shown in Figure 6.3.3, with the length of the sub-interval (or time step) being $\Delta t=t_{i+1}-t_i$. Within each time sub-interval, a local time coordinate $\tau\in[0,r]$ is used to facilitate the approximation and the value of r is determined by the adopted time element. The initial values at time $t=0$ are used in the first sub-interval $[0,t_1]$ to solve the end values at time $t=t_1$, and these end values are utilised as the initial values within the next sub-interval $[t_1,t_2]$ for the end values at $t=t_2$. In this fashion, a recursive

scheme is formed, and the time-history of the structural response is obtained step by step. During this process, the intermediate values (displacement, velocity) at an arbitrary point of time within the time step can also be calculated using the interpolation technique.

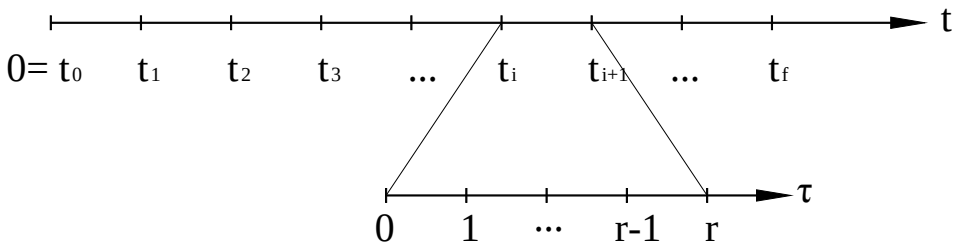

Figure 6.3.3 – Time sub-intervals

From Figure 6.3.3, it is also clear that the relation between the global time coordinate t and the local one τ within an arbitrary time element $[t_i, t_{i+1}]$ is as follows

$$t = t_i + \frac{t_{i+1} - t_i}{r}\tau = t_i + \frac{\Delta t}{r}\tau, \qquad \tau \in [0,\ r] \tag{6.3.21}$$

Using the cubic Hermite element, the approximated displacement field $\tilde{\mathbf{D}}$ expressed in the local time coordinate may be constructed with the displacement vector $\mathbf{D}$ and velocity vector $\dot{\mathbf{D}}$ at the time nodes within the time step. These time nodes include the termini of the time step, and intermediate nodes may be involved as well depending on the time element used.

For the time sub-interval $[t_i, t_{i+1}]$, let

$$\tilde{\mathbf{D}}(\tau) = \boldsymbol{\Psi}(\tau)^T \mathbf{V} \qquad \delta\tilde{\mathbf{D}}(\tau) = \boldsymbol{\Psi}(\tau)^T \delta\mathbf{V} \qquad (\tau \in [0, r]) \tag{6.3.22}$$

where

$$\mathbf{\Psi}(\tau)=\begin{bmatrix}\phi_0(\tau)\times\mathbf{I}\\ \phi_1(\tau)\times\mathbf{I}\\ \vdots\\ \phi_k(\tau)\times\mathbf{I}\\ \varphi_0(\tau)\times\mathbf{I}\\ \varphi_1(\tau)\times\mathbf{I}\\ \vdots\\ \varphi_k(\tau)\times\mathbf{I}\end{bmatrix} \qquad \mathbf{V}=\begin{Bmatrix}\mathbf{D}(t_i)_{n\times1}\\ \mathbf{D}(\tau_{\theta1})_{n\times1}\\ \vdots\\ \mathbf{D}(t_{i+1})_{n\times1}\\ \frac{\Delta t}{r}\times\dot{\mathbf{D}}(t_i)_{n\times1}\\ \frac{\Delta t}{r}\times\dot{\mathbf{D}}(\tau_{\theta1})_{n\times1}\\ \vdots\\ \frac{\Delta t}{r}\times\dot{\mathbf{D}}(t_{i+1})_{n\times1}\end{Bmatrix} \tag{6.3.23}$$

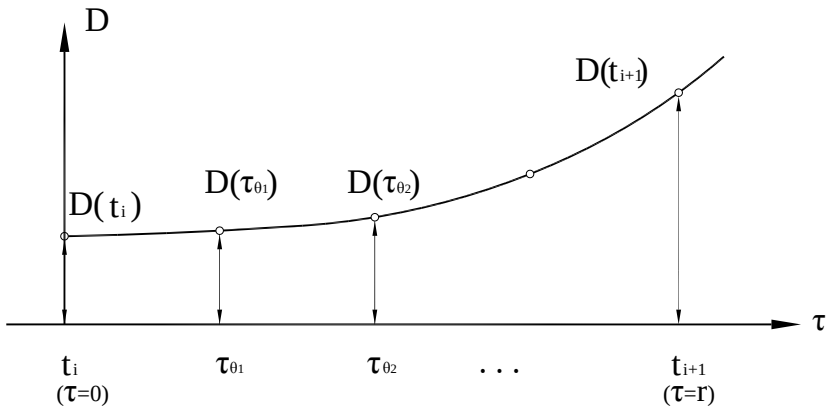

Figure 6.3.4 – Intermediate nodes within time step

$\mathbf{\Psi}$ is the time finite element approximation operator, and $\phi_{(\ )}(\ ),\varphi_{(\ )}(\ )$ are the time element shape functions at the time nodes. $\mathbf{I}$ is the identity matrix of the order n. $\mathbf{V}$ is a state vector for the current time element. $\tau_{\theta1},\tau_{\theta2},\cdots$ are the intermediate time nodes. $\mathbf{D}(\ )$ and $\dot{\mathbf{D}}(\ )$ are the displacement and velocity vectors at the time nodes.

Correspondingly, the first time derivative of the displacement field and its variation may be approximated as

$$\begin{aligned}\dot{\tilde{\mathbf{D}}}(\tau)&=\frac{d\boldsymbol{\Psi}^T}{dt}\mathbf{V}=\frac{d\tau}{dt}\frac{d\boldsymbol{\Psi}^T}{d\tau}\mathbf{V}=\frac{r}{\Delta t}\frac{d\boldsymbol{\Psi}^T}{d\tau}\mathbf{V}\\ \delta\dot{\tilde{\mathbf{D}}}(\tau)&=\frac{r}{\Delta t}\frac{d\boldsymbol{\Psi}^T}{d\tau}\delta\mathbf{V}\end{aligned} \tag{6.3.24}$$

To ensure the approximated displacement and velocity obtaining the corresponding values at all time nodes, which guarantee the initial conditions, the time shape functions ϕ and φ have to satisfy the following conditions

$$\begin{aligned}&\phi_m(n)=\delta_{mn}\\ &\varphi_m(n)=0\\ &\frac{d}{d\tau}\phi_m(n)=0\\ &\frac{d}{d\tau}\varphi_m(n)=\delta_{mn}\\ &(m,n=0,1,\cdots,r)\end{aligned} \tag{6.3.25}$$

where δ_{mn} is the Kronecker delta. It is not difficult to see that the cubic Hermite element fulfils the requirements laid down in Eq. (6.3.25).

For the sub-interval $[t_i,t_{i+1}]$, Eq. (6.3.20) is

$$\begin{aligned}&\int_{t_i}^{t_{i+1}}\left\{\dot{\mathbf{D}}(t)^T\times\mathbf{M}\times\delta\dot{\mathbf{D}}(t)+\left[\mathbf{F}(t)^T+\mathbf{L}(t)^T-\mathbf{D}(t)^T\times\mathbf{K}-\dot{\mathbf{D}}(t)^T\times\mathbf{C}\right]\times\delta\mathbf{D}(t)\right\}dt\\ &-\dot{\mathbf{D}}(t_{i+1})^T\times\mathbf{M}\times\delta\mathbf{D}(t_{i+1})=0\end{aligned} \tag{6.3.26}$$

The substitution of the approximation functions and the corresponding variations in the local time coordinate gives

$$\int_0^r \left\{ \dot{\tilde{\mathbf{D}}}(\tau)^T \mathbf{M} \delta \dot{\tilde{\mathbf{D}}}(\tau) + \left[\mathbf{F}(t)^T + \mathbf{L}(t)^T - \tilde{\mathbf{D}}(\tau)^T \mathbf{K} - \dot{\tilde{\mathbf{D}}}(\tau)^T \mathbf{C} \right] \times \delta \tilde{\mathbf{D}}(\tau) \right\} d\left(\frac{\Delta t}{r} \tau \right)$$
$$- \dot{\tilde{\mathbf{D}}}(r)^T \mathbf{M} \delta \tilde{\mathbf{D}}(r) = 0 \tag{6.3.27}$$

Here the force functions $\mathbf{F}(t)$ and $\mathbf{L}(t)$ with respect to the global time variable t need to be translated into functions $\widehat{\mathbf{F}}(\tau)$ and $\widehat{\mathbf{L}}(\tau)$ with respect to the local time variable τ. This can be easily done within each time step by using Eq. (6.3.21).

Substituting Eqs. (6.3.22) and (6.3.24) into Eq.(6.3.27), one has

$$\mathbf{V}^T \mathbf{M}' \delta \mathbf{V} + \mathbf{L}' \delta \mathbf{V} - \mathbf{V}^T \mathbf{K}' \delta \mathbf{V} - \mathbf{V}^T \mathbf{C}' \delta \mathbf{V} - \mathbf{V}^T \mathbf{M}'_r \delta \mathbf{V} = 0 \tag{6.3.28}$$

in which

$$\mathbf{M}' = \frac{r}{\Delta t} \int_0^r \left\{ \frac{d\boldsymbol{\Psi}(\tau)}{d\tau} \mathbf{M} \frac{d\boldsymbol{\Psi}(\tau)^T}{d\tau} \right\} d\tau$$
$$\mathbf{K}' = \frac{\Delta t}{r} \int_0^r \left\{ \boldsymbol{\Psi}(\tau) \mathbf{K} \boldsymbol{\Psi}(\tau)^T \right\} d\tau$$
$$\mathbf{C}' = \int_0^r \left\{ \frac{d\boldsymbol{\Psi}(\tau)}{d\tau} \mathbf{C} \boldsymbol{\Psi}(\tau)^T \right\} d\tau \tag{6.3.29}$$
$$\mathbf{L}' = \frac{\Delta t}{r} \int_0^r \left\{ \left[\widehat{\mathbf{F}}(\tau)^T + \widehat{\mathbf{L}}(\tau)^T \right] \boldsymbol{\Psi}(\tau)^T \right\} d\tau$$
$$\mathbf{M}'_r = \frac{r}{\Delta t} \frac{d\boldsymbol{\Psi}(r)}{d\tau} \mathbf{M} \boldsymbol{\Psi}(r)^T$$

By re-arranging terms one has

$$\delta \mathbf{V}^T \left\{ \left[\mathbf{M}' - \mathbf{C}' - \mathbf{K}' - \mathbf{M}_r' \right]^T \mathbf{V} + \mathbf{L}'^T \right\} = 0 \tag{6.3.30}$$

Eq. (6.3.30) holds for any choice of $\delta \mathbf{V}$. Therefore the terms in the curly bracket have to vanish, resulting in a set of algebraic equations, viz.

$$\left[\mathbf{M}' - \mathbf{C}' - \mathbf{K}' - \mathbf{M}_r' \right]^T \mathbf{V} = -\mathbf{L}'^T \tag{6.3.31}$$

By removing $2n$ equations corresponding to $\delta \mathbf{D}(0) = 0$ and $\delta \dot{\mathbf{D}}(0) = 0$ in Eq.(6.3.30), the remaining equations can be solved for all unknown nodal displacement and nodal velocity values, including the end values at time $t = t_{i+1}$, which in turn can be utilised in the next time sub-interval as the initial value for the same computation. This process is repeated until the end of the whole time domain is reached.

6.3.2 Two-field variable algorithms

6.3.2.1 Discretisation in the spatial domain

The transformation procedure applied earlier to the displacement field is also applicable to the momentum field. The momentum field $p^{(i)}(x,t)$ of the *i*th rod in the local coordinate system may be interpolated with the rod's global nodal momentum vector $\mathbf{P}^{(i)}(t)$ as

$$p^{(i)}(x,t) = \mathbf{s}(x) \times \mathbf{T}^{(i)} \times \mathbf{P}^{(i)}(t) \tag{6.3.32}$$

with

$$\mathbf{P}^{(i)}(t) = \left\{ P_{aX}, P_{aY}, P_{aZ}, P_{bX}, P_{bY}, P_{bZ} \right\} \tag{6.3.33}$$

Substituting Eqs. (6.3.8), (6.3.9), (6.3.11), (6.3.12b) and (6.3.32) into Eq. (6.2.3) gives

$$
\begin{aligned}
&\delta\sum_{i=1}^{nr}\ \Pi_2{}^{(i)}\left(\mathrm{p},\mathrm{u}\right)= \\
&\delta\sum_{i=1}^{nr}\int_0^{t_f}\int_0^{l^{(i)}}\left\{\begin{array}{l}\mathbf{P}^{(i)}\left(t\right)^T\times\left(\mathbf{T}^T\times\mathbf{s}^T\times\mathbf{s}\times\mathbf{T}\right)^{(i)}\times\dot{\mathbf{D}}^{(i)}\left(t\right)\\ -\mathbf{P}^{(i)}\left(t\right)^T\times\left(\mathbf{T}^T\times\mathbf{s}^T\times\dfrac{1}{2\,\mathrm{m}}\times\mathbf{s}\times\mathbf{T}\right)^{(i)}\times\mathbf{P}^{(i)}\left(t\right)\\ -\mathbf{D}^{(i)}\left(t\right)^T\times\left(\mathbf{T}^T\times\dfrac{\partial\mathbf{s}^T}{\partial x}\times\dfrac{EA}{2}\times\dfrac{\partial\mathbf{s}}{\partial x}\times\mathbf{T}\right)^{(i)}\times\mathbf{D}^{(i)}\left(t\right)\end{array}\right\}dxdt\\
&+\sum_{i=1}^{nr}\int_0^{t_f}\int_0^{l^{(i)}}\left\{\begin{array}{l}\left(\mathbf{T1}\times\mathbf{f}\times\mathbf{s}\times\mathbf{T}\right)^{(i)}\times\delta\mathbf{D}^{(i)}\left(t\right)\\ -\dot{\mathbf{D}}^{(i)}\left(t\right)^T\times\left(\mathbf{T}^T\times\mathbf{s}^T\times c\times\mathbf{s}\times\mathbf{T}\right)^{(i)}\times\delta\mathbf{D}^{(i)}\left(t\right)\end{array}\right\}dxdt\\
&+\sum_{j=1}^{nd}\int_0^{t_f}\left\{\mathbf{L}^{(j)T}\times\delta\mathbf{D}^{(j)}\right\}dt-\sum_{i=1}^{nr}\int_0^{l^{(i)}}\left\{\mathbf{P}^{(i)}\left(t_f\right)^T\times\left(\mathbf{T}^T\times\mathbf{s}^T\times\mathbf{s}\times\mathbf{T}\right)^{(i)}\times\delta\mathbf{D}^{(i)}\left(t_f\right)\right\}dx\\
&=0
\end{aligned}
\tag{6.3.34a}
$$

or

$$
\begin{aligned}
&\delta\sum_{i=1}^{nr}\ \Pi_2^{(i)}\left(\mathrm{p},\mathrm{u}\right)= \\
&\delta\sum_{i=1}^{nr}\int_0^{t_f}\left\{\begin{array}{l}\mathbf{P}^{(i)}\left(t\right)^T\times\mathbf{S}_e^{(i)}\times\dot{\mathbf{D}}^{(i)}\left(t\right)-\mathbf{P}^{(i)}\left(t\right)^T\times\dfrac{\hat{\mathbf{M}}_e^{(i)}}{2}\times\mathbf{P}^{(i)}\left(t\right)\\ -\mathbf{D}^{(i)}\left(t\right)^T\times\dfrac{\mathbf{K}_e^{(i)}}{2}\times\mathbf{D}^{(i)}\left(t\right)\end{array}\right\}dt \\
&+\sum_{i=1}^{nr}\int_0^{t_f}\left\{\mathbf{F}_{(e)}^{(i)}\times\delta\mathbf{D}^{(i)}\left(t\right)-\dot{\mathbf{D}}^{(i)}\left(t\right)^T\times\mathbf{C}_e^{(i)}\times\delta\mathbf{D}^{(i)}\left(t\right)\right\}dt \\
&+\sum_{j=1}^{nd}\int_0^{t_f}\left\{\mathbf{L}^{(j)T}\times\delta\mathbf{D}^{(j)}\right\}dt-\sum_{i=1}^{nr}\left\{\mathbf{P}^{(i)}\left(t_f\right)^T\times\mathbf{S}_e^{(i)}\times\delta\mathbf{D}^{(i)}\left(t_f\right)\right\} \qquad (6.3.34b)\\
&=0
\end{aligned}
$$

where

$$\mathbf{S}_e^{(i)}=\int_0^{l^{(i)}}\left\{\mathbf{T}^T\times\mathbf{s}^T\times\mathbf{s}\times\mathbf{T}\right\}^{(i)}dx \qquad (6.3.35a)$$

$$\hat{\mathbf{M}}_e^{(i)}=\int_0^{l^{(i)}}\left\{\mathbf{T}^T\times\mathbf{s}^T\times\frac{1}{\mathrm{m}}\times\mathbf{s}\times\mathbf{T}\right\}^{(i)}dx \qquad (6.3.35b)$$

To apply the spatial discretisation, let the *n* number of nodal momentum components form a global vector $\mathbf{P}\left(t\right)$

$$\mathbf{P}\left(t\right)=\left\{P_{1X},P_{1Y},P_{1Z},P_{2X},\ldots,P_{ndX},P_{ndY},P_{ndZ}\right\}^T=\left\{P_1,P_2,\ldots,P_n\right\}^T \qquad (6.3.36)$$

The standard discretisation and assemblage of Eq. (6.3.34b) gives

$$\delta\int_0^{t_f}\left\{\mathbf{P}(t)^T\times\mathbf{S}\times\dot{\mathbf{D}}(t)-\frac{1}{2}\mathbf{P}(t)^T\times\hat{\mathbf{M}}\times\mathbf{P}(t)-\frac{1}{2}\mathbf{D}(t)^T\times\mathbf{K}\times\mathbf{D}(t)\right\}dt$$
$$+\int_0^{t_f}\left\{\left[\mathbf{F}(t)^T+\mathbf{L}(t)^T-\dot{\mathbf{D}}(t)^T\times\mathbf{C}\right]\delta\mathbf{D}(t)\right\}dt-\mathbf{P}(t_f)^T\times\mathbf{S}\times\delta\mathbf{D}(t_f)=0 \tag{6.3.37a}$$

or

$$\int_0^{t_f}\left\{\delta\mathbf{P}(t)^T\times\mathbf{S}\times\dot{\mathbf{D}}(t)+\mathbf{P}(t)^T\times\mathbf{S}\times\delta\dot{\mathbf{D}}(t)-\mathbf{P}(t)^T\times\hat{\mathbf{M}}\times\delta\mathbf{P}(t)-\mathbf{D}(t)^T\times\mathbf{K}\times\delta\mathbf{D}(t)\right\}dt$$
$$+\int_0^{t_f}\left\{\left[\mathbf{F}(t)^T+\mathbf{L}(t)^T-\dot{\mathbf{D}}(t)^T\times\mathbf{C}\right]\times\delta\mathbf{D}(t)\right\}dt-\mathbf{P}(t_f)^T\times\mathbf{S}\times\delta\mathbf{D}(t_f)=0 \tag{6.3.37b}$$

in which $\mathbf{S},\hat{\mathbf{M}},\mathbf{K},\mathbf{C}$ are four time-invariant matrices; $\mathbf{P}(t_f)$ and $\mathbf{D}(t_f)$ are the vectors of the momentum and the displacement at the instant $t=t_f$. The time finite element may be introduced at this point.

6.3.2.2 Discretisation in the temporal domain

Following the same principle for constructing a stepwise algorithm, the entire temporal domain is again divided into successive sub-intervals as shown in Figure 6.3.3. Also used is the local time coordinate τ. In the two-field algorithm, the displacement field $\mathbf{D}$ and the momentum fields $\mathbf{P}$ within an arbitrary time element $[t_i,t_{i+1}]$ are approximated simultaneously using an approximation operator.

$$\mathbf{D}(\tau)\cong\tilde{\mathbf{D}}(\tau)=\boldsymbol{\Phi}(\tau)^T\mathbf{U}\qquad\mathbf{P}(\tau)\cong\tilde{\mathbf{P}}(\tau)=\boldsymbol{\Phi}(\tau)^T\mathbf{W}\qquad(\tau\in[0,r]) \tag{6.3.38}$$

where

$$\mathbf{\Phi}(\tau)=\begin{bmatrix}\phi_0(\tau)\times\mathbf{I}\\ \phi_1(\tau)\times\mathbf{I}\\ \phi_2(\tau)\times\mathbf{I}\\ \vdots\\ \phi_r(\tau)\times\mathbf{I}\end{bmatrix}\quad \mathbf{U}=\begin{Bmatrix}\mathbf{D}(t_i)_{n\times1}\\ \mathbf{D}(t_{\theta1})_{n\times1}\\ \mathbf{D}(t_{\theta2})_{n\times1}\\ \vdots\\ \mathbf{D}(t_{i+1})_{n\times1}\end{Bmatrix}\quad \mathbf{W}=\begin{Bmatrix}\mathbf{P}(t_i)_{n\times1}\\ \mathbf{P}(t_{\theta1})_{n\times1}\\ \mathbf{P}(t_{\theta2})_{n\times1}\\ \vdots\\ \mathbf{P}(t_{i+1})_{n\times1}\end{Bmatrix} \tag{6.3.39}$$

$\mathbf{\Phi}(\tau)$ is the time finite element approximation operator, and $\phi_{(\ )}(\ )$ are the time element shape functions at the time nodes. $\mathbf{I}$ is the identity matrix of the order n. $\mathbf{U}$ is a state vector containing all time nodal values of the displacement within the current time element. $\mathbf{W}$ is a state vector containing all time nodal momentums.

For the two-field approximation, the time element shape function only needs to satisfy

$$\phi_m(n)=\delta_{mn}\qquad (m,n=0,1,\cdots,r) \tag{6.3.40}$$

Clearly Lagrange time elements fulfil such requirement. Correspondingly, the first time derivative of the approximated displacement and the variations can be approximated as

$$\begin{aligned}
&\dot{\tilde{\mathbf{D}}}(\tau)=\frac{d\mathbf{\Phi}^T}{dt}\mathbf{U}=\frac{d\tau}{dt}\frac{d\mathbf{\Phi}^T}{d\tau}\mathbf{U}=\frac{r}{\Delta t}\frac{d\mathbf{\Phi}^T}{d\tau}\mathbf{U}\\
&\delta\tilde{\mathbf{D}}(\tau)=\mathbf{\Phi}(\tau)^T\,\delta\mathbf{U}\\
&\delta\tilde{\mathbf{P}}(\tau)=\mathbf{\Phi}(\tau)^T\,\delta\mathbf{W}\\
&\delta\dot{\tilde{\mathbf{D}}}(\tau)=\frac{r}{\Delta t}\frac{d\mathbf{\Phi}^T}{d\tau}\delta\mathbf{U}
\end{aligned} \tag{6.3.41}$$

For the time sub-interval $[t_i,t_{i+1}]$, the substitution of Eqs. (6.3.38) and (6.3.41) into Eq. (6.3.37b) gives

$$\int_0^r \left\{ \begin{array}{l} \delta\mathbf{W}^T \times \mathbf{\Phi}(\tau) \times \mathbf{S} \times \dfrac{r}{\Delta t} \dfrac{d\mathbf{\Phi}^T}{d\tau} \mathbf{U} + \mathbf{W}^T \times \mathbf{\Phi}(\tau) \times \mathbf{S} \times \left(\dfrac{r}{\Delta t} \dfrac{d\mathbf{\Phi}^T}{d\tau} \delta\mathbf{U} \right) \\ -\mathbf{W}^T \times \mathbf{\Phi}(\tau) \times \hat{\mathbf{M}} \times \mathbf{\Phi}(\tau)^T \times \delta\mathbf{W} - \mathbf{U}^T \times \mathbf{\Phi}(\tau) \times \mathbf{K} \times \mathbf{\Phi}(\tau)^T \times \delta\mathbf{U} \end{array} \right\} d\left(\frac{\Delta t}{r} \tau \right)$$
$$+ \int_0^r \left\{ \left[\mathbf{F}(t)^T + \mathbf{L}(t)^T - \frac{r}{\Delta t} \mathbf{U}^T \frac{d\mathbf{\Phi}}{d\tau} \times \mathbf{C} \right] \times \mathbf{\Phi}(\tau)^T \delta\mathbf{U} \right\} d\left(\frac{\Delta t}{r} \tau \right)$$
$$- \mathbf{W}^T \times \mathbf{\Phi}(r) \times \mathbf{S} \times \mathbf{\Phi}(r)^T \delta\mathbf{U} = 0$$

(6.3.42a)

or

$$\delta\mathbf{W}^T \left[\mathbf{S}''\mathbf{U} - \mathbf{M}''^T \mathbf{W} \right] + \delta\mathbf{U}^T \left[\mathbf{L}'' + \left(\mathbf{S}''^T - \mathbf{S}_r''^T \right) \mathbf{W} - \left(\mathbf{C}''^T + \mathbf{K}''^T \right) \mathbf{U} \right] = 0 \quad (6.3.42b)$$

where

$$\begin{aligned} \mathbf{S}'' &= \int_0^r \left\{ \mathbf{\Phi}(\tau) \times \mathbf{S} \times \frac{d\mathbf{\Phi}(\tau)^T}{d\tau} \right\} d\tau \\ \mathbf{M}'' &= \frac{\Delta t}{r} \int_0^r \left\{ \mathbf{\Phi}(\tau) \times \hat{\mathbf{M}} \times \mathbf{\Phi}(\tau)^T \right\} d\tau \\ \mathbf{K}'' &= \frac{\Delta t}{r} \int_0^r \left\{ \mathbf{\Phi}(\tau) \times \mathbf{K} \times \mathbf{\Phi}(\tau)^T \right\} d\tau \\ \mathbf{C}'' &= \int_0^r \left\{ \frac{d\mathbf{\Phi}(\tau)}{d\tau} \times \mathbf{C} \times \mathbf{\Phi}(\tau)^T \right\} d\tau \\ \mathbf{L}'' &= \frac{\Delta t}{r} \int_0^r \left\{ \mathbf{\Phi}(\tau) \times \left[\tilde{\mathbf{F}}(\tau)^T + \tilde{\mathbf{L}}(\tau)^T \right] \right\} d\tau \\ \mathbf{S}_r'' &= \mathbf{\Phi}(r) \times \mathbf{S} \times \mathbf{\Phi}(r)^T \end{aligned} \quad (6.3.43)$$

It should be noted that the force functions $\mathbf{F}(t)$ and $\mathbf{L}(t)$ have been replaced by $\tilde{\mathbf{F}}(\tau)$ and $\tilde{\mathbf{L}}(\tau)$ in the calculation of $\mathbf{L}''$ for each time sub-interval, the transformation are exactly the same as explained in the one-field algorithm. The terms in the square brackets of Eq. (6.3.42b) must vanish to ensure this equation

holds for any variations of the momentum and the displacement, due to the independence between $\delta\mathbf{W}$ and $\delta\mathbf{U}$. This requirement may be couched in a matrix form

$$\begin{bmatrix} \mathbf{S}'' & -\mathbf{M}''^{T} \\ \mathbf{C}''^{T}+\mathbf{K}''^{T} & \mathbf{S}_r''^{T}-\mathbf{S}''^{T} \end{bmatrix} \begin{Bmatrix} \mathbf{U} \\ \mathbf{W} \end{Bmatrix} = \begin{Bmatrix} \mathbf{0} \\ \mathbf{L}'' \end{Bmatrix} \tag{6.3.44}$$

After removing $2n$ equations corresponding to $\delta\mathbf{D}(0)=0$ and $\delta\mathbf{P}(0)=0$, the remaining equations can be solved for all unknown values of displacement and velocity at all time nodes within the time element. The same procedures can be repeated in the successive time elements forming a recurrence scheme.

6.4 Summary

In this chapter, two classes of UHVP algorithms are presented for the direct solution of dynamics of truss structures, based on the variational principles given in Chapter 4. Semi-discretisation of the structure in the spatial and temporal domains is adopted in the derivation of the algorithms. A set of integro-differential equations is obtained after the spatial discretisation, which is then treated with piecewise time finite element approximation to derive the recurrence formulation. In the one-field algorithm the cubic Hermite time finite element is used, while Lagrange elements of various orders are applied to the two-field algorithms.

In the research, the derived algorithms are translated into computer codes using the package Matlab, to evaluate the performance and also to examine the associated numerical properties.

Chapter 7 Stability Analysis

7.1 Introduction

Having obtained the one-field and the two-field UHVP algorithms, their numerical performance are to be evaluated. For any recurrence scheme, the algorithmic stability and consistency need to be investigated to ensure convergence is guaranteed (Hughes, 1987). In this chapter, the stability of the two types of algorithms is examined first in detail. The consistency property is to be investigated in the next chapter.

Stability is a property of a numerical scheme that a small perturbation at an earlier time only produces bounded changes at later time instants in the solution (Geradin, 1974). Stability is an important property for any recurrence schemes, especially for the ones used for long time evaluation. Numerically stable algorithm is required 1) to ensure the initial conditions given is not artificially amplified in the succeeding computation; 2) to prevent the computational errors from accumulating and contaminating the numerical results (Bathe and Wilson, 1972) .

In this chapter, the stability requirement of numerical schemes is briefly discussed, and the method for the evaluation of stability is given. The one-field and two-field equations given in the last chapter are re-organised to derive the amplification matrices, whose spectral radius determine the stabilities of relevant algorithms. These spectral radii are given analytically and evaluated against the stability criterion for each time finite element individually.

7.2 Stability analysis

7.2.1 The stability of numerical schemes

Stability can be classified into three categories: unconditionally stable, conditionally stable and unconditionally unstable. An algorithm for which a time step restriction must be imposed to prevent the result from being divergent is called conditionally stable; while an algorithm does not need such restriction is called unconditionally stable (Hughes, 1987). An algorithm is unconditionally unstable if the divergence is always present. Some higher- order algorithms have been known to be unconditionally unstable (Fung, 1997).

It is desirable to design unconditionally stable algorithms since the time step can be chosen only to meet the accuracy requirement. Many researchers have focused on this perspective (Itzkowitz and Levit, 1987; Tamma and Namburu, 1990; Fung, 1999a, 1999b, Yina, 2011). However, sometimes only conditionally stable algorithms can be achieved with particular methods. For these algorithms the time step has to be restricted below a certain value, which is normally determined by the highest frequency of the system.

7.2.2 Evaluation of algorithmic stability

As the nature of the presented algorithms disclosed, the single-step recurrence scheme can be presented in general as

$$\mathbf{V}_n = \mathbf{A}\mathbf{V}_{n-1} + \mathbf{L}_n \tag{7.2.1}$$

with $\mathbf{V}_n$ and $\mathbf{V}_{n-1}$ being the state (response) vector at time $t = t_n$ and t_{n-1} respectively; $\mathbf{L}_n$ being the load for the time step $\left[t_{n-1}, t_n\right]$, and $\mathbf{A}$ is known as the amplification matrix.

$\mathbf{V}_n$ is related to the initial state vector $\mathbf{V}_0$ at $t_0 = 0$ as

$$\begin{aligned}\mathbf{V}_n &= \mathbf{A}\mathbf{V}_{n-1} + \mathbf{L}_n = \mathbf{A}\left(\mathbf{A}\mathbf{V}_{n-2} + \mathbf{L}_{n-1}\right) + \mathbf{L}_n \\ &= \cdots \\ &= \mathbf{A}^n\mathbf{V}_0 + \mathbf{A}^{n-1}\mathbf{L}_1 + \cdots + \mathbf{A}^2\mathbf{L}_{n-2} + \mathbf{A}\mathbf{L}_{n-1} + \mathbf{L}_n\end{aligned} \tag{7.2.2}$$

It can be seen from the above equation that the stability of a particular algorithm is greatly influenced by the property of $\mathbf{A}$, and the contribution of the load operator is rather limited.

The spectral radius is related to the maximum magnitude of the eigenvalues of $\mathbf{A}$ (Hughes, 1987). If $\lambda^{(i)}$ denotes the eigenvalues of $\mathbf{A}$, which can be complex in some cases, its modulus is defined as

$$\left|\lambda^{(i)}\right| = \sqrt{\lambda^{(i)} \times \overline{\lambda}^{(i)}} \tag{7.2.3}$$

where $\overline{\lambda}^{(i)}$ is the complex conjugate of $\lambda^{(i)}$.

The spectral radius of $\mathbf{A}$, $\rho(\mathbf{A})$, is then defined as

$$\rho(\mathbf{A}) = \max_i \left|\lambda^{(i)}\right| \tag{7.2.4}$$

It is required that $\rho(\mathbf{A})$ should be less than unity for an algorithm to be stable, which means the initial condition will not be amplified artificially and any error induced in the approximation scheme will be bounded in the sequent computation.

Since it has been rigorously established that a MDOF system can be uncoupled as the combination of multiple SDOF components and possesses the same stability properties of these components (Hughes, 1987, Wood, 1990), the presented algorithms can be evaluated with a SDOF system

$$\ddot{x} + 2\xi\omega\dot{x} + \omega^2 x = f(t) \tag{7.2.5}$$

where $\omega = 2\pi/T$ is the natural frequency of the system and T is the corresponding period. ξ is the damping ratio.

7.3 Stability of the one-field algorithm using the Hermite time finite element

The one-field space-time finite element formulation presented in the last chapter, i.e., Eq. (6.3.31), is recalled herein

$$\left[\mathbf{M}' - \mathbf{C}' - \mathbf{K}' - \mathbf{M}'_r\right]^T \mathbf{V} = -\mathbf{L}'^T \tag{7.3.1a}$$

or

$$\begin{aligned} &\mathbf{GV} = -\mathbf{L}'^T \\ &\left(\mathbf{G}(i,j) = \mathbf{M}'^T(i,j) - \mathbf{C}'^T(i,j) - \mathbf{K}'^T(i,j) - \mathbf{M}'^T_r(i,j)\right) \end{aligned} \tag{7.3.1b}$$

with the vector and matrices defined as

$$\begin{aligned} \mathbf{M}' &= \frac{r}{\Delta t}\int_0^r \left\{\frac{d\mathbf{\Psi}(\tau)}{d\tau}\frac{d\mathbf{\Psi}(\tau)^T}{d\tau}\right\} d\tau \\ \mathbf{K}' &= \frac{\omega^2 \Delta t}{r}\int_0^r \left\{\mathbf{\Psi}(\tau)\mathbf{\Psi}(\tau)^T\right\} d\tau \\ \mathbf{C}' &= 2\xi\omega\int_0^r \left\{\frac{d\mathbf{\Psi}(\tau)}{d\tau}\mathbf{\Psi}(\tau)^T\right\} d\tau \\ \mathbf{L}' &= \frac{\Delta t}{r}\int_0^r \left\{\left[\widehat{F}(\tau)^T + \widehat{L}(\tau)^T\right]\mathbf{\Psi}(\tau)^T\right\} d\tau \\ \mathbf{M}'_r &= \frac{r}{\Delta t}\frac{d\mathbf{\Psi}(r)}{d\tau}\mathbf{\Psi}(r)^T \end{aligned} \tag{7.3.2}$$

When the Hermite cubic polynomials are used for the time approximation operator $\mathbf{\Psi}$, the integer r equals to unity correspondingly. The algorithm thus obtained is referred as UHVP_H3 thereafter in this thesis. The state vector and the approximation operator are

$$\mathbf{V}=\begin{Bmatrix} d\left(t_i\right) \\ d\left(t_{i+1}\right) \\ \Delta t\times \dot{d}\left(t_i\right) \\ \Delta t\times \dot{d}\left(t_{i+1}\right) \end{Bmatrix} \qquad \mathbf{\Psi}\left(\tau\right)=\begin{bmatrix} 1-3\tau^2+2\tau^3 \\ 3\tau^2-2\tau^3 \\ \tau-2\tau^2+\tau^3 \\ \tau^3-\tau^2 \end{bmatrix} \tag{7.3.3}$$

and

$$\frac{d\mathbf{\Psi}\left(\tau\right)}{d\tau}==\begin{bmatrix} -6\tau+6\tau^2 \\ 6\tau-6\tau^2 \\ 1-4\tau+3\tau^2 \\ 3\tau^2-2\tau \end{bmatrix} \tag{7.3.4}$$

Let the time step be expressed in terms of the natural period as $\Delta t=\alpha T$, the coefficient matrices become

$$\begin{aligned} \mathbf{M}' &= \frac{1}{\alpha T}\int_0^1\left\{\frac{d\mathbf{\Psi}\left(\tau\right)}{d\tau}\frac{d\mathbf{\Psi}\left(\tau\right)^T}{d\tau}\right\}d\tau \\ \mathbf{K}' &= \omega^2\alpha T\int_0^1\left\{\mathbf{\Psi}\left(\tau\right)\mathbf{\Psi}\left(\tau\right)^T\right\}d\tau \\ \mathbf{C}' &= 2\xi\omega\int_0^1\left\{\frac{d\mathbf{\Psi}\left(\tau\right)}{d\tau}\mathbf{\Psi}\left(\tau\right)^T\right\}d\tau \\ \mathbf{L}' &= \alpha T\int_0^1\left\{\left[\widehat{F}\left(\tau\right)^T+\widehat{L}\left(\tau\right)^T\right]\mathbf{\Psi}\left(\tau\right)^T\right\}d\tau \\ \mathbf{M}'_r &= \frac{1}{\alpha T}\frac{d\mathbf{\Psi}\left(1\right)}{d\tau}\mathbf{\Psi}\left(1\right)^T \end{aligned} \tag{7.3.5}$$

The time-invariant matrices can be expressed explicitly as

$$\mathbf{M}' = \frac{1}{\alpha T}\begin{bmatrix} 6/5 & -6/5 & 1/10 & 1/10 \\ & 6/5 & -1/10 & -1/10 \\ & & 2/15 & -1/30 \\ sym & & & 2/15 \end{bmatrix} \tag{7.3.6a}$$

$$\mathbf{K}' = \omega^2 \alpha T\begin{bmatrix} 13/35 & 9/70 & 11/210 & -13/420 \\ & 13/35 & 13/420 & -11/210 \\ & & 1/105 & -1/140 \\ sym & & & 1/105 \end{bmatrix} \tag{7.3.6b}$$

$$\mathbf{C}' = 2\xi\omega\begin{bmatrix} -1/2 & -1/2 & -1/10 & 1/10 \\ & 1/2 & 1/10 & -1/10 \\ & & 0 & 1/60 \\ -sym & & & 0 \end{bmatrix} \tag{7.3.6c}$$

$$\mathbf{M}'_r = \frac{1}{\alpha T}\begin{bmatrix} 0 & 0 & 0 & 0 \\ 0 & 0 & 0 & 0 \\ 0 & 0 & 0 & 0 \\ 0 & 1 & 0 & 0 \end{bmatrix} \tag{7.3.6d}$$

The state vector at the end of the time step, $\mathbf{V}_1 = \left\{ d\left(t_{i+1}\right) \quad \Delta t \times \dot{d}\left(t_{i+1}\right) \right\}^T$, re-organised from Eq. (7.3.3), is obtained from the initial state vector $\mathbf{V}_0 = \left\{ d\left(t_i\right) \quad \Delta t \times \dot{d}\left(t_i\right) \right\}^T$. To this end, Eq. (7.3.1b) is partitioned as

$$\begin{bmatrix} \mathbf{G}_{00} & \mathbf{G}_{01} \\ \mathbf{G}_{10} & \mathbf{G}_{11} \end{bmatrix} \begin{Bmatrix} \mathbf{V}_0 \\ \mathbf{V}_1 \end{Bmatrix} = \begin{Bmatrix} \mathbf{L}_0 \\ \mathbf{L}_1 \end{Bmatrix} \tag{7.3.7}$$

From which the end state vector can be solved for as

$$\mathbf{V}_1 = -\mathbf{G}_{11}{}^{-1}\mathbf{G}_{10}\mathbf{V}_0 + \mathbf{G}_{11}{}^{-1}\mathbf{L}_1 = \mathbf{A}\mathbf{V}_0 + \mathbf{G}_{11}{}^{-1}\mathbf{L}_1 \tag{7.3.8}$$

It is clear that $-\mathbf{G}_{11}^{-1}\mathbf{G}_{10}$ is the amplification matrix $\mathbf{A}$ whose spectral radius determines the stability of the algorithm. $\mathbf{G}_{11}^{-1}\mathbf{L}_1$ is the load operator for each time step.

The two sub-matrices $\mathbf{G}_{10}$ and $\mathbf{G}_{11}$ are given by

$$\mathbf{G}_{10}=\begin{bmatrix} \frac{2\pi\xi}{T}-\frac{18\alpha\pi^2}{35T}-\frac{6}{5\alpha T} & \frac{2\pi\xi}{5T}-\frac{13\alpha\pi^2}{105T}-\frac{1}{10\alpha T} \\ \frac{-2\pi\xi}{5T}+\frac{13\alpha\pi^2}{105T}+\frac{1}{10\alpha T} & \frac{\alpha\pi^2}{35T}-\frac{1}{30\alpha\pi}-\frac{\pi\xi}{15T} \end{bmatrix} \tag{7.3.9a}$$

$$\mathbf{G}_{11}=\begin{bmatrix} \frac{6}{5\alpha T}-\frac{52\alpha\pi^2}{35T}-\frac{2\xi\pi}{T} & \frac{22\alpha\pi^2}{105T}-\frac{11}{10\alpha T}-\frac{2\xi\pi}{5T} \\ \frac{22\alpha\pi^2}{105T}-\frac{1}{10\alpha T}+\frac{2\xi\pi}{5T} & \frac{2}{15\alpha T}-\frac{4\alpha\pi^2}{105T} \end{bmatrix} \tag{7.3.9b}$$

in which the natural frequency ω has been replaced by $2\pi/T$.

The amplification matrix is hence found to be

$$\mathbf{A} = -\mathbf{G}_{11}^{-1}\mathbf{G}_{10} = \frac{1}{e}\begin{bmatrix} b1 & b2 \\ b3 & b4 \end{bmatrix}$$

$$e = 13440\pi^3\alpha^3\xi^3 + (7680\pi^4\alpha^4 + 25200\pi^2\alpha^2)\xi^2 + (1920\pi^5\alpha^5 + 4320\pi^3\alpha^3 + 25200\pi\alpha)\xi$$
$$+256\pi^6\alpha^6 - 240\pi^4\alpha^4 + 1800\pi^2\alpha^2 + 11025$$

$$b1 = 13440\pi^3\alpha^3\xi^3 + (25200\pi^2\alpha^2 - 5760\pi^4\alpha^4)\xi^2 + (960\pi^5\alpha^5 - 16680\pi^3\alpha^3 + 25200\pi\alpha)\xi$$
$$-64\pi^6\alpha^6 + 3720\pi^4\alpha^4 - 20250\pi^2\alpha^2 + 11025$$

$$b2 = (4200\pi^3\alpha^3\xi^2 + (3150\pi\alpha^2 - 960\pi^3\alpha^4)\xi + 360\pi^4\alpha^5 - 5550\pi^2\alpha^3 + 11025\alpha)T$$

$$b3 = \left(-16800\pi^4\alpha^3\xi^2 + \left(3840\pi^5\alpha^4 - 12600\pi^3\alpha^2\right)\xi - 1440\pi^6\alpha^5 + 22200\pi^4\alpha^3 - 44100\pi^2\alpha\right)/T$$

$$b4 = -3360\pi^3\alpha^3\xi^3 + (12600\pi^2\alpha^2 - 1920\pi^4\alpha^4)\xi^2 + (-480\pi^5\alpha^5 + 5520\pi^3\alpha^3 - 18900\pi\alpha)\xi$$
$$-64\pi^6\alpha^6 + 3720\pi^4\alpha^4 - 20250\pi^2\alpha^2 + 11025$$

(7.3.10)

Correspondingly, the two eigenvalues of the amplification matrix, $\lambda^{(1)}, \lambda^{(2)}$, are

$$\lambda^{(1)} = \frac{\left(72\alpha^4\pi^4 - 582\alpha^2\pi^2 - 204\alpha^3\pi^3\xi + 588\alpha^2\pi^2\xi^2 + 210\alpha\pi\xi + 315\right) + B}{80\alpha^4\pi^4 + 480\alpha^3\pi^3\xi + 1008\alpha^2\pi^2\xi^2 + 48\alpha^2\pi^2 + 840\alpha\pi\xi + 315}$$

$$\lambda^{(2)} = \frac{\left(72\alpha^4\pi^4 - 582\alpha^2\pi^2 - 204\alpha^3\pi^3\xi + 588\alpha^2\pi^2\xi^2 + 210\alpha\pi\xi + 315\right) - B}{80\alpha^4\pi^4 + 480\alpha^3\pi^3\xi + 1008\alpha^2\pi^2\xi^2 + 48\alpha^2\pi^2 + 840\alpha\pi\xi + 315}$$

$$B = 2\alpha\pi\sqrt{\begin{array}{l} 1216\alpha^6\pi^6 - 21960\alpha^4\pi^4 + 88830\alpha^2\pi^2 - 99225 - 6864\alpha^5\pi^5\xi \\ +32964\alpha^4\pi^4\xi^2 - 68040\alpha^3\pi^3\xi^3 + 69300\alpha^3\pi^3\xi + 44100\alpha^2\pi^2\xi^4 \\ -146160\alpha^2\pi^2\xi^2 + 132300\alpha\pi\xi\left(\xi^2 - 1\right) + 99225\xi^2 \end{array}}$$

(7.3.11)

It is found that both $\left|\lambda^{(1)}\right|$ and $\left|\lambda^{(2)}\right|$ will increase over unity when the ratio of the time step to the natural period $\left(\alpha = \Delta t / T\right)$ is sufficiently big, and the ultimate radius is $\left(72 + 2\sqrt{1216}\right)\Big/80 \approx 1.77$ when the ratio approaches infinity. Therefore, the UHVP_H3 algorithm is conditionally stable. Figure 7.3.1 shows the spectral radii of the amplification matrices with various damping ratio ξ

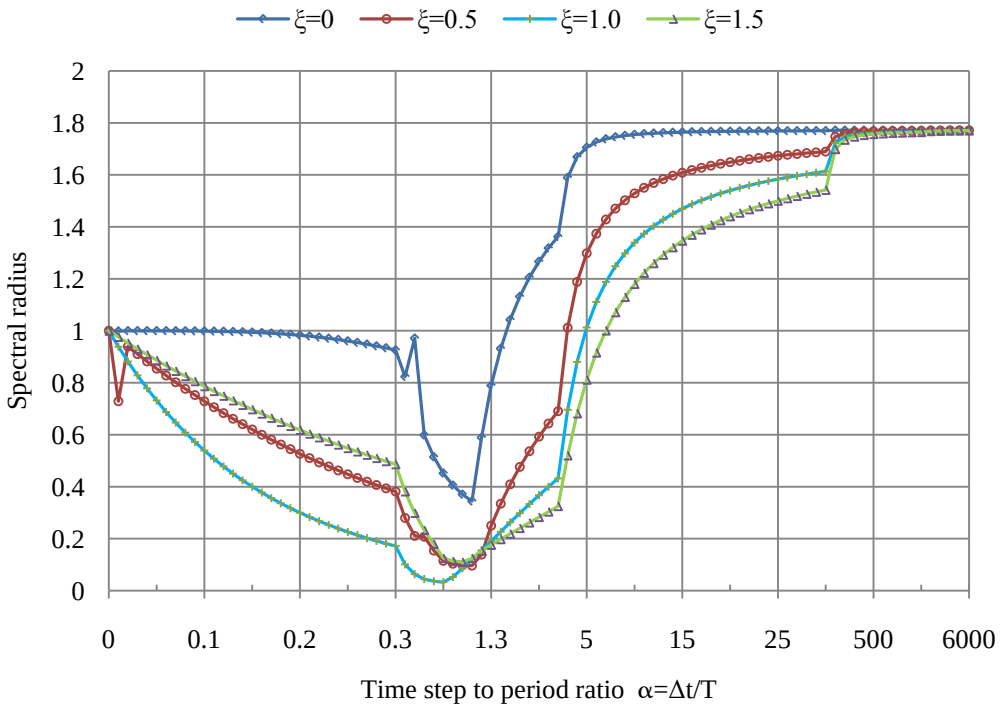

Figure 7.3.1 – Spectral radii for the amplification matrices of UHVP_H3

It is known the maximum length of the time step can be determined conservatively by the undamped case ($\xi = 0$) (Wood, 1990, Hughes, 1987). For this particular algorithm, the maximum ratio $\alpha_{\max}$ equals to $\sqrt{21}/\pi$, which is solved from the following inequality

$$\frac{\left(72\alpha^4\pi^4-582\alpha^2\pi^2+315\right)+2\alpha\pi\sqrt{1216\alpha^6\pi^6-21960\alpha^4\pi^4+88830\alpha^2\pi^2-99225}}{80\alpha^4\pi^4+48\alpha^2\pi^2+315}\le 1$$

(7.3.12)

To ensure convergent solutions are to be obtained, the time step used in the computation must not exceed $\alpha_{\max}T$.

7.4 Stability of the two-field algorithms with Lagrange time finite elements

7.4.1 General form

For the SDOF problem represented by Eq. (7.2.5), the two-field formulation Eq. (6.3.43) is recalled

$$\begin{bmatrix} \mathbf{S}'' & -\mathbf{M}''^T \\ \mathbf{C}''^T+\mathbf{K}''^T & \mathbf{S}_r''^T-\mathbf{S}''^T \end{bmatrix}\begin{Bmatrix}\mathbf{U}\\ \mathbf{W}\end{Bmatrix}=\begin{Bmatrix}\mathbf{0}\\ \mathbf{L}''\end{Bmatrix} \tag{7.4.1}$$

with

$$
\begin{aligned}
&\mathbf{S}'' = \int_0^r \left\{ \mathbf{\Phi}(\tau) \times \mathbf{S} \times \frac{d\mathbf{\Phi}(\tau)^T}{d\tau} \right\} d\tau \\
&\mathbf{M}'' = \frac{\Delta t}{r} \int_0^r \left\{ \mathbf{\Phi}(\tau) \times \hat{\mathbf{M}} \times \mathbf{\Phi}(\tau)^T \right\} d\tau \\
&\mathbf{K}'' = \frac{\Delta t}{r} \int_0^r \left\{ \mathbf{\Phi}(\tau) \times \omega^2 \times \mathbf{\Phi}(\tau)^T \right\} d\tau \\
&\mathbf{C}''^T = \int_0^r \left\{ \mathbf{\Phi}(\tau) \times 2\xi\omega \times \frac{d\mathbf{\Phi}(\tau)^T}{d\tau} \right\} d\tau \\
&\mathbf{L}'' = \frac{\Delta t}{r} \int_0^r \left\{ \mathbf{\Phi}(\tau) \times \left[\tilde{\mathbf{F}}(\tau)^T + \tilde{\mathbf{L}}(\tau)^T \right] \right\} d\tau \\
&\mathbf{S}_r'' = \mathbf{\Phi}(r) \times \mathbf{S} \times \mathbf{\Phi}(r)^T \\
&\mathbf{\Phi}(\tau) = \left\{ \phi_0(\tau) \quad \phi_1(\tau) \quad \phi_2(\tau) \quad \cdots \quad \phi_r(\tau) \right\}^T \\
&\mathbf{U} = \left\{ d(t_i) \quad d(\tau_{\theta 1}) \quad d(\tau_{\theta 2}) \quad \cdots \quad d(t_{i+1}) \right\}^T \\
&\mathbf{W} = \left\{ p(t_i) \quad p(\tau_{\theta 1}) \quad p(\tau_{\theta 2}) \quad \cdots \quad p(t_{i+1}) \right\}^T
\end{aligned}
\tag{7.4.2}
$$

in which $\tau_{\theta 1}, \tau_{\theta 2}, \cdots$ are the intermediate time temporal nodes within the time finite element, and $\mathbf{\Phi}(\tau)$ the Lagrange approximation vector. It should be noted that the matrix $\mathbf{S}$ in the expressions of $\mathbf{S}''$ and $\mathbf{S}_r''$ degenerates to a scalar of unity for the SDOF problem (from Eq. (6.3.35a)). So does $\hat{\mathbf{M}}$ in the expression of $\mathbf{M}''$ (from Eq. (6.3.35b)).

Define state vectors $\mathbf{V}_0$, $\mathbf{V}_\theta$, $\mathbf{V}_r$ as follows

$$
\mathbf{V}_0 = \begin{Bmatrix} d(t_i) \\ p(t_i) \end{Bmatrix}; \quad \mathbf{V}_\theta = \begin{Bmatrix} d(\tau_{\theta 1}) \\ p(\tau_{\theta 1}) \\ d(\tau_{\theta 2}) \\ p(\tau_{\theta 2}) \\ \vdots \\ d\left(\tau_{\theta(r-1)}\right) \\ p\left(\tau_{\theta(r-1)}\right) \end{Bmatrix}; \quad \mathbf{V}_r = \begin{Bmatrix} d(t_{i+1}) \\ p(t_{i+1}) \end{Bmatrix} \tag{7.4.3}
$$

With these definitions, Eq. (7.4.1) can be re-organised and partitioned in the order of the temporal nodes as follows

$$\begin{bmatrix} \mathbf{G}_{00} & \mathbf{G}_{0\theta} & \mathbf{G}_{0r} \\ \mathbf{G}_{\theta 0} & \mathbf{G}_{\theta\theta} & \mathbf{G}_{\theta r} \\ \mathbf{G}_{r0} & \mathbf{G}_{r\theta} & \mathbf{G}_{rr} \end{bmatrix} \begin{Bmatrix} \mathbf{V}_0 \\ \mathbf{V}_\theta \\ \mathbf{V}_r \end{Bmatrix} = \begin{Bmatrix} \mathbf{L}_0 \\ \mathbf{L}_\theta \\ \mathbf{L}_r \end{Bmatrix} \tag{7.4.4}$$

$\mathbf{G}_{(\,)}$ and $\mathbf{L}_{(\,)}$ are the coefficient sub-matrices and the load sub-vectors grouped correspondingly. The end state vector $\mathbf{V}_r$ can be solved in the following procedure. Firstly, one has

$$\begin{Bmatrix} \mathbf{V}_\theta \\ \mathbf{V}_r \end{Bmatrix} = \begin{bmatrix} \mathbf{G}_{\theta\theta} & \mathbf{G}_{\theta r} \\ \mathbf{G}_{r\theta} & \mathbf{G}_{rr} \end{bmatrix}^{-1} \left(-\begin{Bmatrix} \mathbf{G}_{\theta 0} \\ \mathbf{G}_{r0} \end{Bmatrix} \mathbf{V}_0 + \begin{Bmatrix} \mathbf{L}_\theta \\ \mathbf{L}_r \end{Bmatrix} \right) = \begin{bmatrix} \mathbf{A}_\theta \\ \mathbf{A}_r \end{bmatrix} \mathbf{V}_0 + \begin{Bmatrix} \mathbf{GL}_\theta \\ \mathbf{GL}_r \end{Bmatrix} \tag{7.4.5}$$

from which

$$\mathbf{V}_r = \mathbf{A}_r \mathbf{V}_0 + \mathbf{GL}_r \tag{7.4.6}$$

It is obvious the amplification matrix $\mathbf{A}_r$ varies according to the approximation functions adopted. In the following sub-sections, the stability of the algorithms based on the second- and higher-order Lagrange polynomials will be examined in detail.

7.4.2 Algorithm using second-order Lagrange time finite element

When the second-order Lagrange polynomials are used for the time approximation operator $\mathbf{\Phi}$, the integer r equals to two correspondingly. The algorithm thus obtained is referred as UHVP_L2 thereafter in this thesis. The approximation operators are

$$\mathbf{\Phi}(\tau)=\begin{Bmatrix}\frac{1}{2}(\tau-1)(\tau-2)\\ \tau(2-\tau)\\ \frac{1}{2}\tau(\tau-1)\end{Bmatrix}\quad \frac{d\mathbf{\Phi}(\tau)}{d\tau}=\begin{Bmatrix}\tau-\frac{3}{2}\\ 2-2\tau\\ \tau-\frac{1}{2}\end{Bmatrix}\quad (\tau\in[0,2]) \tag{7.4.7}$$

Let the time step be expressed in terms of the natural period as $\Delta t=\alpha T$. The time invariant coefficient matrices in Eq. (7.4.2) become

$$\mathbf{S}''=\begin{bmatrix}-1/2 & 2/3 & -1/6\\ & 0 & 2/3\\ -sym & & 1/2\end{bmatrix} \tag{7.4.8a}$$

$$\mathbf{M}''=\frac{\alpha T}{2}\begin{bmatrix}4/15 & 2/15 & -1/15\\ & 16/15 & 2/15\\ sym & & 4/15\end{bmatrix} \tag{7.4.8b}$$

$$\mathbf{K}''=\frac{2\alpha\pi^2}{T}\begin{bmatrix}4/15 & 2/15 & -1/15\\ & 16/15 & 2/15\\ sym & & 4/15\end{bmatrix} \tag{7.4.8c}$$

$$\mathbf{C}''^{T}=\frac{4\pi\xi}{T}\begin{bmatrix}-1/2 & 2/3 & -1/6\\ & 0 & 2/3\\ -sym & & 1/2\end{bmatrix} \tag{7.4.8d}$$

$$\mathbf{S}_r''=\begin{bmatrix}0 & 0 & 0\\ 0 & 0 & 0\\ 0 & 0 & 1\end{bmatrix} \tag{7.4.8e}$$

The sub-matrices in Eq. (7.4.5) related to the amplification matrix $\mathbf{A}_r$ can be written explicitly as follows

$$\mathbf{G}_{\theta\theta}=\begin{bmatrix}\mathbf{S}''(2,2) & -\mathbf{M}''^{T}(2,2)\\ \mathbf{C}''^{T}(2,2)+\mathbf{K}''^{T}(2,2) & \mathbf{S}_r''^{T}(2,2)-\mathbf{S}''^{T}(2,2)\end{bmatrix} \tag{7.4.9a}$$

$$=\begin{bmatrix}0 & \dfrac{-8\alpha T}{15}\\ \dfrac{32\pi^2\alpha}{15T} & 0\end{bmatrix}$$

$$\mathbf{G}_{\theta r}=\begin{bmatrix}\mathbf{S}''(2,3) & -\mathbf{M}''^{T}(2,3)\\ \mathbf{C}''^{T}(2,3)+\mathbf{K}''^{T}(2,3) & \mathbf{S}_r''^{T}(2,3)-\mathbf{S}''^{T}(2,3)\end{bmatrix} \tag{7.4.9b}$$

$$=\begin{bmatrix}\dfrac{2}{3} & \dfrac{-\alpha T}{15}\\ \dfrac{4\pi^2\alpha}{15T}+\dfrac{8\pi\xi}{3T} & \dfrac{2}{3}\end{bmatrix}$$

$$\mathbf{G}_{r\theta}=\begin{bmatrix}\mathbf{S}''(3,2) & -\mathbf{M}''^{T}(3,2)\\ \mathbf{C}''^{T}(3,2)+\mathbf{K}''^{T}(3,2) & \mathbf{S}_r''^{T}(3,2)-\mathbf{S}''^{T}(3,2)\end{bmatrix} \tag{7.4.9c}$$

$$=\begin{bmatrix}\dfrac{-2}{3} & \dfrac{-\alpha T}{15}\\ \dfrac{4\pi^2\alpha}{15T}-\dfrac{8\pi\xi}{3T} & \dfrac{-2}{3}\end{bmatrix}$$

$$\mathbf{G}_{rr}=\begin{bmatrix}\mathbf{S}''(3,3) & -\mathbf{M}''^{T}(3,3)\\ \mathbf{C}''^{T}(3,3)+\mathbf{K}''^{T}(3,3) & \mathbf{S}_r''^{T}(3,3)-\mathbf{S}''^{T}(3,3)\end{bmatrix} \tag{7.4.9d}$$

$$=\begin{bmatrix}\dfrac{1}{2} & \dfrac{-2\alpha T}{15}\\ \dfrac{8\pi^2\alpha}{15T}+\dfrac{2\pi\xi}{T} & \dfrac{1}{2}\end{bmatrix}$$

$$\mathbf{G}_{\theta 0}=\begin{bmatrix}\mathbf{S}''(2,1) & -\mathbf{M}''^{T}(2,1)\\ \mathbf{C}''^{T}(2,1)+\mathbf{K}''^{T}(2,1) & \mathbf{S}_r''^{T}(2,1)-\mathbf{S}''^{T}(2,1)\end{bmatrix}$$

(7.4.9e)

$$=\begin{bmatrix}\frac{-2}{3} & \frac{-\alpha T}{15}\\ \frac{4\pi^2\alpha}{15T}-\frac{8\pi\xi}{3T} & \frac{-2}{3}\end{bmatrix}$$

$$\mathbf{G}_{r0}=\begin{bmatrix}\mathbf{S}''(3,1) & -\mathbf{M}''^{T}(3,1)\\ \mathbf{C}''^{T}(3,1)+\mathbf{K}''^{T}(3,1) & \mathbf{S}_r''^{T}(3,1)-\mathbf{S}''^{T}(3,1)\end{bmatrix}$$

(7.4.9f)

$$=\begin{bmatrix}\frac{1}{6} & \frac{\alpha T}{30}\\ \frac{2\pi\xi}{3T}-\frac{2\pi^2\alpha}{15T} & \frac{1}{6}\end{bmatrix}$$

The amplification matrix $\mathbf{A}_r$ is found to be

$$\mathbf{A}_r=\begin{bmatrix}1-\frac{2\pi^2\alpha^2\left(3\pi^2\alpha^2+30\pi\xi\alpha+25\right)}{b} & \frac{-\alpha T\left(9\pi^2\alpha^2-10\pi\xi\alpha-25\right)}{e}\\ \frac{40\pi^2\alpha\left(9\pi^2\alpha^2-10\pi\xi\alpha-25\right)}{bT} & \frac{1}{3}-\frac{46\pi^2\alpha^2+60\pi\xi\alpha-50/3}{e}\end{bmatrix}$$

$$b=9\pi^4\alpha^4+36\pi^3\alpha^3\xi+60\pi^2\xi^2\alpha^2+6\pi^2\alpha^2+60\pi\xi\alpha+25 \qquad (7.4.10)$$

$$e=6\pi^2\alpha^2\left(10\xi^2+1\right)+9\pi^4\alpha^4+36\pi^3\alpha^3\xi+60\pi\xi\alpha+25$$

The two eigenvalues of the amplification matrix $\mathbf{A}_r$, $\lambda^{(1)},\lambda^{(2)}$, are

$$\lambda^{(1)} = \mathrm{Re} + \mathrm{Im}; \quad \lambda^{(2)} = \mathrm{Re} - \mathrm{Im}$$

$$\mathrm{Re} = \left(3\pi^4\alpha^4 - 44\pi^2\alpha^2 - 6\pi^3\alpha^3\xi + 10\pi\alpha\xi + 40\pi^2\alpha^2\xi^2 + 25\right) \Big/ b \tag{7.4.11}$$

$$\mathrm{Im} = \left(-18\pi^3\alpha^3\sqrt{\xi^2-1} + 50\pi\alpha\sqrt{\xi^2-1} + 20\pi^2\alpha^2\xi\sqrt{\xi^2-1}\right) \Big/ b$$

It is clear that the two eigenvalues are complex conjugates when the system is undamped or under-damped, i.e., $\xi < 1$, consequently the spectral radius of $\mathbf{A}_r$ is

$$\begin{aligned} \rho(\mathbf{A}_r) &= \left|\lambda^{(1,2)}\right| = \sqrt{\lambda^{(1)} \times \lambda^{(2)}} \\ &= \frac{\sqrt{\left(3\pi^4\alpha^4 - 44\pi^2\alpha^2 - 6\pi^3\alpha^3\xi + 10\pi\alpha\xi + 40\pi^2\alpha^2\xi^2 + 25\right)^2 + \left(-18\pi^3\alpha^3 + 50\pi\alpha + 20\pi^2\alpha^2\xi\right)^2\left(1-\xi^2\right)}}{9\pi^4\alpha^4 + 36\pi^3\alpha^3\xi + 60\pi^2\xi^2\alpha^2 + 6\pi^2\alpha^2 + 60\pi\xi\alpha + 25} \\ &(\xi < 1) \end{aligned} \tag{7.4.12}$$

It is required $\rho(\mathbf{A}_r) \le 1$ for an algorithm to be stable. In order to evaluate the stability, let $\rho^2(\mathbf{A}_r) \le 1$, which leads to an inequality

$$\begin{aligned} 0 \le\ & 72\pi^8\alpha^8 + 684\pi^7\alpha^7\xi + 2424\pi^6\alpha^6\xi^2 + 48\pi^6\alpha^6 + 4080\pi^5\alpha^5\xi^3 \\ & + \pi^5\alpha^5\xi(1704 - 60\xi) + 2400\pi^4\alpha^4\xi^4 + 120\pi^4\alpha^4\xi^3 + 6360\pi^4\alpha^4\xi^2 \\ & + 200\pi^4\alpha^4 + 100\pi^3\alpha^3\xi^3(92 - 8\xi) + 880\pi^3\alpha^3\xi^2 + 820\pi^3\alpha^3\xi \\ & + 100\pi^2\alpha^2\xi^2(71 - \xi^2) + 100\pi\alpha\xi(30 - 5\xi) \end{aligned} \tag{7.4.13}$$

It can be seen that this inequality holds for any value of $\xi < 1$, therefore the algorithm is unconditionally stable for undamped and under-damped cases.

When the system is critically-damped or over-damped, the two eigenvalues become real numbers. In this case, the spectral radius is determined by the larger

value of $\left|\lambda^{(1)}\right|$ and $\left|\lambda^{(2)}\right|$. Both values are considered here since it is not possible to determine in advance which one is larger in the case of over-damped systems.

Let $\left|\lambda^{(1)}\right|^2 \le 1$, then one has

$$\begin{aligned}&\left(\begin{aligned}&3\pi^4\alpha^4-44\pi^2\alpha^2-6\pi^3\alpha^3\xi+10\pi\alpha\xi+40\pi^2\alpha^2\xi^2+25\\&-18\pi^3\alpha^3\sqrt{\xi^2-1}+50\pi\alpha\sqrt{\xi^2-1}+20\pi^2\alpha^2\xi\sqrt{\xi^2-1}\end{aligned}\right)^2\\&\le\left(9\pi^4\alpha^4+36\pi^3\alpha^3\xi+60\pi^2\xi^2\alpha^2+6\pi^2\alpha^2+60\pi\xi\alpha+25\right)^2\end{aligned}\tag{7.4.14a}$$

or

$$\begin{aligned}&72\pi^8\alpha^8+684\pi^7\alpha^7\xi+108\pi^7\alpha^7\sqrt{\xi^2-1}+696\pi^6\alpha^6+\left(1776\xi-336\sqrt{\xi^2-1}\right)\pi^6\alpha^6\xi\\&+204\pi^5\alpha^5\xi+\left(5520\xi^3-1884\sqrt{\xi^2-1}\right)\pi^5\alpha^5+1680\pi^5\alpha^5\xi^2\sqrt{\xi^2-1}+\left(10880\xi^2-3400\right)\pi^4\alpha^4\\&+2720\pi^4\alpha^4\xi\sqrt{\xi^2-1}+1600\pi^4\alpha^4\xi^3\left(\xi-\sqrt{\xi^2-1}\right)+4400\pi^3\alpha^3\xi^2\left(\xi-\sqrt{\xi^2-1}\right)\\&+5700\pi^3\alpha^3\xi+5300\pi^3\alpha^3\sqrt{\xi^2-1}+5000\pi^2\alpha^2+2000\pi^2\alpha^2\xi\left(\xi-\sqrt{\xi^2-1}\right)\\&+2500\pi\alpha\left(\xi-\sqrt{\xi^2-1}\right)\ge 0\end{aligned}\tag{7.4.14b}$$

This inequality holds for any value of $\xi \ge 1$.

Similarly let $\left|\lambda^{(2)}\right|^2 \le 1$, then one has

$$\begin{aligned}&\left(\begin{aligned}&3\pi^4\alpha^4-44\pi^2\alpha^2-6\pi^3\alpha^3\xi+10\pi\alpha\xi+40\pi^2\alpha^2\xi^2+25\\&+18\pi^3\alpha^3\sqrt{\xi^2-1}-50\pi\alpha\sqrt{\xi^2-1}-20\pi^2\alpha^2\xi\sqrt{\xi^2-1}\end{aligned}\right)^2\\&\le\left(9\pi^4\alpha^4+36\pi^3\alpha^3\xi+60\pi^2\xi^2\alpha^2+6\pi^2\alpha^2+60\pi\xi\alpha+25\right)^2\end{aligned}\tag{7.4.15a}$$

or

$$72\pi^8\alpha^8+\left(684\xi-108\sqrt{\xi^2-1}\right)\pi^7\alpha^7+696\pi^6\alpha^6+\left(1776\xi+336\sqrt{\xi^2-1}\right)\pi^6\alpha^6\xi$$
$$+204\pi^5\alpha^5\xi+\left(5520\xi-1680\sqrt{\xi^2-1}\right)\pi^5\alpha^5\xi^2+1884\pi^5\alpha^5\sqrt{\xi^2-1}$$
$$+\left(10880\xi^2-2720\xi\sqrt{\xi^2-1}-3400\right)\pi^4\alpha^4+1600\pi^4\alpha^4\xi^3\left(\xi+\sqrt{\xi^2-1}\right)$$
$$+4400\pi^3\alpha^3\xi^2\left(\xi+\sqrt{\xi^2-1}\right)+\left(5700\xi-5300\sqrt{\xi^2-1}\right)\pi^3\alpha^3$$
$$+5000\pi^2\alpha^2+2000\pi^2\alpha^2\xi\left(\xi+\sqrt{\xi^2-1}\right)+2500\pi\alpha\left(\xi-\sqrt{\xi^2-1}\right)\geq 0 \tag{7.4.15b}$$

This inequality also holds for any value of $\xi \geq 1$.

It concludes that $\rho(\mathbf{A}_r)\leq 1$ for any ξ values, therefore the UHVP_L2 algorithm is unconditionally stable. The spectral radii of the amplification matrices with various damping ratio ξ are plotted in Figure 7.4.1. The ultimate spectral radius is $1/3$.

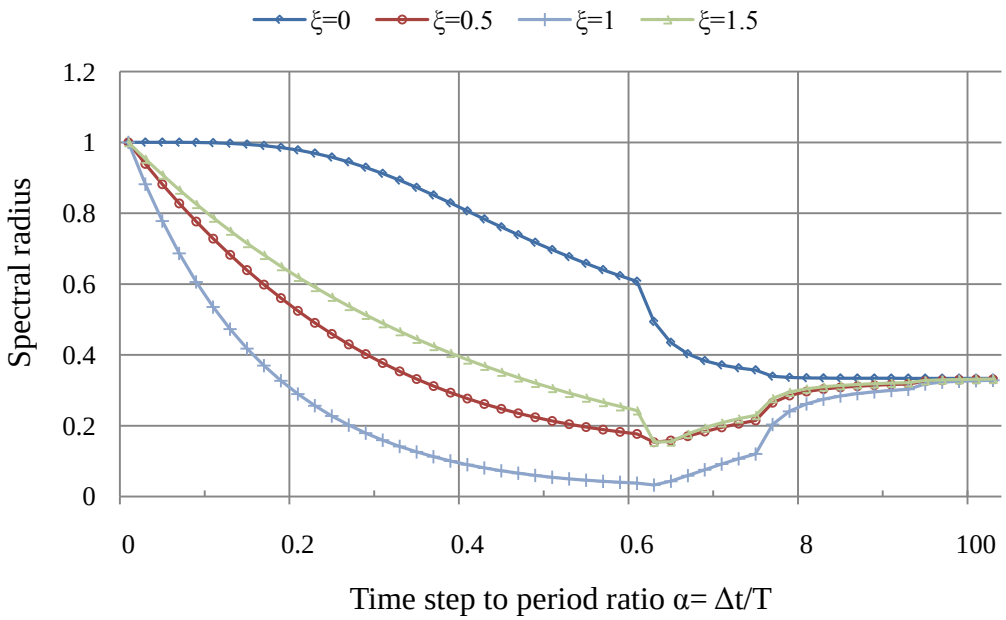

Figure 7.4.1 – Spectral radii for the amplification matrices of UHVP_L2

7.4.3 Algorithm using third-order Lagrange time finite element

When the third-order Lagrange polynomials are used for the time approximation operator $\mathbf{\Phi}$, the integer r equals to three correspondingly. The algorithm thus obtained is referred as UHVP_L3 thereafter in this thesis. The approximation operators are

$$\mathbf{\Phi}(\tau)=\begin{Bmatrix} \frac{-1}{6}(\tau-1)(\tau-2)(\tau-3) \\ \frac{1}{2}\tau(\tau-2)(\tau-3) \\ \frac{-1}{2}\tau(\tau-1)(\tau-3) \\ \frac{1}{6}\tau(\tau-1)(\tau-2) \end{Bmatrix} \quad \frac{d\mathbf{\Phi}(\tau)}{d\tau}=\begin{Bmatrix} -\frac{1}{2}\tau^2+2\tau-\frac{11}{6} \\ \frac{3}{2}\tau^2-5\tau+3 \\ \frac{-3}{2}\tau^2+4\tau-\frac{3}{2} \\ \frac{1}{2}\tau^2-\tau+\frac{1}{3} \end{Bmatrix} \quad (\tau\in[0,3]) \tag{7.4.16}$$

Correspondingly the time invariant coefficient matrices in Eq. (7.4.2) are now

$$\mathbf{S}''=\begin{bmatrix} -1/2 & 57/80 & -3/10 & 7/80 \\ & 0 & 81/80 & -3/10 \\ & & 0 & 57/80 \\ -sym & & & 1/2 \end{bmatrix} \tag{7.4.17a}$$

$$\mathbf{M}''=\frac{\alpha T}{3}\begin{bmatrix} 8/35 & 99/560 & -9/140 & 19/560 \\ & 81/70 & -81/560 & -9/140 \\ & & 81/70 & 99/560 \\ sym & & & 8/35 \end{bmatrix} \tag{7.4.17b}$$

$$\mathbf{K}''=\frac{4\alpha\pi^2}{3T}\begin{bmatrix} 8/35 & 99/560 & -9/140 & 19/560 \\ & 81/70 & -81/560 & -9/140 \\ & & 81/70 & 99/560 \\ sym & & & 8/35 \end{bmatrix} \tag{7.4.17c}$$

$$\mathbf{C}''^{T} = \frac{4\pi\xi}{T}\begin{bmatrix} -1/2 & 57/80 & -3/10 & 7/80 \\ & 0 & 81/80 & -3/10 \\ & & 0 & 57/80 \\ -sym & & & 1/2 \end{bmatrix} \tag{7.4.17d}$$

$$\mathbf{S}_r'' = \begin{bmatrix} 0 & 0 & 0 & 0 \\ & 0 & 0 & 0 \\ & & 0 & 0 \\ sym & & & 1 \end{bmatrix} \tag{7.4.17e}$$

The sub-matrices in Eq. (7.4.5) related to the amplification matrix $\mathbf{A}_r$ can be written explicitly as follows

$$\mathbf{G}_{\theta\theta} = \begin{bmatrix} 0 & \frac{-27\alpha T}{70} & \frac{81}{80} & \frac{27\alpha T}{560} \\ \frac{54\alpha\pi^2}{35T} & 0 & \frac{81\pi\xi}{20T} - \frac{27\alpha\pi^2}{140T} & \\ \frac{-81}{80} & \frac{27\alpha T}{560} & & \\ \frac{-81\pi\xi}{20T} - \frac{27\alpha\pi^2}{140T} & & & sym \end{bmatrix} \tag{7.4.18a}$$

$$\mathbf{G}_{\theta r} = \begin{bmatrix} \frac{-3}{10} & \frac{3\alpha T}{140} \\ \frac{-3\pi^2\alpha}{35T} - \frac{6\pi\xi}{5T} & \frac{-3}{10} \\ \frac{57}{80} & \frac{-33\alpha T}{560} \\ \frac{33\pi^2\alpha}{140T} + \frac{57\pi\xi}{20T} & \frac{57}{80} \end{bmatrix} \tag{7.4.18b}$$

$$\mathbf{G}_{r\theta} = \begin{bmatrix} \frac{3}{10} & \frac{3\alpha T}{140} & \frac{-57}{80} & \frac{-33\alpha T}{560} \\ \frac{6\pi\xi}{5T} - \frac{3\pi^2\alpha}{35T} & \frac{3}{10} & \frac{-57\pi\xi}{20T} + \frac{33\pi^2\alpha}{140T} & \frac{-57}{80} \end{bmatrix} \tag{7.4.18c}$$

$$\mathbf{G}_{rr} = \begin{bmatrix} \frac{1}{2} & \frac{-8\alpha T}{105} \\ \frac{32\pi^2\alpha}{105T} + \frac{2\pi\xi}{T} & \frac{1}{2} \end{bmatrix} \tag{7.4.18d}$$

$$\mathbf{G}_{\theta 0} = \begin{bmatrix} \frac{57}{80} & \frac{-33\alpha T}{560} \\ \frac{33\pi^2\alpha}{140T} - \frac{57\pi\xi}{20T} & \frac{57}{80} \\ \frac{3}{10} & \frac{3\alpha T}{140} \\ \frac{-3\pi^2\alpha}{35T} + \frac{6\pi\xi}{5T} & \frac{3}{10} \end{bmatrix} \tag{7.4.18e}$$

$$\mathbf{G}_{r0} = \begin{bmatrix} \frac{-7}{80} & \frac{-19\alpha T}{1680} \\ \frac{-7\pi\xi}{20T} + \frac{19\pi^2\alpha}{420T} & \frac{-7}{80} \end{bmatrix} \tag{7.4.18f}$$

The amplification matrix $\mathbf{A}_r$ is hence

$$\mathbf{A}_r = \begin{bmatrix} 1 - \frac{b_1}{b_2} & \frac{15T\alpha b_3}{b_2} \\ \frac{-60\pi^2\alpha b_3}{b_2 T} & \frac{b_4}{b_2} - \frac{1}{4} \end{bmatrix} \tag{7.4.19}$$

where

$$
\begin{aligned}
b_1 &= 13440\pi^4\alpha^4\xi^2 + 10\pi^2\alpha^2\left(32\pi^4\alpha^4 - 396\pi^2\alpha^2 + 2205\right) + 10\pi^2\alpha^2\xi\left(96\pi^3\alpha^3 + 2100\pi\alpha\right) \\
b_2 &= 256\pi^6\alpha^6 + 1920\pi^5\alpha^5\xi + \left(7680\xi^2 - 240\right)\pi^4\alpha^4 + \left(4320\xi + 13440\xi^3\right)\pi^3\alpha^3 + \\
&\quad \left(1800 + 25200\xi^2\right)\pi^2\alpha^2 + 25200\pi\alpha\xi + 11025 \\
b_3 &= 24\pi^4\alpha^4 - 64\pi^3\alpha^3\xi + 280\pi^2\alpha^2\xi^2 - 370\pi^2\alpha^2 + 210\pi\alpha\xi + 735 \\
b_4 &= 3660\pi^4\alpha^4 + 6600\pi^3\alpha^3\xi + \left(18900\xi^2 - 19800\right)\pi^2\alpha^2 - 12600\pi\alpha\xi + {}^{55125}\!/_{4}
\end{aligned}
\tag{7.4.20}
$$

The two eigenvalues of the amplification matrix $\mathbf{A}_r$, $\lambda^{(1)}, \lambda^{(2)}$, are

$$
\lambda^{(1)} = \mathrm{Re} + \mathrm{Im}; \quad \lambda^{(2)} = \mathrm{Re} - \mathrm{Im} \tag{7.4.21}
$$

where

$$
\begin{aligned}
\mathrm{Re} &= {}^{Nu_{\mathrm{Re}}}\!/_{b_2} \\
\mathrm{Im} &= {}^{Nu_{\mathrm{Im}}}\!/_{b_2}
\end{aligned}
\tag{7.4.22}
$$

$$
Nu_{\mathrm{Re}} = \begin{pmatrix} -64\pi^6\alpha^6 + 3720\pi^4\alpha^4 - 20250\pi^2\alpha^2 + 11025 \\ +240\pi^5\alpha^5\xi - 3840\pi^4\alpha^4\xi^2 + 5040\pi^3\alpha^3\xi^3 \\ -5580\pi^3\alpha^3\xi + 18900\pi^2\alpha^2\xi^2 + 3150\pi\alpha\xi \end{pmatrix}
$$

$$
Nu_{\mathrm{Im}} = \begin{pmatrix} 720\pi^4\alpha^4 - 11100\pi^2\alpha^2 + 22050 \\ -1920\pi^3\alpha^3\xi + 8400\pi^2\alpha^2\xi^2 + 6300\pi\alpha\xi \end{pmatrix} \pi\alpha\sqrt{\xi^2 - 1}
$$

Again, that the two eigenvalues are complex conjugates when $\xi < 1$, consequently the spectral radius of $\mathbf{A}_r$ is

$$
\rho\left(\mathbf{A}_r\right) = \sqrt{\lambda^{(1)} \times \lambda^{(2)}} = \sqrt{\mathrm{Re}^2 - \mathrm{Im}^2} \qquad \left(\xi < 1\right) \tag{7.4.23}
$$

Let $\rho^2\left(\mathbf{A}_r\right)\le 1$, one has

$$
\begin{aligned}
0 \le\ & 61440\pi^{12}\alpha^{12}+1013760\pi^{11}\alpha^{11}\xi+\left(7587840\xi^2-165120\right)\pi^{10}\alpha^{10} \\
& +36096000\pi^{9}\alpha^{9}\xi^3+1555200\pi^{9}\alpha^{9}\xi+109209600\pi^{8}\alpha^{8}\xi^4 \\
& +27705600\pi^{8}\alpha^{8}\xi^2+532800\pi^{8}\alpha^{8}+212889600\pi^{7}\alpha^{7}\xi^5 \\
& +151200000\pi^{7}\alpha^{7}\xi^3+17683200\pi^{7}\alpha^{7}\xi+225792000\pi^{6}\alpha^{6}\xi^6 \\
& +423360000\pi^{6}\alpha^{6}\xi^4+167832000\pi^{6}\alpha^{6}\xi^2+1890000\pi^{6}\alpha^{6} \\
& +592704000\pi^{5}\alpha^{5}\xi^5+762048000\pi^{5}\alpha^{5}\xi^3+15606000\pi^{5}\alpha^{5}\xi \\
& +\left(1333584000\xi^4+463428000\xi^2-4630500\right)\pi^{4}\alpha^{4} \\
& +1614060000\pi^{3}\alpha^{3}\xi^3+158760000\pi^{3}\alpha^{3}\xi+1250235000\pi^{2}\alpha^{2}\xi^2 \\
& +486202500\pi\alpha\xi
\end{aligned}
\tag{7.4.24}
$$

The above inequality will be invalid when ξ and α are small enough, which means $\rho\left(\mathbf{A}_r\right)>1$ for certain combinations of ξ and α. It is clear the most extreme case is obtained when $\xi=0$ for an undamped system, then Eq. (7.4.24) degenerates to

$$
0\le\alpha^4\left(61440\pi^8\alpha^8-165120\pi^6\alpha^6+532800\pi^4\alpha^4+1890000\pi^2\alpha^2-4630500\right)
\tag{7.4.25}
$$

From which the unstable range of α is found to be $\left]0,\sqrt{7}/2\pi\right[$, and the algorithm becomes stable once $\alpha=\Delta t/T\ge\sqrt{7}/2\pi\approx 0.421$. Interestingly, this hints for an undamped multi-degree-of-freedom system the stability of the results is determined by the lowest frequency of the system. This is in contrast to the stability properties of many conditionally stable algorithms whose stability restriction are determined by the highest frequency.

On the other hand, for a critically-damped or over-damped system, the two eigenvalues become real numbers. In this case, the spectral radius is determined by the larger value of $\left|\lambda^{(1)}\right|$ and $\left|\lambda^{(2)}\right|$. Let $\left|\lambda^{(1)}\right|^2 \le 1$, which leads to

$$\left(Nu_{\mathrm{Re}} + Nu_{\mathrm{Im}}\right)^2 \le {b_2}^2 \tag{7.4.26a}$$

or

$$\begin{aligned}
&61440\pi^{12}\alpha^{12} + \left(92160\sqrt{\xi^2-1} + 1013760\xi\right)\pi^{11}\alpha^{11} + 871680\pi^{10}\alpha^{10} \\
&+ \left(6551040\xi - 591360\sqrt{\xi^2-1}\right)\pi^{10}\alpha^{10}\xi + \left(7526400\xi^2 - 6777600\right)\pi^9\alpha^9\sqrt{\xi^2-1} \\
&+ \left(41625600\xi^3 - 3974400\xi\right)\pi^9\alpha^9 + \left(91238400\xi^2 - 31435200\right)\pi^8\alpha^8 \\
&+ \left(77644800\xi - 26035200\sqrt{\xi^2-1}\right)\pi^8\alpha^8\xi^3 + 28454400\pi^8\alpha^8\xi\sqrt{\xi^2-1} \\
&+ \left(277401600\xi^3 - 199411200\sqrt{\xi^2-1}\right)\pi^7\alpha^7\xi^2 + 114566400\pi^7\alpha^7\sqrt{\xi^2-1} \\
&+ \left(83865600\xi\sqrt{\xi^2-1} - 16704000\right)\pi^7\alpha^7\xi^3 + 121075200\pi^7\alpha^7\xi \\
&+ \left(326592000\xi^2 - 263628000\right)\pi^6\alpha^6\xi\sqrt{\xi^2-1} + 311814000\pi^6\alpha^6 \\
&+ \left(985824000\xi^2 - 563436000\right)\pi^6\alpha^6\xi^2 + 84672000\pi^6\alpha^6\xi^5\left(\xi - \sqrt{\xi^2-1}\right) \\
&+ \left(1422792000\xi^2 - 433458000\right)\pi^5\alpha^5\xi + 381024000\pi^5\alpha^5\xi^4\left(\xi - \sqrt{\xi^2-1}\right) \\
&+ \left(1011528000\xi^2 - 629478000\right)\pi^5\alpha^5\sqrt{\xi^2-1} + 613494000\pi^4\alpha^4\xi\sqrt{\xi^2-1} \\
&+ \left(2262708000\xi^2 - 983650500\right)\pi^4\alpha^4 + 513324000\pi^4\alpha^4\xi^3\left(\xi - \sqrt{\xi^2-1}\right) \\
&+ 1137780000\pi^3\alpha^3\sqrt{\xi^2-1} + 1058400000\pi^3\alpha^3\xi^2\left(\xi - \sqrt{\xi^2-1}\right) \\
&+ 714420000\pi^3\alpha^3\xi + 972405000\pi^2\alpha^2 + 277830000\pi^2\alpha^2\xi\left(\xi - \sqrt{\xi^2-1}\right) \\
&+ 486202500\pi\alpha\left(\xi - \sqrt{\xi^2-1}\right) \\
&\ge 0
\end{aligned} \tag{7.4.26b}$$

It is clear that Eq. (7.4.26b) holds for any $\xi \ge 1$.

Similarly, let $\left|\lambda^{(2)}\right|^2 \le 1$, one has

$$\left(Nu_{\mathrm{Re}} - Nu_{\mathrm{Im}}\right)^2 \le {b_2}^2 \tag{7.4.27a}$$

or

$$\begin{aligned}
&61440\pi^{12}\alpha^{12} + \left(1013760\xi - 92160\sqrt{\xi^2-1}\right)\pi^{11}\alpha^{11} + 871680\pi^{10}\alpha^{10} \\
&+\left(6551040\xi + 591360\sqrt{\xi^2-1}\right)\pi^{10}\alpha^{10}\xi + 6777600\pi^9\alpha^9\sqrt{\xi^2-1} \\
&+\left(41625600\xi^2 - 7526400\xi - 3974400\right)\pi^9\alpha^9\xi + \left(91238400\xi^2 - 31435200\right)\pi^8\alpha^8 \\
&+\left(77644800\xi^3 - 28454400\sqrt{\xi^2-1}\right)\pi^8\alpha^8\xi + 26035200\pi^8\alpha^8\xi^3\sqrt{\xi^2-1} \\
&+\left(199411200\xi^2 - 114566400 - 83865600\xi\right)\pi^7\alpha^7\sqrt{\xi^2-1} \\
&+\left(121075200\xi - 114566400\sqrt{\xi^2-1}\right)\pi^7\alpha^7 \\
&+\left(277401600\xi^2 - 16704000\right)\pi^7\alpha^7\xi^3 + 84672000\pi^6\alpha^6\xi^5\left(\xi + \sqrt{\xi^2-1}\right) \\
&+\left(985824000\xi^2 - 326592000\xi\sqrt{\xi^2-1} - 563436000\right)\pi^6\alpha^6\xi^2 \\
&+263628000\pi^6\alpha^6\xi\sqrt{\xi^2-1} + 311814000\pi^6\alpha^6 \\
&+\left(1011528000\xi - 1011528000\sqrt{\xi^2-1}\right)\pi^5\alpha^5\xi^2 \\
&+\left(411264000\xi^2 + 381024000\xi^4 - 433458000\right)\pi^5\alpha^5\xi \\
&+381024000\pi^5\alpha^5\xi^4\left(\sqrt{\xi^2-1}\right) + \left(629478000\right)\pi^5\alpha^5\sqrt{\xi^2-1} \\
&+\left(2262708000\xi^2 - 613494000\xi\sqrt{\xi^2-1} - 983650500\right)\pi^4\alpha^4 \\
&+513324000\pi^4\alpha^4\xi^3\left(\xi + \sqrt{\xi^2-1}\right) \\
&\left(1058400000\xi^2\left(\xi + \sqrt{\xi^2-1}\right) - 1137780000\sqrt{\xi^2-1}\right)\pi^3\alpha^3 \\
&+714420000\pi^3\alpha^3\xi + 972405000\pi^2\alpha^2 + 277830000\pi^2\alpha^2\xi\left(\xi + \sqrt{\xi^2-1}\right) \\
&+486202500\pi\alpha\left(\xi + \sqrt{\xi^2-1}\right) \\
&\ge 0
\end{aligned} \tag{7.4.27b}$$

Which also holds for any $\xi \geq 1$, therefore for critically-damped and over-damped systems the algorithm is "unconditionally" stable. Overall UHVP_L3 algorithm is conditionally stable because of the criteria to be satisfied for under-damped systems. The spectral radii of the amplification matrices with various damping ratio ξ are plotted in Figure 7.4.2. The ultimate spectral radius is $1/4$.

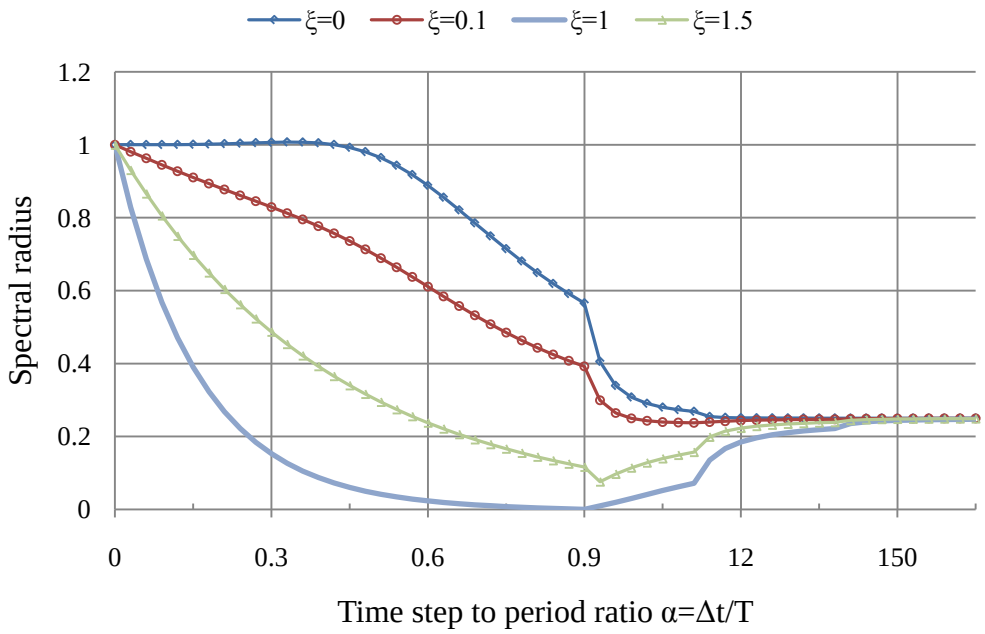

Figure 7.4.2 – Spectral radii for the amplification matrices of UVHP_L3

Figure 7.4.3 shows the localised region where the spectral radius exceeds unity for the undamped system.

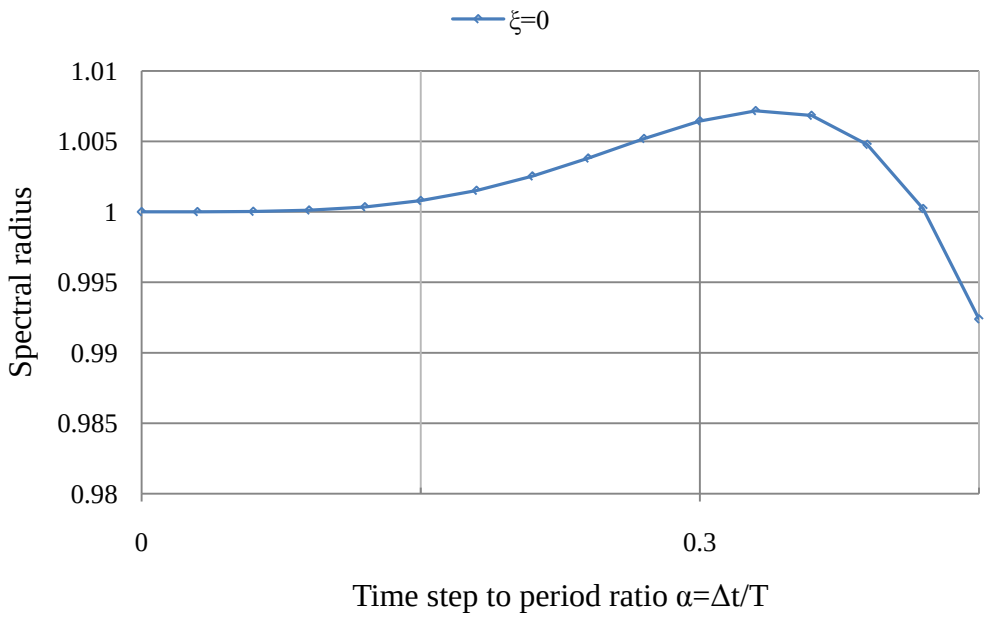

Figure 7.4.3 – Range of the unstable ratio α of UVHP_L3

7.4.4 Algorithm using fifth-order Lagrange time finite element

When the fifth-order Lagrange polynomials are used for the time approximation operator $\mathbf{\Phi}$, the integer r equals to five. The algorithm thus obtained is referred as UHVP_H5 thereafter in this thesis. The approximation operators are

$$\boldsymbol{\Phi}(\tau)=\begin{Bmatrix}\frac{-1}{120}(\tau-1)(\tau-2)(\tau-3)(\tau-4)(\tau-5)\\ \frac{1}{24}\tau(\tau-2)(\tau-3)(\tau-4)(\tau-5)\\ \frac{-1}{12}\tau(\tau-1)(\tau-3)(\tau-4)(\tau-5)\\ \frac{1}{12}\tau(\tau-1)(\tau-2)(\tau-4)(\tau-5)\\ \frac{-1}{24}\tau(\tau-1)(\tau-2)(\tau-3)(\tau-5)\\ \frac{1}{120}\tau(\tau-1)(\tau-2)(\tau-3)(\tau-4)\end{Bmatrix}$$

$$\frac{d\boldsymbol{\Phi}(\tau)}{d\tau}=\begin{Bmatrix}-\tau^4/24+\tau^3/2-17\tau^2/8+15\tau/4-137/60\\ 5\tau^4/24-7\tau^3/3+71\tau^2/8+77\tau/6+5\\ -5\tau^4/12+13\tau^3/3-59\tau^2/4+107\tau/6-5\\ 5\tau^4/12-4\tau^3+49\tau^2/4-13\tau+10/3\\ -5\tau^4/24+11\tau^3/6-41\tau^2/8+61\tau/12-5/4\\ \tau^4/24-\tau^3/3+7\tau^2/8-5\tau/6+1/5\end{Bmatrix}\quad(\tau\in[0,5]) \tag{7.4.28}$$

The procedure to evaluate the algorithmic stability condition is identical to the ones for UHVP_L2 and UHVP_L3. It is found the algorithm employing the fifth-order element is also conditionally stable as illustrated in Figure 7.4.4 below. Similar to UHVP_L3 algorithm, the unstable range of α of UHVP_L5 algorithm is bounded, which means the algorithm will become stable when the length of the time step increases. Another observation is made that the stability property varies in accordance with the damping ratio; the conditional stability is only at presence for a certain range of damping ratio. For the undamped case, the unstable region for α is approximately $(0.45T,1.3T)$.

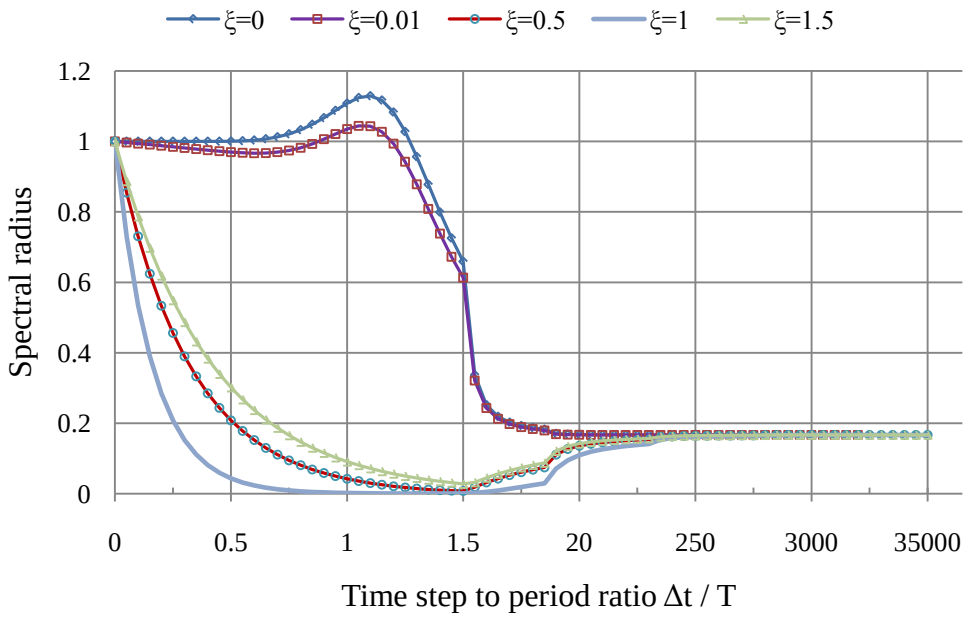

Figure 7.4.4 – Spectral radii for the amplification matrices of UHVP_L5

7.5 Conclusion

In this chapter, the stability of the one- and two- field algorithms based on Unconventional Hamilton-type Variational Principles are examined in combination with the time finite elements reviewed in Chapter 5. It is found that the UHVP_H3 algorithm is conditionally stable, and the maximum length of the time step is $\sqrt{21}/\pi \approx 1.45$ times the natural period to guarantee stable results. The UHVP_L3 and UHVP_L5 algorithms are also found to be conditionally stable. However, their conditional stability can shift to unconditional stability when the damping ratio increases. In addition, the unstable range of the time step is bounded, therefore, large time steps can be accepted for the stability consideration as long as it stays outside of the unstable range. The best UHVP algorithm with regards to the stability property is the UHVP_L2, which possesses the desired characteristic of unconditionally stable.

Chapter 8 Consistency Analysis

8.1 Introduction

If an algorithm is stable and consistent, its convergence is assured. Stability having been investigated in the last chapter, the consistency properties of the algorithms are to be evaluated next. The consistency is judged by the examination of the local truncation error. Two approaches for this exercise are briefly reviewed, and the second approach (i.e., comparing the amplification matrices and the load operators) is adopted in the subsequent investigation. Both the analytical solution and three approximation solutions generated from the presented algorithms are expanded in Taylor series and compared. Conclusions for the consistency associated the UVHP_H3, the UVHP_L2 and UVHP_L3 algorithms are reached in Section 8.3. However, it is not successful to obtain a theoretical conclusion for the UVHP_L5 scheme, its performance will be illustrated numerically in the next chapter.

8.2 Consistency analysis

8.2.1 Consistency

As reviewed in Chapter 7 (Eq. (7.2.1)), the formulation of a single step recursive scheme can be expressed in general as

$$\mathbf{V}_n = \mathbf{A}\mathbf{V}_{n-1} + \mathbf{L}_n \tag{8.2.1}$$

When the scheme is an approximation, $\mathbf{A}$ and $\mathbf{L}_n$ are the approximated amplification matrix and load operator. If an analytical scheme is available, these two quantities are then exact – denoted as $\mathbf{A}_{Exact}$ and $\mathbf{L}_{Exact}$. The exact solution

$\mathbf{V}(t)=\{u(t),\dot{u}(t)\}^T$ or $\mathbf{V}=\{u(t),p(t)\}^T$ at the time instants t_{n-1} and $t_n=t_{n-1}+\Delta t$ satisfy

$$\mathbf{V}(t_n)=\mathbf{A}_{Exact}\mathbf{V}(t_{n-1})+\mathbf{L}_{Exact} \tag{8.2.2}$$

The essence of all numerical schemes is to simulate Eq. (8.2.2) as closely as possible. Nevertheless a certain amount of errors always occur in all numerical schemes. When the analytical solution $\mathbf{V}(t_n)$ and $\mathbf{V}(t_{n-1})$ are substituted in the approximation formulation, Eq. (8.2.1), the local truncation error $\tau(t_n)$ can be defined as

$$\tau(t_n)=\left(\mathbf{V}(t_n)-\mathbf{A}\mathbf{V}(t_{n-1})-\mathbf{L}_n\right)/\Delta t \tag{8.2.3}$$

If $|\tau(t)|\le c\Delta t^k$ for all t within the temporal domain, where c is a constant independent of the time step and k>0, the numerical scheme defined by Eq. (8.2.1) is called consistent, and k is referred as the order of accuracy (Hughes, 1987).

In order to investigate the algorithmic consistency, two approaches can be utilised. The first one is to find the local truncation error and evaluate the consistency directly by the definition. The other way is to compare the approximation amplification matrix and the load operator against the analytical ones, respectively (Fung, 1997). The truncation errors of the relevant entries in the matrix and load operator will determine the error of the numerical scheme under consideration. Both ways lead to the same conclusion, and the latter approach is adopted in this research since insights may be gained in this approach.

Similar to the stability analysis, an SDOF system is used for the investigation, the applicability of the findings to MDOF systems were proven by Hughes (1987) and Wood (1990). This SDOF problem is again

$$\begin{aligned} &\ddot{u}(t)+2\xi\omega\dot{u}(t)+\omega^2 u(t)=f(t) \\ &u\big|_{t=0}=u_0;\ \ \dot{u}\big|_{t=0}=v_0 \end{aligned} \tag{8.2.4}$$

8.2.2 The analytical solution of an SDOF system

If $\hat{u}(t)$ is the exact solution to Eq. (8.2.4), it can be divided into two parts – the homogenous solution $\hat{u}_h(t)$ and the particular solution $\hat{u}_p(t)$

$$\hat{u}(t)=\hat{u}_h(t)+\hat{u}_p(t) \tag{8.2.5}$$

The particular solution varies according to the type of the excitation force, $f(t)$, and the closed form are only available for limited types of loads. However, an arbitrary load can be expanded into a Taylor series about $t=0$ within a small time interval $[0,\Delta t]$

$$\begin{aligned} &f(t)=f(0)+\frac{\partial f(0)}{\partial t}t+\frac{\partial^2 f(0)}{\partial t^2}t^2+\frac{\partial^3 f(0)}{\partial t^3}t^3+\cdots \\ &(0\le t\le \Delta t) \end{aligned} \tag{8.2.6}$$

Subsequently the response corresponding to each term of the load expansion can be combined linearly to obtain the overall response of the dynamic system under a wide class of excitation forces. Without losing of generality, only one term needs to be considered in the following discussion. The excitation force is assumed to be

$$f(t)=Ft^n \tag{8.2.7}$$

where F is the amplitude coefficient, n is an integer and $n\ge 1$ .The motion equation under consideration is now

$$\ddot{u}(t)+2\xi\omega\dot{u}(t)+\omega^2 u(t)=Ft^n \tag{8.2.8}$$

The homogenous solution to Eq. (8.2.8) is

$$\hat{u}_h(t) = e^{-\xi\omega t}\left\{\left[\cos(\omega_d t) + \frac{\xi\omega}{\omega_d}\sin(\omega_d t)\right]u_0 + \frac{\sin(\omega_d t)}{\omega_d}v_0\right\} \tag{8.2.9}$$

The particular solution to Eq. (8.2.8) is an indefinite series related to the excitation.

$$\hat{u}_p(t) = F\left(\frac{1}{(n+2)!}t^{n+2} - \frac{2\xi\omega}{(n+3)!}t^{n+3} - \frac{(1-4\xi^2)\omega^2}{(n+4)!}t^{n+4} + \frac{4\xi(1-2\xi^2)\omega^3}{(n+5)!}t^{n+5} + \cdots\right)n! \tag{8.2.10}$$

However, it can be proven that the sum of the first four terms will give a solution of at least fourth-order accurate simply by substituting the sum of these terms back into Eq. (8.2.8).

The analytical amplification matrix $\mathbf{A}_{Exact}$ can be derived from Eq. (8.2.9) and its first time derivatives

$$\mathbf{A}_{Exact}(t) = e^{-\xi\omega t}\begin{bmatrix} \cos(\omega_d t) + \frac{\xi\omega}{\omega_d}\sin(\omega_d t) & \frac{1}{\omega_d}\sin(\omega_d t) \\ -\frac{\omega^2}{\omega_d}\sin(\omega_d t) & \cos(\omega_d t) - \frac{\xi\omega}{\omega_d}\sin(\omega_d t) \end{bmatrix} \tag{8.2.11}$$

with $\omega_d = \sqrt{1-\xi^2}\omega$ being the damped system frequency. When $t = \Delta t$, the Taylor expansion of the entries of $\mathbf{A}_{Exact}$ is (Fung, 1997)

$$\mathbf{A}_{Exact}(1,1)=1-\frac{1}{2}\omega^2\Delta t^2+\frac{1}{3}\xi\omega^3\Delta t^3-\frac{1}{24}\left(4\xi^2-1\right)\omega^4\Delta t^4+\frac{1}{30}\xi\left(2\xi^2-1\right)\omega^5\Delta t^5+\cdots$$

$$\mathbf{A}_{Exact}(1,2)=\Delta t-\xi\omega\Delta t^2+\frac{1}{6}\left(4\xi^2-1\right)\omega^2\Delta t^3-\frac{1}{6}\xi\left(2\xi^2-1\right)\omega^3\Delta t^4+\frac{1}{120}\left(16\xi^4-12\xi^2+1\right)\omega^4\Delta t^5+\cdots$$

$$\mathbf{A}_{Exact}(2,1)=-\omega^2\Delta t+\xi\omega^3\Delta t^2-\frac{1}{6}\left(4\xi^2-1\right)\omega^4\Delta t^3+\frac{1}{6}\xi\left(2\xi^2-1\right)\omega^5\Delta t^4-\frac{1}{120}\left(16\xi^4-12\xi^2+1\right)\omega^6\Delta t^5+\cdots$$

$$\mathbf{A}_{Exact}(2,2)=1-2\xi\omega\Delta t+\frac{1}{2}\left(4\xi^2-1\right)\omega^2\Delta t^2-\frac{2}{3}\xi\left(2\xi^2-1\right)\omega^3\Delta t^3+\frac{1}{24}\left(16\xi^4-12\xi^2+1\right)\omega^4\Delta t^4-\frac{1}{60}\xi\left(16\xi^4-16\xi^2+3\right)\omega^5\Delta t^5+\cdots$$

(8.2.12)

The analytical load operator $\mathbf{L}_{Exact}(t)$ is related to the particular solution $\hat{u}_p(t)$. A truncated Taylor series of at least fourth-order accurate can be obtained from Eq. (8.2.10) and its first time derivative, let $t=\Delta t$

$$\mathbf{L}_{Exact,trun}(\Delta t)=\left\{\begin{array}{l}\frac{1}{(n+2)!}\Delta t^{n+2}-\frac{2\xi\omega}{(n+3)!}\Delta t^{n+3}-\frac{\left(1-4\xi^2\right)\omega^2}{(n+4)!}\Delta t^{n+4}+\frac{4\xi\left(1-2\xi^2\right)\omega^3}{(n+5)!}\Delta t^{n+5}\\ \frac{1}{(n+1)!}\Delta t^{n+1}-\frac{2\xi\omega}{(n+2)!}\Delta t^{n+2}-\frac{\left(1-4\xi^2\right)\omega^2}{(n+3)!}\Delta t^{n+3}+\frac{4\xi\left(1-2\xi^2\right)\omega^3}{(n+4)!}\Delta t^{n+4}\end{array}\right\}n!F$$

(8.2.13)

In the subsequent examination, Taylor expansions of amplification matrices and load operators of the presented algorithms will be compared against $\mathbf{A}_{Exact}$ and $\mathbf{L}_{Exact,trun}$, to evaluate the local truncation errors.

8.3 Consistency of the one-field and two-field algorithms

8.3.1 Consistency of UVHP_H3 algorithm

The one-field formulation given in Eq. (7.3.8) is recalled here for convenience. Let $t = \Delta t$, one has

$$\begin{Bmatrix} d(t_i) \\ \Delta t \times \dot{d}(t_i) \end{Bmatrix} = -\mathbf{G}_{11}{}^{-1}\mathbf{G}_{10} \begin{Bmatrix} d(t_{i-1}) \\ \Delta t \times \dot{d}(t_{i-1}) \end{Bmatrix} + \mathbf{G}_{11}{}^{-1}\mathbf{L}_1 \tag{8.3.1}$$

or

$$\begin{bmatrix} 1 & 0 \\ 0 & \Delta t \end{bmatrix} \begin{Bmatrix} d(t_i) \\ \dot{d}(t_i) \end{Bmatrix} = -\mathbf{G}_{11}{}^{-1}\mathbf{G}_{10} \begin{bmatrix} 1 & 0 \\ 0 & \Delta t \end{bmatrix} \begin{Bmatrix} d(t_{i-1}) \\ \dot{d}(t_{i-1}) \end{Bmatrix} + \mathbf{G}_{11}{}^{-1}\mathbf{L}_1 \tag{8.3.2}$$

Compared with Eq. (8.2.1), it is clear that the corresponding approximating amplification matrix $\mathbf{A}_{H3}$ and the approximating load operator $\mathbf{L}_{H3}$ are the following

$$\mathbf{A}_{H3}(\Delta t) = \begin{bmatrix} 1 & 0 \\ 0 & \Delta t \end{bmatrix}^{-1} \left(-\mathbf{G}_{11}{}^{-1}\mathbf{G}_{10}\right) \begin{bmatrix} 1 & 0 \\ 0 & \Delta t \end{bmatrix} \tag{8.3.3}$$

$$\mathbf{L}_{H3}(\Delta t) = \begin{bmatrix} 1 & 0 \\ 0 & \Delta t \end{bmatrix}^{-1} \mathbf{G}_{11}{}^{-1}\mathbf{L}_1 \tag{8.3.4}$$

Using Eq. (7.3.10a) and substituting in $\alpha T = t$ and $\omega = {2\pi}/{T}$, the Taylor series of $\mathbf{A}_{H3}(\Delta t)$ entries can be obtained as

$$\mathbf{A}_{H3}(1,1) = 1 - \frac{1}{2}\omega^2\Delta t^2 + \frac{1}{3}\xi\omega^3\Delta t^3 - \frac{1}{90}\left(4\xi^2 - 1\right)\omega^4\Delta t^4 + \left(\frac{64}{945}\xi - \frac{28}{135}\xi^3\right)\omega^5\Delta t^5 + \cdots$$

$$\mathbf{A}_{H3}(1,2) = \Delta t - \xi\omega\Delta t^2 + \frac{1}{6}\left(4\xi^2 - 1\right)\omega^2\Delta t^3 + \frac{2}{45}\left(1 - 2\xi^2\right)\xi\omega^3\Delta t^4 + \left(-\frac{56}{135}\xi^4 + \frac{226}{945}\xi^2 - \frac{1}{126}\right)\omega^4\Delta t^5 + \cdots$$

$$\mathbf{A}_{H3}(2,1) = -\omega^2\Delta t + \xi\omega^3\Delta t^2 + \frac{1}{15}\left(2 - 8\xi^2\right)\omega^4\Delta t^3 - \left(\frac{4}{45}\xi^3 + \frac{8}{315}\xi\right)\omega^5\Delta t^4 + \cdots$$

$$\mathbf{A}_{H3}(2,2) = 1 - 2\xi\omega\Delta t + \frac{1}{2}\left(4\xi^2 - 1\right)\omega^2\Delta t^2 + \frac{8}{15}\left(1 - 2\xi^2\right)\xi\omega^3\Delta t^3 - \left(\frac{8}{45}\xi^4 + \frac{2}{315}\xi^2 - \frac{1}{42}\right)\omega^4\Delta t^4 + \left(\frac{736}{675}\xi^5 - \frac{512}{675}\xi^3 + \frac{118}{1575}\xi\right)\omega^5\Delta t^5 + \cdots \tag{8.3.5}$$

Comparing Eq. (8.3.5) with Eq. (8.2.12), it can be seen that the local truncation errors are $O\left(\Delta t^3\right)$ for $\mathbf{A}_{H3}(2,1)$ and $O\left(\Delta t^4\right)$ for the other entries, hence the displacement homogenous solution is consistent and third-order accurate.

From Eq. (7.3.2), one has

$$\mathbf{L}_1 = \Delta t\int_0^1 \begin{Bmatrix} 3\tau^2 - 2\tau^3 \\ \tau^3 - \tau^2 \end{Bmatrix}\left(F\tau^n\right)d\tau \tag{8.3.6}$$

Therefore one can obtain $\mathbf{L}_{H3}(\Delta t)$ from Eq. (8.3.4) as

$$\mathbf{L}_{H3}\left(\Delta t\right) = \left\{ \begin{array}{c} \dfrac{30\left(63\Delta t^{n+2}-28n\Delta t^{n+2}+42\xi\omega\Delta t^{n+3}+\omega^2\Delta t^{n+4}+2n\omega^2\Delta t^{n+4}\right)}{\left(n^2+7n+12\right)\left(315+5\omega^4\Delta t^4+60\xi\omega^3\Delta t^3+252\xi^2\omega^2\Delta t^2+12\omega^2\Delta t^2+420\xi\omega\Delta t\right)} \\ \dfrac{30\left(126\Delta t^{n+1}-21n\Delta t^{n+1}+42\left(n+1\right)\xi\omega\Delta t^{n+2}-12\omega^2\Delta t^{n+3}+11n\omega^2\Delta t^{n+3}\right)}{\left(n^2+7n+12\right)\left(315+5\omega^4\Delta t^4+60\xi\omega^3\Delta t^3+252\xi^2\omega^2\Delta t^2+12\omega^2\Delta t^2+420\xi\omega\Delta t\right)} \end{array} \right\} F$$

(8.3.7)

Comparing with Eq. (8.3.7) with Eq. (8.2.13), it can be seen that the leading error for the displacement particular solution is $\mathrm{O}\left(t^{n+2}\right)$, therefore, the particular solution is consistent and at least second-order accurate for the displacement when $n=1$, and higher when $n>1$. Overall, the UVHP_H3 algorithm is consistent and the accuracy of the solution is at least second-order, third-order if the excitation force is of second- or higher-order.

8.3.2 Consistency of UVHP_L2 algorithm

The approximating amplification matrix with the second-order Lagrange element $\mathbf{A}_{L2}$ is given by Eq. (7.4.9). With the substitution of Δt and ω, its entries can be expanded as

$$\mathbf{A}_{L2}(1,1)=1-\frac{1}{2}\omega^2\Delta t^2+\frac{1}{3}\xi\omega^3\Delta t^3+\left(\frac{3}{200}-\frac{3}{50}\xi^2\right)\omega^4\Delta t^4+\left(\frac{27}{500}-\frac{27}{250}\xi^2\right)\xi\omega^5\Delta t^5+\cdots$$

$$\mathbf{A}_{L2}(1,2)=\Delta t-\xi\omega\Delta t^2+\frac{3}{20}\left(4\xi^2-1\right)\omega^2\Delta t^3-\frac{3}{50}\left(2\xi^2-1\right)\xi\omega^3\Delta t^4-\left(\frac{27}{125}\xi^4+\frac{81}{500}\xi^2-\frac{27}{2000}\right)\omega^4\Delta t^5+\cdots$$

$$\mathbf{A}_{L2}(2,1)=-\omega^2\Delta t+\xi\omega^3\Delta t^2-\frac{3}{20}\left(4\xi^2-1\right)\omega^4\Delta t^3+\frac{3}{50}\left(2\xi^2-1\right)\xi\omega^5\Delta t^4+\left(\frac{27}{125}\xi^4-\frac{81}{500}\xi^2+\frac{27}{2000}\right)\omega^6\Delta t^5+\cdots$$

$$\mathbf{A}_{L2}(2,2)=1-2\xi\omega\Delta t+\frac{1}{2}\left(4\xi^2-1\right)\omega^2\Delta t^2-\frac{3}{5}\left(2\xi^2-1\right)\xi\omega^3\Delta t^3+\left(\frac{6}{25}\xi^4-\frac{9}{50}\xi^2+\frac{3}{200}\right)\omega^4\Delta t^4+\left(\frac{54}{125}\xi^4-\frac{54}{125}\xi^2+\frac{81}{1000}\right)\xi\omega^5\Delta t^5+\cdots \tag{8.3.8}$$

Compared with Eq. (8.2.12), it can be seen that the truncation errors are $O\left(\Delta t^4\right)$ for $\mathbf{A}_{L2}(1,1)$ and $O\left(\Delta t^3\right)$ for the other entries, hence the displacement homogenous solution is consistent and second-order accurate.

The load operator $\mathbf{L}_{L2}$ at the end of the time step alongside with the one $\mathbf{L}_{\theta,L2}$ for the intermediate time node can be obtained from Eqs. (7.4.4) and (7.4.8a-d), where they were referred as $\mathbf{GL}_r$ and $\mathbf{GL}_\theta$, respectively. When the second-order Lagrange element is used, one has

$$\mathbf{L}_\theta = \begin{Bmatrix} 0 \\ \dfrac{\Delta t}{2}\int_0^2 \left(2\tau - \tau^2\right) A\left(\dfrac{\Delta t}{2}\tau\right)^n d\tau \end{Bmatrix} = \frac{A\Delta t^{n+1}}{(n+2)(n+3)}\begin{Bmatrix} 0 \\ 4 \end{Bmatrix}$$
$$\mathbf{L}_r = \begin{Bmatrix} 0 \\ \dfrac{\Delta t}{2}\int_0^2 \left(\dfrac{\tau^2}{2} - \dfrac{\tau}{2}\right) A\left(\dfrac{\Delta t}{2}\tau\right)^n d\tau \end{Bmatrix} = \frac{(n+1)A\Delta t^{n+1}}{(n+2)(n+3)}\begin{Bmatrix} 0 \\ 1 \end{Bmatrix} \tag{8.3.9}$$

Therefore the load operator is found to be

$$\mathbf{L}_{L2} = \begin{Bmatrix} \dfrac{(1200-480n)\Delta t^{(n+2)} + 720\xi\omega\Delta t^{(n+3)} + (36+72n)\omega^2\Delta t^{(n+4)}}{(n^2+5n+6)(400+9\omega^4\Delta t^4 + 72\xi\omega^3\Delta t^3 + 240\xi^2\omega^2\Delta t^2 + 24\omega^2\Delta t^2 + 480\xi\omega\Delta t)} \\ \dfrac{2400\Delta t^{(n+1)} + (480+960n)\xi\omega\Delta t^{(n+2)} + (288n-216)\omega^2\Delta t^{(n+3)}}{(n^2+5n+6)(400+9\omega^4\Delta t^4 + 72\xi\omega^3\Delta t^3 + 240\xi^2\omega^2\Delta t^2 + 24\omega^2\Delta t^2 + 480\xi\omega\Delta t)} \end{Bmatrix} F \tag{8.3.10}$$

Compared with Eq. (8.2.13), it is trivial to see that the leading error term for the displacement particular solution is $\mathrm{O}\left(t^{n+2}\right)$, therefore, the displacement particular solution is consistent and at least second-order accurate when $n=1$, and higher when $n>1$. Considering both the homogenous and particular solution, the algorithm is consistent and the solution obtained is second-order accurate.

8.3.3 Consistency of UVHP_L3 algorithm

The approximating amplification matrix with the third-order Lagrange element $\mathbf{A}_{L3}$ is given by Eq. (7.4.18). With the substation of Δt and ω, its entries can be expanded as

$$\mathbf{A}_{L3}(1,1)=1-\frac{1}{2}\omega^2\Delta t^2+\frac{1}{3}\xi\omega^3\Delta t^3-\frac{1}{70}\left(12\xi^2-3\right)\omega^4\Delta t^4+\frac{2}{49}\left(2\xi^2-1\right)\xi\omega^5\Delta t^5+\cdots$$

$$\mathbf{A}_{L3}(1,2)=\Delta t-\xi\omega\Delta t^2+\frac{1}{6}\left(4\xi^2-1\right)\omega^2\Delta t^3-\frac{6}{35}\left(2\xi^2-1\right)\xi\omega^3\Delta t^4+\frac{1}{98}\left(16\xi^4-12\xi^2+1\right)\omega^4\Delta t^5+\cdots$$

$$\mathbf{A}_{L3}(2,1)=-\omega^2\Delta t+\xi\omega^3\Delta t^2-\frac{1}{6}\left(4\xi^2-1\right)\omega^4\Delta t^3+\frac{1}{35}\left(12\xi^2-6\right)\xi\omega^5\Delta t^4-\frac{1}{98}\left(16\xi^4-12\xi^2+1\right)\omega^6\Delta t^5+\cdots$$

$$\mathbf{A}_{L3}(2,2)=1-2\xi\omega\Delta t+\frac{1}{2}\left(4\xi^2-1\right)\omega^2\Delta t^2-\frac{2}{3}\xi\left(2\xi^2-1\right)\omega^3\Delta t^3+\cdots$$

(8.3.11)

Compared with Eq. (8.2.12), it can be seen that the truncation error is $O\left(\Delta t^4\right)$, for all entries, hence the displacement homogenous solution is consistent and third-order accurate.

The load operator $\mathbf{L}_{L3}$ at the end of the time step alongside with the one $\mathbf{L}_\theta$ for the intermediate time nodes associated with the third-order Lagrange element can be obtained from Eqs. (7.4.4), (7.4.17a-d). When the third-order Lagrange element is used, one has

$$\mathbf{L}_{\theta}=\begin{Bmatrix}0\\ \dfrac{\Delta t}{3}\int_0^3\left(\dfrac{1}{2}\tau(\tau-2)(\tau-3)\right)A\left(\dfrac{\Delta t}{3}\tau\right)^n d\tau\\ 0\\ \dfrac{\Delta t}{3}\int_0^3\left(\dfrac{-1}{2}\tau(\tau-1)(\tau-3)\right)A\left(\dfrac{\Delta t}{3}\tau\right)^n d\tau\end{Bmatrix}=\frac{A\Delta t^{n+1}}{(n+2)(n+3)(n+4)}\begin{Bmatrix}0\\ \dfrac{-9}{2}(n-2)\\ 0\\ 9(n+1)\end{Bmatrix}$$

$$\mathbf{L}_{r}=\begin{Bmatrix}0\\ \dfrac{\Delta t}{3}\int_0^3\left(\dfrac{1}{6}\tau(\tau-1)(\tau-2)\right)A\left(\dfrac{\Delta t}{3}\tau\right)^n d\tau\end{Bmatrix}=\frac{(n+1)A\Delta t^{n+1}}{(n+2)(n+3)(n+4)}\begin{Bmatrix}0\\ \dfrac{2n^2+5n+6}{2}\end{Bmatrix}$$

(8.3.12)

The load operator $\mathbf{L}_{L3}$ is found to be

$$\mathbf{L}_{L3}=\frac{30}{Dom}\begin{Bmatrix}\left(4410-1155n+420n^2\right)\Delta t^{n+2}+O\left(\Delta t^{n+2}\right)\\ \left(8820+1470n+735n^2\right)\Delta t^{n+1}+O\left(\Delta t^{n+1}\right)\end{Bmatrix}F$$

$$Dom=(n^3+9n^2+26n+24)(11025+4\omega^6\Delta t^6+60\xi\omega^5\Delta t^5+$$
$$480\xi^2-15\omega^4\Delta t^4+1680\xi^3\omega^3\Delta t^3+540\xi\omega^3\Delta t^3+6300\xi^2\omega^2\Delta t^2+450\omega^2\Delta t^2+12600\xi\omega\Delta t)$$

(8.3.13)

The leading error term for the displacement particular solution is also $\mathrm{O}\left(t^{n+2}\right)$, therefore, the particular solution is at least consistent and second-order accurate for the displacement when $n=1$, and higher when $n>1$. Considering both the homogenous and particular solution, the algorithm is consistent and the solution obtained is at least second-order accurate, and third-order if the excitation force is of second- or higher-order.

8.3.4 Consistency of UVHP_L5 algorithm

For this fifth-order approximation, a meaningful Taylor expansion of the amplification matrix is not able to be obtained due to the machine epics. However its performance will be demonstrated numerically in the next chapter.

8.4 Conclusion

In this chapter, the consistency of the presented space-time finite element schemes is examined. It is found that the UVHP_H3, the UVHP_L2 and the UVHP_L3 algorithms are consistent. However, it is not successful to verify the consistency of the UVHP_L5 analytically. Furthermore the order of accuracy for the verified schemes is at least second-order, and can be third-order for the UVHP_H3 and the UVHP_L3 algorithms if the excitation force is in the proper form.

Chapter 9 Numerical Examples

9.1 Introduction

Numerical tests carried out using Matlab are given in this chapter to verify the proposed UVHP algorithms and to evaluate their performance. Displacement time-histories of selected nodes obtained with these algorithms are compared with two reference schemes, one is the analytical method - the modal decomposition method; the other is the Average Acceleration Method (AAM) of the Newmark family, which is known to be second-order accurate. The results of these schemes are evaluated in terms of the accuracy of the results, as well as the computational cost associated with different level of accuracy. The absolute error and relative error are used for the evaluation, which are defined as follows, respectively

$$absolute\ error = \left| analytical\ result - approximation\ result \right| \tag{9.1.1}$$

$$relative\ error = \left| \frac{absolute\ error}{analytical\ result} \right| \times 100\% \tag{9.1.2}$$

Four numerical examples are presented in the following sections. The trusses in these examples include a two-degree-of-freedom planar truss, a seven-node planar truss and a space truss with one hundred and fifteen numbers of DOFs. A periodical load and a chaotic load are used in the examples. In the evaluation, the damping is not considered so that the difference of various algorithms can be fully preserved.

9.2 Example One – A three-node planar truss

A planar truss made up of three isotropic and prismatic rods is illustrated in Figure 9.2.1. A harmonic load $L(t)=30\cos 50t\,(kN)$ is applied to the node C in the Y direction. The values of mechanical parameters are: elastic modulus $E=210GPa$; cross-sectional area $A=500mm^2$ for all rods; material density $7800kg/m^3$. Damping and the self-weight of rods are not considered in this example. The initial displacement and initial velocity are given as zero at time $t=0$. The Y-displacement of node C is used to evaluate the UVHP schemes against the two reference schemes.

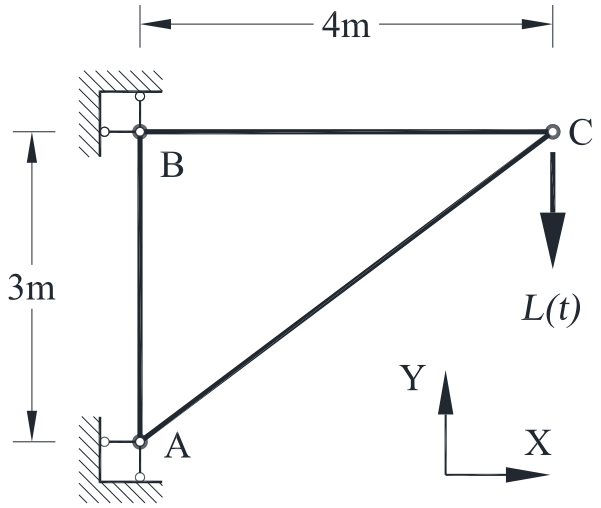

Figure 9.2.1 – Three- node truss

The degree of freedom of this system is two. The time-history of the Y-displacement of the node C with a time step $\Delta t=3.5E-04\,s$ is given in Table 9.2.1, where the relative errors are also given. The time step is taken as one tenth of the bigger natural period of the system as commonly adopted in the engineering practice. It should be noted that this time step satisfies the stability conditions of the UVHP_H3 and UVHP_L5 algorithms, while not the one for UVHP_L3. However for the first one hundred steps, the amplification error of UVHP_L3 is $\rho(\mathbf{A}_r)^{100}-1=1.000172317965^{100}-1\approx 0.017$, therefore the results of UVHP_L3 are still meaningful for the comparison.

Time	analytical	AAM		UVHP_H3		UVHP_L2		UVHP_L3		UVHP_L5	
	Y Displacement	Y Displacement	Relative error	Y Displacement	Relative error	Y Displacement	Relative error	Y Displacement	Relative error	Y Displacement	Relative error
0	0	0	0	0	0	0	0	0	0	0	0
0.00175	-1.14E-02	-1.16E-02	1.97%	-1.13E-02	0.91%	-1.13E-02	0.95%	-1.14E-02	0.04%	-1.14E-02	0.00%
0.0035	-1.96E-03	-1.29E-03	34.11%	-2.17E-03	10.44%	-2.16E-03	10.27%	-1.96E-03	0.14%	-1.96E-03	0.00%
0.00525	-8.31E-03	-9.12E-03	9.77%	-8.14E-03	2.00%	-8.16E-03	1.86%	-8.31E-03	0.03%	-8.31E-03	0.00%
0.007	-3.70E-03	-3.47E-03	6.24%	-3.67E-03	0.83%	-3.67E-03	0.88%	-3.70E-03	0.07%	-3.70E-03	0.00%
0.00875	-8.01E-03	-6.96E-03	13.08%	-8.25E-03	2.98%	-8.21E-03	2.56%	-8.02E-03	0.13%	-8.01E-03	0.00%
0.0105	-1.17E-03	-3.64E-03	212.08%	-9.23E-04	20.80%	-1.00E-03	13.92%	-1.13E-03	2.85%	-1.17E-03	0.00%
0.01225	-1.04E-02	-7.11E-03	31.38%	-1.03E-02	0.64%	-1.02E-02	1.68%	-1.04E-02	0.53%	-1.04E-02	0.00%
0.014	1.41E-03	-1.44E-03	202.30%	8.41E-04	40.30%	7.46E-04	47.00%	1.47E-03	4.24%	1.41E-03	0.01%
0.01575	-9.58E-03	-8.22E-03	14.16%	-8.62E-03	10.04%	-8.57E-03	10.48%	-9.62E-03	0.44%	-9.58E-03	0.00%
0.0175	2.02E-05	4.67E-04	2213.84%	-9.40E-04	4755.94%	-9.27E-04	4689.77%	3.19E-05	57.92%	2.02E-05	0.01%
0.01925	-5.89E-03	-7.36E-03	24.98%	-5.37E-03	8.71%	-5.40E-03	8.21%	-5.87E-03	0.20%	-5.89E-03	0.00%
0.021	-1.05E-03	-1.43E-04	86.33%	-9.31E-04	11.34%	-9.45E-04	9.94%	-1.06E-03	0.73%	-1.05E-03	0.00%
0.02275	-5.14E-03	-3.86E-03	24.91%	-5.64E-03	9.67%	-5.54E-03	7.73%	-5.17E-03	0.55%	-5.14E-03	0.00%
0.0245	2.07E-03	-2.20E-03	206.47%	2.36E-03	14.23%	2.19E-03	5.79%	2.15E-03	3.86%	2.07E-03	0.00%
0.02625	-7.04E-03	-2.60E-04	96.31%	-6.57E-03	6.59%	-6.39E-03	9.26%	-7.16E-03	1.68%	-7.04E-03	0.00%
0.028	4.97E-03	-2.73E-03	154.93%	3.60E-03	27.57%	3.47E-03	30.11%	5.09E-03	2.37%	4.97E-03	0.00%
0.02975	-5.77E-03	9.49E-04	116.44%	-3.90E-03	32.40%	-3.88E-03	32.85%	-5.85E-03	1.32%	-5.77E-03	0.00%
0.0315	3.81E-03	-6.88E-04	118.07%	2.18E-03	42.66%	2.23E-03	41.46%	3.82E-03	0.44%	3.81E-03	0.00%
0.03325	-1.85E-03	4.43E-04	123.98%	-1.09E-03	40.77%	-1.13E-03	38.78%	-1.82E-03	1.21%	-1.85E-03	0.00%
0.035	3.01E-03	1.67E-03	44.62%	3.20E-03	6.54%	3.15E-03	4.74%	2.99E-03	0.40%	3.01E-03	0.00%

Table 9.2.1 – Three-node truss – time history of Y displacements of node C (time step = 3.5E-4 s)

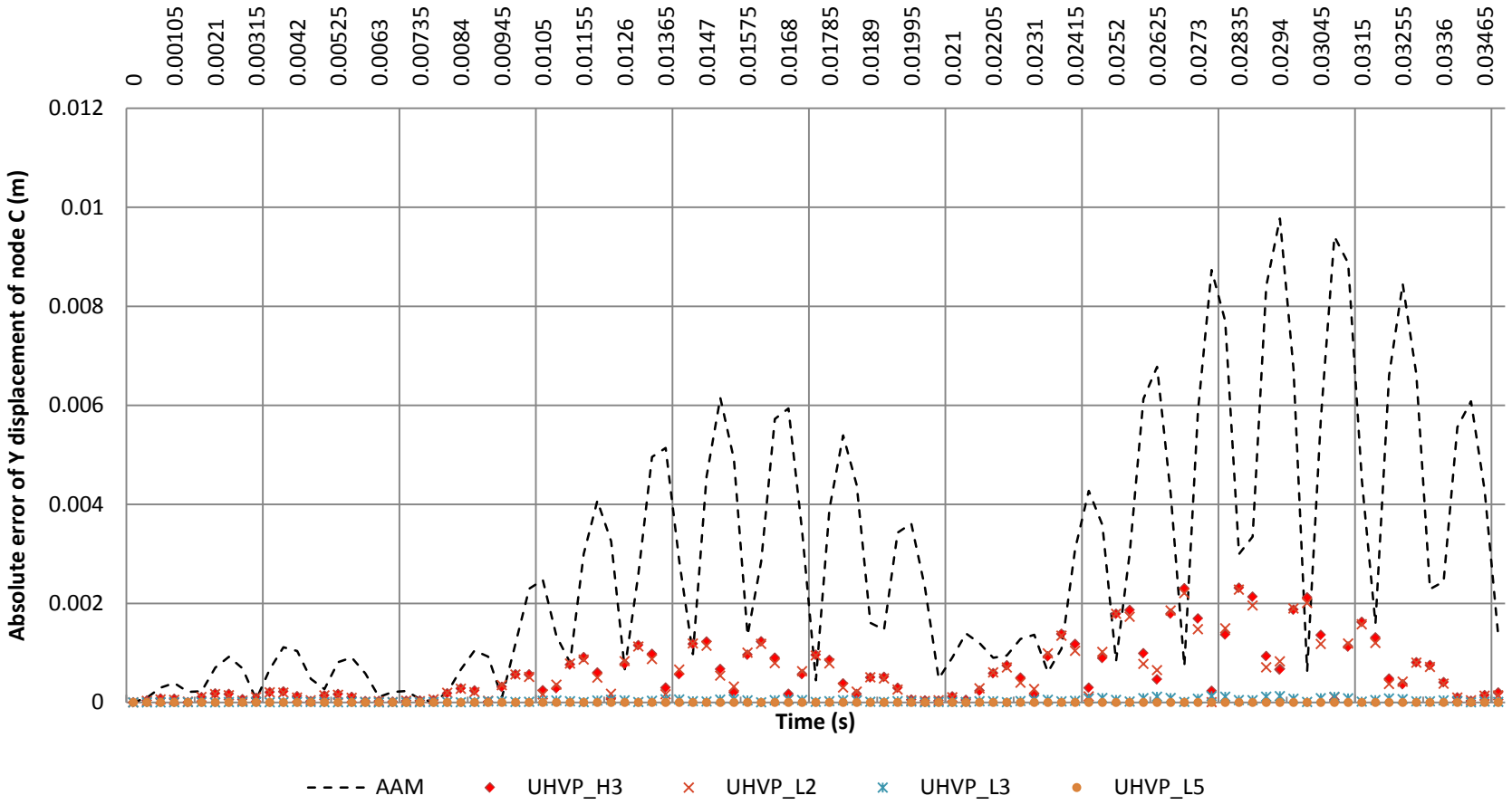

Figure 9.2.2 – Three-node truss – absolute error of Y displacement of node C (time step = 3.5E-4 s)

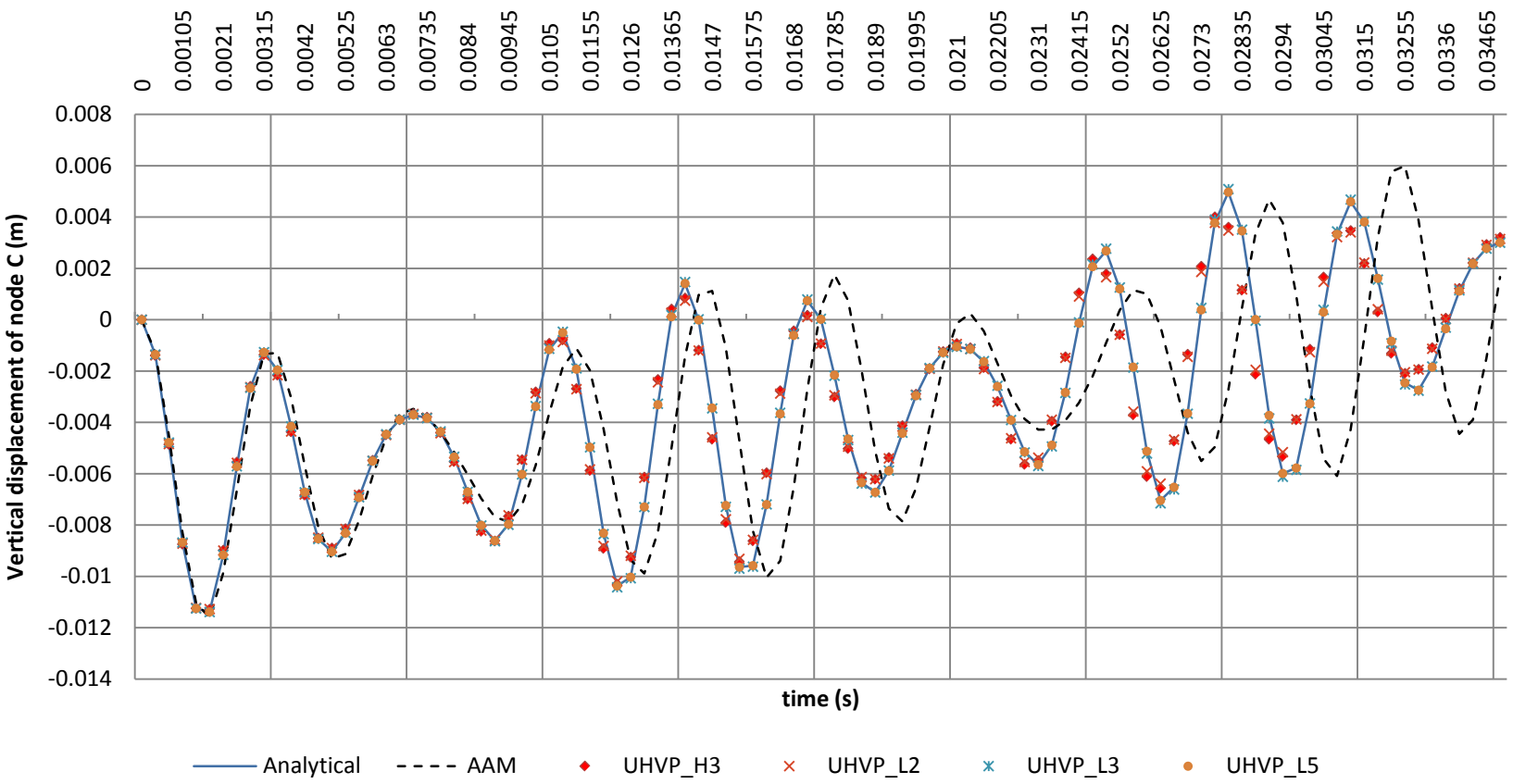

Figure 9.2.3 – Three-node truss – time history plot of Y displacements of node C (time step = 3.5E-4 s)

From Table 9.2.1 and Figure 9.2.2, it can be observed that the results of the UVHP algorithms agree with the analytical solutions better than the result of the AAM scheme. The relative errors of the higher-order schemes (UVHP_L3 & UVHP_L5) are reduced significantly.

It can be further seen from Figure 9.2.3 that the period elongation and amplitude variation of the AAM scheme is clearly evident. In contrast, the UHVP algorithms have much better agreement in both aspects, which means for a MDOF problem the period of each mode can be preserved better with the presented UVHP algorithms, thus making the overall solution more accurate.

To improve the accuracy of the AAM results, smaller time steps have to be used. This will increase the computational cost as a result. The computational cost is measured in terms of the computation time consumed by a desktop with an Intel Core™ i7 CPU (2.93GHz) and 3GB RAM. It is found that the time step has to be halved to 1.75E-04s to get roughly equivalently accurate results to those of the UHVP_L2 and UHVP_H3 schemes. To match the accuracy of the UHVP_L5 results, the time step has to be further reduced to 7.00E-06s, which is 2% of the original time step. The costs for the calculation of the dynamic response during the period [0, 0.035s] are summarised in Table 9.2.2, from which it can be seen that:

- UVHP_H3 is the most efficient scheme for this example. As shown in Figure 9.2.3, it offers better accuracy than the AAM scheme using the same time step.
- UHVP algorithms are more computationally efficient than the AAM schemes for the same level of accuracy in this particular example.
- On the consideration of the equivalent accuracy, the UHVP algorithms are shown to demand much less additional computational efforts compared to the AAM, especially when highly accurate results are required.

Algorithm	Time step (s)	Computation time (s)	Ratio of computational cost
AAM	7.00E-06	0.1809	82.23
	1.75E-04	0.0071	3.23
	3.50E-04	0.0036	1.64
UVHP_H3	3.50E-04	0.0022	1.00
UVHP_L2		0.0035	1.59
UVHP_L3		0.0045	2.05
UVHP_L5		0.0088	4.0

Table 9.2.2 - Comparison of computational costs for Example One

Further numerical test shows that an even bigger time step ($\Delta t = 7E-04\,s$) can be used for the UVHP_L5 algorithms to produce a relatively accurate solution compared to the AAM, as illustrated in Figure 9.2.4, which clearly demonstrates the advantage of using the higher order approximation.

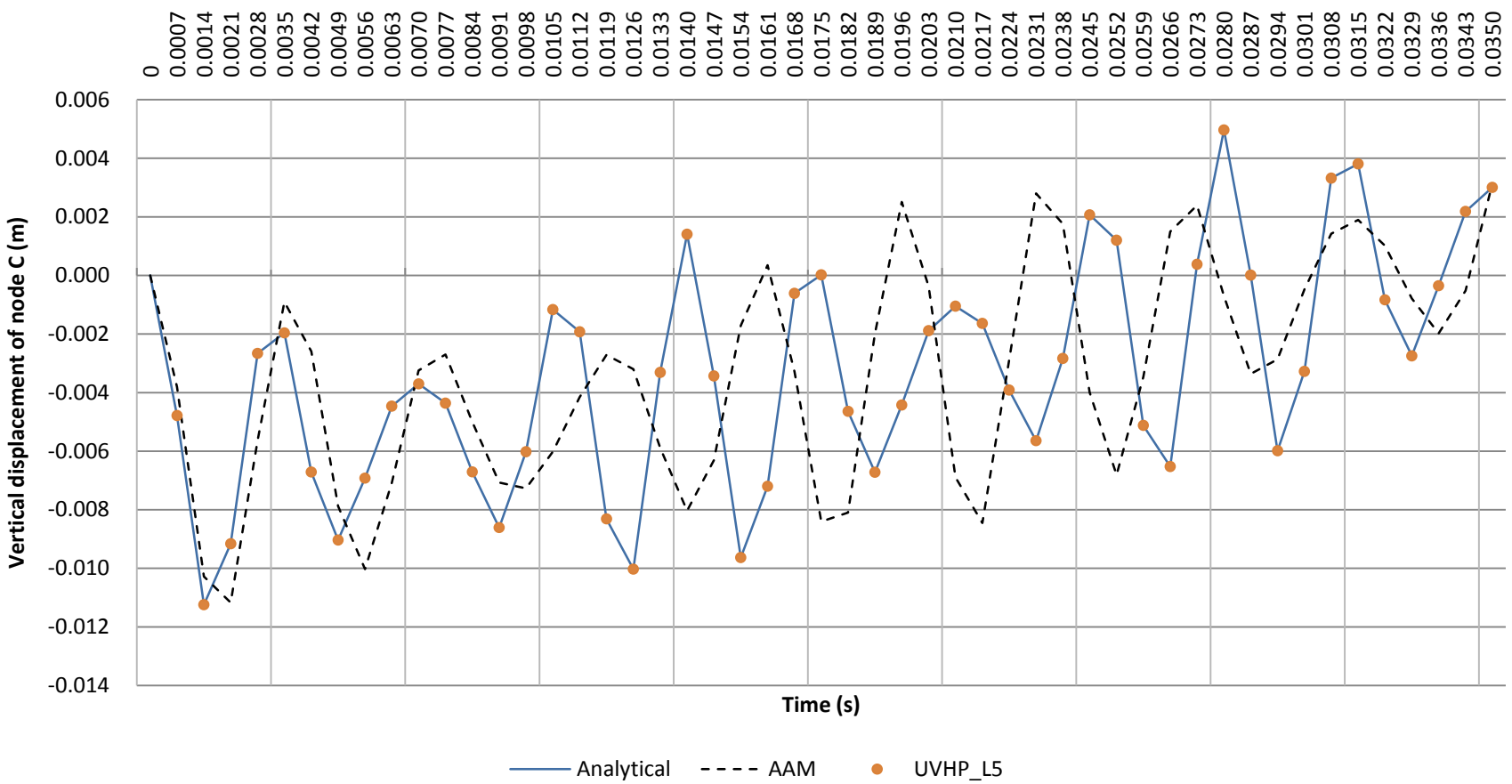

Figure 9.2.4 – Three-node truss – time history plot of Y displacements of node C (time step = 7E-4s)

9.3 Example Two – A seven-node planar truss

A simply supported truss of seven nodes is subject to a vertical dynamic load $L(t) = 30\cos 50t\,(kN)$, as shown in Figure 9.3.1. The degrees of freedom are eleven for this structure. The mechanical parameters of this system are: elastic modulus $E = 210GPa$; cross-sectional area $A = 2827mm^2$ for all rods; material density $7800kg/m^3$. The damping and the self-weight of the rods are not considered. The initial displacement and initial velocity are given as zero at time $t = 0$. The vertical (Y) displacement of node F is used for the evaluation.

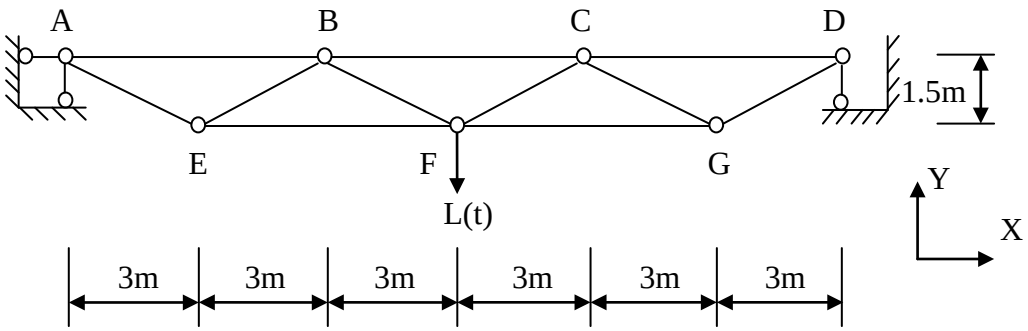

Figure 9.3.1 – Simply supported seven – node truss

The results for the first one hundred steps with a time step $\Delta t = 5E-04\,s$ are compared in Table 9.3.1. The time step is so selected to ensure stable results or meaningful results (for UVHP_L3) are obtained. It can be seen that all the results agree with the analytical solution for the given time step. However, the UVHP algorithms obtain better accuracy than the AAM, as shown in Figure 9.3.2, and the improvement with the UVHP_L5 algorithm is clearly evident.

Time	analytical	AAM		UVHP_H3		UVHP_L2		UVHP_L3		UVHP_L5	
	Y Displacement	Y Displacement	Relative error	Y Displacement	Relative error	Y Displacement	Relative error	Y Displacement	Relative error	Y Displacement	Relative error
0	0	0	0	0	0	0	0	0	0	0	0
0.0025	-2.30E-03	-2.40E-03	4.32%	-2.35E-03	1.92%	-2.34E-03	1.57%	-2.30E-03	0.09%	-2.30E-03	0.00%
0.005	-5.90E-03	-5.88E-03	0.34%	-5.97E-03	1.09%	-5.96E-03	0.87%	-5.93E-03	0.35%	-5.90E-03	0.00%
0.0075	-9.74E-03	-9.89E-03	1.55%	-9.84E-03	1.05%	-9.84E-03	0.96%	-9.77E-03	0.29%	-9.74E-03	0.00%
0.01	-1.10E-02	-1.10E-02	0.06%	-1.11E-02	0.40%	-1.11E-02	0.38%	-1.11E-02	0.42%	-1.10E-02	0.00%
0.0125	-1.01E-02	-1.02E-02	1.18%	-1.01E-02	0.05%	-1.01E-02	0.09%	-1.02E-02	0.89%	-1.01E-02	0.01%
0.015	-8.28E-03	-8.40E-03	1.49%	-8.36E-03	0.96%	-8.35E-03	0.91%	-8.36E-03	1.03%	-8.28E-03	0.01%
0.0175	-6.12E-03	-6.05E-03	1.11%	-6.15E-03	0.60%	-6.15E-03	0.62%	-6.19E-03	1.28%	-6.11E-03	0.02%
0.02	-4.34E-03	-4.38E-03	0.78%	-4.29E-03	1.24%	-4.29E-03	1.24%	-4.46E-03	2.75%	-4.34E-03	0.05%
0.0225	-8.62E-04	-8.59E-04	0.25%	-9.48E-04	10.00%	-9.47E-04	9.90%	-9.30E-04	7.90%	-8.59E-04	0.25%
0.025	2.12E-03	2.00E-03	5.64%	2.20E-03	3.73%	2.20E-03	3.74%	2.11E-03	0.70%	2.12E-03	0.12%
0.0275	4.54E-03	4.72E-03	3.98%	4.57E-03	0.57%	4.57E-03	0.58%	4.50E-03	0.87%	4.55E-03	0.07%
0.03	3.76E-03	3.66E-03	2.68%	3.76E-03	0.04%	3.76E-03	0.08%	3.80E-03	1.04%	3.77E-03	0.07%
0.0325	4.29E-04	6.93E-04	61.76%	4.50E-04	5.06%	4.53E-04	5.80%	5.52E-04	28.73%	4.31E-04	0.65%
0.035	-3.19E-03	-3.04E-03	4.78%	-3.15E-03	1.36%	-3.15E-03	1.31%	-3.11E-03	2.44%	-3.19E-03	0.11%
0.0375	-4.55E-03	-4.57E-03	0.38%	-4.47E-03	1.68%	-4.47E-03	1.74%	-4.42E-03	2.86%	-4.55E-03	0.05%
0.04	-2.26E-03	-2.31E-03	1.96%	-2.25E-03	0.70%	-2.25E-03	0.76%	-2.05E-03	9.46%	-2.26E-03	0.08%
0.0425	1.75E-03	1.63E-03	6.81%	1.97E-03	12.25%	1.97E-03	12.05%	1.86E-03	6.11%	1.76E-03	0.13%
0.045	6.03E-03	6.21E-03	3.08%	5.97E-03	0.89%	5.98E-03	0.81%	6.14E-03	1.81%	6.03E-03	0.01%
0.0475	8.26E-03	8.20E-03	0.72%	8.38E-03	1.49%	8.38E-03	1.42%	8.44E-03	2.16%	8.26E-03	0.00%
0.05	9.32E-03	9.67E-03	3.70%	9.37E-03	0.50%	9.38E-03	0.57%	9.34E-03	0.23%	9.32E-03	0.00%

Table 9.3.1 – Seven-node truss – time history of Y displacements of node F (time step = 5E-4 s)

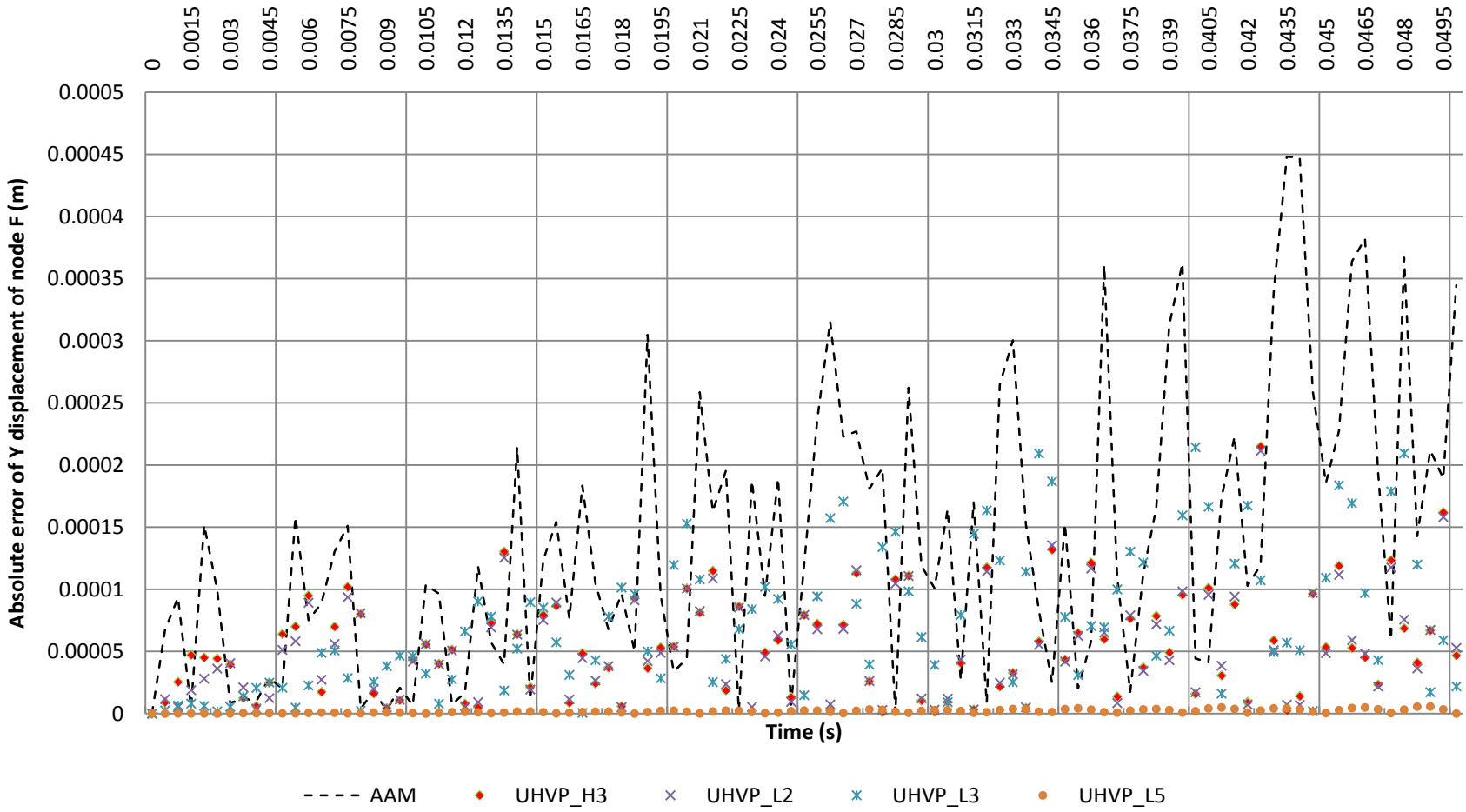

Figure 9.3.2 – Seven-node truss – absolute error of Y displacements of node F (time step = 5E-4 s)

In order to improve the accuracy of the AAM results, smaller time steps are used. The improved results are compared with the results of UVHP algorithms in Table 9.3.2. From this table, it can be seen that the time step has to be reduced by more than half to 1.67e-4s to obtain results roughly matching the results of UHVP_H3, UHVP_L2 and UHVP_L3; and it has to be further reduced to 1.25e-5s to match the results obtained with the UHVP_L5 algorithm, which is as small as 2.5% of the UHVP time step.

Time	**UHVP_H3 (time step = 5e-4s)**	**UHVP_L2 (time step = 5e-4s)**	**UHVP_L3 (time step = 5e-4s)**	**UHVP_L5 (time step = 5e-4s)**	**AAM (time step = 1.67e-4s)**	**AAM (time step = 1.25e-5s)**
0	0	0	0	0	0	0
0.0025	1.92%	1.57%	0.09%	0.00%	0.61%	0.00%
0.005	1.09%	0.87%	0.35%	0.00%	0.12%	0.01%
0.0075	1.05%	0.96%	0.29%	0.00%	0.92%	0.00%
0.01	0.40%	0.38%	0.42%	0.00%	0.72%	0.01%
0.0125	0.05%	0.09%	0.89%	0.01%	0.65%	0.01%
0.015	0.96%	0.91%	1.03%	0.01%	2.20%	0.02%
0.0175	0.60%	0.62%	1.28%	0.02%	0.67%	0.03%
0.02	1.24%	1.24%	2.75%	0.05%	0.40%	0.07%
0.0225	10.00%	9.90%	7.90%	0.25%	10.18%	0.31%
0.025	3.73%	3.74%	0.70%	0.12%	3.56%	0.11%
0.0275	0.57%	0.58%	0.87%	0.07%	2.77%	0.09%
0.03	0.04%	0.08%	1.04%	0.07%	0.84%	0.08%
0.0325	5.06%	5.80%	28.73%	0.65%	37.92%	0.61%
0.035	1.36%	1.31%	2.44%	0.11%	4.24%	0.12%
0.0375	1.68%	1.74%	2.86%	0.05%	0.75%	0.04%
0.04	0.70%	0.76%	9.46%	0.08%	1.02%	0.05%
0.0425	12.25%	12.05%	6.11%	0.13%	0.24%	0.11%
0.045	0.89%	0.81%	1.81%	0.01%	0.63%	0.00%
0.05	0.50%	0.57%	0.23%	0.00%	1.45%	0.00%

Table 9.3.2 - Comparison of relative errors of node F displacements

The computation costs for each scheme using these time steps are compared in Table 9.3.3, which are measured in terms of the computation time for the period [0, 0.05s] using the same desktop for Example One. Combining Tables 9.3.1, 9.3.2 and 9.3.3, It can be seen that:

- UVHP_H3 has the same computational efficiency as the AAM with the same time step, while providing more accurate results.

- For the same level of accuracy, UVHP_H3 and UVHP_L2 algorithms require less computational effort than the corresponding AAM schemes.
- For highly accurate results, the additional computational cost for UVHP_L5 is lower than the corresponding AAM scheme.

It summaries that the UVHP algorithms provide a more accurate and efficient means than the AAM in this particular example.

Algorithm	Time step (s)	Computation time (s)	Ratio of computational cost
AAM	1.25E-05	0.2510	40.48
	1.67E-04	0.018	2.90
	5.00E-04	0.0062	1.00
UVHP_H3	5.00E-04	0.0062	1.00
UVHP_L2		0.0108	1.74
UVHP_L3		0.0237	3.82
UVHP_L5		0.1818	29.32

Table 9.3.3 - Comparison of computational costs for Example Two

9.4 Example Three – A forty one-node space truss

In this example a space truss of forty-one nodes is subject to a dynamic load $L(t) = 30\cos 50t\,(kN)$ applied to node 6 vertically as shown in Figure 9.4.1. The mechanical parameters are the same as Example Two. Again, the initial displacement and initial momentum/velocity are null, and the self-weight and damping are not considered. The degrees of freedom are one hundred and fifteen for this system.

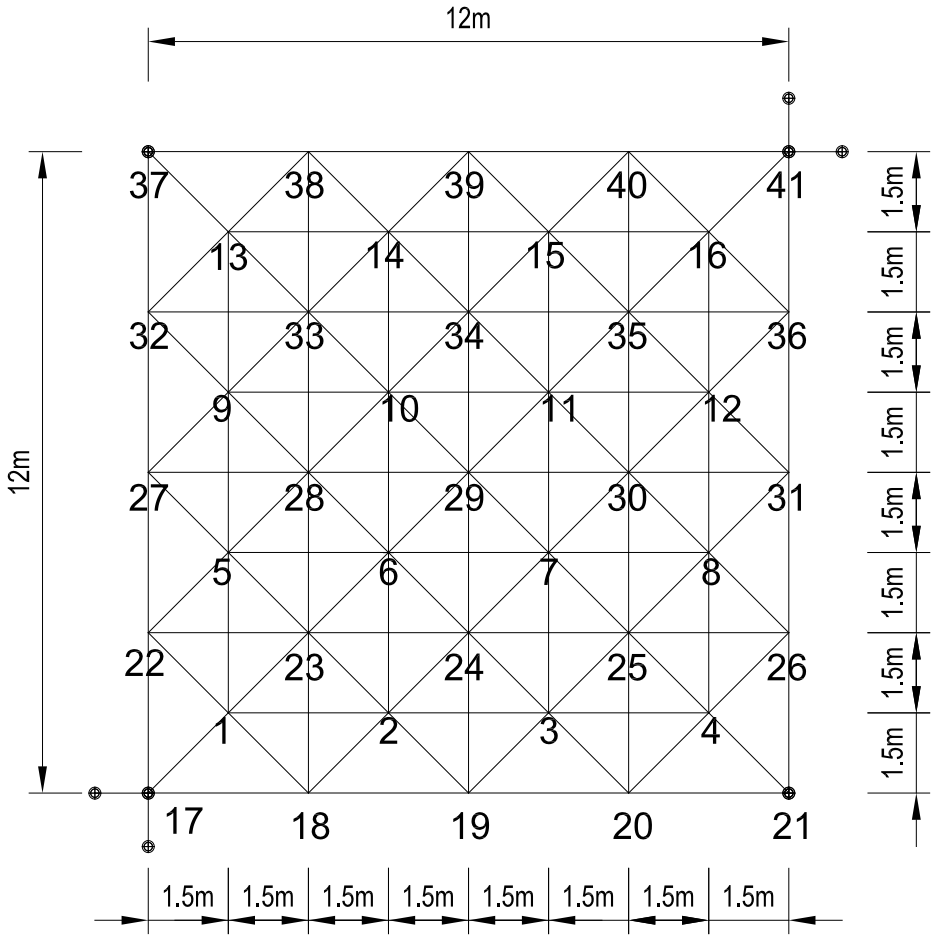

(a) space truss - plan view and node numbers

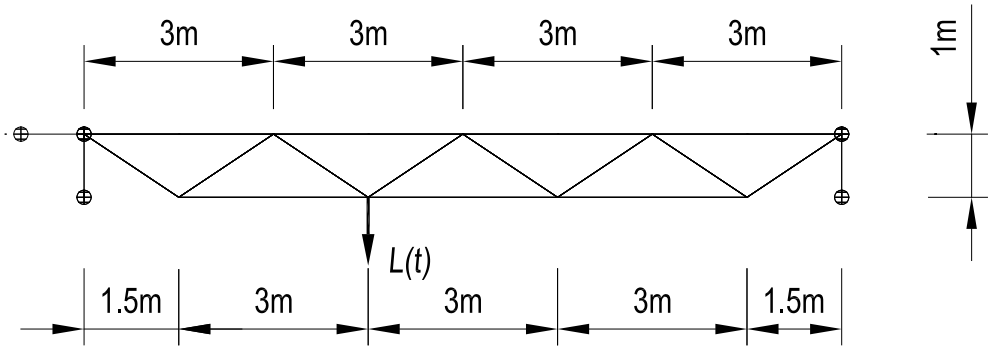

(b) space truss - elevation

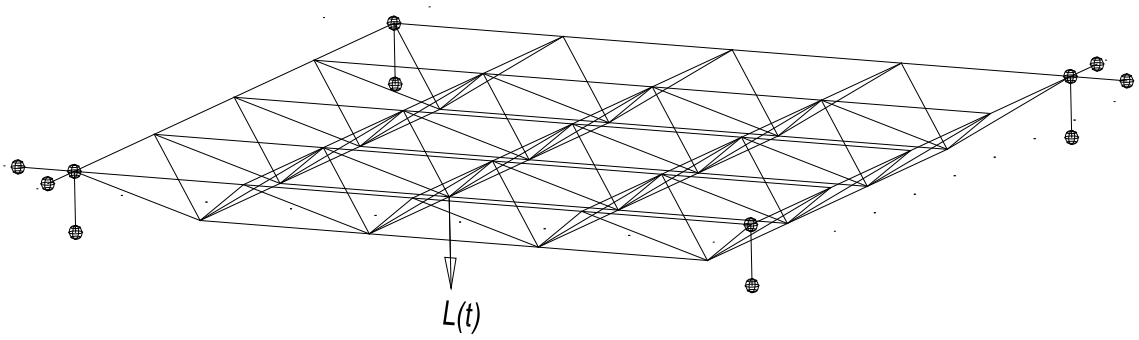

(c) space truss - isometric view

Figure 9.4.1 – Model of the 41 node space truss

The vertical displacement of node 6 is used for the comparison. Initially a time step of 3E-4s is selected to meet the stability requirements of all algorithms apart from the UVHP_L3, however as explained earlier the result obtained with the UVHP_L3 is still meaningful for the first one hundred steps. The results are compared in Table 9.4.1 and Figure 9.4.2.

Time	analytical	AAM		H3 algorithm		L2 algorithm		L3 algorithm		L5 algorithm	
	Y Displacement	Y Displacement	Relative error	Y Displacement	Relative error	Y Displacement	Relative error	Y Displacement	Relative error	Y Displacement	Relative error
0	0	0	0	0.00E+00	0	0.00E+00	0	0	0	0	0
0.0015	-4.99E-04	-5.04E-04	1.06%	-4.85E-04	2.79%	-4.90E-04	1.74%	-4.97E-04	0.39%	-4.99E-04	0.00%
0.003	-9.11E-04	-9.60E-04	5.42%	-9.08E-04	0.26%	-9.06E-04	0.47%	-9.13E-04	0.30%	-9.11E-04	0.00%
0.0045	-1.31E-03	-1.31E-03	0.06%	-1.31E-03	0.25%	-1.31E-03	0.36%	-1.30E-03	0.21%	-1.31E-03	0.00%
0.006	-1.82E-03	-1.81E-03	0.51%	-1.81E-03	0.53%	-1.81E-03	0.42%	-1.82E-03	0.08%	-1.82E-03	0.00%
0.0075	-2.20E-03	-2.24E-03	1.79%	-2.20E-03	0.17%	-2.20E-03	0.09%	-2.20E-03	0.03%	-2.20E-03	0.00%
0.009	-2.61E-03	-2.59E-03	0.81%	-2.59E-03	0.67%	-2.59E-03	0.58%	-2.61E-03	0.00%	-2.61E-03	0.00%
0.0105	-3.17E-03	-3.10E-03	2.19%	-3.16E-03	0.33%	-3.16E-03	0.33%	-3.16E-03	0.16%	-3.17E-03	0.00%
0.012	-3.54E-03	-3.48E-03	1.74%	-3.52E-03	0.65%	-3.52E-03	0.68%	-3.54E-03	0.03%	-3.54E-03	0.00%
0.0135	-3.38E-03	-3.44E-03	1.58%	-3.40E-03	0.34%	-3.39E-03	0.31%	-3.39E-03	0.31%	-3.38E-03	0.00%
0.015	-3.22E-03	-3.23E-03	0.56%	-3.22E-03	0.09%	-3.22E-03	0.06%	-3.21E-03	0.33%	-3.22E-03	0.00%
0.0165	-2.88E-03	-2.88E-03	0.08%	-2.87E-03	0.24%	-2.87E-03	0.26%	-2.90E-03	0.64%	-2.88E-03	0.01%
0.018	-2.42E-03	-2.41E-03	0.27%	-2.44E-03	1.07%	-2.44E-03	1.00%	-2.42E-03	0.13%	-2.42E-03	0.01%
0.0195	-2.06E-03	-2.04E-03	0.82%	-2.07E-03	0.21%	-2.06E-03	0.16%	-2.04E-03	0.94%	-2.06E-03	0.00%
0.021	-1.52E-03	-1.52E-03	0.01%	-1.53E-03	0.42%	-1.52E-03	0.31%	-1.53E-03	0.47%	-1.52E-03	0.01%
0.0225	-5.87E-04	-6.63E-04	12.96%	-5.98E-04	1.77%	-5.98E-04	1.77%	-5.84E-04	0.55%	-5.87E-04	0.01%
0.024	1.14E-04	1.26E-04	10.34%	9.87E-05	13.62%	9.84E-05	13.89%	1.02E-04	10.77%	1.14E-04	0.01%
0.0255	7.00E-04	6.81E-04	2.67%	7.16E-04	2.24%	7.14E-04	1.99%	7.10E-04	1.39%	7.00E-04	0.02%
0.027	1.18E-03	1.20E-03	1.02%	1.20E-03	1.35%	1.20E-03	1.16%	1.18E-03	0.25%	1.18E-03	0.00%
0.0285	1.29E-03	1.35E-03	4.55%	1.30E-03	0.58%	1.30E-03	0.54%	1.31E-03	1.13%	1.29E-03	0.00%
0.03	1.44E-03	1.42E-03	1.17%	1.47E-03	2.30%	1.47E-03	2.15%	1.44E-03	0.09%	1.44E-03	0.02%

Table 9.4.1 – Space truss – time history of vertical displacement of node 6 (time step = 3E-4s)

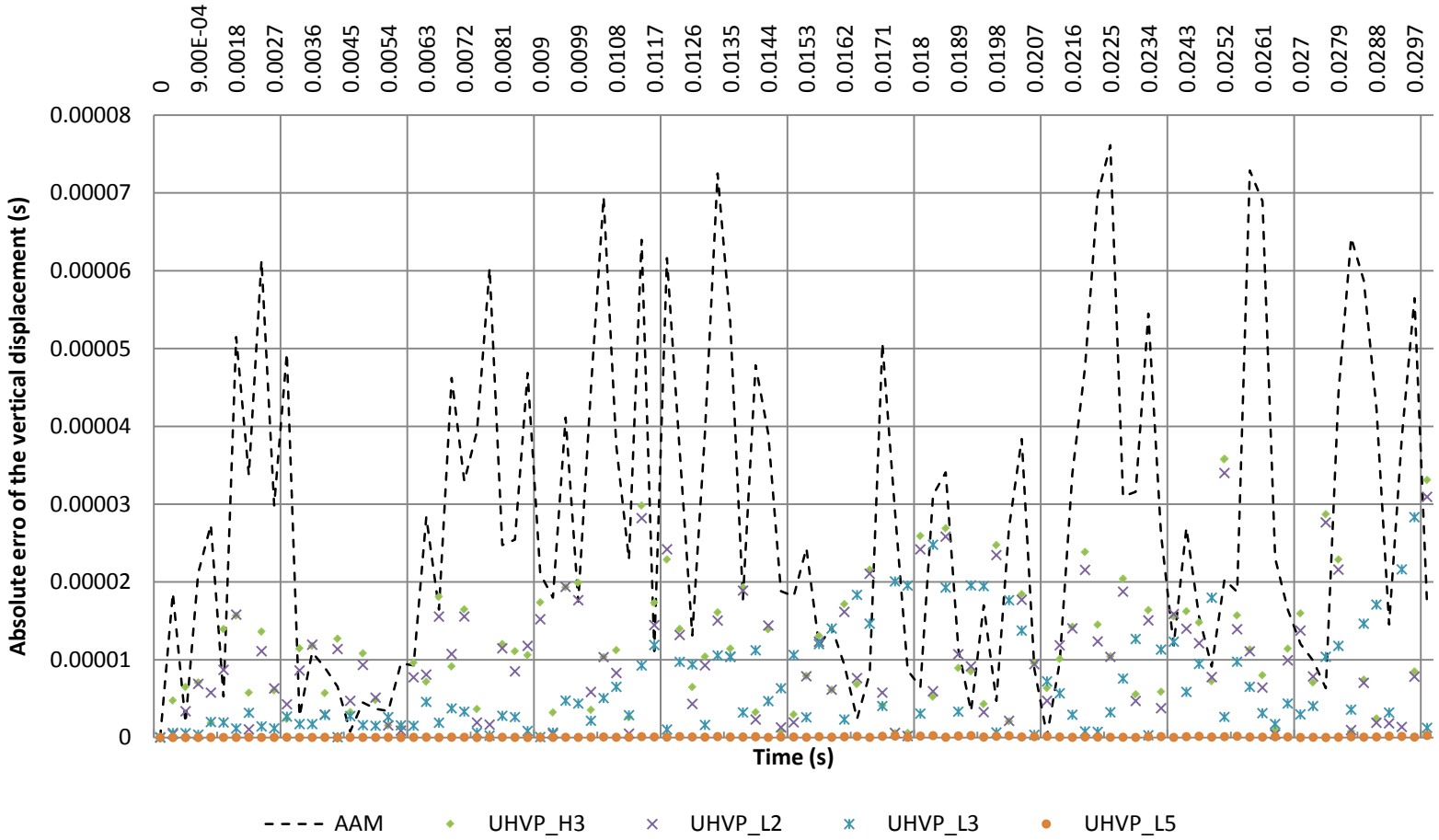

Figure 9.4.2 – Space truss – absolute error of the vertical displacements of node 6 (time step = 3E-4s)

It can be seen from Table 9.4.1 that the results of all algorithms match the analytical one well for the given time step, however, it is clear from Figure 9.4.2 that the UHVP algorithms approximate the analytical solution even better, especially the UHVP_L5 scheme.

Smaller time steps are used to improve the accuracy of the AAM results, the relative errors of each scheme with various time steps are listed in Table 9.4.2.

Time	**UHVP_H3 (time step = 3E-4s)**	**UHVP_L2 (time step = 3E-4s)**	**UHVP_L3 (time step = 3E-4s)**	**UHVP_L5 (time step = 3E-4s)**	**AAM (time step = 1E-4s)**	**AAM (time step = 7.5E-6s)**
0	0	0	0	0	0	0
0.003	0.26%	0.47%	0.30%	0.00%	1.05%	0.01%
0.006	0.53%	0.42%	0.08%	0.00%	0.37%	0.00%
0.009	0.67%	0.58%	0.00%	0.00%	0.32%	0.00%
0.012	0.65%	0.68%	0.03%	0.00%	0.84%	0.00%
0.015	0.09%	0.06%	0.33%	0.00%	0.48%	0.01%
0.018	1.07%	1.00%	0.13%	0.01%	0.21%	0.01%
0.021	0.42%	0.31%	0.47%	0.01%	1.24%	0.02%
0.024	13.62%	13.89%	10.77%	0.01%	22.77%	0.08%
0.027	1.35%	1.16%	0.25%	0.00%	0.30%	0.00%
0.03	2.30%	2.15%	0.09%	0.02%	0.48%	0.02%

Table 9.4.2 - Comparison of relative errors of the vertical displacements of node 6

From the above table, it is clear that the time step for AAM has to be reduced to 1E-4s to get the results close to those of UHVP_L2 and UVHP_H3 algorithms. The time step has to be further reduced to 7.5E-6s to obtain the AAM results matching the results of UHVP_L5 scheme. The corresponding computational costs for these schemes are listed in Table 9.4.3.

Algorithm	**Time step (s)**	**Computation time (s)**	**Ratio of computational cost**
AAM	7.50E-06	2.0411	24.18
	1.00E-04	0.2428	2.88
	3.00E-04	0.0844	1.00
UVHP_H3	3.00E-04	0.2764	3.27
UVHP_L2		0.8853	10.49
UVHP_L3		2.3578	27.94
UVHP_L5		8.9389	105.91

Table 9.4.3 - Comparison of computational costs for Example Three

It can be seen that:

- The AAM scheme with the time step of 3.00E-04s is the most efficient scheme, although its accuracy is known the lowest within all schemes compared.
- For the same level of accuracy, the UVHP_H3 algorithm requires slightly higher computational effort than the corresponding AAM scheme.
- The rest of UVHP algorithms are more computationally expensive than the corresponding AAM schemes in this particular example, due to more degrees of freedom involved in the calculation.

9.5 Example Four – A seven-node planar truss subject to a chaotic excitation force

In this example, the same planar truss used in Example Two (Figure 9.3.1) is excited from the static equilibrium position by a chaotic force depicted in Figure 9.5.1. The load is applied vertically to the node F. The damping and the self-weight of the truss are not considered.

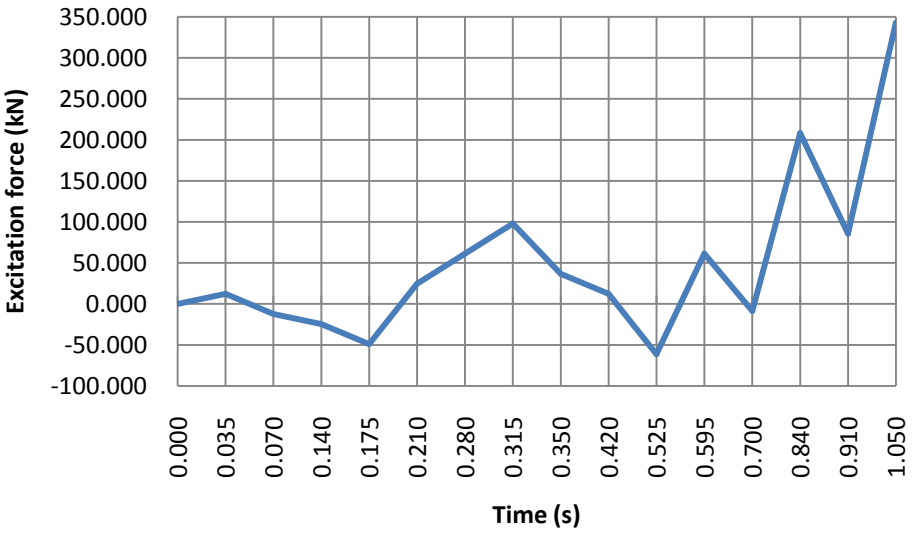

Figure 9.5.1 – Time history of the excitation force applied to the node F

The length of the time step used is again 5E-4 seconds, and the results for the period [0, 0.035s] are compared in Table 9.5.1. It can be seen that these numerical schemes, including the AAM and all UVHP algorithms, give accurate results for this initial period, especial the UVHP_L5 results show very high accuracy.

However, similar to the previous examples, the difference starts to appear when the calculation is repeated. This is clearly visible in Figures 9.5.2 and 9.5.3 where the AAM results “drift” away from the UVHP results.

To improve the accuracy of the AAM results, much smaller time steps have to be used. It can be seen from Figure 9.5.4 that the results of the AAM with the time step ten times smaller match the results of UHVP_L5 using the original time step. Table 9.5.2 confirms this observation from the relative error perspective, and it can also be seen from the same table, when the time step is taken as 2.5E-4 seconds, the AAM results are roughly as accurate as the UVHP_L2 and UVHP_H3 results using the original time step, but are still less accurate than the UVHP_L3 results.

Time	analytical	AAM		UVHP_H3		UVHP_L2		UVHP_L3		UVHP_L5	
	Y Displacement	Y Displacement	Relative Error %	Y Displacement	Relative Error %	Y Displacement	Relative Error %	Y Displacement	Relative Error %	Y Displacement	Relative Error %
0.0035	6.35E-05	6.36E-05	0.16%	6.34E-05	0.13%	6.34E-05	0.20%	6.35E-05	0.04%	6.35E-05	0.00%
0.007	3.29E-04	3.28E-04	0.39%	3.29E-04	0.00%	3.29E-04	0.02%	3.29E-04	0.01%	3.29E-04	0.00%
0.0105	7.73E-04	7.72E-04	0.12%	7.73E-04	0.02%	7.73E-04	0.02%	7.73E-04	0.01%	7.73E-04	0.00%
0.014	1.23E-03	1.23E-03	0.01%	1.23E-03	0.03%	1.23E-03	0.03%	1.23E-03	0.02%	1.23E-03	0.00%
0.0175	1.61E-03	1.61E-03	0.08%	1.61E-03	0.00%	1.61E-03	0.00%	1.61E-03	0.01%	1.61E-03	0.00%
0.021	1.93E-03	1.92E-03	0.06%	1.93E-03	0.00%	1.93E-03	0.00%	1.93E-03	0.01%	1.93E-03	0.00%
0.0245	2.12E-03	2.12E-03	0.06%	2.12E-03	0.00%	2.12E-03	0.00%	2.12E-03	0.01%	2.12E-03	0.00%
0.028	2.20E-03	2.20E-03	0.18%	2.20E-03	0.04%	2.20E-03	0.04%	2.20E-03	0.01%	2.20E-03	0.00%
0.0315	2.31E-03	2.32E-03	0.11%	2.31E-03	0.02%	2.31E-03	0.02%	2.31E-03	0.01%	2.31E-03	0.00%
0.035	2.65E-03	2.65E-03	0.11%	2.65E-03	0.03%	2.65E-03	0.03%	2.65E-03	0.01%	2.65E-03	0.00%

Table 9.5.1 – Seven-node truss under a chaotic excitation –Y displacements of node F for the period [0, 0.035s] (time step = 5E-4 s)

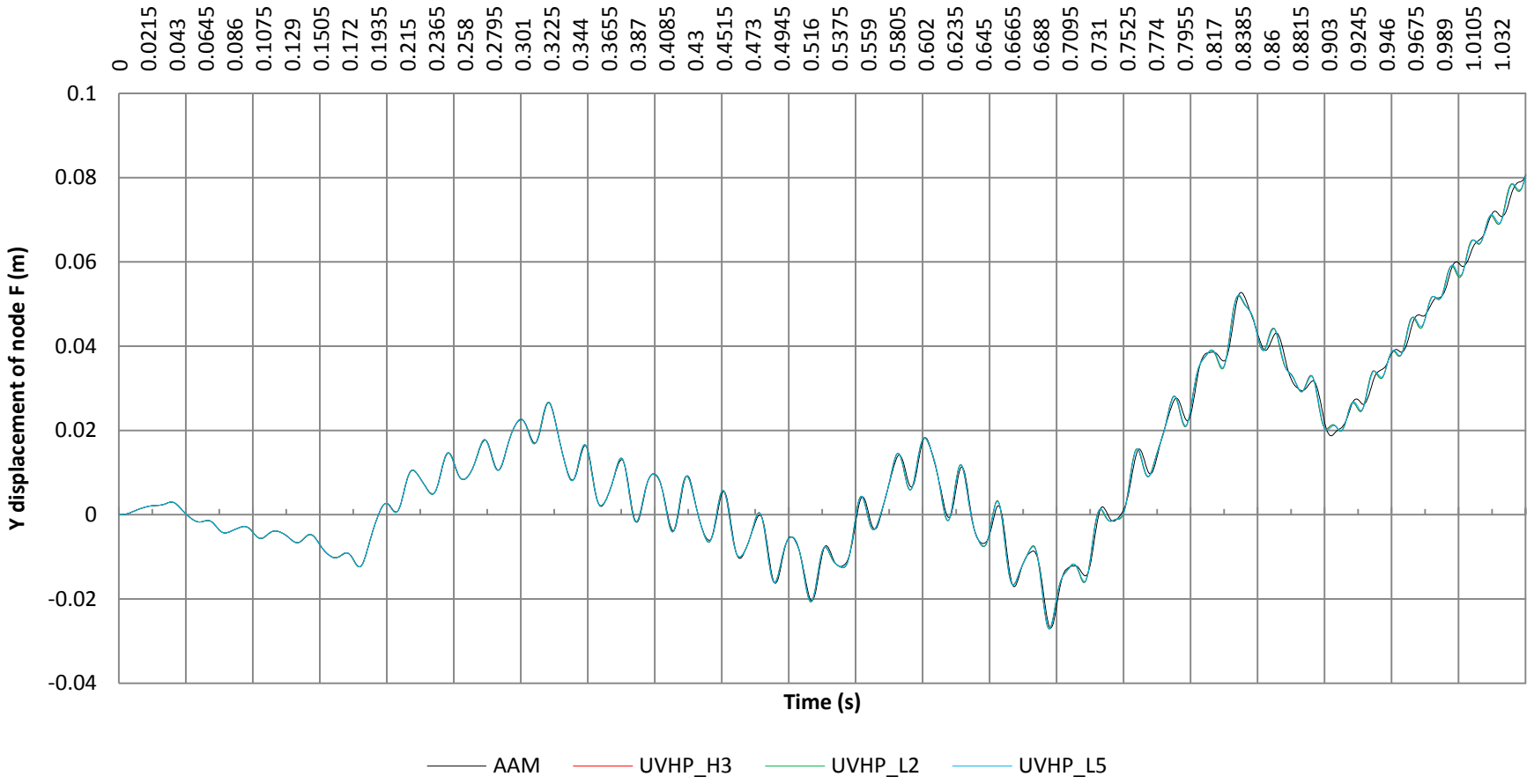

Figure 9.5.2 – Seven-node truss under a chaotic excitation – time history plot of Y displacements of node F (time step = 5E-4 s)

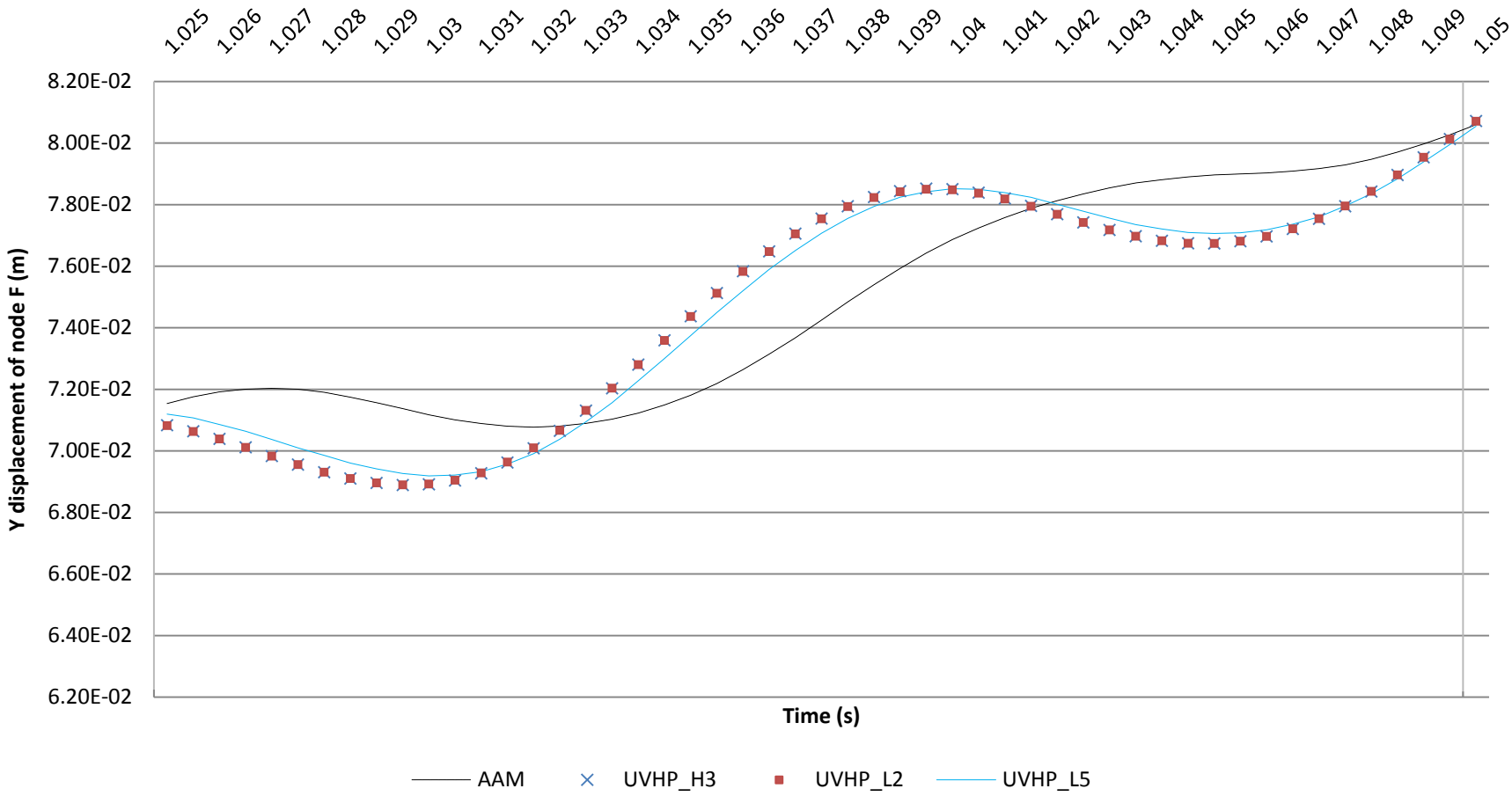

Figure 9.5.3 – “close up” of time history plot between [1.00s, 1.05s] (time step = 5E-4 s)

Time (s)	**UVHP_H3 (Δt=5E-4s)**	**UVHP_L2 (Δt=5E-4s)**	**UVHP_L3 (Δt=5E-4s)**	**UVHP_L5 (Δt=5E-4s)**	**AAM (Δt=5E-4s)**	**AAM (Δt=2.5E-4s)**	**AAM (Δt=5E-5s)**
0.0035	0.13%	0.20%	0.04%	0.00%	0.16%	0.09%	0.01%
0.007	0.00%	0.02%	0.01%	0.00%	0.39%	0.20%	0.01%
0.0105	0.02%	0.02%	0.01%	0.00%	0.12%	0.04%	0.01%
0.014	0.03%	0.03%	0.02%	0.00%	0.01%	0.01%	0.00%
0.0175	0.00%	0.00%	0.01%	0.00%	0.08%	0.05%	0.00%
0.021	0.00%	0.00%	0.01%	0.00%	0.06%	0.01%	0.01%
0.0245	0.00%	0.00%	0.01%	0.00%	0.06%	0.02%	0.00%
0.028	0.04%	0.04%	0.01%	0.00%	0.18%	0.02%	0.00%
0.0315	0.02%	0.02%	0.01%	0.00%	0.11%	0.03%	0.00%
0.035	0.03%	0.03%	0.01%	0.00%	0.11%	0.02%	0.00%

Table 9.5.2 – Comparison of the relative errors of node F displacements

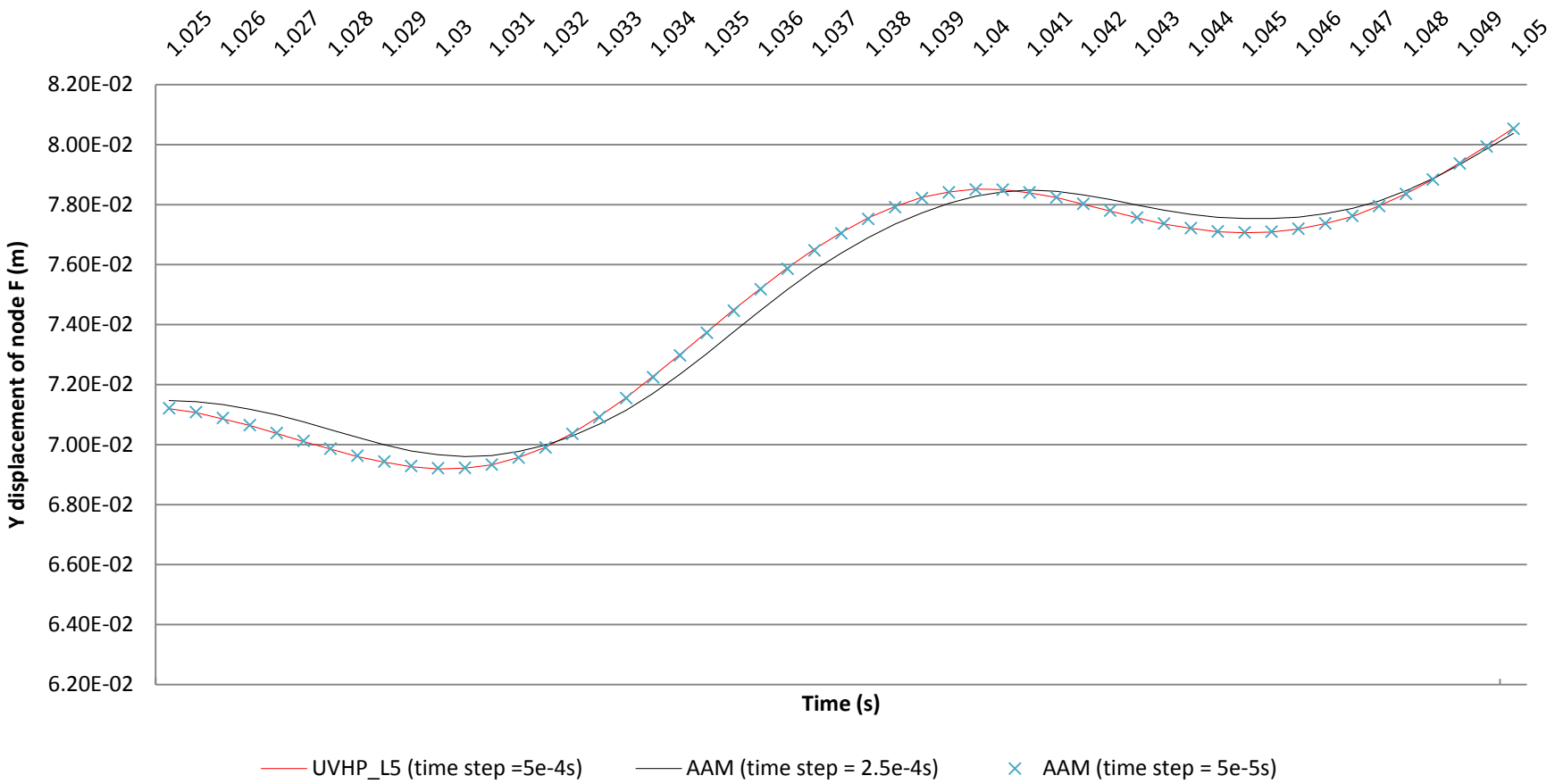

Figure 9.5.4 – Time history plot of Y displacements of node F between [1.00s, 1.05s] with various time steps

The computational cost of each scheme for the period [0, 1.05s], measured in terms of the computation time consumed by the same desktop used for Example One are listed in Table 9.5.3. It can be seen that:

- The UVHP_H3 algorithm again uses less time than the AAM with the same time step, while producing more accurate results.
- The computational cost for the UVHP_L2 algorithm is less than the corresponding AAM scheme for equivalent accuracy.
- Both UVHP_L5 algorithm and the AAM scheme with the smallest time step produce equally high- order results, with much increased computational costs.

Algorithm	Time step (s)	Computation time (s)	Ratio of computational cost
AAM	5.00e-05	1.134	10.70
	2.50e-04	0.267	2.52
	5.00e-04	0.130	1.23
UVHP_H3	5.00e-04	0.106	1.00
UVHP_L2		0.227	2.14
UVHP_L3		0.780	7.36
UVHP_L5		1.627	15.35

Table 9.5.3 - Comparison of computational costs of Example Four

9.6 Conclusion

Four examples have been given in this chapter to demonstrate the accuracy and efficiency of the proposed UVHP algorithms. It is found in these examples:

- The validity of the UVHP algorithms has been verified through the comparison with the reference schemes. Both homogeneous and chaotic loads are tested, and the UVHP results match the analytical ones very well.
- All UVHP algorithms have less period elongation and amplitude variation than the AAM.
- With the given time steps, the UVHP algorithms produce much improved results compared to the AAM, especially the UVHP_L5 algorithm. At the

same time, the computational cost for UVHP algorithms can be lower than the AAM schemes for the equivalent level of accuracy.

- To improve the accuracy of the AAM results, much increased computational cost is demanded. In contrast, these additional costs can be lower for UVHP algorithms by using higher order approximations.
- Large time step may be used to produce results with decent accuracy with the UVHP algorithm.

Chapter 10 Conclusion and Future Work

10.1 Summary

This research aims to construct a new method for the linear dynamic analysis of truss-type structures. The proposed method is a space-time finite element method, based on Unconventional Hamilton-type Variational Principles tailored for this type of structures. The dynamic equilibrium equation and all essential conditions are preserved naturally in simple functionals. A fundamental integral relation was given, from which five bespoke Unconventional Hamilton-type Variational Principles were derived. The intrinsic relations between these principles were also revealed. The one-field and two-field principles were used to underpin the development of the proposed space-time finite element algorithms.

To construct the proposed method, the semi-discretisation approach of the space-time domain was adopted. The structure was first discretised with rod element in the spatial domain, followed by a separate time finite element treatment in the temporal domain. The resultant system equations were a set of algebraic equations which could be solved conveniently. The time finite elements utilised in the study included the cubic Hermite element, the second-, third- and fifth-order Lagrange elements. The stability and consistency of these UVHP algorithms were examined in detail, and the accuracy and efficiency of the proposed algorithms were verified via four numerical examples. The performance of the proposed UVHP algorithms was compared against the popular Average Acceleration Method.

10.2 Conclusions

The main findings of the research are as follows:

1. The Hamilton's principle is not a suitable variational principle for initial-value problems, despite it is still in use in some modern texts. The reason lies in the assumption of the variation vanishing at the upper time boundary cannot be justified for initial-value problems in the context of the calculus of variation.

2. A system of Unconventional Hamilton-type Variational Principles has been developed, which have been proved to be suitable for developing a tailored method for the dynamic analysis of truss-type structures. Existing variational principles/ law (Hamilton's Principle, Hamilton's Weak Principle, and Hamilton's Law of Varying Action) can be verified as special cases of Unconventional Hamilton-type Variational Principle in the general form.

3. The proposed method for developing the variational principles is unique. Starting from an identical equation, the Unconventional Hamilton-type Variational Principles for truss-type structures can be developed in a systematic approach.

4. Five tailored Unconventional Hamilton-type Variational Principles suitable for the linear dynamic analysis of truss structures have been derived with various independent variable fields. These five principles are interlinked and the relations between them are revealed. The functionals in each of the principles always appear in complementary pairs, and either one can be used for the construction of the variational algorithm. These principles also lay a solid foundation for the extension to other applications, by introducing relevant governing conditions for particular behaviour to be addressed, such as non-linear analysis.

5. Two types of space-time finite element algorithms are derived based on the one-field and two-field principles, respectively. It is shown that these algorithms are capable of producing second- and higher-order results when various time finite elements are employed.

6. The accuracy of the proposed UVHP algorithms has been verified through the numerical examples. It was found that the UVHP algorithms give much improved results compared to the popular Average Acceleration Method (AAM).

7. The efficiency of the proposed UVHP algorithms has been verified. As demonstrated in the numerical examples, the computational cost for the UVHP algorithms can be lower than the AAM schemes. Therefore, in addition to structural dynamics, the UVHP algorithms may be also considered for applications where fast and highly accurate algorithms are required, such as the positive control of vibrations.

8. The stability and consistency of the UVHP algorithms have been proven.

In summary, this study has provided a new approach to develop a space-time finite element method for truss-type structures, from the variational theory to the space-time discretisation. The proposed method is very useful for engineering applications that require efficient and accurate dynamic response analysis. It can also be extended to other particular applications, such as non-linear analysis and multi-physics analysis.

10.3 Future work

1. UVHP_H3, UVHP_L3 and UVHP_L5 algorithms are conditionally stable although they can give very accurate results. It is worthwhile to explore the means of amending these algorithms to obtain unconditional stability. In the literature, three approaches have been proven successful in this respect:

    1) Unconditionally stable algorithm may be obtained by combining the evaluations at other locations rather than at the end node of the time step as demonstrated in (Geradin, 1974, Fung, 1998).

2) Unconditionally stable algorithm may be obtained by the combination of different methods as demonstrated in (Wang and Au, 2004).

3) Stabilising terms may be considered to be introduced into the formulation (Hughes and Hulbert, 1988).

2. The ultimate spectral radii of the presented algorithms are all “fixed” for each particular algorithm. Therefore, it is desirable to find suitable measures to obtain adjustable ultimate spectral radius to have a better dissipation.

3. A further study considering the post-buckling behaviour of the truss structure is worth exploring. Although it is not intended to push truss-type structures into the non-linear stage during its service period, unexpected circumstances do occur in reality. To prevent adverse deformations and to have more assurance on the safety for both the occupants and the structure, a complete theory suitable for both linear and non-linear analysis will be more advantageous. This research has demonstrated a means to introduce any necessary condition into the variational principle and provided a platform for the development of a complete theory.

REFERENCE

Argyris, J. H., & Scharpf, D. W., 1969. Finite elements in time and space. *Nuclear Engineering and Design,* 10**,** pp. 456-464.

Bailey, C. D., 1975a. A new look at Hamilton's principle. *Foundations of Physics,* 5**,** pp. 433-451.

Bailey, C. D., 1975b. Application of Hamilton's law of varying action. *AIAA Journal,* 13**,** pp. 1154-1157.

Bailey, C. D., 1976. Hamilton, Ritz and elastodynamics. *Journal of Applied Mechanics Transactions of the Asme,* 43**,** pp. 684-688.

Bailey, C., 1987. Dynamics and the calculus of variations. *Computer methods in applied mechanics and engineering,* 60**,** pp. 275-287.

Bajer, C. I., 1986. Triangular and tetrahedral space - time finite elements in vibration analysis. *International journal for numerical methods in engineering,* 23**,** pp. 2031-2048.

Baruch, M. & Riff, R., 1982. Hamilton's Principle, Hamilton's Law - 6^n Correct Formulations. *AIAA Journal,* 20**,** pp. 687-692.

Baruch, M. & Riff, R., 1984. Stability of time finite elements. *AIAA journal,* 22**,** pp. 1171-1173.

Bathe, K. J. & Wilson, E. L., 1972. Stability and accuracy analysis of direct integration methods. *Earthquake Engineering & Structural Dynamics,* 1**,** pp. 283-291.

Bathe, K.J., 1996. *Finite element procedures,* Prentice hall Englewood Cliffs: Prentice Hall.

Bazzi, G. & Anderheggen, E., 1982. The ρ-family of algorithms for time-step integration with improved numerical dissipation. *Earthquake Engineering & Structural Dynamics,* 10**,** pp. 537-550.

Bellman, R. & Casti, J., 1971. Differential quadrature and long-term integration. *Journal of Mathematical Analysis and Applications,* 34**,** pp. 235-238.

Bhutani, O. P. & Gupta, N., 1982. Variational principle for linear initial value problems. *International Journal of Engineering Science,* 20**,** pp. 1303-1309.

Borri, M., Ghiringhelli, G. L., Lanz, M., Mantegazza, P. & Merlini, T., 1985. Dynamic response of mechanical systems by a weak Hamiltonian formulation. *Computers & Structures,* 20**,** pp. 495-508.

Cella, A., Lucchesi, M. & Pasquinelli, G., 1980. Space–time elements for the shock wave propagation problem. *International Journal for Numerical Methods in Engineering,* 15**,** pp. 1475-1488.

Chen, G., 1990. Unconstrained variational statements for initial and boundary-value problems via the principle of total virtual action. *International Journal of Engineering Science,* 28**,** pp. 875-887.

Chung, J. & Hulbert, G. M., 1993. A time integration algorithm for structural dynamics with improved numerical dissipation: the generalized-α method. *Journal of applied mechanics,* 60**,** pp. 371-375.

Chung, J. & Hulbert, G. M., 1994. A family of single-step Houbolt time integration algorithms for structural dynamics. *Computer methods in applied mechanics and engineering,* 118**,** pp. 1-11.

Clough, R. W. & Penzien, J., 1993. *Dynamics of structures,* New York: McGraw-Hill.

Courant, R., 1943. Variational methods for the solution of problems of equilibrium and vibrations. *Bulletin of the American mathematical society,* 49**,** pp. 1-23.

Cushman, J. H., 1979. Difference schemes or element schemes? *International Journal for Numerical Methods in Engineering,* 14**,** pp. 1643-1651.

Dokainish, M. & Subbaraj, K., 1989. A survey of direct time-integration methods in computational structural dynamics—I. Explicit methods. *Computers & Structures,* 32**,** pp. 1371-1386.

Fan, S., Fung, T. & Sheng, G., 1997a. A comprehensive unified set of single-step algorithms with controllable dissipation for dynamics Part II. Algorithms and analysis. *Computer methods in applied mechanics and engineering,* 145**,** pp. 99-107.

Fan, S. C., Fung, T. C. & Sheng, G., 1997b. A comprehensive unified set of single-step algorithms with controllable dissipation for dynamics Part I. Formulation. *Computer methods in applied mechanics and engineering,* 145**,** pp. 87-98.

Fang, J., Li, Q. & Jeary, A., 1999. A new function transform technique for the solution of FEM dynamic equations. *Computers & structures,* 70**,** pp. 345-355.

Fox, L. & Goodwin, E., Some new methods for the numerical integration of ordinary differential equations. Proc. Cambridge Philos. Soc, 1949. Cambridge Univ Press, pp. 373-388.

Fung, T. C., 1996. Unconditionally stable higher-order accurate Hermitian time finite elements. *International journal for numerical methods in engineering,* 39**,** pp. 3475-3495.

Fung, T. C. 1997a. A precise time-step integration method by step-response and impulsive-response matrices for dynamic problems. *International Journal for Numerical Methods in Engineering,* 40**,** pp. 4501-4527.

Fung, T. C., 1997b. Third-order time-step integration methods with controllable numerical dissipation. *Communications in numerical methods in engineering,* 13**,** pp. 307-315.

Fung, T. C., 1997c. Unconditionally stable higher-order Newmark methods by sub-stepping procedure. *Computer Methods in Applied Mechanics and Engineering,* 147**,** pp. 61-84.

Fung, T. C., 1998a. Complex-time-step Newmark methods with controllable numerical dissipation. *International Journal for numerical methods in Engineering,* 41**,** pp. 65-93.

Fung, T. C., 1998b. Higher order time-step integration methods with complex time steps. *Journal of sound and vibration,* 210**,** pp. 69-89.

Fung, T. C., 1999a. Weighting parameters for unconditionally stable higher-order accurate time step integration algorithms. Part 1—first-order equations. *International journal for numerical methods in engineering,* 45**,** pp. 941-970.

Fung, T. C., 1999b. Weighting parameters for unconditionally stable higher-order accurate time step integration algorithms. Part 2—second-order equations. *International journal for numerical methods in engineering,* 45**,** pp. 971-1006.

Fung, T. C., 2000a. Weighting parameters for time-step integration algorithms with predetermined coefficients. *International Journal for Numerical Methods in Engineering,* 49**,** pp. 1397-1430.

Fung, T. C., 2000b. Unconditionally stable higher-order accurate collocation time-step integration algorithms for first-order equations. *Computer methods in applied mechanics and engineering,* 190**,** pp. 1651-1662.

Fung, T. c., 2001a. Solving initial value problems by differential quadrature method—part 1: first-order equations. *International Journal for Numerical Methods in Engineering,* 50**,** pp. 1411-1427.

Fung, T. C., 2001b. Third order complex-time-step methods for transient analysis. *Computer methods in applied mechanics and engineering,* 190**,** pp. 2789-2802.
Fung, T. C., 2002b. On the equivalence of the time domain differential quadrature method and the dissipative Runge-Kutta collocation method. *International journal for numerical methods in engineering,* 53**,** pp. 409-431.

Fung, T. C., 2005. Construction of higher-order accurate time-step integration algorithms by equal-order polynomial projection. *Journal of Vibration and Control,* 11**,** pp. 19-49.

Fung, T. C., 2001c. Solving initial value problems by differential quadrature method - part 2: second- and higher-order equations. *International journal for numerical methods in engineering,* 50**,** pp. 1429-1454.

Fung, T. C., 2003a. Bi-discontinuous time step integration algorithms—Part 1: first order equations. *Computer methods in applied mechanics and engineering,* 192**,** pp. 331-349.

Fung, T. C., 2003b. Bi-discontinuous time step integration algorithms—Part 2: second-order equations. *Computer methods in applied mechanics and engineering,* 192**,** pp. 351-374.

Fung, T. C., 2003c. Time step integration algorithms with predetermined coefficients for second order equations. *Computers and Structures,* 81**,** pp. 2557-2577.

Fung, T.C., 2003d. Numerical dissipation in time-step integration algorithms for structuraldynamic analysis. *Progress in Structural Engineering and Materials,*5, pp. 167–180.

Fung, T. C., & Chen, Z., 2006. Krylov precise time-step integration method. *International journal for numerical methods in engineering,* 68**,** pp. 1115-1136.

Fung, T. C. & Chow, S., 1999. Responses of blast loading by complex time step method. *Journal of sound and vibration,* 223**,** pp. 23-48.
Fung, T. C. & Chow, S., 2002. Solving non-linear problems by complex time step methods. *Communications in numerical methods in engineering,* 18**,** pp. 287-303.

Fung, T. C., Fan, S. C. & Sheng, G., 1998. Mixed time finite elements for vibration response analysis. *Journal of Sound and Vibration,* 213**,** pp. 409-428.

Fried, I., 1969. Finite-element analysis of time-dependent phenomena. *AIAA Journal,* 7**,** pp. 1170-173.

Gao, W., 2007. Random seismic response analysis of truss structures with uncertain parameters. *Engineering Structures,* 29 (7), pp. 1487-1498.

Gellert, M., 1978. A new algorithm for integration of dynamic systems. *Computers & Structures,* 9**,** pp. 401-408.

Geradin, M., 1974. On the variational method in the direct integration of the transient structural response. *Journal of Sound and Vibration,* 34**,** pp. 479-487.
Gerald, C. F. & Wheatley, P. O., 1994. *Applied numerical analysis,* Reading, Mass. Wokingham : Addison-Wesley.

Golley, B. W., 1996. A time-stepping procedure for structural dynamics using gauss point collocation. *International journal for numerical methods in engineering,* 39**,** pp. 3985-3998.

Golley, B. W. & Amer, M., 1999. An unconditionally stable time-stepping procedure with algorithmic damping: a weighted integral approach using two general weight functions. *Earthquake engineering & structural dynamics,* 28**,** pp. 1345-1360.

Grossi, R. O. & Albaracin, C.M., 2007. A variational approach to vibrating frames. *Journal of Multi-body Dynamics, 221***,** pp. 247-259.

Gu, Y., Chen, B., Zhang, H. & Guan, Z., 2001. Precise time-integration method with dimensional expanding for structural dynamic equations. *AIAA journal,* 39**,** pp. 2394-2399.

Gurtin, M. E., 1963. Variational principles in the linear theory of viscoelasticity. *Archive for Rational Mechanics and Analysis,* 13**,** pp. 179-191.

Gurtin, M. E., 1964a. Variational principles for linear elastodynamics. *Archive for Rational Mechanics and Analysis,* 16**,** pp. 34-50.

Gurtin, M. E., 1964b. Variational principles for linear initial-value problems. *The Quarterly of Applied Mathematics,* 22**,** pp. 252-256.

Hamilton, W. R., 1834. On a General Method in Dynamics. *Philosophical Transactions of the Royal Society of London,* 124**,** pp. 247-308.

Hamilton, W. R., 1835. Second essay on a general method in dynamics. *Philosophical Transactions of the Royal Society of London,* 125**,** pp. 95-144.

Heppler, G., Oguamanam, D. & Hansen, J., 2003. Vibration of a two-member open frame. *Journal of sound and vibration,* 263**,** pp. 299-317.

Herrera, I. & Bielak, J., 1974. A simplified version of Gurtin's variational principle. *Archive for Rational Mechanics and Analysis,* 53**,** pp. 131-149.

Hilber, H. M. & Hughes, T. J. R., 1978. Collocation, dissipation and overshoot for time integration schemes in structural dynamics. *Earthquake Engineering &*

Structural Dynamics, 6**,** pp. 99-117.

Hilber, H. M., Hughes, T. J. R. & Taylor, R. L., 1977. Improved numerical dissipation for time integration algorithms in structural dynamics. *Earthquake Engineering & Structural Dynamics,* 5**,** pp. 283-292.

Houbolt, J. C., 1950. A recurrence matrix solution for the dynamic response of elastic aircraft. *Journal of the Aeronautical Sciences (Institute of the Aeronautical Sciences),* 17(9), pp. 540-550.

Howard, G. & Penny, J., 1978. The accuracy and stability of time domain finite element solutions. *Journal of Sound and Vibration,* 61**,** pp. 585-595.

Huang, W., Luo, E. & She, H., 2006. Unconventional Hamilton-type variational principles for dynamics of reissner sandwich plate. *Applied Mathematics and Mechanics,* 27**,** pp. 75-82.

Hughes, T. J., 1987. *The finite element method: linear static and dynamic finite element analysis.* Englewood Cliffs, New Jersey: Prentice Hall.

Hughes, T. J. R. & Hulbert, G. M., 1988. Space-Time Finite-Element Methods for Elastodynamics - Formulations and Error-Estimates. *Computer Methods in Applied Mechanics and Engineering,* 66**,** pp. 339-363.

Hughes, T. J. R. & Stewart, J. R., 1996. A space-time formulation for multiscale phenomena. *Journal of Computational and Applied Mathematics,* 74**,** pp. 217-229.

Hulbert, G. M., 1992. Time finite element methods for structural dynamics. *International Journal for Numerical Methods in Engineering,* 33**,** pp. 307-331.

Hulbert, G. M. & Hughes, T. J. R., 1990. Space-Time Finite-Element Methods for Second-Order Hyperbolic-Equations. *Computer Methods in Applied Mechanics and Engineering,* 84**,** pp. 327-348.

Idesman, A., 2011. A new exact, closed ‐ form a priori global error estimator for second ‐ and higher ‐ order time ‐ integration methods for linear elastodynamics. *International Journal for Numerical Methods in Engineering,* 88**,** pp. 1066-1084.

Idesman, A. V., 2007. A new high-order accurate continuous Galerkin method for linear elastodynamics problems. *Computational Mechanics,* 40**,** pp. 261-279.

Itzkowitz, I. & Levit, I., 1987. An explicit, unconditionally stable, time integration algorithm with a controlled accuracy. *Computers & structures,* 27**,** pp. 351-355.

Jiang, F. & Luo, E. 2008. Unconventional Hamilton-type incremental variational principles for piecewise linear elastodynamics of thin plates. *Journal of Vibration and Shock,* 11**,** pp. 31-39.

Kantorovich, L., Akilov, G., Vainberg, M. & Feinstein, A., 1964. *Variational methods for the study of nonlinear operators*. San Francisco: Holden-Day.

Kim, C. K., 2001. On the Numerical Computation for Solving the Two-Dimensional Parabolic Equations by Space-Time Finite Element Method. *JSME International Journal Series B,* 44**,** pp. 434-438.

Kim, C. K., 2003. Discontinuous Time-Space Galerkin Finite Element Discretization Technique for the Analysis of Two-Dimensional Heat Conduction. *JSME International Journal Series A,* 46**,** pp. 103-108.

Kim, S. J., Cho, J. Y. & Kim, W. D., 1997. From the trapezoidal rule to higher-order accurate and unconditionally stable time-integration method for structural dynamics. *Computer Methods in Applied Mechanics and Engineering,* 149**,** pp. 73-88.

Koohestani, K. & Kaven, A., 2010. Efficient buckling and free vibration analysis of cyclically repeated space truss structures. *Finite Elements in Analysis and Design,* 46**,** pp. 943-948.

Lanczos, C., 1970. *The Variational Principles of Mechanics*. Toronto, University of Toronto Press, 1970.

Lee, D. I. & Kwak, B. M., 1993. A direct integration method of elastodynamics using finite element time discretization. *Computers & structures,* 47**,** pp. 201-211.

Leung, A., 1986. Steady state response of undamped systems to excitations expressed as polynomials in time. *Journal of sound and vibration,* 106**,** pp. 145-151.

Levinson, M., 1976. Application of an extended Hamilton's principle to damped discrete and continuous systems. *Mechanics Research Communications,* 3**,** pp. 125-131.

Li, W. & Luo, E., 2007. Unconventional Hamilton-type variational principles for nonlinear elastodynamics of membrane structures. *Journal of Dynamics and Control,* 3**,** pp. 45-51.

Li, W., Luo, E. & Huang, W., 2007. Unconventional Hamilton-type variational principles for nonlinear elastodynamics of orthogonal cable-net structures. *Applied Mathematics and Mechanics-English Edition,* 28**,** pp. 931-942.

Lin, J., Shen, W. & Williams, F., 1995. A high precision direct integration scheme for structures subjected to transient dynamic loading. *Computers & structures,* 56**,** pp. 113-120.

Liu, J. & Wang, X., 2008. An assessment of the differential quadrature time integration scheme for nonlinear dynamic equations. *Journal of Sound and Vibration,* 314**,** pp. 246-253.

Liu, J. L., 2001. Solution of dynamic response of SDOF system using piecewise Lagrange polynomial. *Earthquake Engineering & Structural Dynamics,* 30**,** pp. 613-619.

Liu, J. L., 2002. Solution of dynamic response of framed structure using piecewise Birkhoff polynomial. *Journal of Sound and Vibration,* 251**,** pp. 847-857.

Luo, E. & Cheung, Y., 1988. On the variational principles in linear elastodynamics. *Acta Mechanica Sinica,* 4**,** pp. 337-349.

Luo, E., Huang, W. & Zhang, H.X., 2003. Unconventional Hamilton-type variational principle in phase space and symplectic algorithm. *Science in China Series G: Physics Mechanics and Astronomy,* 46**,** pp. 248-258.

Luo, E., Liang, L. F. & Li, W.H., 2007. Unconventional Hamilton-type variational principles for analytical mechanics. *Science in China Series G: Physics Mechanics and Astronomy,* 50**,** pp. 152-162.

Luo, E., Kuang, J., Huang, W. & Luo, Z., 2002. Unconventional Hamilton-type variational principles for nonlinear coupled thermoelastodynamics. *Science in China Series A: Mathematics,* 45**,** pp. 783-794.

Luo, E., Zhu, H. & Yuan, L., 2006. Unconventional Hamilton-type variational principles for electromagnetic elastodynamics. *Science in China Series G: Physics Mechanics and Astronomy,* 49**,** pp. 119-128.

Nickell, R. E. & Sackman, J. L., 1968. Approximate solutions in linear, coupled thermoelasticity. *Journal of Applied Mechanics,* 35**,** pp. 255.

Newmark, N. M., 1959. A Method of Computation for Structural Dynamics. *Transactions of the American Society of Civil Engineers,* 127**,** pp. 1406-1432.

Newmark, N. M., 1962. A Method of Computation for Structural Dynamics. *Transactions of the American Society of Civil Engineers,* 127**,** pp. 1406-1432.

Oden, J. T., 1969. A general theory of finite elements. II. Applications. *International Journal for Numerical Methods in Engineering,* 1**,** pp. 247-259.

Oden, J. T. & Reddy, J. N., 1974. On dual-complementary variational principles in mathematical physics. *International Journal of Engineering Science,* 12**,** pp. 1-29.

Panagiotopoulos, C. & Manolis, G., 2011. Three-dimensional BEM for transient elastodynamics based on the velocity reciprocal theorem. *Engineering Analysis with Boundary Elements,* 35**,** pp. 507-516.

Peng, J., Lewis, R. & Zhang, J., 1996. A semi-analytical approach for solving forced vibration problems based on a convolution-type variational principle. *Computers & structures,* 59**,** pp. 167-177.

Peters, D. & Izadpanah, A., 1988. hp-version finite elements for the space-time domain. *Computational Mechanics,* 3**,** pp. 73-88.

Park, K., 1975. Evaluating time integration methods for nonlinear dynamics analysis. *Finite element analysis of transient nonlinear structural behavior***,** pp. 35-58.

Rajan, M. & Junkins, J. L., 1983. Perturbation methods based upon varying action integrals. *International Journal of Non-Linear Mechanics,* 18**,** pp. 335-351.

Reddy, J. N., 1976. Modified Gurtins variational principles in linear dynamic theory of viscoelasticity. *International Journal of Solids and Structures,* 12**,** pp. 227-235.

Richtmyer, R. D. & Morton, K. W., 1967. *Difference Methods for Initial-Value Problems. 2nd ed.* New York : Interscience Publishers.

Riff, R. & Baruch, M., 1984. Time Finite Element Discretization of Hamilton's Law of Varying Action. *AIAA Journal,* 22**,** pp. 1310-1318.

Roelandts, T,(n.d.) [photograph] Available at: <http://tomroelandts.com/sites/tomroelandts.com/files/forth-rail-bridge.jpg> [Accessed 14 October 2013]

Rosen, P., 1954. Use of restricted variational principles for the solution of differential equations. *Journal of Applied Physics,* 25**,** pp. 336-338.

Rostami, S., Shojaee, S. & Moeinadini, A., 2012. A parabolic acceleration time integration method for structural dynamics using quartic B-spline functions. *Applied Mathematical Modelling,* 36**,** pp. 5162-5182.

Preumont, A., 2011. *Vibration control of active structures, an introduction*. 3rd ed. Berlin: Springer

Sandhu, R. S. & Pister, K. S., 1970. A variational principle for linear, coupled field problems in continuum mechanics. *International Journal of Engineering Science,* 8**,** pp. 989-999.

Sandhu, R. S. & Pister, K. S., 1971. Variational principles for boundary value and initial-boundary value problems in continuum mechanics. *International Journal of*

Solids and Structures, 7**,** pp. 639-654.

Sanz‐Serna, J. M., 1983. On finite elements simultaneously in space and time. *International Journal for Numerical Methods in Engineering,* 19**,** pp. 623-624.

Schueller, W., 1983. *Horizontal-span building structures,* New York: John Wiley & Sons.

Segerlind, L. J., 1989. Weighted residual solutions in the time domain. *International journal for numerical methods in engineering,* 28**,** pp. 679-685.

Shen, W., Lin, J. & Williams, F., 1995. Parallel computing for the high precision direct integration method. *Computer methods in applied mechanics and engineering,* 126**,** pp. 315-331.

Sheng, G., Fung, T. C. & Fan, S. C., 1998a. Parametrized formulations of Hamilton's law for numerical solutions of dynamic problems: Part I. Global approximation. *Computational Mechanics,* 21**,** pp. 441-448.

Sheng, G., Fung, T. C. & Fan, S. C., 1998b. Parametrized formulations of Hamilton's law for numerical solutions of dynamic problems: Part II. Time finite element approximation. *Computational Mechanics,* 21**,** pp. 449-460.

Simkins, T. E., 1978. Unconstrained variational statements for initial and boundary-value problems. *AIAA journal,* 16, pp. 559-563.

Simkins, T. E., 1979. Reply by author to C.V.Smith Jr. *AIAA Journal,* 17**,** pp. 127-128.

Simkins, T. E., 1981. Finite Elements for Initial Value Problems in Dynamics. *AIAA Journal,* 19**,** pp. 1357-1362.

Simkins, T. E., 1983. Reply by author to Riff,Weler, and Baruch. *AIAA journal,* 21**,** pp. 319-320.

Smith, C. V. & Smith, D. R., 1977. Comment on "Application of Hamilton's Law of Varying Action". *AIAA Journal,* 15**,** pp. 284-286.

Smith, C. V., 1979. Comment on "Unconstrained variational statements for initial and boundary-value problems". *AIAA Journal,* 17**,** pp. 126-127.

Smith, C. V., 1977. Discussion:“Hamilton, Ritz, and Elastodynamics”(Bailey, CD, 1976, ASME J. Appl. Mech., 43, pp. 684–688). *Journal of Applied Mechanics,* 44**,** pp. 796.

Soares Jr, D., 2011. A new family of time marching procedures based on Green’s function matrices. *Computers & structures,* 89**,** pp. 266-276.

Subbaraj, K. & Dokainish, M., 1989. A survey of direct time-integration methods in computational structural dynamics—II. Implicit methods. *Computers & Structures,* 32**,** pp. 1387-1401.

Tamma, K. K. & Namburu, R. R., 1990. Applicability and evaluation of an implicit self-starting unconditionally stable methodology for the dynamics of structures. *Computers & structures,* 34**,** pp. 835-842.

Tarnow, N. & Simo, J., 1994. How to render second order accurate time-stepping algorithms fourth order accurate while retaining the stability and conservation properties. *Computer Methods in Applied Mechanics and Engineering,* 115**,** pp. 233-252.

Tedesco, J. W., McDougal, W. G. & Ross, C. A., 1999. *Structural dynamics : theory and applications,* Menlo Park, Calif: Addison Wesley Longman.

Thai, H.T. & Kim, S.E. 2011. Nonlinear inelastic time-history analysis of truss structures. *Journal of Constructional Steel Research,* 67**,** pp. 1966-1972.

Tiersten, H. F., 1968. Natural boundary and initial conditions from a modification of Hamilton's principle. *Journal of Mathematical Physics,* 9**,** pp. 1445-1451.

Tonti, E., 1973. On the variational formulation for linear initial value problems. *Annali di Matematica Pura ed Applicata,* 95**,** pp. 331-359.

Wang, M. F. & Au, F. T. K., 2004. Higher-order mixed method for time integration in dynamic structural analysis. *Journal of Sound and Vibration*, 278, pp. 690–698.

Wang, M. & Au, F. T. K., 2009. On the precise integration methods based on Padé approximations. *Computers & Structures,* 87**,** pp. 380-390.

Wang, Y., Tian, X. & Zhou, G., 2002. Homogenized high precision direct integration scheme and its applications in engineering. *Communications in numerical methods in engineering,* 18**,** pp. 429-439.

Wilson, E. L., 1968. A computer program for the dynamic stress analysis of underground structures, SESM report No. 68-1, Division of structural engineering and structural mechanics, University of California, Berkeley, CA.

Wilson, E. L. & Nickell, R. E., 1966. Application of the finite element method to heat conduction analysis. *Nuclear Engineering and Design,* 4**,** pp. 276-286.

Wood, W., 1990. *Practical time-stepping schemes,* Clarendon Press Oxford.

Wood, W., Bossak, M. & Zienkiewicz, O., 1980. An alpha modification of

Newmark's method. *International Journal for Numerical Methods in Engineering,* 15**,** pp. 1562-1566.

Wu, J., 1977. Solutions to initial value problems by use of finite elements—Unconstrained variational formulations. *Journal of Sound and Vibration,* 53**,** pp. 341-356.

Yina, S., 2011. An unconditionally stable explicit method for structural dynamics. *Procedia Engineering,* 14**,** pp. 2519-2526.

Yu, J. R. & Hsu, T. R., 1985. Analysis of heat conduction in solids by space-time finite element method. *International Journal for Numerical Methods in Engineering,* 21**,** pp. 2001-2012.

Yu, Y., Li, R. & Luo, Y., 2011. Progressive collapse simulation of truss structures based on the Finite Particle Method. Electric Technology and Civil Engineering (ICETCE), 2011 International Conference on, IEEE, pp. 567-571.

Zhong, W., Jianing, Z. & Zhong, X. X., 1996. On a new time integration method for solving time dependent partial differential equations. *Computer methods in applied mechanics and engineering,* 130**,** pp. 163-178.

Zhong, W. & Williams, F., 1994. A precise time step integration method. *Proceedings of the Institution of Mechanical Engineers, Part C: Journal of Mechanical Engineering Science,* 208**,** pp. 427-430.

Zienkiewicz, O. C., 1977. *The finite element method,* London ; New York, McGraw-Hill.

Zienkiewicz, O. C., Taylor, R. L. & Zhu, J. Z., 2005. *The finite element method : its basis and fundamentals,* Oxford, Elsevier Butterworth-Heinemann.

Zienkiewicz, O. C., Wood, W. L., Hine, N. W. & Taylor, R. L., 1984. A unified set of single step algorithms. Part 1: General formulation and applications. *International Journal for Numerical Methods in Engineering,* 20**,** pp. 1529-1552.